



Control of Particulate Matter Emissions

Student Manual

APTI Course 413
Fifth Edition
(Version 2)

Authors

Jerry W. Crowder, PhD, PE
Crowder Environmental Associates, Inc.

Timothy Smith
U.S. Environmental Protection Agency

Control of Particulate Matter Emissions

Student Manual

APTI Course 413

Fifth Edition

(Version 2)

Authors

Jerry W. Crowder, Ph.D., P.E.
Crowder Environmental Associates, Inc.
120 Cherry Circle
Dyersburg, Tennessee 38024

Timothy Smith
Office of Air Quality Planning and Standards
U.S. Environmental Protection Agency
Research Triangle Park, North Carolina 27711

Notice

This is not an official policy and standards document. The opinions and selections are those of the authors and not necessarily those of the U.S. Environmental Protection Agency. Every attempt has been made to represent the present state of environmental knowledge as well as subject areas still under evaluation. Any mention of products or organizations does not constitute endorsement or recommendation by the United States Environmental Protection Agency.

Table of Contents

Chapter 1 - Basic Concepts	1-1
Gas Temperature	1-1
Absolute Temperature	1-2
Standard Temperature	1-2
Gas Pressure	1-3
Barometric Pressure	1-3
Gauge Pressure	1-3
Absolute Pressure	1-4
Molecular Weight and the Mole	1-5
Equation of State	1-5
Volume Correction	1-6
Molar Volume	1-7
Gas Density	1-8
Viscosity	1-9
Liquid Viscosity	1-9
Gas Viscosity	1-10
Kinematic Viscosity	1-10
Reynolds Number	1-11
Calculation of Dew Point	1-13
Review Questions	1-15
Review Question Answers	1-17
Review Problems	1-19
Review Problem Solutions	1-21
References	1-23
Chapter 2 - Particulate Matter Formation and Regulation	2-1
Particle Formation	2-1
Primary and Secondary Particulate Matter	2-5
Sources of Particulate Matter	2-6
Particulate Matter Regulation	2-7
Before the Clean Air Act	2-7
The Clean Air Act	2-8
National Ambient Air Quality Standards	2-9
State Implementation Plans	2-10
New Source Performance Standards and New Source Permitting	2-13
National Emissions Standard for Hazardous Air Pollutants	2-15
Visibility	2-16
Title V Operating Permits	2-16
Review Questions	2-19
Review Question Answers	2-21
References	2-24

Chapter 3 - Particle Sizing	3-1
Particle Size	3-1
Particle Size Measurement	3-5
Microscopy	3-6
Optical Counters	3-7
Bahco Analyzer	3-8
Electrical Aerosol Analyzer	3-8
Cascade Impactors	3-9
Comparison of Particle Sizing Devices	3-11
Particle Size Distributions	3-11
Review Problems	3-17
Review Problem Solutions	3-19
References	3-23
Chapter 4 - Particle Collection Mechanisms	4-1
Collection Mechanisms	4-1
Steps in Particulate Matter Control	4-2
Gravitational Settling	4-3
Gravitational Force	4-3
Buoyant Force	4-3
Drag Force	4-4
Drag Coefficient	4-5
Cunningham Slip Correction Factor	4-6
Calculation of Drag Force	4-7
Terminal Settling Velocity	4-8
Determination of Flow Region	4-9
Summary	4-11
Centrifugal Inertial Force	4-12
Inertial Impaction	4-14
Brownian Motion	4-15
Electrostatic Attraction	4-16
Thermophoresis and Diffusiophoresis	4-19
Particle Size-Collection Efficiency Relationships	4-19
Review Questions	4-21
Review Question Answers	4-23
Review Problems	4-25
Review Problem Solutions	4-27
References	4-29
Chapter 5 - Settling Chambers	5-1
Types and Components	5-1
Simple Expansion Chamber	5-1
Howard Settling Chamber	5-1
Momentum Separators	5-2
Performance Evaluation	5-3

Review Questions	5-9
Review Question Answers	5-11
Review Problem	5-13
Review Problem Solutions	5-15
References	5-17
Chapter 6 - Cyclones	6-1
Operating Principles	6-1
Cyclone Systems	6-3
Large Diameter Cyclones	6-3
Small Diameter Multi-Cyclones	6-6
Performance Evaluation	6-10
Collection Efficiency	6-10
Lapple Technique	6-10
Leith Technique	6-12
Pressure Drop	6-15
Instrumentation	6-17
Static Pressure Drop Gauges	6-17
Inlet and Outlet Gas Temperature Gauges	6-17
Review Questions	6-19
Review Question Answers	6-23
Review Problems	6-25
Review Problem Solutions	6-27
References	6-31
Chapter 7 - Fabric Filters	7-1
Operating Principles	7-1
Particle Collection	7-1
Pressure Drop	7-3
Filter Media Blinding and Bag Blockage	7-7
Fabric Filter Applicability Limitations	7-8
Fabric Filter Systems	7-8
Shaker Fabric Filters	7-9
Reverse Air Fabric Filters	7-11
Pulse Jet Fabric Filters	7-14
Cartridge Filters	7-20
Fabrics	7-21
Performance Evaluation	7-25
Air-to-Cloth Ratio	7-26
Approach Velocity	7-29
Bag Spacing and Length	7-31
Bag Accessibility	7-33
Hopper Design	7-33
Bypass Dampers	7-34
Instrumentation	7-35
Static Pressure Drop Gauges	7-35

Inlet and Outlet Gas Temperature Gauges	7-36
Opacity Monitors	7-36
Review Questions	7-39
Review Question Answers	7-41
Review Problems	7-43
Review Problem Solutions	7-45
References	7-49
Chapter 8 - Wet Scrubbers	8-1
Operating Principles	8-1
Collection Mechanisms	8-1
Inertial Impaction	8-2
Brownian Motion	8-3
Static Pressure Drop	8-3
Gas Cooling	8-6
Liquid Recirculation	8-6
Liquid-to-Gas Ratio	8-7
Liquid Purge Rates	8-8
Alkali Addition	8-9
Wastewater Treatment	8-11
Mist Elimination	8-11
Chevrons	8-11
Mesh and Woven Pads	8-12
Tube Bank	8-13
Cyclones	8-13
Fans, Ductwork and Stacks	8-16
Fans	8-16
Ductwork	8-16
Stacks	8-16
Wet Scrubber Capabilities and Limitations	8-17
Wet Scrubber Systems	8-18
Spray Tower Scrubbers	8-19
Mechanically Aided Scrubbers	8-20
Orifice Scrubbers	8-21
Packed Bed Scrubbers	8-22
Ionizing Wet Scrubbers	8-24
Fiber Bed Scrubbers	8-25
Moving Bed Scrubbers	8-26
Tray Scrubbers	8-26
Catenary Grid Scrubbers	8-28
Condensation Growth Scrubbers	8-29
Venturi Scrubbers	8-30
Rod Deck Scrubbers	8-33
Collision Scrubbers	8-34
Ejector Scrubbers	8-34
Performance Evaluation	8-35
Empirical Evaluation	8-35
Pilot Scale Tests	8-36

Mathematical Models	8-37
Counter-Current Spray Tower Scrubbers	8-37
Packed Bed Scrubbers	8-39
Tray Scrubbers	8-40
Venturi scrubbers	8-41
Instrumentation	8-44
Review Questions	8-47
Review Question Answers	8-51
Review Problems	8-53
Review Problem Solutions	8-55
References	8-61
Chapter 9 - Electrostatic Precipitators	9-1
Operating Principles	9-1
Precipitator Energization	9-1
Particle Charging and Migration	9-5
Dust Layer Resistivity	9-7
Applicability Limitations	9-12
Precipitator Systems	9-13
Dry, Negative Corona Precipitators	9-14
Wet, Negative Corona Precipitators	9-23
Wet, Positive Corona Precipitators	9-27
Performance Evaluation	9-27
Collection Efficiency	9-28
Specific Collection Area	9-33
Sectionalization	9-34
Aspect Ratio	9-37
Gas Superficial Velocity	9-38
Collector Plate Spacing	9-38
Summary of Sizing Parameters	9-38
Discharge Electrodes	9-39
Rapping Systems	9-39
Hopper Design	9-40
Flue Gas Conditioning Systems	9-41
Instrumentation	9-44
Review Questions	9-47
Review Question Answers	9-51
Review Problems	9-55
Review Problem Solutions	9-57
References	9-59
Chapter 10 - Hoods and Fans	10-1
Hoods	10-1
Hood Operating Principles	10-4
Hood Designs for Improved Performance	10-6
Monitoring Hood Capture Effectiveness	10-8

	Transport Velocity	10-11
	Summary	10-13
Fans		10-13
	Types of Fans and Fan Components	10-13
	Centrifugal Fan Operating Principles	10-16
	Effect of Gas Temperature and Density	10-24
	Summary	10-26
	Review Problems	10-27
	Review Problem Solutions	10-31
	References	10-35

CHAPTER 1

BASIC CONCEPTS

Gas Temperature

There are several scales available for measuring temperature, all of them entirely arbitrary. The two that have come into common use are the Fahrenheit scale and the Celsius or Centigrade scale. As shown in Figure 1-1, the Fahrenheit scale sets 32°F as the freezing temperature of water and divides the scale between the freezing and boiling points into 180 degree units, making 212°F the boiling temperature of water. The Celsius scale sets 0°C as the freezing temperature of water and divides the scale between the freezing and boiling points into 100 degree units, making 100°C the boiling temperature of water. The following relationships convert one scale to another:

$$^{\circ}\text{F} = 1.8^{\circ}\text{C} + 32 \quad (1-1)$$

$$^{\circ}\text{C} = \frac{^{\circ}\text{F} - 32}{1.8} \quad (1-2)$$

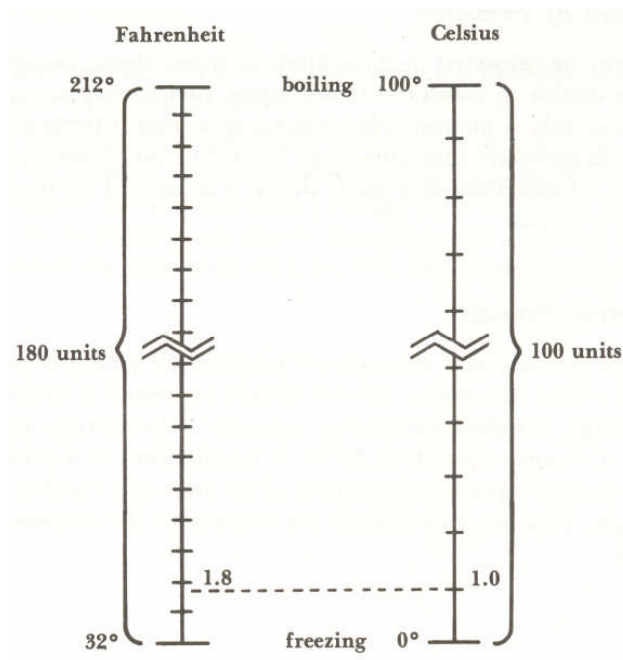


Figure 1-1. Comparison of Fahrenheit and Celsius temperature scales

Absolute Temperature

Although these two scales are very serviceable, their use causes difficulties when forming temperature ratios or when taking roots and powers of negative temperatures. What is needed in these situations is a temperature scale that has zero as its lowest value. These scales are referred to as *absolute temperature* scales. Experiments with perfect gases have shown that, under constant pressure, for each change in Fahrenheit degree below 32°F the volume of gas changes 1/491.69. Similarly, for each Celsius degree the volume changes 1/273.16. Therefore, if this change in volume per temperature degree is constant, the volume of gas would, theoretically, become zero at 491.69 Fahrenheit degrees below 32°F, or at -459.69°F. On the Celsius scale, this condition occurs at 273.16 Celsius degrees below 0°C, or at a temperature of -273.16°C.

Absolute temperatures determined by using Fahrenheit units are expressed as degrees Rankine (°R); those determined by using Celsius units are expressed as Kelvin (K). The following approximate relationships convert one scale to the other:

$$^{\circ}\text{R} = ^{\circ}\text{F} + 460 \quad (1-3)$$

$$\text{K} = ^{\circ}\text{C} + 273 \quad (1-4)$$

Standard Temperature

One particular temperature of interest is *standard temperature*. Unfortunately, there is no common temperature that is recognized by all groups. Even USEPA has two standard temperatures, one for air monitoring and one for all other applications. The standard temperatures used by various groups are listed in Table 1-1.

Group	T_{std}
USEPA (General)	68°F (20°C)
USEPA (Air monitoring)	77°F (25°C)
Industrial hygiene	70°F (21.1°C)
Combustion	60°F (15.6°C)
Science	32°F (0°C)

In this course, the USEPA standard temperature of 68°F will be used.

Example 1-1

The gas temperature in the stack of a wet scrubber system is 130°F. What is the absolute temperature in Rankine and Kelvin?

Solution:

$$\text{Absolute Temperature, } ^{\circ}\text{R} = 460^{\circ}\text{R} + 130^{\circ}\text{F} = 590^{\circ}\text{R}$$

$$\text{Absolute Temperature, K} = \frac{590^{\circ}\text{R}}{1.8} = 327.8\text{K}$$

Gas Pressure

A body may be subjected to three kinds of stress: shear, compression and tension. Fluids are unable to withstand tensile stress; hence, they are subject only to shear and compression. Unit compressive stress in a fluid is termed *pressure* and is expressed as force per unit area (e.g., lb_f/in² and Newtons/m²). Pressure is equal in all directions at a point within a volume for fluid and acts perpendicular to a surface.

Barometric Pressure

Barometric pressure and atmospheric pressure are synonymous. These pressures are measured with a barometer and are usually expressed as inches or millimeters of mercury (Hg). Standard barometric pressure is agreed to by all groups and is the average atmospheric pressure at sea level, 45°N latitude and at 35°F. It is equivalent to a pressure of 14.696 pounds force per square inch exerted at the base of a column of mercury 29.92 inches high. Other equivalents to standard pressure are listed in Table 1-2. Weather and altitude are responsible for barometric pressure variations.

Units	Value
Atmosphere (atm)	1
Pounds force per square inch (psi)	14.70
Inches of mercury (in Hg)	29.92
Millimeters of mercury (mm Hg)	760
Feet of water column (ft WC)	33.92
Inches of water column (in WC)	407
Kilopascals (kPa)	101.3
Millibars (mb)	1013

Gauge Pressure

The pressure inside an air pollution control system is termed the *gauge or static pressure* and is measured relative to the prevailing atmospheric pressure, as shown in Figure 1-2. If the system pressure is greater than atmospheric, the gauge pressure is expressed as a positive value. If smaller, the gauge pressure is expressed as negative. The term *vacuum* designates a negative gauge pressure. Gauge or static pressures in air pollution systems are usually expressed in inches of water column (in WC).

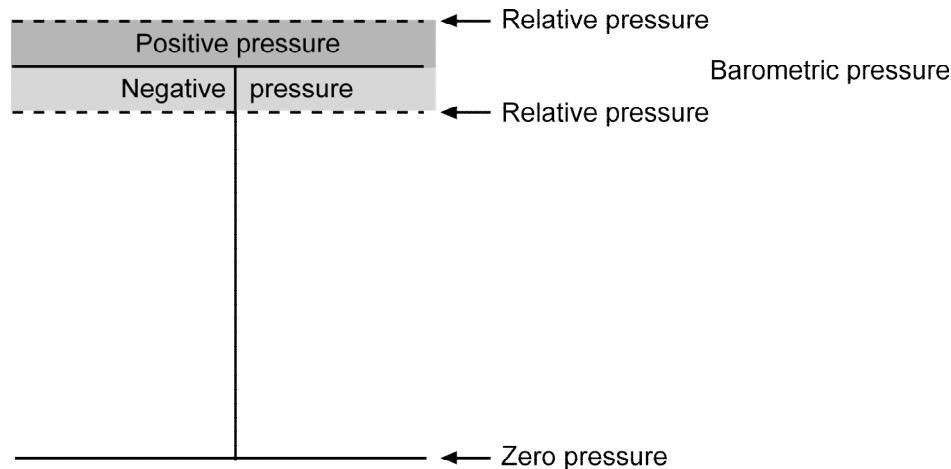


Figure 1-2. Definition of positive and negative gauge pressures

Absolute Pressure

The gauge pressures commonly used in reference to air pollution control systems share an attribute that caused difficulties in the use of normal temperature scales—they can have negative values. As a result, calculations involving pressure ratios and roots and powers of pressure must use *absolute pressure*. Absolute pressure is the algebraic sum of the atmospheric pressure and the gauge pressure:

$$P = P_b + p_g \quad (1-5)$$

where

P = absolute pressure

P_b = barometric or atmospheric pressure

P_g = gauge pressure

Example 1-2

An air pollution control device has an inlet static pressure of -25 in WC. What is the absolute static pressure at the inlet of the air pollution control device if the barometric pressure at the time is 29.85 in Hg?

Solution:

Convert the barometric pressure units to in WC:

$$P_b = 29.85 \text{ in Hg} \left(\frac{407 \text{ in WC}}{29.92 \text{ in Hg}} \right) = 406 \text{ in WC}$$

Add the barometric and gauge (static) pressures:

$$P = 406 \text{ in WC} + (-25 \text{ in WC}) = 381 \text{ in WC}$$

Molecular Weight and the Mole

The molecular weight of a compound is simply the sum of the atomic weights of all the atoms in the molecule. The atomic weight of an atom is based on an arbitrary scale of the relative masses of the elements, usually based on a carbon value of 12. The chemical identity of an atom is determined by the number of protons in its nucleus and is called the atomic number. Values of atomic number and atomic weight can be found in a Periodic Table of Elements.

Mixtures of molecules do not have a true molecular weight; however, they do have an apparent molecular weight that can be calculated from the composition of the mixture:

$$MW_{\text{mixture}} = \sum_{i=1}^n \chi_i MW_i \quad (1-6)$$

where χ_i is the mole fraction of component i and MW_i is its molecular weight. Many times, properties of a contaminated gas can be approximated by the properties of air, itself a mixture of molecules. The apparent molecular weight of air is 28.95, or approximately 29.

A mole is a mass of material that contains a certain number of molecules. Moles can be expressed in terms of any mass unit; thus, e.g., there are gram-moles, kilogram-moles, ounce-moles, pound-moles and ton-moles. The relationship between the different types of moles is the same as the relationship between the corresponding mass units. Thus, there are 1,000 gram-moles in a kilogram-mole, 453.6 gram-moles in a pound-mole, 16 ounce-moles in a pound-mole and 2,000 pound-moles in a ton-mole.

The gram-mole is the mass of material that contains Avogadro's number of molecules, approximately 6.023×10^{23} . The mass of a mole is numerically equal to the molecular weight. For oxygen, which has a molecular weight of 32, there are 32 grams per gram-mole, 32 kilograms per kilogram-mole, and 32 pounds per-pound mole. However, only the gram-mole contains Avogadro's number of molecules. The kilogram-mole contains 1,000 times Avogadro's number of molecules, and the pound-mole contains 453.6 times.

Equation of State

Equations of state relate the pressure, volume and temperature properties of a pure substance or mixture by semi-theoretical or empirical relationships. Over the range of temperature and pressure usually encountered in air pollution control systems, these values may be related by the ideal or perfect gas law:

$$PV = nRT \quad (1-7)$$

where

P = absolute pressure

V = gas volume

n = number of moles

R = constant

T = absolute temperature

Here, R is referred to as the universal gas constant, and its value depends on the units of the other terms in the equation. Values of R include:

$$\begin{aligned} &10.73 \text{ psia}\cdot\text{ft}^3/\text{lb-mole}\cdot^\circ\text{R} \\ &0.73 \text{ atm}\cdot\text{ft}^3/\text{lb-mole}\cdot^\circ\text{R} \\ &82.06 \text{ atm}\cdot\text{cm}^3/\text{g-mole}\cdot\text{K} \\ &8.31 \times 10^3 \text{ kPa}\cdot\text{m}^3/\text{kg-mole}\cdot\text{K} \end{aligned}$$

Volume Correction

A useful relationship may be developed from the ideal gas law by noting that $PV/T = nR$, and that, for a given number of moles of a gas, nR is a constant. Thus, at two different conditions for the same gas, we may write:

$$\frac{P_1 V_1}{T_1} = \frac{P_2 V_2}{T_2} \quad (1-8)$$

or

$$V_1 = V_2 \left(\frac{P_2}{P_1} \right) \left(\frac{T_1}{T_2} \right) \quad (1-9)$$

Equation 1-9 allows volumes (or volume rates) to be corrected from one set of temperature and pressure conditions to another. One common calculation is to convert volumetric flow rate from actual conditions to standard conditions, or vice versa:

$$\text{SCFM} = \text{ACFM} \left(\frac{P_{\text{actual}}}{P_{\text{std}}} \right) \left(\frac{T_{\text{std}}}{T_{\text{actual}}} \right) \quad (1-10)$$

$$\text{ACFM} = \text{SCFM} \left(\frac{P_{\text{std}}}{P_{\text{actual}}} \right) \left(\frac{T_{\text{actual}}}{T_{\text{std}}} \right) \quad (1-11)$$

Example 1-3

A particulate control system consists of a hood, ductwork, fabric filter, fan, and stack. The total gas flow entering the fabric filter is 8,640 scfm. The gas temperature in the inlet duct is 320°F and the static pressure is -10 in WC. The barometric pressure is 28.30 in Hg. If the inlet duct has inside dimensions of 3 feet by 4 feet, what is the velocity into the fabric filter?

Solution:

Velocity must be calculated from the actual volumetric flow rate.

Convert the static pressure to absolute pressure:

$$P = 28.30 \text{ in Hg} \left(\frac{407 \text{ in WC}}{29.92 \text{ in Hg}} \right) + (-10 \text{ in WC}) = 375 \text{ in WC}$$

Convert the gas temperature to absolute temperature:

$$T_{\text{actual}} = 320^\circ\text{F} + 460^\circ = 780^\circ\text{R}$$

Convert the inlet flow rate to actual conditions:

$$Q_{\text{actual}} = 8,640 \text{ scfm} \left(\frac{780^\circ\text{R}}{528^\circ\text{R}} \right) \left(\frac{407 \text{ in WC}}{375 \text{ in WC}} \right) = 13,853 \text{ acfm}$$

Calculate the velocity:

$$V = \frac{13,853 \frac{\text{ft}^3}{\text{min}}}{(3 \text{ ft})(4 \text{ ft})} = 1,154 \frac{\text{ft}}{\text{min}}$$

Molar Volume

The ideal gas law may also be rearranged to calculate the volume occupied by a mole of gas, called the *molar volume*:

$$\frac{V}{n} = \frac{RT}{P} \quad (1-12)$$

Example 1-4

What is the molar volume of an ideal gas at 68°F and 1 atm? At 200°F and 1 atm?

Solution:

At 68°F and 1 atm:

$$\frac{V}{n} = \frac{RT}{P} = \frac{\left(0.73 \frac{\text{atm} \cdot \text{ft}^3}{\text{lb-mole } ^\circ\text{R}}\right)(528^\circ\text{R})}{(1 \text{ atm})} = 385.4 \frac{\text{ft}^3}{\text{lb-mole}}$$

At 200°F and 1 atm:

$$\frac{V}{n} = \frac{RT}{P} = \frac{\left(0.73 \frac{\text{atm} \cdot \text{ft}^3}{\text{lb-mole } ^\circ\text{R}}\right)(660^\circ\text{R})}{(1 \text{ atm})} = 481.8 \frac{\text{ft}^3}{\text{lb-mole}}$$

or

$$\frac{V}{n} = 385.4 \left(\frac{660^\circ\text{R}}{528^\circ\text{R}} \right) = 481.8 \frac{\text{ft}^3}{\text{lb-mole}}$$

Gas Density

Finally, we may use the ideal gas law to estimate gas density. Density is the ratio of the mass of a material to the volume that material occupies. For accurate values, gas densities should be determined from reference texts. However, an estimate of the gas density can be determined from the ideal gas law. Recognizing that the number of moles is given by mass (m) divided by molecular weight (MW), the ideal gas law may be written:

$$PV = \left(\frac{m}{MW} \right) RT \quad (1-13)$$

The gas density (ρ) can then be estimated from:

$$\rho = \frac{m}{V} = \frac{P \cdot MW}{RT} \quad (1-14)$$

Density can also be estimated from the molecular weight and molar volume:

$$\rho = \left(\frac{MW}{385.4} \right) \left(\frac{528}{T} \right) \left(\frac{P}{29.92} \right) \quad (1-15)$$

where

P = absolute pressure (in. Hg)

T = absolute temperature ($^\circ\text{R}$)

Viscosity

Viscosity is the proportionality constant associated with a fluid resistance to flow. Viscosity is the result of two phenomena: (1) intermolecular cohesive forces, and (2) momentum transfer between flowing strata caused by molecular agitation perpendicular to the direction of motion. Between adjacent strata of a moving Newtonian fluid, a shearing stress, σ , occurs that is directly proportional to the velocity gradient or shear rate, Γ (see Figure 1-3). This is expressed in the equation:

$$\sigma = \mu\Gamma = \mu \frac{dv}{dy} \quad (1-16)$$

where

σ = shear stress

μ = proportionality constant

Γ = shear rate or velocity gradient (dv/dy)

The proportionality constant, μ , is called the coefficient of viscosity, the absolute viscosity or merely viscosity. It should be noted that the pressure does not appear in Equation 1-16, indicating that the shear stress and viscosity are independent of pressure. Actually, viscosity increases very slightly with pressure, but this variation is negligible in most engineering calculations.

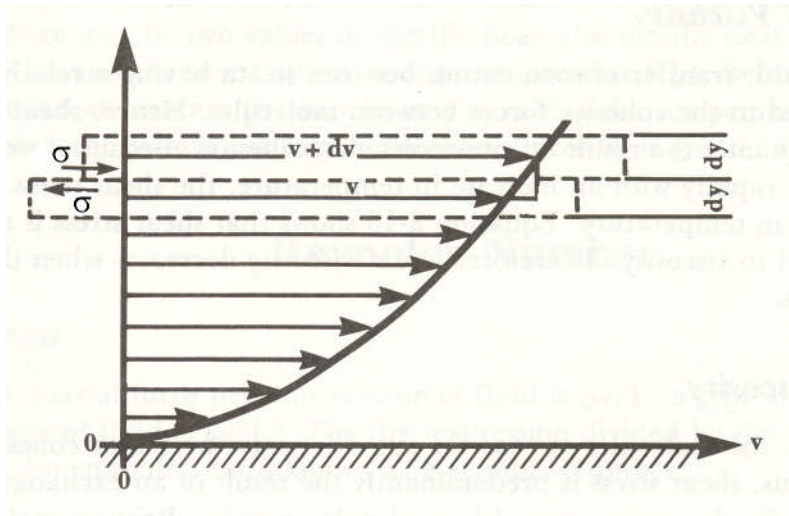


Figure 1-3. Shearing stress in a moving fluid

Liquid Viscosity

In a liquid, transfer of momentum between strata flowing at slightly different velocities is small compared to the cohesive forces between molecules. Hence, viscosity in liquids is predominantly the result of intermolecular cohesion. Because forces of cohesion decrease

rapidly with an increase in temperature, liquid viscosity decreases with an increase in temperature.

Gas Viscosity

In a gas, the molecules are too far apart for intermolecular cohesion to be effective. Thus, the viscosity in gases is predominantly the result of an exchange of momentum between flowing strata caused by molecular transfer. Since molecular motion increases as temperature increases, gas viscosity increases with an increase in temperature.

The viscosity of air at any temperature may be estimated from:

$$\frac{\mu}{\mu_{\text{ref}}} = \left(\frac{T}{T_{\text{ref}}} \right)^{0.768} \quad (1-17)$$

where

- μ = absolute viscosity
- μ_{ref} = absolute viscosity at reference temperature
- T = absolute temperature
- T_{ref} = reference absolute temperature

The viscosity of air and other gases important in air pollution control applications can also be estimated from:

$$\mu = 51.05 + 0.207T + 3.24 \times 10^{-5}T^2 - 74.14x + 53.417y \quad (1-18)$$

where

- μ = absolute viscosity (micropoise)
- T = absolute temperature ($^{\circ}\text{R}$)
- x = water vapor content (fraction)
- y = oxygen content (fraction)

The viscosity of air at 68°F is 1.21×10^{-5} lb_m/ft·sec.

Kinematic Viscosity

The ratio of the absolute viscosity to the density of a fluid often appears in dimensionless numbers, such as the Reynolds Number. Kinematic viscosity is defined according to the following relationship, and is used to simplify calculations:

$$\nu = \frac{\mu}{\rho} \quad (1-19)$$

where

- ν = kinematic viscosity

μ = absolute viscosity

ρ = density

Reynolds Number

Reynolds Number is the ratio of inertial forces to viscous forces in a flowing fluid. A typical inertial force per unit volume of fluid is $\rho v^2/L$. A typical viscous force per unit volume of fluid is $\mu v/L^2$. The first expression divided by the second provides the dimensionless ratio known as the Reynolds Number:

$$\text{Re} = \frac{Lv\rho}{\mu} \quad (1-20)$$

where

Re = Reynolds Number

L = characteristic system dimension

v = fluid velocity

ρ = fluid density

μ = fluid viscosity

The linear dimension, L, is a length characteristic of the flow system. It is equal to four times the mean hydraulic radius, which is the cross-sectional area divided by the wetted perimeter. Thus, for a circular pipe, L is the pipe diameter, D, and the Reynolds Number, sometimes termed the *Flow Reynolds Number*, takes the form:

$$\text{Re} = \frac{Dv\rho}{\mu} \quad (1-21)$$

Reynolds Number in this form is used to distinguish between laminar and turbulent flow. In laminar flow, the fluid is constrained to motion in layers, or laminae, by the action of viscosity. These layers of fluid move in parallel paths that remain distinct from one another. Laminar flow occurs when the Reynolds Number is less than about 2,000. In turbulent flow, the fluid is not restricted to parallel paths but moves forward in a random, chaotic manner. Fully turbulent flow occurs when the Reynolds Number is greater than about 3,000. Between Reynolds Numbers of 2,000 and 3,000, the flow may be laminar or turbulent, depending on the flow system conditions. Pipe or duct vibration, for example, can cause turbulent conditions to exist at Reynolds Numbers significantly below 3,000. It is worth noting that, primarily because of the size, flow in air pollution control equipment is always turbulent. Laminar conditions are present only in the very thin boundary layers that form near surfaces.

A form of Reynolds Number that is of greater interest in this course is the *Particle Reynolds Number*. Here, the characteristic system dimension is the particle diameter, d_p , and the velocity, v_p , is the particle velocity relative to the gas stream:

$$\text{Re}_p = \frac{d_p v_p \rho}{\mu} \quad (1-22)$$

Particle Reynolds Number is used to characterize flow conditions when particles move through or with a flowing fluid. Particle Reynolds Numbers less than about 1 indicate laminar conditions and define what is commonly termed the *Stokes Region*. Values over about 1,000 indicate turbulent conditions and define what is commonly termed the *Newton Region*. Particle Reynolds Numbers between 1 and 1,000 indicate transitional conditions. Most particle motion in air pollution control devices occurs in the Stokes and Transitional Regions.

Example 1-5

Calculate the Particle Reynolds Number for a 2 μm diameter particle moving through 10°C still air at a velocity of 6 m/sec.

Solution:

From Appendix B, the density of air at 20°C is $1.20 \times 10^{-3} \text{ g/cm}^3$ and the viscosity is $1.80 \times 10^{-4} \text{ g/cm}\cdot\text{sec}$.

Estimate the gas density at 10°C:

$$\rho = 1.20 \times 10^{-3} \left(\frac{293 \text{ K}}{283 \text{ K}} \right) = 1.24 \times 10^{-3} \frac{\text{g}}{\text{cm}^3}$$

Estimate the gas viscosity at 10°C:

$$\mu = 1.80 \times 10^{-4} \left(\frac{283 \text{ K}}{293 \text{ K}} \right)^{0.768} = 1.75 \times 10^{-4} \frac{\text{g}}{\text{cm}\cdot\text{sec}}$$

Calculate Particle Reynolds Number:

$$\text{Re}_p = \frac{d_p v_p \rho}{\mu} = \frac{(2 \times 10^{-4} \text{ cm}) \left(6 \times 10^2 \frac{\text{cm}}{\text{sec}} \right) \left(1.24 \times 10^{-3} \frac{\text{g}}{\text{cm}^3} \right)}{1.75 \times 10^{-4} \frac{\text{g}}{\text{cm}\cdot\text{sec}}} = 0.85$$

Example 1-6

Calculate the Particle and Flow Reynolds Numbers for a gas stream moving through a 200 cm diameter duct at a velocity of 1,500 cm/sec. Assume that the particles are moving at the

same velocity as the gas stream and are not settling due to gravity. Assume a gas temperature of 20°C and standard pressure.

Solution:

Since there is no difference in velocity between the gas stream and the particle, the Particle Reynolds Number is zero.

The Flow Reynolds Number is:

$$Re = \frac{Dv\rho}{\mu} = \frac{(200 \text{ cm}) \left(1,500 \frac{\text{cm}}{\text{sec}} \right) \left(1.20 \times 10^{-3} \frac{\text{g}}{\text{cm}^3} \right)}{1.80 \times 10^{-4} \frac{\text{g}}{\text{cm} \cdot \text{sec}}} = 2.00 \times 10^6$$

Calculation of Dew Point

Many gas streams that must be treated for particulate emissions may also contain significant amounts of water vapor or another condensable component. If particulate control is to be accomplished using fabric filters, it is necessary that the gas stream be maintained at a temperature sufficient to prevent the water from condensing, since condensation will cause the particulate matter to collect on the filters as a paste that cannot be easily cleaned.

The temperature at which condensation occurs is also known as the dew point temperature. At the dew point temperature, the partial pressure of the condensable component is equal to its vapor pressure. Since pressure fraction, mole fraction and volume fraction are equal for an ideal gas:

$$p_i = p^* = y_i P \quad (1-23)$$

where

- p_i = partial pressure of the condensable component
- p^* = vapor pressure of the condensable component
- y_i = mole fraction of the condensable component in the gas
- P = total pressure

Vapor pressure is a function of temperature and, for some materials, can be obtained from the Antoine equation:

$$\log_{10} p^* = A - \frac{B}{T + C} \quad (1-24)$$

where

- p^* = vapor pressure, mm Hg

T = Temperature, °C
A, B, and C are constants

Antoine constants for different materials may be found in numerous standard references. For water, values of the vapor pressure as a function of temperature may be obtained directly from vapor pressure tables that are widely available on the internet.

Example 1-7

The mole fraction of water in the stack gas from a combustion process contains 14% water vapor by volume. What is the dew point temperature if the total pressure is 1 atm? The Antoine constants for water are:

$$\begin{aligned}A &= 8.10765 \\B &= 1750.286 \\C &= 235.000\end{aligned}$$

Solution:

Note that volume fraction equals mole fraction. At the dew point temperature:

$$P^* = P_i = y_i P = 0.14(1) = 0.14 \text{ atm or } 106.4 \text{ mm Hg}$$

From the Antoine equation:

$$\begin{aligned}\log_{10} P^* &= 8.10765 - \frac{1750.286}{T + 235.000} \\ \log_{10} (106.4) &= 8.10765 - \frac{1750.286}{T + 235.000} \\ T &= 53^\circ\text{C}\end{aligned}$$

Review Questions

1. How does the particle Reynolds number change when the gas temperature is increased?
 - a. Increases
 - b. Decreases
 - c. Remains unchanged

2. How does the gas viscosity change as the temperature is increased?
 - a. Increases
 - b. Decreases
 - c. Remains unchanged

This page intentionally left blank.

Review Question Answers

1. How does the particle Reynolds number change when the gas temperature is increased?
 - b. Decreases

2. How does the gas viscosity change as the temperature is increased?
 - a. Increases

This page intentionally left blank.

Review Problems

1. The flows from Ducts A and B are combined into a single Duct C. The flow rate in Duct A is 5,000 scfm, the gas stream temperature is 350°F and the static pressure is -32 in WC. The flow rate in Duct B is 4,000 acfm, the gas stream temperature is 400°F and the static pressure is -35 in WC. What is the flow rate in Duct C? Assume a barometric pressure of 29.15 in Hg.
2. Calculate the Particle Reynolds Numbers for the following particles. Assume a gas temperature of 20°C and a pressure of 1 atm.
 - a. 10 μm particle moving at 1 ft/sec relative to the gas stream
 - b. 10 μm particle moving at 10 ft/sec relative to the gas stream
 - c. 100 μm particle moving at 1 ft/sec relative to the gas stream
 - d. 100 μm particle moving at 10 ft/sec relative to the gas stream

This page intentionally left blank.

Review Problem Solutions

1. The flows from Ducts A and B are combined into a single Duct C. The flow rate in Duct A is 5,000 scfm, the gas stream temperature is 350°F and the static pressure is -32 in WC. The flow rate in Duct B is 4,000 acfm, the gas stream temperature is 400°F and the static pressure is -35 in WC. What is the flow rate in Duct C? Assume a barometric pressure of 29.15 in Hg.

Solution:

Calculate the absolute pressure in Duct B:

$$P = 29.15 \text{ in Hg} \left(\frac{407 \text{ in WC}}{29.92 \text{ in Hg}} \right) + (-35 \text{ in WC}) = 361.5 \text{ in WC}$$

Convert the flow in Duct B to standard conditions:

$$Q_B = 4,000 \text{ acfm} \left(\frac{528^\circ\text{R}}{860^\circ\text{R}} \right) \left(\frac{361.5 \text{ in WC}}{407 \text{ in WC}} \right) = 2,181 \text{ scfm}$$

Combine flows:

$$Q_C = 5,000 \text{ scfm} + 2,181 \text{ scfm} = 7,181 \text{ scfm}$$

2. Calculate the Particle Reynolds Numbers for the following particles. Assume a gas temperature of 20°C and a pressure of 1 atm.

Solution:

- a. 10 μm particle moving at 1 ft/sec relative to the gas stream

$$\text{Re}_p = \frac{d_p v_p \rho}{\mu} = \frac{(10 \times 10^{-4} \text{ cm}) \left[\left(1.0 \frac{\text{ft}}{\text{sec}} \right) \left(30.48 \frac{\text{cm}}{\text{ft}} \right) \right] \left(1.20 \times 10^{-3} \frac{\text{g}}{\text{cm}^3} \right)}{1.80 \times 10^{-4} \frac{\text{g}}{\text{cm} \cdot \text{sec}}} = 0.203$$

- b. 10 μm particle moving at 10 ft/sec relative to the gas stream

$$\text{Re}_p = \frac{d_p v_p \rho}{\mu} = \frac{(10 \times 10^{-4} \text{ cm}) \left[\left(10.0 \frac{\text{ft}}{\text{sec}} \right) \left(30.48 \frac{\text{cm}}{\text{ft}} \right) \right] \left(1.20 \times 10^{-3} \frac{\text{g}}{\text{cm}^3} \right)}{1.80 \times 10^{-4} \frac{\text{g}}{\text{cm} \cdot \text{sec}}} = 2.03$$

c. 100 μm particle moving at 1 ft/sec relative to the gas stream

$$\text{Re}_p = \frac{d_p v_p \rho}{\mu} = \frac{(100 \times 10^{-4} \text{ cm}) \left[\left(1.0 \frac{\text{ft}}{\text{sec}} \right) \left(30.48 \frac{\text{cm}}{\text{ft}} \right) \right] \left(1.20 \times 10^{-3} \frac{\text{g}}{\text{cm}^3} \right)}{1.80 \times 10^{-4} \frac{\text{g}}{\text{cm} \cdot \text{sec}}} = 2.03$$

d. 100 μm particle moving at 10 ft/sec relative to the gas stream

$$\text{Re}_p = \frac{d_p v_p \rho}{\mu} = \frac{(100 \times 10^{-4} \text{ cm}) \left[\left(10.0 \frac{\text{ft}}{\text{sec}} \right) \left(30.48 \frac{\text{cm}}{\text{ft}} \right) \right] \left(1.20 \times 10^{-3} \frac{\text{g}}{\text{cm}^3} \right)}{1.80 \times 10^{-4} \frac{\text{g}}{\text{cm} \cdot \text{sec}}} = 20.3$$

References

Cengel, Y.A., and M.A. Boles, *Thermodynamics: An Engineering Approach*, McGraw-Hill, New York, 1989.

Himmelblau, D.M., *Basic Principles and Calculations in Chemical Engineering*, Prentice-Hall, Englewood Cliffs, 1982.

This page intentionally left blank.

CHAPTER 2

PARTICULATE MATTER FORMATION AND REGULATION

Particle Formation

The range of particle sizes formed in a process is largely dependent on the types of particle formation mechanisms present. It is possible to estimate the general size range simply by recognizing which of these is important in the process being evaluated. The most important particle formation mechanisms in air pollution sources include the following:

- Physical attrition/mechanical dispersion
- Combustion particle burnout
- Homogeneous condensation
- Heterogeneous nucleation
- Droplet evaporation

Physical attrition occurs when two surfaces rub together. For example, the grinding of a rod on a grinding wheel (as shown in Figure 2-1) yields small particles that break off from both surfaces. The compositions and densities of these particles are identical to the parent materials.

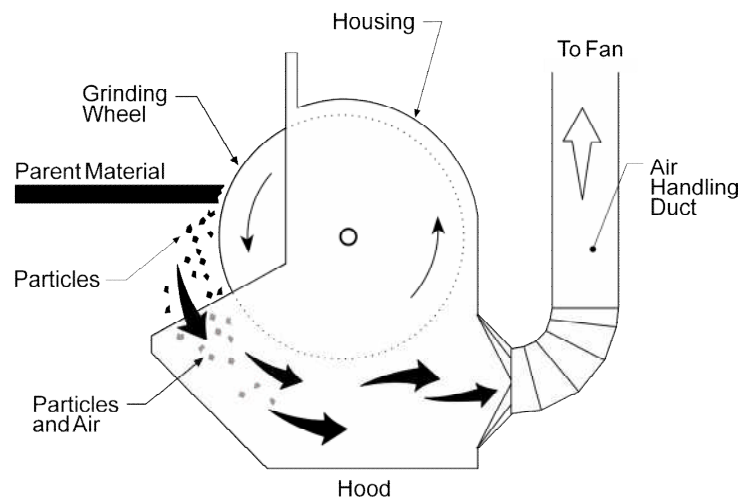


Figure 2-1. Grinding wheel

The tertiary stone crusher shown in Figure 2-2 is an example of an industrial source of particles that involves only physical attrition. The particles formed range from approximately 1 μm to almost 1,000 μm . However, the limited energy used in the crushing operation, very little of the particulate matter is less than 10 μm . Physical attrition generates primarily large particles.



Figure 2-2. Tertiary crusher

In order for fuel to burn, it must be pulverized (solid fuel) or atomized (liquid fuel) so that sufficient surface area is exposed to oxygen and high temperature. The surface area of particles increases substantially as more and more of the material is reduced in size. Accordingly, most industrial-scale combustion processes use one or more types of physical attrition in order to prepare or introduce their fuel into the furnace. For example, coal-fired boilers use pulverizers to reduce the chunks of coal to sizes that can be burned quickly. Oil-fired boilers use atomizers to disperse the oil as fine droplets. In both cases, the fuel particle size range is reduced primarily to the 100-1,000 μm range. Coal pulverizers and oil burner atomizers are examples of physical attrition and mechanical dispersion.

When the fuel particles are injected into the hot furnace area of the combustion process (Figure 2-3), most of the organic compounds are vaporized and oxidized in the gas stream. The fuel particles get smaller as the volatile matter leaves. The fuel particles are quickly reduced to only the incombustible matter (ash) and slow burning char composed of organic compounds. Eventually, most of the char will also burn, leaving primarily the incombustible material. As oxidation progresses, the fuel particles, which started as 100-1,000 μm particles, are reduced to ash and char particles that are primarily in the 1 to 10 μm range. This mechanism for particle formation can be termed combustion fuel burnout.

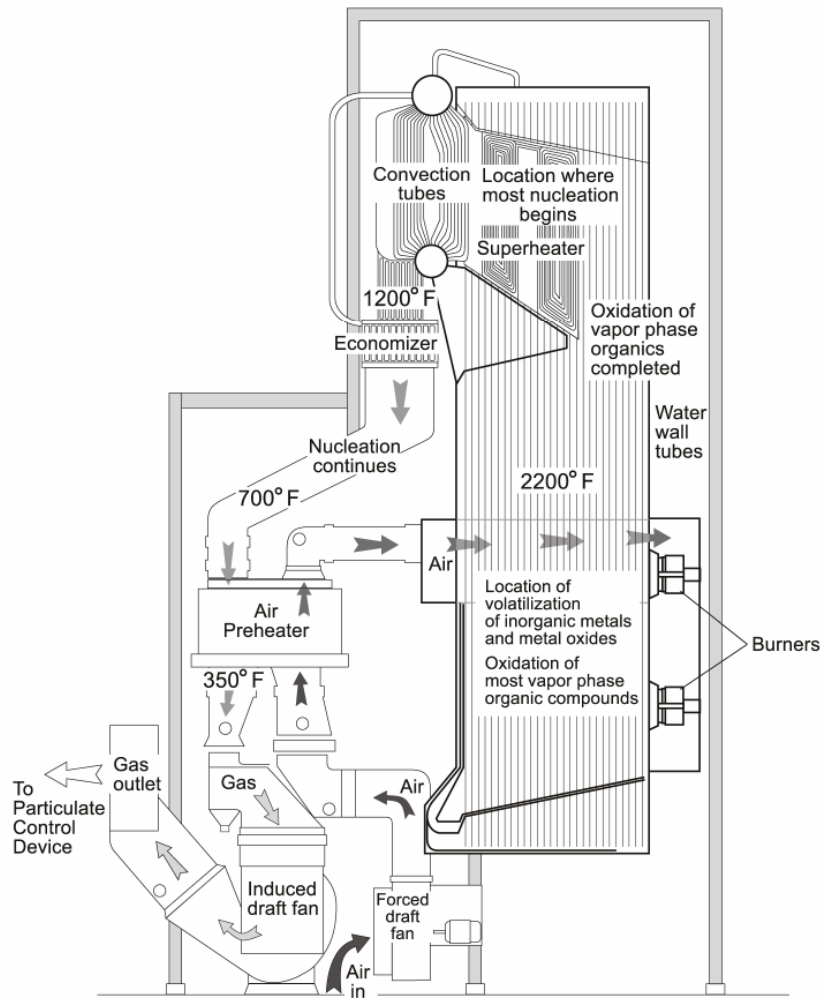


Figure 2-3. Combustion process

Homogeneous nucleation and heterogeneous nucleation involve the conversion of vapor phase materials to a particulate matter form. Homogeneous nucleation is the formation of new particles composed almost entirely of the vapor phase material. Heterogeneous nucleation is the accumulation of material on the surfaces of particles that have formed due to other mechanisms. In both cases, the vapor-containing gas streams must cool to the temperature at which nucleation can occur. The temperature at which vapors begin to condense is called the dew point, and it depends on the concentration of the vapors. The dew point increases with increases in the vapor concentration. Some compounds condense in relatively hot gas zones (>1,000°F), while others do not reach their dew point temperature until the gas stream cools below 300°F.

There are three main categories of vapor phase material that can nucleate in air pollution source gas streams: (1) organic compounds, (2) inorganic metals and metal compounds, and (3) chloride compounds. For example, in a waste incinerator organic vapor that has

volatilized from the waste due to the high temperature is generally oxidized completely to carbon dioxide and water. However, if there is a combustion upset, a portion of the organic compounds or their partial oxidation products remain in the gas stream as they leave the incinerator. These organic vapors can condense in downstream equipment. Volatile metals and metal compounds such as mercury, lead, lead oxide, cadmium, cadmium oxide, cadmium chloride, and arsenic trioxide can also volatilize in the hot incinerator. Once the gas stream passes through the heat exchange equipment used to produce steam, the organic vapors and metal vapors can homogeneously or heterogeneously condense. Generally, the metals and metal compounds reach their dew point first and begin to nucleate in relatively hot zones of the unit. The organic vapors and/or chloride compounds begin to condense in downstream areas of the process where the gas temperatures are cooler. These particles must then be collected in the downstream air pollution control systems. Homogeneous and heterogeneous nucleation generally creates particles that are very small, often between 0.05 and 1.0 μm .

Heterogeneous nucleation facilitates a phenomenon called *enrichment* in particles in the submicrometer size range. The elemental metals and metal compounds volatilized during high temperature operations (e.g., fossil fuel combustion, incinerator, and metallurgical processes) nucleate preferentially on these very small particles. This means that these particles have more of these materials than the very large particles leaving the processes. These small particles are described as enriched with respect to their concentration of metals and metal compounds. Heterogeneous nucleation contributes to the formation of particle distributions that have quite different chemical compositions in different size ranges.

Another consequence of heterogeneous nucleation is that the metals are deposited in small quantities on the surfaces of a large number of small particles (Figure 2-4). In this form, the metals are available to participate in catalytic reactions with gases or other vapor phase materials that are continuing to nucleate. Accordingly, heterogeneous nucleation also increases the types of chemical reactions that can occur as the particles travel in the gas stream from the process source and through the air pollution control device.

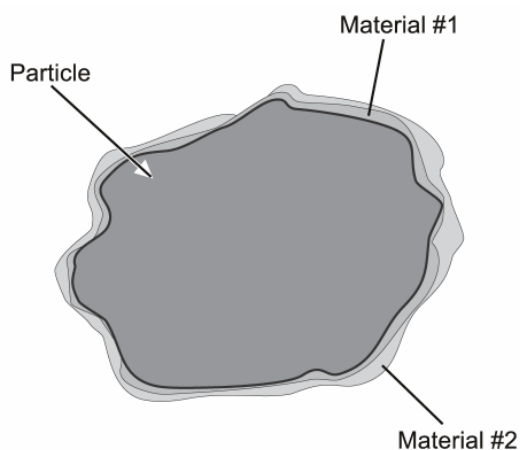


Figure 2-4. Heterogeneous nucleation

Some air pollution control systems use solids-containing water recycled from wet scrubbers to cool the gas streams. This practice inadvertently creates another particle formation mechanism that is very similar to fuel burnout. The water streams are atomized during injection into the hot gas streams. As these small droplets evaporate to dryness, the suspended and dissolved solids are released as small particles. The particle size range created by this mechanism has not been extensively studied; however, it probably creates particles that range in size from 0.1-2.0 μm . All of these particles must then be collected in the downstream air pollution control systems.

A summary of the particle size ranges generated by the different formation mechanisms is provided in Figure 2-5. Several particle formation mechanisms can be present in many air pollution sources. As a result, the particles created can have a wide range of sizes and chemical compositions.

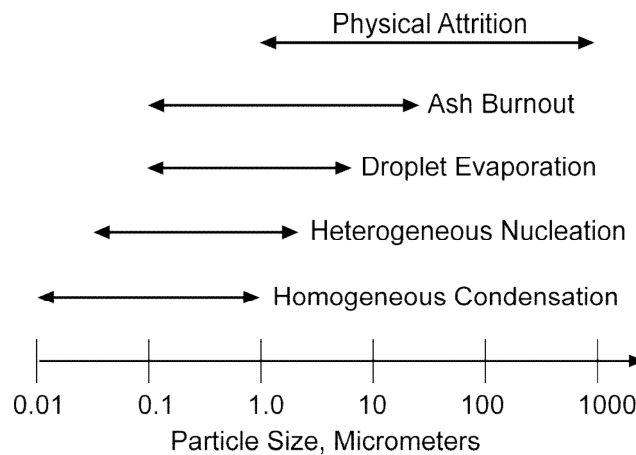


Figure 2-5. Approximate size distributions for various formation mechanisms

Primary and Secondary Particulate Matter

Particulate matter in the atmosphere can be divided into the following two categories:

- Primary particulate matter
- Secondary particulate matter

Primary particulate matter includes both: (1) material emitted directly into the atmosphere as particulate, and (2) condensable particulate matter formed quickly from condensed vapors.

Direct-emitted primary particulate emissions have always been of concern to air quality programs. Primary particulate matter can consist of particles less than 0.1 micrometer to more than 100 micrometers. Very large particles have the potential for a dust nuisance in the near vicinity of their emissions. Smaller particles become airborne and are transported, thereby contributing to particulate levels in the atmosphere, both within urban areas and over broader regions.

High molecular weight volatile organic compounds and sulfuric acid are two common examples of emissions that are gaseous at stack conditions, but which condense to form particulate matter. These materials pass through particulate matter control systems, including high efficiency devices, due to their vapor form in the stationary source gas stream. However, at ambient temperature the vapor phase material condenses in the ambient air to form particles measured by ambient sampling systems.

EPA stack sampling methods for particulate matter include methods for collecting direct emitted particles matter on a filter (Method 5) and for collecting condensable particulate matter by cooling the gas stream in impingers downstream of the filter (Method 202). Direct-emitted particulate matter is sometimes referred to as “filterable” or “front half” particulate matter, while condensable particulate matter is sometimes referred to as the “back half.” EPA emissions inventory reporting systems contain separate reporting of filterable and condensable particulate matter.

Secondary particulate matter refers to particles formed due to atmospheric reactions of gaseous precursors. Ammonium sulfate and ammonium nitrate are two common examples of material present in secondary particles formed by atmospheric reactions. These materials form over periods of hours to days as gaseous precursors in plumes and in large air masses move across the country. With the promulgation of the PM_{2.5} standard aimed at fine particles, there is increasing attention concerning secondary particulate matter. Secondary formation processes can result in the formation of new particles or the addition of material to pre-existing particles. The gases most commonly associated with secondary particulate matter formation include sulfur dioxide, nitrogen oxides, ammonia, and volatile organic compounds. Most of these gaseous precursors are emitted from anthropogenic sources; however, biogenic sources also contribute some nitrogen oxides, ammonia, and volatile organic compounds.

Sources of Particulate Matter

Primary PM is emitted from a wide variety of stationary sources, mobile sources and fugitive dust sources. Figure 2-6 displays national PM_{2.5} emissions contributions from various source types. Similar data for PM₁₀ indicate greater contributions from fugitive dust sources.

This course addresses industrial sources of both fine (PM_{2.5}) and coarse (PM₁₀ and greater than PM₁₀) particulate matter. The control devices discussed in subsequent chapters mitigated many of the industrial source categories in the above figure. It is important to note that in the near vicinity of an industrial source, the concentrations of PM_{2.5} in the air can be dominated by that source. In addition, that local source may have the potential to create a serious dust nuisance problem from particles too large to be airborne for any appreciable length of time.

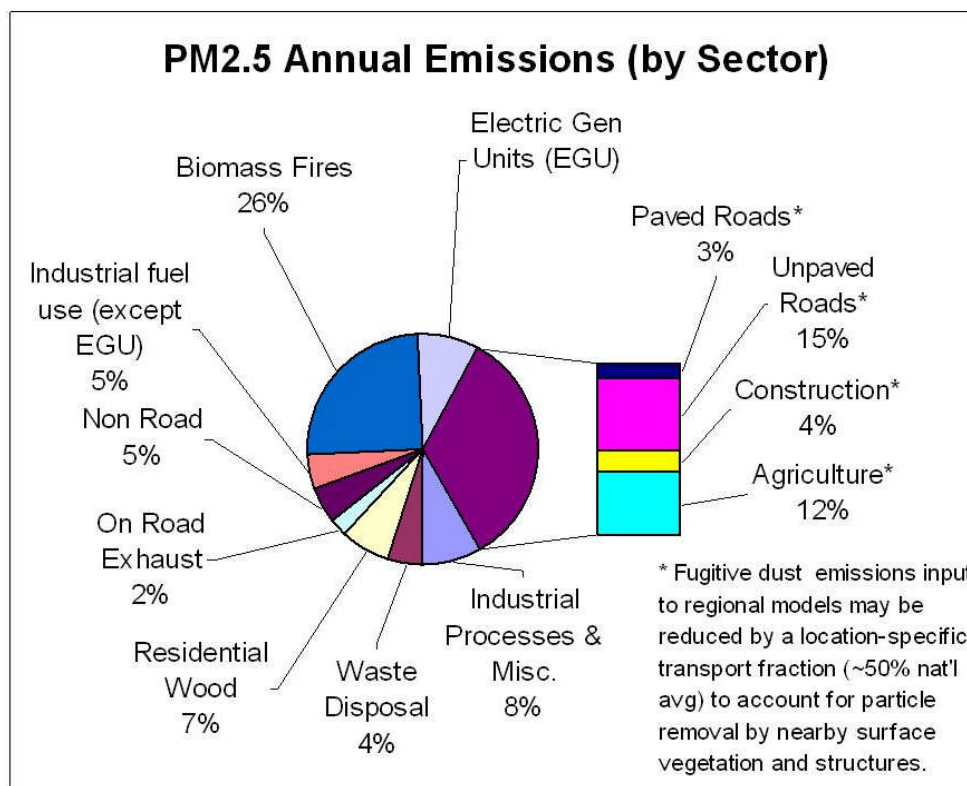


Figure 2-6. Source contributions to national annual PM_{2.5} emissions

Particulate Matter Regulation

Before the Clean Air Act

The regulation of particulate matter emissions dates back to the early stages of the industrial revolution. Even in the 1600s, people could see the relationship between particulate matter emissions and problems such as solids deposition, fabric soiling, material corrosion, and building discoloration. As technology and public awareness expanded, it became apparent that particulate matter emissions also contributed to certain types of lung disease and related illnesses. Particulate matter emissions were an important factor in the air pollution-related fatalities that occurred during a multi-day atmospheric inversion in Donora, Pennsylvania in 1948 and London in 1952-53. Since that time, particulate matter emissions have been identified as causal factors in many toxicological and epidemiological studies, and there continues to be a strong public demand for particulate matter control.

Conditions such as those shown in Figure 2-7 were common in the United States until particulate matter control devices were routinely required to be installed. Since the enactment of the Clean Air Act Amendments of 1970 (the first comprehensive Federal Clean Air law), many particulate control devices have been installed, and many new types of systems have been commercialized. Over time, particulate control requirements have become increasingly stringent as additional regulations have been developed, as more and

more equipment has been replaced by new sources subject to stringent new source standards, and as national standards for particles in outdoor air have been changed to reflect the latest scientific health studies.



Figure 2-7. Northeast U.S. community near a steel mill, 1967

The Clean Air Act

Most of the provisions in the Federal Clean Air Act were put into the Act in the Clean Air Amendments of 1970, 1977 and 1990. The Clean Air Act contains a number of ways to regulate particulate matter, including:

- National ambient air quality standards (NAAQS) for particulate matter.
- State Implementation Plans (SIPs), regulations developed by State and local air quality agencies and approved by EPA, that provide the emissions reductions needed to bring nonattainment areas (areas with monitored air quality above the NAAQS) into attainment”.
- New source performance standards (NSPS), national emissions standards for many source categories developed by EPA.
- Permitting requirements for new major-emitting sources (usually developed by State and local air agencies with EPA oversight) which provide for best available control technology (BACT) and lowest achievable emission rate (LAER).
- State permitting requirements for new sources.
- National emissions standards for hazardous air pollutants (NESHAP) which are required by the Clean Air Act to apply maximum achievable control technology (MACT).

- Implementation plans to protect visibility in certain federally protected scenic areas, including requirements to apply best available retrofit technology (BART) to certain older sources.
- Title V operating permits, which provide a single repository for all federally-enforceable requirements and which provide for periodic monitoring and compliance assurance monitoring.

National Ambient Air Quality Standards

Over time, the NAAQS for particulate matter have reflected the growing evidence of health problems caused by particles of smaller sizes. The first standards, published in 1971, were for total suspended particulate matter (TSP). Due to increasing concerns about the possible health and welfare effects of ambient particulate matter, regulatory agencies in the late 1960s began to measure the ambient concentrations of TSP using High-Volume (Hi-Vol) ambient samplers that provided a single concentration value for a 24-hour sampling period. Particulate matter that was sufficiently small to remain suspended in the atmosphere and captured in the sampling systems of the Hi-Vol samplers was defined as TSP. TSP included particles smaller than approximately 35-45 micrometers—approximately the diameter of a human hair.

In 1987, the USEPA revised the NAAQS for particulate matter to include only particles equal to or smaller than 10 micrometers (μm). This change was made to focus regulatory attention on those particles that are sufficiently small to penetrate into the respiratory system and, therefore, contribute to adverse health effects. Particles larger than 10 μm are effectively filtered out by the nose and upper respiratory tract. Therefore, only particles equal to or smaller than 10 μm were measured in evaluating ambient air quality levels with respect to the NAAQS. These particulate matters are collectively designated as PM_{10} to differentiate them from TSP.

In 1997, the USEPA added a new NAAQS applicable to $\text{PM}_{2.5}$, that is, particulate matter equal to or less than 2.5 μm . The USEPA concluded that the $\text{PM}_{2.5}$ NAAQS was needed in response to health effects research indicating that particulate matter in this size category was most closely associated with adverse health effects. Many areas of the country showed measured exceedences of the 15 $\mu\text{g}/\text{m}^3$ annual standard, but only a few areas exceeded the 24-hour standard of 65 $\mu\text{g}/\text{m}^3$. Small size increases the probability that the particles will penetrate deeply into the respiratory tract and be retained. In 2006, the USEPA completed a review of the 1997 standards and reduced the 24-hour standard from 65 $\mu\text{g}/\text{m}^3$ to 35 $\mu\text{g}/\text{m}^3$.

The NAAQS for PM_{10} and $\text{PM}_{2.5}$ are given in Table 2-1. The TSP NAAQS was retired in 1987 when the PM_{10} standard was first adopted. Table 2-1 reflects the 2006 revision of the 24-hour standard.

Pollutant	Primary Standard		Secondary Standard	
	Type of Average	Concentration	Type of Average	Concentration
PM ₁₀	Annual Arithmetic Mean	50 µg/m ³	Same as Primary Standard	
	24-hour ^a	150 µg/m ³	Same as Primary Standard	
PM _{2.5}	Annual Arithmetic Mean ^b	15 µg/m ³	Same as Primary Standard	
	24-hour ^c	35 µg/m ³	Same as Primary Standard	

^anot to be exceeded more than once per year on average over a three year period

^bthree-year average of the annual average

^cdetermined from the 98th percentile, averaged over three years

As noted above different particle formation mechanisms lead to different particle sizes. Distinct tri-modal ambient particle size distributions that are generally observed in research studies. As indicated in Figure 2-8, there are ultrafine particles smaller than 0.1 micrometer (nuclei mode), fine particles approximately 0.1 to 2.5 micrometers (accumulated and nuclei modes), and coarse particles larger than 2.5 micrometers.

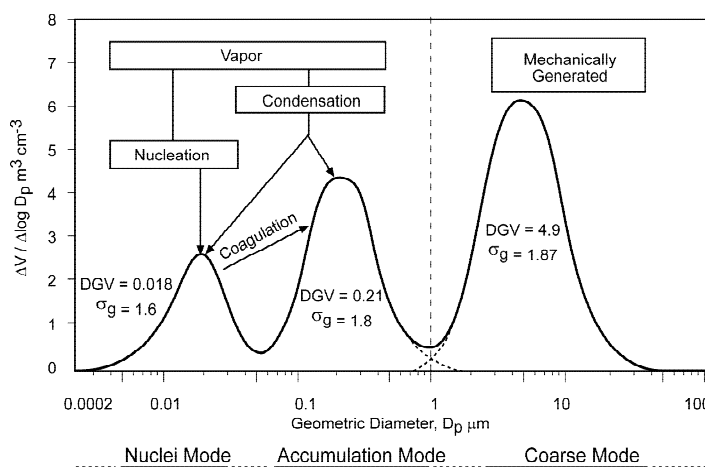


Figure 2-8. Typical ambient air particulate matter size distribution

The particles in the ultrafine and fine distributions are formed mainly by chemical reactions between gases in the atmosphere. The particles in the coarse distribution are formed primarily by physical grinding (attrition) and by combustion burnout of ash particles. Current particulate matter standards do not have any special treatment of ultrafine particles.

State Implementation Plans

Control strategies for the achievement of the original TSP NAAQS were developed and adopted as part of the State Implementation Plans (SIPs) required by the Clean Air Act Amendments of 1970. These control strategies were designed by each state and local regulatory agency having areas above the NAAQS limits. Particulate matter emission

regulations were adopted by the states and local agencies to implement the SIP control strategies and were approved by EPA.

These 1970's particulate matter emission limitations took many regulatory forms, many of which are still in effect today. Regulations included: (1) fuel burning regulations with allowable lb/MMBTU limits that became more stringent with increased boiler capacity, (2) process-weight-based particulate matter equations for which an allowable emissions rate is calculated for a given process operating rate, and (3) opacity limitations.

Opacity is a measure of the extent to which the particulate matter emissions reduce the ambient light passing through the plume, as indicated in Figure 2-9. Opacity is a convenient indirect indicator of particulate matter emissions and can be determined by a trained visible emissions observer without the need for special instruments. Opacity can also be determined by continuous monitors. Generally, opacity is a separately enforceable emission characteristic. As PM limits become more stringent, EPA and States have greater concerns with reliance on opacity as a surrogate and have expressed a greater preference for methods that produce continuous measurement of PM stack concentrations.

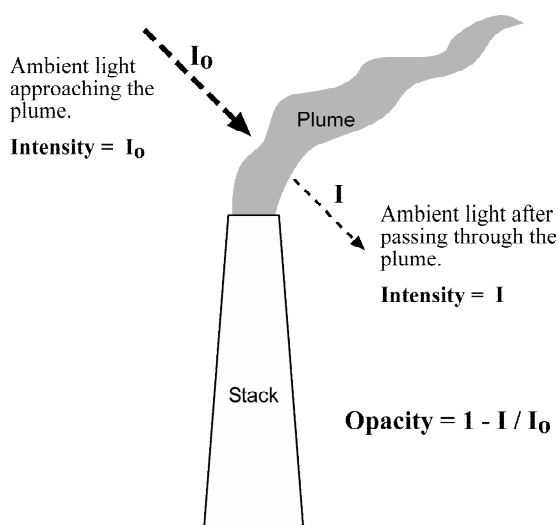


Figure 2-9. Opacity of a plume emitted by a stationary source

In addition to regulations applying to particulate matter emitted from stacks and vents, the regulations included in the SIPs applied to fugitive particulate matter emissions. As illustrated in Figure 2-10, fugitive emission sources include sources where a portion of the particulate matter generated escapes collection hoods and is emitted directly to the atmosphere. Fugitive emissions also include unpaved roads, storage piles, dust from unpaved construction sites, and other similar dust sources that cannot be captured by hoods and controlled by air pollution control systems.

Fugitive emission regulations were adopted to control process related fugitive emissions. Due to the diversity of these sources and the difficulty in measuring fugitive emissions, regulations have taken many forms. Regulations include but are not limited to (1) required

work practices, (2) visible emission (opacity) limits at plant boundary lines, and (3) visible emission limits at the process source.



Figure 2-10. Fugitive particulate matter escaping a hood

During the late 1980s after the PM_{10} standards were published, EPA adopted a PM_{10} policy dividing all areas of the country into three categories based upon their probability of violating the standards. The Clean Air Act amendments of 1990 set into motion substantially modified provisions, including the formal designation of nonattainment areas. The 1990 amendments also included certain minimum requirements for the content of PM_{10} SIPs. It also required EPA to develop technology documents. This included guidance documents for reasonable available control measures (RACM) and best available control measures (BACM) for urban fugitive dust, residential wood combustion and prescribed silvicultural and agricultural burning. Many of the areas of the United States which violated the 1987 PM_{10} standards were in the western United States, with some areas in the industrialized eastern United States. Because PM_{10} includes both coarse and fine particles, the overall mass of PM_{10} is usually dominated by coarse particles. Accordingly, the PM_{10} SIPs gave considerable attention to coarse particle fugitive dust measures in most areas. Other areas of attention included woodstoves for certain areas of the west, particularly areas in mountain valleys. For a few areas, such as the San Joaquin Valley and Los Angeles, secondarily-formed particles from gases were important contributors.

In contrast to PM_{10} , many of the areas exceeding the 1997 $PM_{2.5}$ standards are in the eastern United States. For $PM_{2.5}$, which includes only fine particles, both primary and secondarily formed particles from gaseous precursors are important as shown in Figure 2-11. Primary $PM_{2.5}$ consists of elemental carbon (soot) and organic matter (often referred to as “organic carbon”) emitted from cars, trucks, industrial sources, forest fires, and burning waste, and crustal material from unpaved roads, stone crushing, construction sites, and metallurgical operations such as steel mills and foundries. Fugitive dust sources, which primarily emit coarse particles, tend to be much less important for $PM_{2.5}$ than for PM_{10} . Secondary $PM_{2.5}$ includes: (1) sulfates formed from sulfur dioxide emissions from power plants and industrial facilities, (2) nitrates formed from nitrogen oxide emissions from cars, trucks, power plants, and other combustion sources, and (3) organic carbon formed from reactive organic gas emissions from cars, trucks, industrial facilities, solvent usage, forest fires, and biogenic sources such as trees. The due date for SIPs addressing $PM_{2.5}$ nonattainment areas (under the

1997 standards) is April 2008. For stationary sources, the SIPs will need to address Clean Air Act requirements for RACT and RACM for sources located within nonattainment areas.

Automobiles, Power Generation, and Other Sources Contribute to Fine Particle Levels

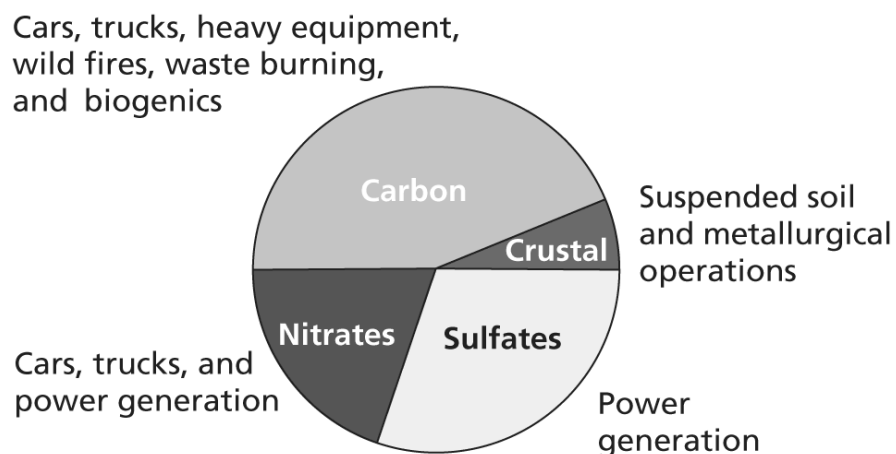


Figure 2-11. Source contributions to ambient PM_{2.5} levels (including contributions from secondary precursors)

Likely, PM_{2.5} SIPs will need to focus on a mix of regional and local strategies and control measures. In the troposphere, coarse and fine particles behave in different ways. Large coarse particles may settle out from the air more rapidly than fine particles and usually will be found relatively close to their emission sources. Fine particles, however, can be transported long distances by wind and weather and can be found in the air thousands of miles from where they were formed. Figure 2-12 provides estimates of regional versus local contributions for a number of U.S. cities.

EPA's 2006 revisions to the PM_{2.5} standards maintained the previous annual average standard of 15 µg/m³, but lowered the 24-hour standard from 65 µg/m³ to 35 µg/m³. Very few areas violated the 65 µg/m³ standard, but a number of areas show monitored violations of the lower standard. Many of the nonattainment areas added by the revisions are in the western United States. The SIPs addressing geographic areas violating the revised standards, but which did not violate the previous standards, will be due in approximately 2013.

New Source Performance Standards and New Source Permitting

The Clean Air Act Amendments of 1970 required EPA to develop emission limitations that would apply to new sources on a nationwide basis. These new source-oriented standards were titled New Source Performance Standards (NSPS). These standards, adopted by the USEPA for many source categories, are based on air pollution control systems that represent the best demonstrated technology for a particular type of industrial source category. For particulate matter, NSPS will include mass emission standards (variously expressed as lb PM per ton of process rate, grains/dry standard cubic foot stack concentration, or pounds per

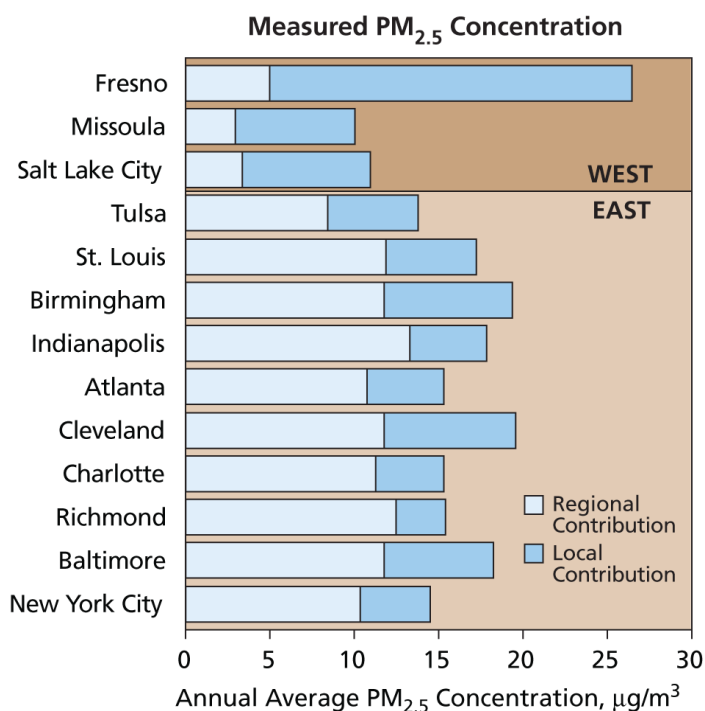


Figure 2-12. Regional and local contributions to PM_{2.5}

million BTU for combustion sources), and often will also include opacity limits and continuous opacity monitoring requirements. The NSPS emissions limits appear in the Code of Federal Regulations in 40 CFR Part 60. Examples of regulated source categories are listed in Table 2-2.

Table 2-2. Examples of NSPS with PM limits	
Source Category	Subpart
Industrial-Commercial-Institutional Steam Generating Units	Db
Small Industrial-Commercial-Institutional Steam Generating Unit	Dc
Large Municipal Waste Combustors	Eb
Hospital/Medical/Infectious Waste Incinerators	Ec
Portland Cement Plants	F
Hot Mix Asphalt Facilities	I
Petroleum Refineries	J
Secondary Brass and Bronze Production Plants	M
Secondary Emissions From Basic Oxygen Process Steelmaking	Na
Sewage Treatment Plants	O
Kraft Pulp Mills	BB
Glass Manufacturing Plants	CC

Source Category	Subpart
Grain Elevators	DD
Lime Manufacturing Plants	HH
Asphalt Processing and Asphalt Roofing Manufacture	UU
New Residential Wood Heaters	AAA

The Clean Air Act Amendments of 1977 included provisions for case-by-case permit reviews for sources in attainment areas, referred to as the Prevention of Significant Deterioration (PSD) program, and in nonattainment areas, referred to as the Nonattainment New Source Review (NSR) program. For both PSD and nonattainment NSR programs, proposed new sources must exceed major source thresholds for the program to apply. PSD and NSR permits are almost always issued by State and local air quality agencies, and require stringent technology levels to be approved. PSD permits must meet best available control technology (BACT) while nonattainment NSR permits must meet a somewhat more stringent level called the lowest achievable emission rate (LAER). Because PSD and NSR permits are a case-by-case review based upon up-to-date technology information, the resulting emissions limits tend to be more stringent than NSPS standards.

Proposed new emitting equipment that would emit less than major sources levels may require a minor source permit from State and local agencies. The permit will ensure that applicable State and federal regulations would be met.

National Emissions Standard for Hazardous Air Pollutants

The Clean Air Act of 1970 authorized the promulgation by EPA of regulations for pollutants that are considered highly toxic or hazardous. This set of regulations is titled National Emission Standards for Hazardous Air Pollutant Sources (NESHAPS). The Clean Air Act Amendments of 1990 required a major revision and expansion of these regulations. The 1990 Amendments specified 189 specific pollutants as hazardous. This list includes many compounds and elements such as heavy metals that are generally in particulate matter form. Title III provisions of the CAAA of 1990 require that EPA develop a list of source categories emitting HAPs, and develop an emissions standard for each category. Notably, NESHAP standards affect both new and existing sources, in contrast to NSPS/BACT/LAER limits which affect only new sources. Major-emitting HAP sources subject to the regulation are required to install Maximum Achievable Control Technology (MACT) for that source category. For existing sources, MACT standards must be as stringent as a “floor” defined by the best performing 12 percent of the category. Especially for the existing source population, MACT standards may be a driver for further control of particulate matter. While the MACT regulations are not directed at the control of particulate matter per se, they will require the high efficiency control of the hazardous air pollutants that may be a constituent of the particulate matter. A number of NESHAP standards use PM as a surrogate emissions limit rather than emissions limits for individual HAPs.

Visibility

One of the most obvious effects of particulate pollution is visibility impairment, which occurs when fine particles scatter and absorb light, creating a haze that limits the distance we can see. The Clean Air Act contains provisions providing for protection of visibility in a number of scenic areas collectively referred to as Class I areas. In 1999, EPA published a regulation requiring States to submit implementation plans that provide for reasonable progress towards the Act's goal of natural background conditions. Another requirement of the regional haze rule is that older (i.e., too old to be covered by PSD or nonattainment NSR), major-emitting sources in 26 source categories meet a requirement to install best available retrofit technology (BART). Implementation plans are required by the end of 2007, and periodic implementation plans are due every 10 years thereafter.

Title V Operating Permits

Title V of the Clean Air Act requires all major sources and some other types of sources to obtain operating permits. Approximately 16,000 Title V permits have been issued by state permitting agencies and several hundred by EPA regions to facilities on tribal lands. A Title V permit includes every federally-enforceable air pollution requirement that applies to a particular facility. A federally-enforceable requirement stems from the Clean Air Act and includes all federal and state air quality regulations that apply to a facility. After a Title V permit is issued for a facility, a member of the public who wants to know which air pollution requirements apply to that facility can simply request to see the facility's Title V permit or obtain it online.

Every year, a representative from each facility with a Title V permit must sign a statement certifying whether the facility is in compliance with its permit. For example, if the permit requires continuous monitoring and a company failed to perform monitoring for several days, this failure would show up on this compliance certification. The compliance statement is based on records, monitoring and other information that indicates whether the company has complied with its permit requirements. There are stiff fines--or even criminal charges--for a false statement.

Title V permits are required to add monitoring where the underlying requirement (1) requires no monitoring, (2) requires only a start-up test, or (3) does not specify a monitoring frequency. This is called periodic monitoring, and it applies to control devices and uncontrolled units with air pollution control requirements. Periodic monitoring is created case-by-case, taking into account factors such as the margin of compliance, emissions variability and frequency of operation. For example, for an uncontrolled glass furnace with a 20% opacity standard and a 0.04 gr/scf PM emission limit, a state might determine that periodic monitoring is a weekly visible emission reading for the opacity standard and an annual stack test for the emission limit.

Title V permits must be renewed and updated every 5 years to incorporate any new requirements. As of 2007, almost all Title V permits have been issued, and several thousand have been renewed. Upon the first renewal, many Title V permits must include the

compliance assurance monitoring (CAM) requirements. CAM requirements are found in 40 CFR Part 64, and CAM applies only to relatively large units at major sources that have underlying federal or state requirements. For example, a large boiler subject to a NSPS and using a baghouse or ESP could be subject to CAM. CAM does not apply to facilities subject to MACT requirements because monitoring for MACT standards is presumed to meet CAM. CAM monitoring is proposed by the facility in its permit application and if approved by the state, incorporated into the Title V permit. CAM is determined case-by-case and relies on monitoring of representative parameters of a control device, such as pressure drop and liquid flow for a scrubber or temperature for a thermal oxidizer. Typically the indicator ranges for the parameters are set by testing. If parameter ranges are exceeded, this is not necessarily a violation, provided the facility takes steps to correct the problem.

This page intentionally left blank

Review Questions

1. What is total suspended particulate matter?
 - a. Particulate matter measured in the ambient air having a size less than approximately 1,000 micrometers
 - b. Particulate matter measured in the ambient air having a size less than approximately 100 micrometers
 - c. Particulate matter measured in the ambient air having a size less than approximately 45 micrometers
 - d. Particulate matter measured in the ambient air having a size less than approximately 10 micrometers
 - e. None of the above

2. What are ultrafine particles?
 - a. Particulate matter measured in the ambient air having a size less than approximately 10 micrometers
 - b. Particulate matter measured in the ambient air having a size less than approximately 0.1 micrometers
 - c. Particulate matter measured in the ambient air having a size less than approximately 0.01 micrometers
 - d. Particulate matter measured in the ambient air having a size less than approximately 0.001 micrometers
 - e. None of the above

3. Particles that form by homogeneous condensation and/or heterogeneous nucleation are mainly in which size range?
 - a. Greater than 10 micrometers
 - b. Between 1 and 10 micrometers
 - c. Between 0.1 and 1 micrometers
 - d. Between 0.01 and 0.1 micrometers
 - e. None of the above

4. What types of mechanisms are responsible for the formation of condensable particulate matter? Select all that apply.
 - a. Condensation of vapor phase material emitted from stationary sources
 - b. Condensation of organic vapors emitted from stationary sources
 - c. Atmospheric reactions involving sulfur dioxide and ammonia
 - d. Grinding of one material against another (attrition)
 - e. All of the above

5. The accurately measured ambient concentration of PM_{10} is 78 micrograms per cubic meter. Which of the following could be true?
 - a. The ambient concentration of $PM_{2.5}$ is 125 micrograms per cubic meter.
 - b. The ambient concentration of $PM_{2.5}$ is 26 micrograms per cubic meter.
 - c. The ambient concentration of $PM_{2.5}$ is 158 micrograms per cubic meter.
 - d. The ambient concentration of total suspended particulate matter is 65 micrograms per cubic meter.

6. Which compounds are known to participate in atmospheric reactions that result in the formation of secondary particulate matter? Select all that apply.
 - a. Sulfur dioxide
 - b. Nitrogen oxides
 - c. Ammonia
 - d. All of the above

Review Question Answers

1. What is total suspended particulate matter?
 - c. Particulate matter measured in the ambient air having a size less than approximately 45 micrometers
2. What are ultrafine particles?
 - b. Particulate matter measured in the ambient air having a size less than approximately 0.1 micrometers
3. Particles that form by homogeneous condensation and/or heterogeneous nucleation are mainly in which size range?
 - c. Between 0.1 and 1 micrometers
4. What types of mechanisms are responsible for the formation of condensable particulate matter? Select all that apply.
 - a. Condensation of vapor phase material emitted from stationary sources
 - b. Condensation of organic vapors emitted from stationary sources
 - c. Atmospheric reactions involving sulfur dioxide and ammonia
5. The accurately measured ambient concentration of PM_{10} is 78 micrograms per cubic meter. Which of the following could be true?
 - b. The ambient concentration of $PM_{2.5}$ is 26 micrograms per cubic meter.
6. Which compounds are known to participate in atmospheric reactions that result in the formation of secondary particulate matter? Select all that apply.
 - d. All of the above

This page intentionally left blank

References

Nizich, S.V., A.A. Pope, L.M. Driver and Pechan-Avanti Group, *National Air Pollutant Emission Trends, 1900-1998*, EPA-454/R-00-002, March 2000.

This page intentionally left blank.

CHAPTER 3

PARTICLE SIZING

Particle size distribution is one of the most important factors affecting the performance of particulate matter control systems. Determination of the size distribution is often necessary in order to prepare equipment design specifications, evaluate expected performance of new systems, or to analyze the actual performance of existing systems. Several methods are used to obtain particle size data from industrial sources. This chapter will briefly describe a number of these methods and their operating principles. The mathematical treatment of collected data will also be presented.

Particle Size

The range of particle sizes of concern in air pollution control is extremely broad. Some of the droplets collected in the mist eliminators of wet scrubbers and the solid particles collected in large diameter cyclones are as large as raindrops. Some of the small particles created in high temperature incinerators and metallurgical processes are so small that more than 500 of them could be lined up across the diameter of a human hair.

To appreciate the difference in sizes, it is helpful to compare the diameters, areas, and volumes of a variety of particles. Assume that all of the particles are simple spheres. The raindrop shown in Figure 3-1 is 500 μm in diameter. The term *micrometer* (μm) simply means one millionth of a meter. One thousand micrometers are equivalent to 0.1 cm or 1.0 mm. In some texts, the term *micron* is often used as an abbreviation for micrometer.

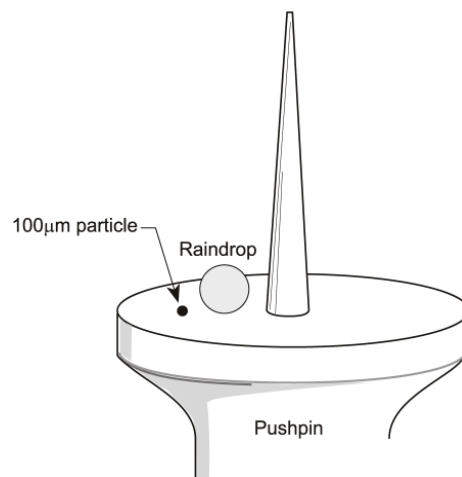


Figure 3-1. Very large particle and a raindrop

A 100 μm particle shown next to the raindrop in Figure 3-1 looks like a small speck compared to the pushpin. However, both the raindrop and the 100 μm particle are on the large end of the particle size range of interest in air pollution control. Particles in the range of 10-100 μm are also on the large end of the particle size scale of interest in this course.

The particle size range between 1 and 10 μm is especially important in air pollution control. A major fraction of the particulate matter generated in some industrial sources is in this size range. Furthermore, all particles less than or equal to 10 μm are considered respirable and are regulated as PM_{10} . Figure 3-2 shows a comparison of 1, 10, and 100 μm particles. It is apparent that there is a substantial difference in size between these particles.

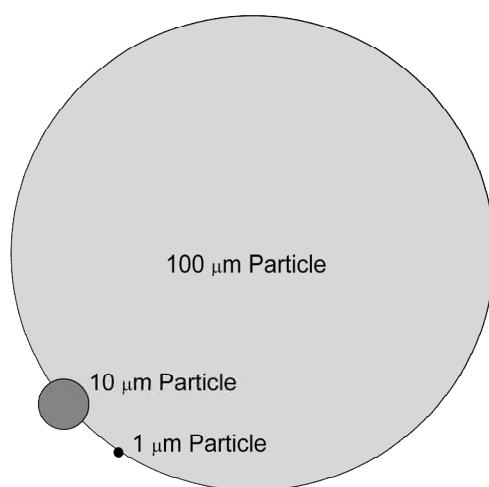


Figure 3-2. 1 μm and 10 μm particles compared to a 100 μm particle

Particles in the range of 0.1 to 1.0 μm are important in air pollution control because they can represent a significant fraction of the particulate matter emissions from some types of industrial sources and because they are relatively hard to collect. Some industrial processes, such as combustion and metallurgical sources, generate particles in the range of 0.01 to 0.1 μm . These sizes are approaching the size of individual gas molecules, which are in the range of 0.0002 to 0.001 μm . However, particles in this size range tend to agglomerate rapidly to yield particles in the greater than 0.1 μm range. Accordingly, very little of the particulate matter entering an air pollution control device remains in the size range of 0.01 to 0.1 μm .

Throughout this manual, small particles are defined as less than 1 μm , moderately-sized particles are classified as 1 to 10 μm , and large particles are classified as 10 to 1,000 μm . The volumes and surface areas of particles over this size range are shown in Table 3-1.

The data in Table 3-1 indicate that 1,000 μm particles are more than 1,000,000,000,000 times (one trillion) larger in volume than 0.1 μm particles. As an analogy, assume that a 1,000 μm particle was a large domed sports stadium. A basketball in this stadium would be equivalent

to a 5 μm particle. Approximately 100,000 spherical particles of 0.1 μm diameter would fit into this 5 μm basketball. The entire 1,000 μm stadium is the size of a small raindrop. Particles over this extremely large size range of 0.1 to 1,000 μm are of interest in air pollution control.

Diameter (μm)	Volume (cm^3)	Area (cm^2)
0.1	5.23×10^{-16}	3.14×10^{-10}
1.0	5.23×10^{-13}	3.14×10^{-8}
10.0	5.23×10^{-10}	3.14×10^{-6}
100.0	5.23×10^{-7}	3.14×10^{-4}
1,000.0	5.23×10^{-4}	3.14×10^{-2}

Particle size itself is difficult to define in terms that accurately represent the types of particles. This difficulty stems from the fact that particles exist in a wide variety of shapes, not just as spheres as shown earlier. The photomicrograph shown in Figure 3-3 has a variety of spherical particles and irregularly shaped particles. For spherical particles, the definition of particle size is easy--it is simply the diameter. For the irregularly shaped particles, size can be defined in a variety of ways. For example, when measuring the size of particles on a microscope slide, size can be based on the diameter of the particle parallel to the microscope scan that divides the particle into equal areas (Martin's diameter) or the mean length between two tangents on opposite sides of the particle that are perpendicular to the fixed direction of the microscope scan (Ferret's diameter).

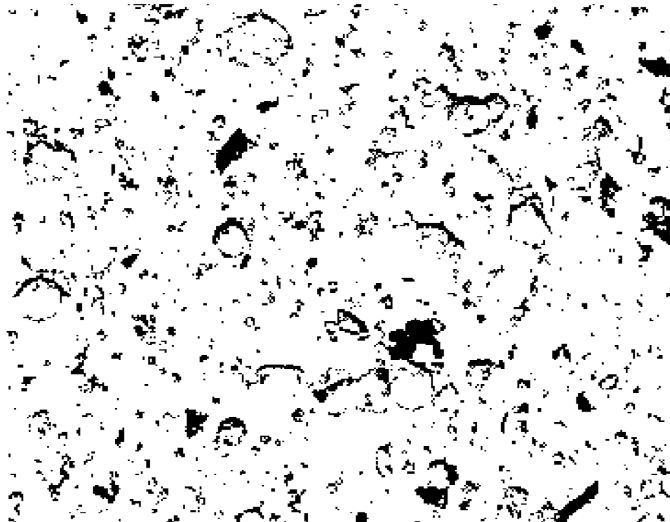


Figure 3-3. Photomicrograph of coal fly ash (reprinted courtesy of Research Triangle Institute)

Neither of these microscopically based size definitions, however, is directly related to how particles behave in a fluid such as air. The particle size definition that is most useful for evaluating particle motion in a fluid is termed the *aerodynamic diameter*. For all particles greater than 0.5 μm , the aerodynamic diameter can be approximated by:

$$d_p = d\sqrt{\rho_p C_c} \quad (3-1)$$

where:

d_p = aerodynamic particle diameter (μm)

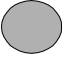
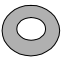

d = physical diameter (μm)

ρ_p = particle density (g/cm^3)


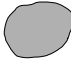

C_c = Cunningham slip correction

The Cunningham slip correction accounts for particle motion through a non-continuous medium and become increasingly more significant as the particle diameter decreases below about 3 μm . Calculation of the Cunningham slip correction factor will be discussed in Chapter 4.

Aerodynamic particle diameter is determined by inertial sampling devices such as the cascade impactor, which is discussed later in this chapter. Particles that appear to be different in physical size and shape can have the same aerodynamic diameter, as illustrated in Table 3-2. Conversely, as illustrated in Table 3-3, some particles that appear to be visually similar can have somewhat different aerodynamic diameters.

	Solid sphere	$\rho_p = 2.0 \text{ g}/\text{cm}^3$ $d = 1.4 \mu\text{m}$	$d_p = 2.0 \mu\text{m}$
	Hollow sphere	$\rho_p = 0.50 \text{ g}/\text{cm}^3$ $d = 2.80 \mu\text{m}$	
	Irregular shape	$\rho_p = 2.3 \text{ g}/\text{cm}^3$ $d = 1.3 \mu\text{m}$	

The term *aerodynamic diameter* is useful for all particles including the fibers and particle clusters shown in Figure 3-4. The aerodynamic diameter provides a simple means of categorizing the sizes of particles with a single dimension and in a way that relates to how particles move in a fluid. Unless otherwise noted, particle size is expressed in terms of aerodynamic diameter throughout the remainder of this manual.

	$\rho = 1.0 \text{ g/cm}^3$ $d = 2.0 \text{ }\mu\text{m}$	$d_p = 2.0 \text{ }\mu\text{m}$
	$\rho = 2.0 \text{ g/cm}^3$ $d = 2.0 \text{ }\mu\text{m}$	$d_p = 2.8 \text{ }\mu\text{m}$
	$\rho = 3.0 \text{ g/cm}^3$ $d = 2.0 \text{ }\mu\text{m}$	$d_p = 3.5 \text{ }\mu\text{m}$

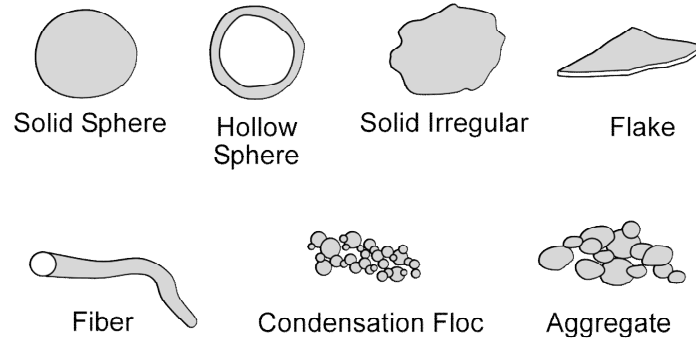


Figure 3-4. Different shapes of particles

Particle Size Measurement

Several alternative methods are used to evaluate the size distribution of particulate matter in industrial gas streams. An ideal particle measuring device would be able to do the following:

- Measure the exact size of each particle
- Determine the composition of each particle
- Report real-time data instantaneously

It would be an extremely difficult task to produce such an instrument. At this time, there are devices that incorporate only one or two of these ideal functions. In this section, various sizing techniques will be examined and compared to such an ideal device, listing advantages and disadvantages of each. While this discussion is not intended to be exhaustive, it will review the more commonly employed methods.

Microscopy

Various types of microscopy analyses can be performed on filters or slides that have been exposed to the gas stream. The representativeness of the sample depends in part on the characteristics of the sampling equipment and in part on the adequacy of the sampling procedures. It is important to minimize the sampling times to avoid overloading the surface. Particles should be deposited as a single layer to the extent possible. Sampling times are usually in the range of one to five minutes.

There are several common types of microscopic analyses used to evaluate particle size. Polarizing light microscopy (PLM) uses visible light that is focused on the particle and magnified in a set of lenses mounted in a conventional microscope (Figure 3-5). With the appropriate lenses and sample preparation techniques, PLM analyses can be used to size particles as small as 1 micrometer. Generally speaking, the chemical composition of the particle can not be determined by using an optical microscope. However, a subsequent chemical analysis can be performed on the sample.

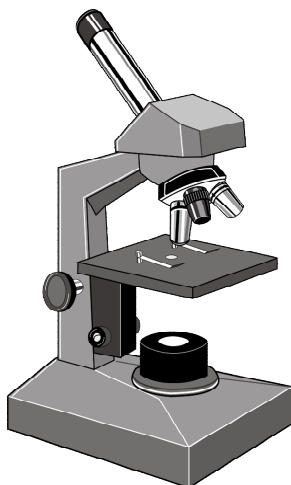


Figure 3-5. Optical microscope used for PLM analyses

The size of a particle is estimated by comparing each particle to a scale in the eyepiece, usually calibrated to micrometers. Each particle, presented in a fixed area of the eyepiece, is sized and tallied into a number of size categories. The number of particles sized may range from 100 to several thousand per sample, depending on the accuracy desired. Typically, 400 or more particles per filter sample section are individually counted to compile a particle size distribution estimate. This method can be time consuming and extremely tedious. Training is needed to properly identify and size particles using this technique.

The particles are usually collected by deposition on a glass slide or filter and later analyzed by a microscope in the lab. In general, size distributions determined from particles collected in the field and transported to the lab must be viewed with caution. First of all, it is difficult to collect a truly representative sample, and then it is almost impossible to maintain the original size distribution while transferring the samples to the laboratory. For example, it is

not known whether agglomerates seen on the sample were agglomerates in the gas stream or existed as separate particles. As a result, methods that involve analysis of bulk samples generally overestimate particle size. In spite of the limitations of the microscopic method, this method is useful in the determination of some properties of interest.

Scanning electron microscopy (SEM) can provide greater magnification of the particles than with PLM. With SEM, it is possible to resolve particles as small as 0.001 micrometers. Furthermore, an electron beam microprobe can be used to obtain elemental chemical analyses of individual small particles and even localized areas of large particles. These electron beam analyses are usually termed *energy dispersive x-ray spectroscopy* or EDX. As in the case with PLM, particle size distributions determined by SEM involve the comparison of the projected area of the particle with a calibrated graticule mounted into the viewing port of the SEM.

Optical Counters

Optical particle counters have not been widely used for particle sizing because they cannot be directly applied to the stack exhaust gas stream. The sample must be extracted, cooled, and diluted before entering the counter. This procedure must be done with extreme care to avoid introducing serious errors in the analyses. A major benefit of an optical counter is the ability to observe emission (particle) fluctuations on a real time, instantaneous basis. Particles as small as 0.3 μm can be determined with an optical counter.

Optical particle counters work on the principle of light scattering. Each particle in a continuously flowing sample stream passes through a small illuminated viewing chamber. Light scattered by the particle is observed by the photodetector during the time the particle is in the viewing chamber (Figure 3-6). The intensity of the scattered light is a function of particle size, shape, and index of refraction. Optical counters give reliable particle size information only when one particle is in the viewing chamber at a time. The simultaneous presence of more than one particle can be interpreted by the photodetector as a larger sized particle. This error can be minimized by maintaining sample dilution ratios to ensure less than 300 particles per cubic centimeter.

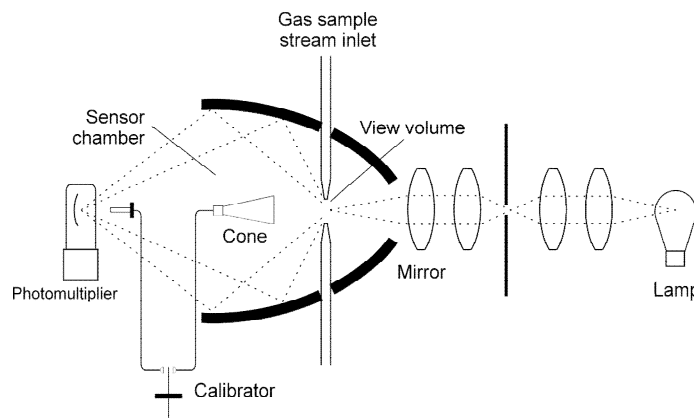


Figure 3-6. Optical particle counter

A drawback of the optical counter is the dependence of the instrument calibration on the index of refraction and the shape of the particle. Errors in counting can also occur due to the presence of high concentrations of very small particles, which are sensitive to the light wavelength used.

Bahco Analyzer

The Bahco analyzer (Figure 3-7) uses centrifugal force to separate particles ranging in size from 1 to 60 μm . A weighed sample, usually 5 grams, is introduced into a rotating gas stream. The larger particles move to the wall of the chamber and are separated. The rotational speed is then increased in steps in order to separate smaller and smaller size fractions. The separated size fractions are weighed to determine the mass in each size range. Chemical analysis could also be done on each size fraction.

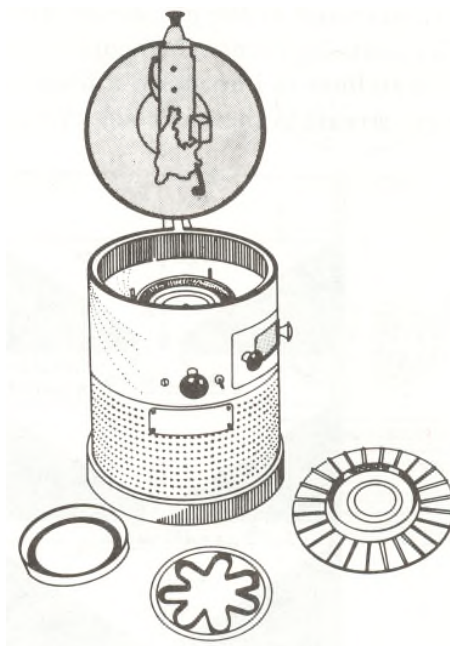


Figure 3-7. Bahco analyzer

The Bahco provides information on aerodynamic particle size. However, because the analysis is performed on a bulk sample, it suffers from the same agglomeration related problems discussed for microscopy and, likewise, tends to overestimate particle size.

Electrical Aerosol Analyzer

The electrical aerosol analyzer (EAA) is a submicrometer particle size measuring device that was commercially developed at the University of Minnesota. The EAA uses an electrical field to separate particles ranging in size from 0.003 to 0.5 μm on the basis of their mobility, a diffusional property that increases as the particle size decreases. One type of EAA is shown in Figure 3-8.

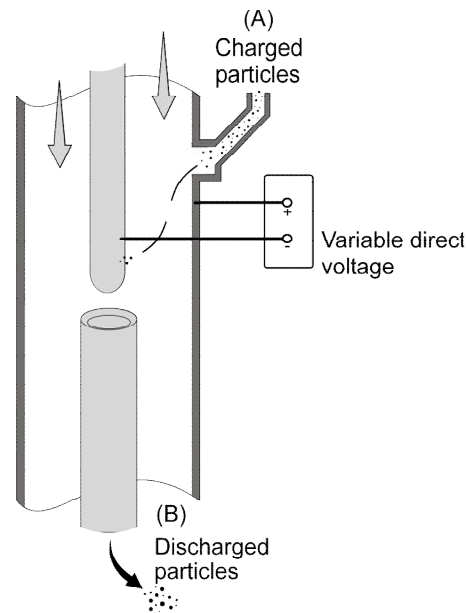


Figure 3-8. Electrical aerosol analyzer

A particle-laden sample stream is extracted from the stack and introduced into the analyzer. The concentration range for the most efficient operation of the EAA is from 1 to 1,000 $\mu\text{g}/\text{m}^3$. Since stack gas concentrations usually exceed 1,000 $\mu\text{g}/\text{m}^3$, sample dilution with clean air is usually required.

The analyzer first places a unipolar charge on the particles being measured. These charged particles are then passed through an electrostatic field imposed between the sample-cell wall and a central sampling aperture. For the imposed field level, a certain segment of the particles will have enough mobility to make it to the sampling aperture and be collected. These separated particles are counted with an optical particle counter or a charge counter. The strength of the imposed field is then increased in steps, each step allowing for a larger segment of particles to be separated and counted. The resulting data are numerically analyzed to determine the number size distribution. No information on the chemical composition of the particles is obtainable since the particles are not collected.

Cascade Impactors

Cascade impactors are used most frequently to determine the particle size distribution of exhaust streams from industrial sources. Cascade impactors utilize the inertia of the particles to separate the particulate matter in the sample gas stream into a number of size categories. Impactors measure the aerodynamic diameter of the particles.

The mechanism by which an impactor operates is illustrated in Figure 3-9. This impactor is constructed using a succession of stages, each containing orifice openings with an impaction slide or collection plate opposite the openings. In each stage, the gas stream passes through the orifice opening and forms a jet that is directed toward the impaction plate. Particles will

impact on the plate if their inertia is large enough to overcome the drag of the air stream as it moves around the plate. Since each successive orifice opening is smaller than those on the preceding stage, the velocity of the air stream, and therefore that of the dispersed particles, is increased as the gas stream advances through the impactor. Consequently, smaller particles eventually acquire enough momentum to break away from the gas streamlines to impact on a plate. Particles passing the last stage are collected on a filter. A complete particle size classification of the gas stream is therefore achieved.

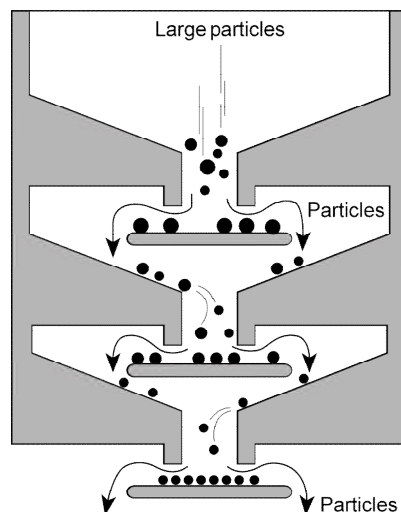


Figure 3-9. Operation of a cascade impactor

Typical impactors consist of a series of stacked stages and collection surfaces. Depending on the calibration requirements, each stage contains from one to as many as 400 precisely drilled jet orifices, identical in diameter on each stage but decreasing in diameter in each succeeding stage (Figure 3-10). Particles are collected on preweighed individual stages, usually filters made of glass fiber or thin metal foil. Some dusts are difficult to collect and require grease on the collection surface for adequate particle capture. The sampling period is usually in the range of 5 minutes to 30 minutes depending on the concentration of particulate matter in the gas stream being tested. It is important to avoid excessively long sampling periods because this can lead to the reentrainment of particles initially captured on each stage. This results in a bias to lower-than-true measured particle sizes. Once the sampling is complete, the collection surfaces from each stage and the final filter are reweighed to determine the mass of particle in each size range. Chemical analyses can also be performed on the separated particles.

The effective range for measuring the aerodynamic diameter is generally between 0.3 and 20 μm . However, some cascade manufacturers have achieved size fractionalization as small as 0.02 μm with low pressure operation. Factors limiting the accuracy of cascade impactors include particle bounce on the impactor stages, particle reentrainment from the impactor stages, and particle agglomerate fracturing in the impactor jets. The latter problem is caused by the high velocities created by the jets in subsequent stages. Other practical problems include the nucleation of vapors due to heat transfer to the large metal cascade impactor

sampling heads and air infiltration into one of more of the numerous sealing surfaces of cascade impactor heads.

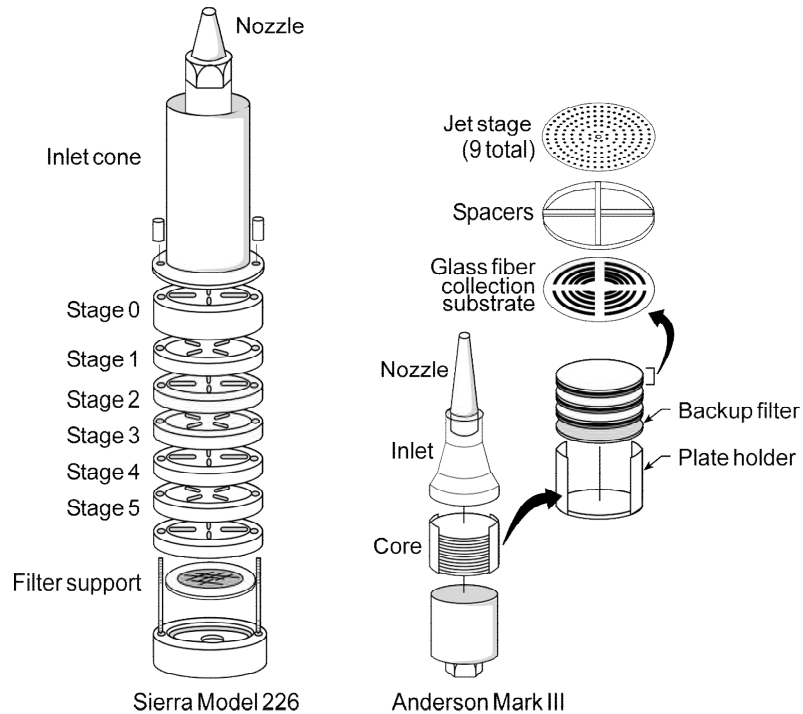


Figure 3-10. Cascade impactors

Comparison of Particle Sizing Devices

Five particle sizing instruments have been briefly described in the previous sections. Figure 3-11 shows the particle size range for each instrument, and Figure 3-12 compares their analytical capabilities. If an analyzer is able to resolve particle size or composition to the single particle level or to provide instantaneous real-time response, an open wedge symbol is indicated. A segmented wedge indicates that the analyzer is capable of providing particle size or composition information for discrete size ranges or for discrete time intervals. An integral symbol indicates that the particle sample is composited over some time period. As previously stated, the ideal measuring instrument would measure the exact size of each particle, determine the composition of each particle, and give an instantaneous real-time response. Accordingly, in Figure 3-12, open wedges are indicated in the size, time and composition columns for the ideal instrument.

Particle Size Distributions

Particulate matter emissions from both anthropogenic and biogenic sources do not consist of particles of just one size. Instead, they are composed of particles over a relatively wide size range. It is often necessary to describe this size range.

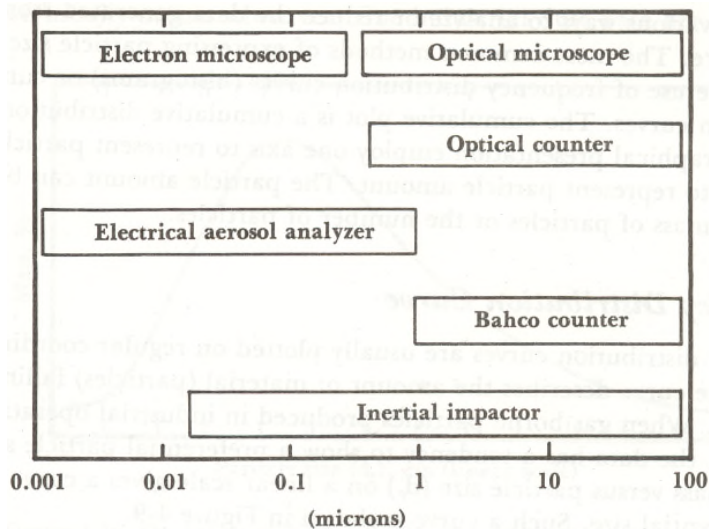


Figure 3-11. Size range capabilities of measuring devices

Device	Size	Time	Composition
Ideal	◁	◁	◁
Microscope	◁	∫	
Optical counter	◁	◁	
EEA	◁	◁	
Bahco counter	◁	∫	◁
Impactor	◁	∫	◁

- ◁ Single particle level
- ◁ Discrete ranges
- ∫ Integrated averaging process

Figure 3-12. Comparison of particle sizing devices

One of the simplest means of describing a particle size distribution is a histogram as shown in Figure 3-13. This simply shows the number of particles in a set of arbitrary size ranges specified on the horizontal axis. The terms used to characterize the particle size distribution are also shown in the figure.

The *median* particle size divides the frequency distribution in half: 50% of the mass has particles with a larger diameter, and 50% of the mass has particles with a smaller diameter.

The *mean* is the mathematical average of the distribution. The value of the mean is sensitive to the quantities of particulate matter at the extreme lower and upper ends of the distribution.

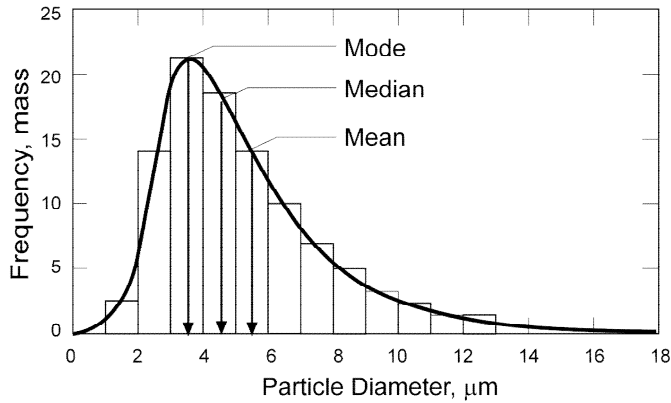


Figure 3-13. Particle size distribution

For many stationary and mobile sources, the observed particulate matter distribution in the effluent gas stream approximates a lognormal distribution. When the log of the particle diameter is plotted against the frequency of occurrence, a normal bell-shaped curve is generated. The histogram for a lognormal curve is shown in Figure 3-14. Note that the percent mass on the vertical axis is divided by the difference in the logarithms of the particle sizes defining the range ($\Delta \log d_p = \log d_{pmax} - \log d_{pmin}$). This is done to avoid any bias from the measurement range capabilities of the analyzer.

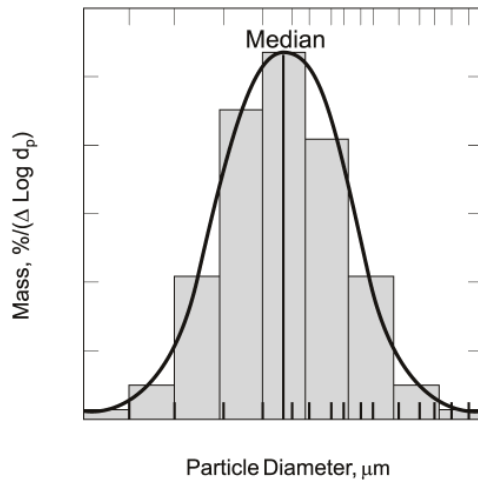


Figure 3-14. Lognormal size distribution

Lognormal distributions plot as a straight line on log-probability paper. This straight line can be characterized by two parameters: the intercept, represented by the geometric mass mean diameter, and the slope, represented by the geometric standard deviation. The geometric mass mean diameter is the particle size that is equivalent to the 50% probability point (zero standard deviations from the mean). The diversity of the particle sizes is described by the

geometric standard deviation. A distribution with a broad range of sizes has a larger geometric standard deviation (σ_g) than one in which the particles are relatively similar in size. When the data are plotted in terms of the cumulative percent larger than size, the geometric standard deviation is determined by dividing the particle size at the 15.87 percent probability (-1 standard deviations from the mean) by the geometric mean size or by dividing the geometric mean size by the particle size at the 84.13 percent probability (+1 standard deviations from the mean):

$$\sigma_g = \frac{d_{15.87}}{d_{50}} \quad (3-2)$$

$$\sigma_g = \frac{d_{50}}{d_{84.13}} \quad (3-3)$$

where

- σ_g = geometric standard deviation of particle mass distribution
- d_{50} = mass mean particle diameter
- $d_{15.87}$ = particle diameter which 15.87% of the mass is larger than
- $d_{84.13}$ = particle diameter which 84.13% of the mass is larger than

If the data are plotted in terms of the cumulative percent smaller than size, the curve slopes the other way. Accordingly, the geometric standard deviation is given by the inverse of Equations 3-2 and 3-3. The easiest way to be sure of forming the proper ratio is to remember that d_{50} is always used in the ratio and that σ_g can not be less than 1. A σ_g equal to 1 indicates that all of the particles are the same size. Thus, the ratio of d_{50} to either $d_{15.87}$ or $d_{84.13}$ must be such that it yields an answer that is greater than 1.

Particle size distributions resulting from complex particle formation mechanisms or several simultaneous formation mechanisms may not be lognormal. As shown in Figure 3-15, these distributions may exhibit more than one peak. In these cases, plots of the data on log-probability paper will not yield a straight line.

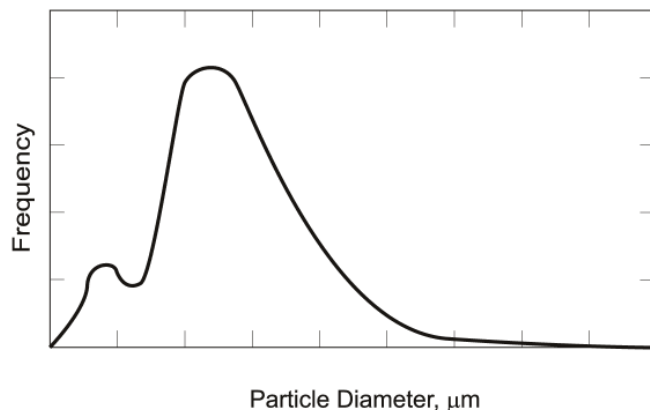


Figure 3-15. Bi-modal particle size distribution

Example 3-1

Determine the mass mean diameter and the geometric standard deviation of the particle collection represented by the following distribution:

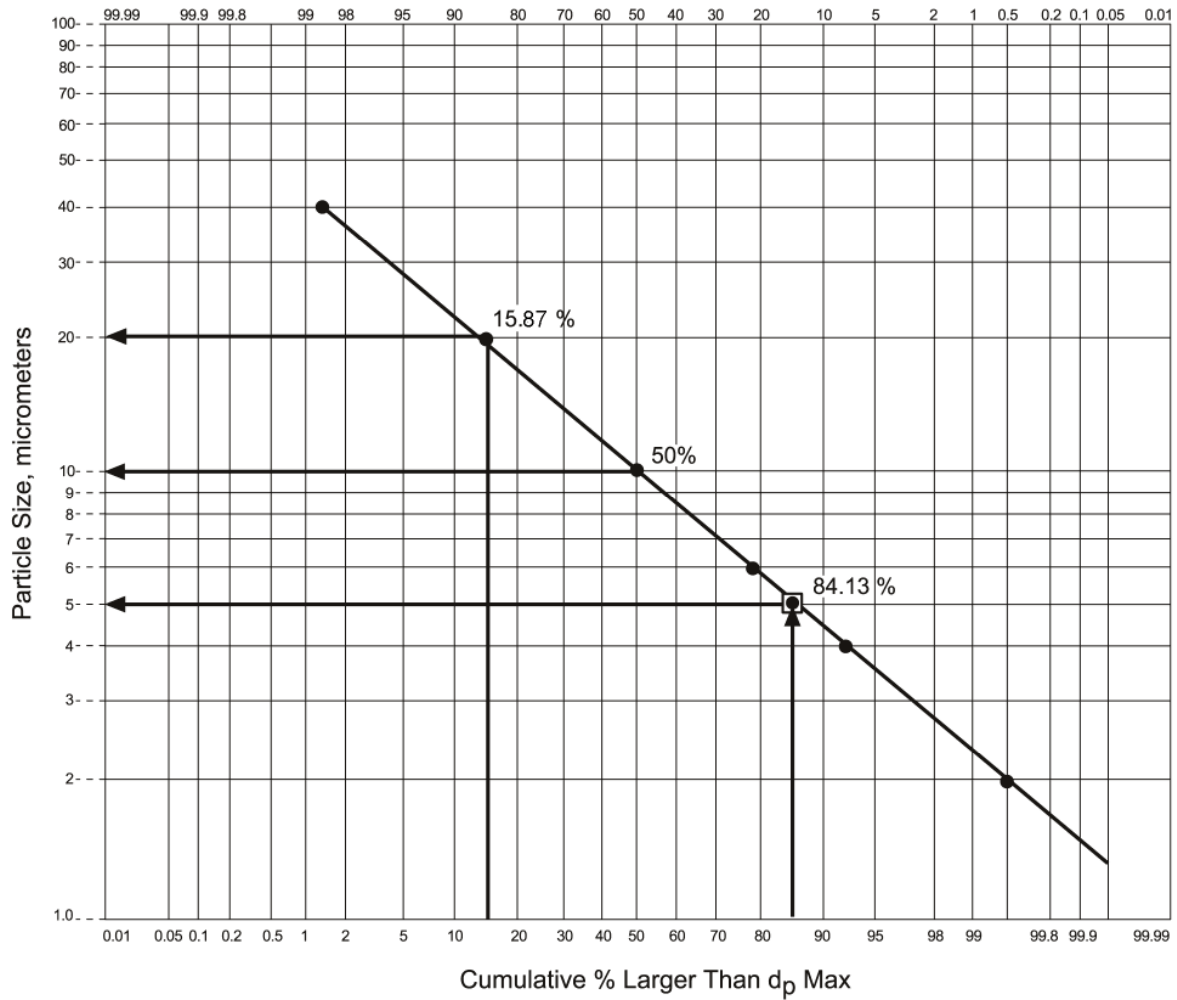
Size Range (μm)	Mass (mg)
<2	1.0
2 to 4	14.5
4 to 6	24.7
6 to 10	59.8
10 to 20	68.3
20 to 40	28.9
>40	2.8

Solution:

Refer to the following table. Determine the total mass and calculate the percentage in each size range. Starting with the size range for the smallest particles (<2 μm), subtract the percent mass in that range (0.50%) from 100.00 to determine the cumulative percent mass greater than 2 μm (99.50%). For each subsequent size range, subtract the percent mass in that range from the cumulative percent mass of the previous size range to determine the cumulative percent mass greater than $d_{p\text{max}}$ for that size range. For example, for the 2 to 4 μm size range, $99.50\% - 7.25\% = 92.25\%$, the cumulative percent mass greater than 4 μm .

Example Particle Size Data			
Size Range (μm)	Mass (mg)	Percent Mass in Size Range	Cumulative Percent Mass Greater Than $d_{p\text{max}}$
<2	1.0	0.50	99.50
2 to 4	14.5	7.25	92.25
4 to 6	24.7	12.35	79.90
6 to 10	59.8	29.90	50.00
10 to 20	68.3	34.15	15.85
20 to 40	28.9	14.45	1.40
>40	2.8	1.40	---
TOTAL	200.0	100.0	

Plot $d_{p\text{max}}$ versus Cumulative Percent Mass Greater Than $d_{p\text{max}}$ on log-probability paper:



The mass mean particle diameter is found at the 50th percentile and is 10 μm . The geometric standard deviation is calculated from:

$$\sigma_g = \frac{d_{15.87}}{d_{50}} = \frac{20 \mu\text{m}}{10 \mu\text{m}} = 2.0$$

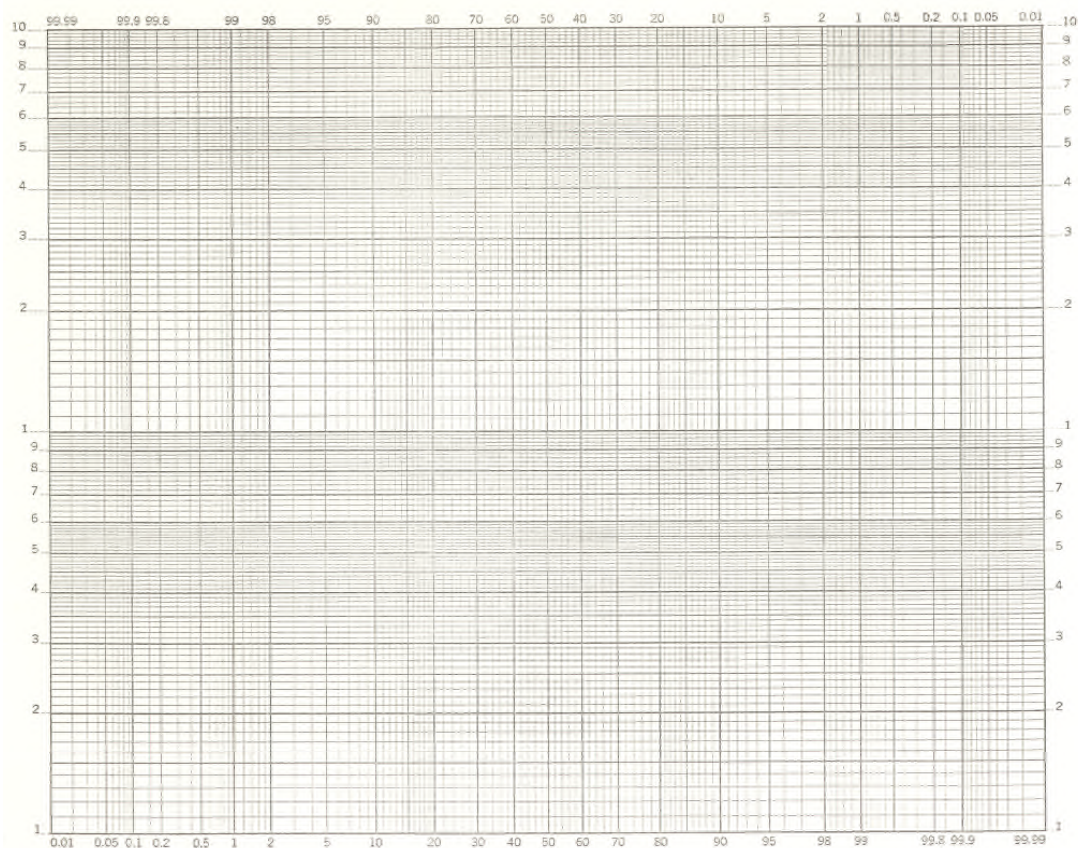
or

$$\sigma_g = \frac{d_{50}}{d_{84.13}} = \frac{10 \mu\text{m}}{5 \mu\text{m}} = 2.0$$

Review Problems

1. Calculate the aerodynamic diameter of a spherical particle having a true diameter of $2\ \mu\text{m}$ and a density of $2.7\ \text{g/cm}^3$.
2. Given the following distributions:
 - (a) Is either distribution lognormal?
 - (b) If yes, what is the geometric mass mean diameter and the geometric standard deviation?

Size Range (μm)	Sample A Mass (mg)	Sample B Mass (mg)
<0.6	25.50	8.50
0.6 to 1.0	33.15	11.05
1.0 to 1.2	17.85	7.65
1.2 to 3.0	102.00	40.80
3.0 to 8.0	63.75	15.30
8.0 to 10.0	5.10	1.69
>10.0	7.65	0.01



This page intentionally left blank.

Review Problem Solutions

1. Calculate the aerodynamic diameter of a spherical particle having a true diameter of $2\ \mu\text{m}$ and a density of $2.7\ \text{g/cm}^3$.

Solution:

Assume that the Cunningham slip correction factor is 1.

$$d_p = d \sqrt{\rho_p C_c} = 2 \sqrt{(2.7)(1.0)} = 3.29\ \mu\text{m}$$

2. Given the following distributions:
- Is either distribution lognormal?
 - If yes, what are the geometric mass mean diameter and the geometric standard deviation?

Size Range (μm)	Sample A Mass (mg)	Sample B Mass (mg)
<0.6	25.50	8.50
0.6 to 1.0	33.15	11.05
1.0 to 1.2	17.85	7.65
1.2 to 3.0	102.00	40.80
3.0 to 8.0	63.75	15.30
8.0 to 10.0	5.10	1.69
>10.0	7.65	0.01

Solution:

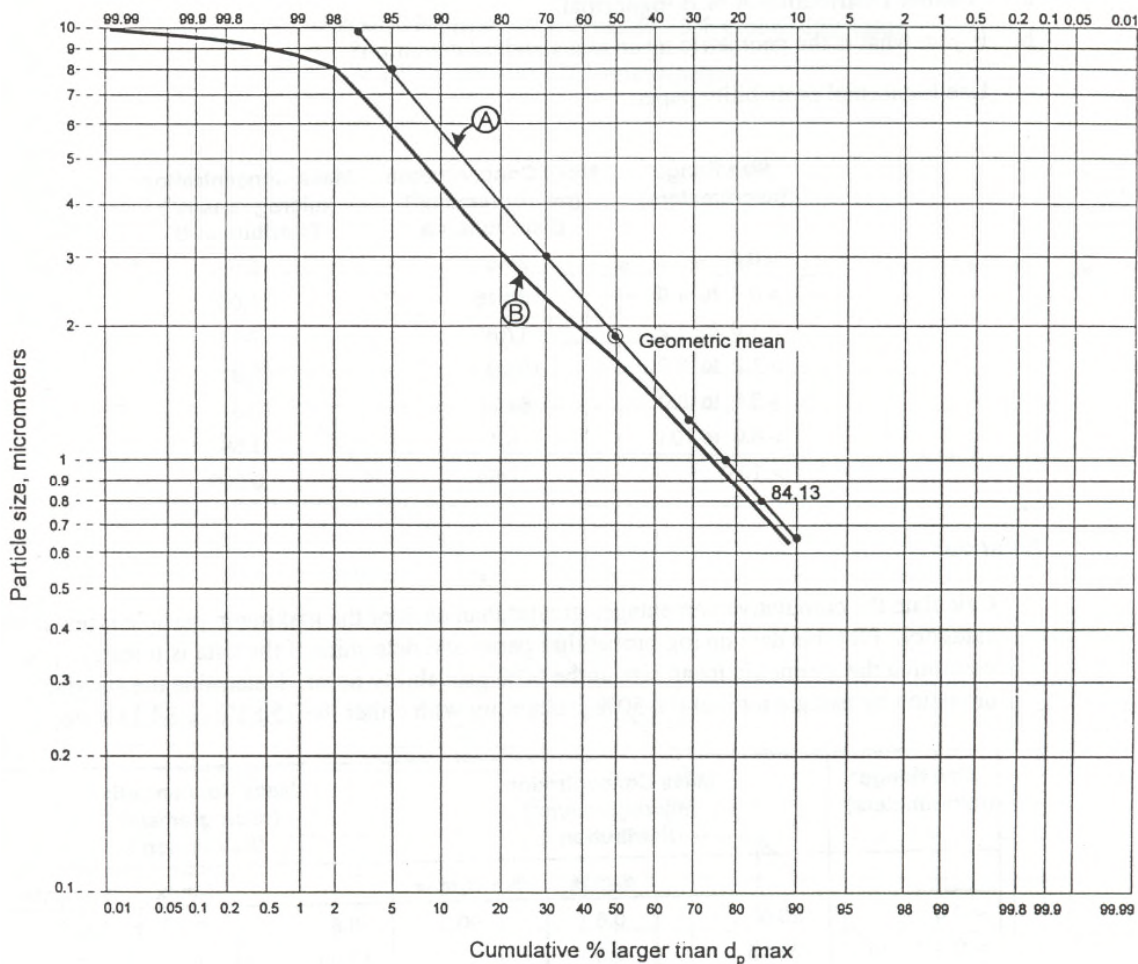
For Sample A—

Size Range (μm)	Mass (mg)	Percent Mass in Size Range	Cumulative Percent Mass Greater Than $d_{p\text{max}}$
<0.6	25.50	10	90
0.6 to 1.0	33.15	13	77
1.0 to 1.2	17.85	7	70
1.2 to 3.0	102.00	40	30
3.0 to 8.0	63.75	25	5
8.0 to 10.0	5.10	2	3
>10.0	7.65	3	---
TOTAL	255.0	100.0	

For Sample B—

Size Range (μm)	Mass (mg)	Percent Mass in Size Range	Cumulative Percent Mass Greater Than $d_{p\text{max}}$
<0.6	8.50	10	90
0.6 to 1.0	11.05	13	77
1.0 to 1.2	7.65	9	68
1.2 to 3.0	40.80	48	20
3.0 to 8.0	15.30	18	2
8.0 to 10.0	1.69	1.99	0.01
>10.0	0.01	0.01	---
TOTAL	85.0	100.0	

For each sample, plot $d_{p\text{max}}$ versus Cumulative Percent Mass Greater Than $d_{p\text{max}}$ on log-probability paper:



- a. Sample A is lognormal; Sample B is not lognormal.
- b. The geometric mass mean diameter and the geometric standard deviation for Sample A are:

$$d_{50} = 1.9 \text{ } \mu\text{m}$$

$$\sigma_g = \frac{d_{50}}{d_{84.13}} = \frac{1.9 \text{ } \mu\text{m}}{0.8 \text{ } \mu\text{m}} = 2.4$$

This page intentionally left blank.

References

Hewitt, G.W., *The Charging of Small Particles for Electrostatic Precipitation*, Paper No. 73-283, Presented at the AIEE Winter General Meeting, New York, NY, 1957.

U.S. Environmental Protection Agency, *Guidelines for Particulate Sampling in Gaseous Effluents from Industrial Processes*, EPA 600/7-79-028, 1979.

This page intentionally left blank.

CHAPTER 4

PARTICLE COLLECTION MECHANISMS

Collection Mechanisms

There are several mechanisms that can act to cause particles to be separated from a gas stream. Which specific mechanism or combination of mechanisms acts and which particular mechanism dominates is strongly dependent on particle size.

- Gravitational settling
- Centrifugal inertial force
- Inertial impaction
- Brownian motion
- Electrostatic attraction
- Thermophoresis
- Diffusiophoresis

Each of these mechanisms applies one or more forces to a particle, such as electrostatic force or inertial force, to cause it to move to a collecting surface. If it were possible to account for all of the forces acting on a particle, then particle motion could be evaluated from:

$$\Sigma F = m_p a_p = m_p \frac{dv_p}{dt} \quad (4-1)$$

where

ΣF = sum of all forces acting on the particle ($\text{g}\cdot\text{cm}/\text{sec}^2$)

m_p = mass of the particle (g)

a_p = acceleration of the particle (cm/sec^2)

v_p = velocity of the particle (cm/sec)

t = time (sec)

It should be noted that Equation 4-1 is sometimes written:

$$\Sigma F = \frac{m_p a_p}{g_c} \quad (4-2)$$

where

ΣF = sum of all forces acting on the particle (lb_f)

m_p = mass of the particle (lb_m)

a_p = acceleration of the particle (ft/sec^2)

$$g_c = 32.2 \frac{\text{lb}_m \text{ ft}}{\text{lb}_f \text{ sec}^2}$$

As indicated, this form is used in the English system, where g_c is needed to convert pounds of mass to pounds of force.

Steps in Particulate Matter Control

Three fundamental steps are involved in the collection of particulate matter in high efficiency particulate control systems, such as fabric filters and electrostatic precipitators.

- Initial capture of particles on surfaces
- Gravity settling of solids into the hopper
- Removal of solids from the hopper

The particle collection mechanisms described in this section control the effectiveness of the first two steps: initial capture of the incoming particles and gravity settling of the collected solids. Particle size distribution is important in each of these steps. As indicated in the following examples, there are significant differences in the particle size ranges involved.

A pulse jet fabric filter uses inertial impaction, Brownian motion and electrostatic attraction to capture particles in the size range of 100 μm to less than 0.01 μm onto the dust layers present on the exterior surfaces of the bags. At regular intervals, the bag cleaning cycle is activated. Large chunks of dust cake are dislodged from the bag surface and fall into the hopper. These agglomerated chunks of solids are usually in the range of 10,000 to 50,000 micrometers (1.0 cm to 5.0 cm). Due to their relatively large size, they fall rapidly into the hopper. However, if the bag compartment is cleaned improperly, the solids can be dislodged in very small agglomerates that might settle too slowly. Proper gravity settling of the solids, Step 2 of particle collection, is crucial to the proper operation of the fabric filter.

In electrostatic precipitators, the dust is deposited on collection plates by electrostatic forces. The initial capture of particles is efficient over the entire size range of 0.1 μm to 100 μm . The particulate matter that accumulates on these collection plates must be discharged to the hoppers below during routine intervals. The cleaning systems in precipitators create disturbances that break off layers or clumps of accumulated solids that fall by gravity into the hopper. As the solids fall downward, they are swept toward the outlet of the precipitator by the horizontally moving gas stream. If the solids clumps are too small, gravity settling is too slow to allow the solids to reach the hopper before the gas stream carries them out of the collector. For this reason, gravity settling is an important second step in particulate matter control in electrostatic precipitators.

The performance of air pollution control equipment is dependent on all three of these steps. Inertial impaction, Brownian motion and electrostatic attraction primarily control the effectiveness of initial capture. Gravity settling is responsible for settling of large clunks of solids during Step 2.

Gravitational Settling

To determine the extent to which a particle or agglomerated solid clumps can be collected by gravitational settling, it is necessary to calculate the forces exerted on the material. These forces are the *gravitational force*, F_G , the *buoyant force*, F_B , and the *drag force*, F_D .

Gravitational Force

The gravitational force F_G , which causes particles and masses to fall, can be expressed:

$$F_G = m_p g = \rho_p V_p g \quad (4-3)$$

where

- F_G = force of gravity ($\text{g}\cdot\text{cm}/\text{sec}^2$)
- m_p = mass of the particle (g)
- g = acceleration of particle due to gravity ($980 \text{ cm}/\text{sec}^2$)
- ρ_p = density of the particle (g/cm^3)
- V_p = volume of the particle (cm^3)

To simplify calculations, particles are assumed to be spheres. Accordingly, the volume of the particle is:

$$V_p = \frac{\pi d_p^3}{6} \quad (4-4)$$

where

- d_p = physical diameter of the particle (cm)

Substituting Equation 4-4 into Equation 4-3 gives:

$$F_G = \frac{\pi d_p^3 \rho_p g}{6} \quad (4-5)$$

Buoyant Force

Acting to resist the downward force of gravity is the upward force of buoyancy. This force occurs because of the gas displaced by the particle and is given by:

$$F_B = m_g g = \rho_g V_p g \quad (4-6)$$

where

- F_B = force of buoyancy ($\text{g} \cdot \text{cm}/\text{sec}^2$)
- m_g = mass of the displaced gas (g)
- g = acceleration of particle due to gravity ($980 \text{ cm}/\text{sec}^2$)
- ρ_g = density of the gas (g/cm^3)
- V_p = volume of the particle (cm^3)

Substituting Equation 4-4 into Equation 4-6 gives:

$$F_B = \frac{\pi d_p^3 \rho_g g}{6} \quad (4-7)$$

The force of buoyancy depends on the gas density, which is on the order of $10^{-2} \text{ lb}_m/\text{ft}^3$, while the gravitational force depends on the particle density, which is on the order of $10^2 \text{ lb}_m/\text{ft}^3$. Accordingly, the buoyant force is comparatively very small and can be neglected.

Drag Force

As the particle begins to move downward as a result of the force of gravity, it encounters a resistive force that increases as the downward velocity increases (see Figure 4-1). This force is called the drag force:

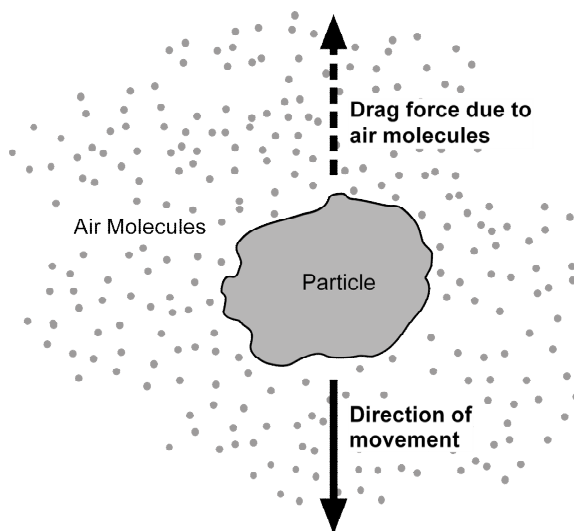


Figure 4-1. Drag force on a particle

$$F_D = \frac{A_p \rho_g v_p^2 C_D}{2} = \frac{\pi d_p^2 \rho_g v_p^2 C_D}{8} \quad (4-8)$$

where

F_D = force of drag ($\text{g}\cdot\text{cm}/\text{sec}^2$)

A_p = cross-sectional area of the particle (cm^2) = $\frac{\pi d_p^2}{4}$

ρ_g = density of the gas (g/cm^3)

v_p = velocity of the particle (cm/sec)

C_D = drag coefficient (dimensionless)

When a particle moves through a gas, it displaces the gas immediately in front of it, imparting momentum to the gas. The drag force produced is equal to the momentum per unit time imparted to the gas by the particle. A portion of the particle's velocity, v_p , is transferred by momentum to the gas as gas velocity, v_g . The amount of energy imparted from v_p to v_g is related to a friction factor which is called the drag coefficient, C_D .

Drag Coefficient

The value of C_D is related to the velocity of the particle and the flow pattern of the gas around the particle. The particle Reynolds number discussed in Chapter 1 is used as an indicator of this flow pattern:

$$\text{Re}_p = \frac{d_p v_p \rho_g}{\mu_g} \quad (4-9)$$

where

Re_p = particle Reynolds number (dimensionless)

d_p = particle diameter (cm)

v_p = particle velocity relative to the gas (cm/sec)

ρ_g = gas density (g/cm^3)

μ_g = gas viscosity ($\text{g}/(\text{cm}\cdot\text{sec})$)

From experimentation, it has been observed that three particle flow regions exist: laminar (sometimes termed *Stokes*), transition, and turbulent (sometimes termed *Newton*). These regions are related to the particle Reynolds number, as shown in Figure 4-2.

For low values of the particle Reynolds number ($\text{Re}_p < 1$), the flow is considered laminar. Laminar flow is defined as flow in which the fluid moves in layers smoothly over an adjacent particle surface. For much higher values of the particle Reynolds number ($\text{Re}_p > 1,000$), the flow is turbulent. Turbulent flow is characterized by erratic motion of fluid, with a violent interchange of momentum throughout the fluid near the particle surface. For particle Reynolds numbers between 1 and 1,000, the flow is said to be in the transition region, where the flow can be either laminar or turbulent, depending on local conditions. In most air pollution control applications, particles less than 100 μm are in the laminar flow region. Transition and turbulent flow conditions are relevant primarily to the gravity settling of large agglomerates in fabric filters and electrostatic precipitators.

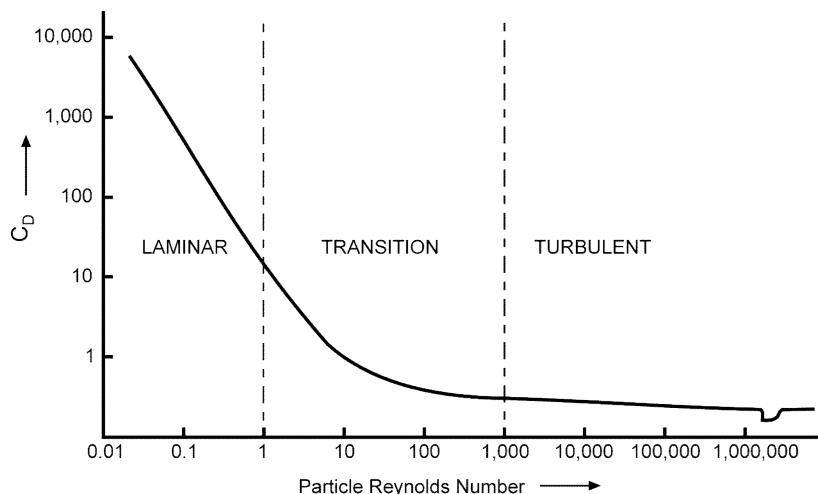


Figure 4-2. Relationship between C_D and Re_p for spheres

Mathematical expressions relating the values of C_D and Re_p can be derived from the data illustrated in Figure 4-2. Equations for determining C_D in each flow region are as follows:

$$\text{Laminar } (Re_p < 1) \quad C_D = \frac{24}{Re_p} \quad (4-10)$$

$$\text{Transition } (1 < Re_p < 1,000) \quad C_D = \frac{18.5}{Re_p^{0.6}} \quad (4-11)$$

$$\text{Turbulent } (Re_p > 1,000) \quad C_D = 0.44 \quad (4-12)$$

Cunningham Slip Correction Factor

If the size of the particle is greater than approximately $3 \mu\text{m}$ in diameter, the gas appears *continuous* around the particle, and mathematical relationships developed for continuous media, like those above, are applicable. However, if the particles are smaller than $3 \mu\text{m}$ in diameter, the gas appears as individual molecules. These small particles are able to slip between the gas molecules and fall faster than relationships developed for continuous media predict. To correct for this, Cunningham deduced that the drag coefficient should be reduced for small particles. Thus, the drag coefficient equation for the laminar region is modified to include a term called the *Cunningham slip correction factor*, C_c .

$$C_D = \frac{24}{Re_p C_c} \quad (4-13)$$

The Cunningham slip correction factor can be estimated from:

$$C_c = 1 + \frac{6.21 \times 10^{-4} T}{d_p} \quad (4-14)$$

where

T = absolute temperature (K)

d_p = particle diameter (μm)

Figure 4-3 illustrates the effect of particle size and gas stream temperature on the Cunningham slip correction factor.

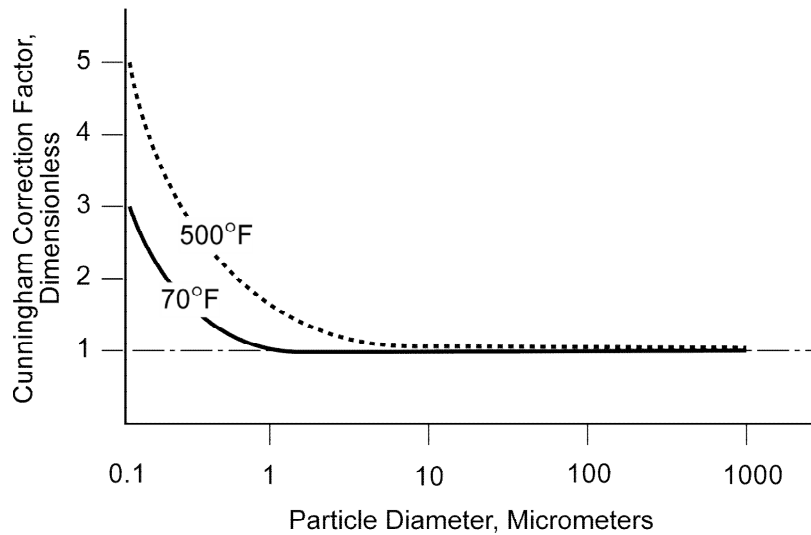


Figure 4-3. Cunningham correction as a function of particle size and gas temperature

Calculation of Drag Force

The drag force for each region can now be calculated by substituting Equation 4-13, 4-11 or 4-12 into Equation 4-8:

Laminar ($Re_p < 1$)
$$F_D = \frac{3\pi\mu_g v_p d_p}{C_c} \quad (4-15)$$

Transition ($1 < Re_p < 1,000$)
$$F_D = 2.31\pi(d_p v_p)^{1.4} \mu_g^{0.6} \rho_g^{0.4} \quad (4-16)$$

Turbulent ($Re_p > 1,000$)
$$F_D = 0.055\pi(d_p v_p)^2 \rho_g \quad (4-17)$$

where

μ_g = gas viscosity (g/(cm·sec))

d_p = physical particle diameter (cm)

ρ_g = gas density (g/cm³)

v_p = velocity of particle relative to gas (cm/sec)

C_c = Cunningham slip correction factor (dimensionless)

Terminal Settling Velocity

Recalling Equation 4-1 and referring to Figure 4-4:

$$\Sigma F = F_G - F_D = m_p a_p = m_p \frac{dv_p}{dt} \quad (4-18)$$

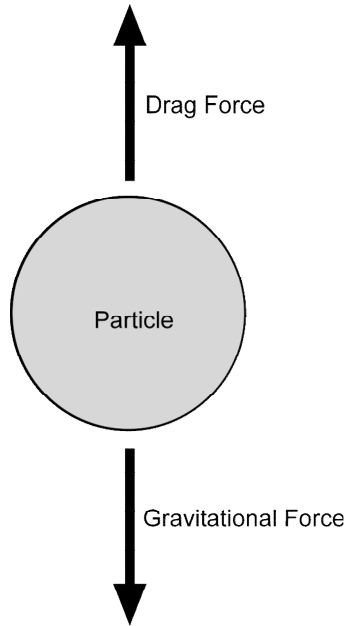


Figure 4-4. Gravitational and drag forces

Note that the buoyant force has been neglected. As the particle accelerates, the velocity will increase. The drag force on the particle also increases with increasing velocity. At some point, a velocity value will be reached where the drag force will be as large as the gravitational force. At this point, the net force will be zero, and the particle will no longer accelerate. If the particle is not accelerating, it is at a constant velocity. This constant velocity, where all the forces balance, is called the *terminal settling velocity*. At the terminal settling velocity:

$$F_G - F_D = 0 \quad (4-19)$$

Terminal settling velocity equations for each region are derived by substituting Equation 4-5 for F_G and Equation 4-15, 4-16 or 4-17, as appropriate, for F_D into Equation 4-19 and solving for particle velocity:

$$\text{Laminar (Re}_p < 1) \quad v_t = \frac{g C_c \rho_p d_p^2}{18 \mu_g} \quad (4-20)$$

$$\text{Transition } (1 < \text{Re}_p < 1,000) \quad v_t = \frac{0.153 g^{0.71} \rho_p^{0.71} d_p^{1.14}}{\mu_g^{0.43} \rho_g^{0.29}} \quad (4-21)$$

$$\text{Turbulent } (\text{Re}_p > 1,000) \quad v_t = 1.74 \left(\frac{g \rho_p d_p}{\rho_g} \right)^{0.5} \quad (4-22)$$

where

- v_t = terminal settling velocity (cm/sec)
- g = acceleration of particle due to gravity (980 cm/sec²)
- C_c = Cunningham slip correction factor (dimensionless)
- ρ_p = particle density (g/cm³)
- μ_g = gas viscosity (g/(cm·sec))
- d_p = physical particle diameter (cm)
- ρ_g = gas density (g/cm³)

Determination of Flow Region

In order to determine the settling velocity of a particle, the flow region must be known so that the appropriate terminal settling velocity equation can be selected. However, in order to determine the flow region, the particle Reynolds number must be calculated and this requires knowledge of the particle velocity we are trying to determine. The following equation allows the flow region to be determined without first determining the particle Reynolds number:

$$K = d_p \left(\frac{g \rho_p \rho_g}{\mu_g^2} \right)^{0.33} \quad (4-23)$$

where

- g = acceleration of particle due to gravity (980 cm/sec²)
- ρ_p = particle density (g/cm³)
- μ_g = gas viscosity (g/(cm·sec))
- d_p = physical particle diameter (cm)
- ρ_g = gas density (g/cm³)

Values of K correspond to the different flow regions, as shown in Table 4-1. Once the flow region has been determined, the appropriate equation can be used to calculate the settling velocity of the particle.

Laminar region	$K < 2.62$
Transitional region	$2.62 < K < 69.12$
Turbulent region	$K > 69.12$

Example 4-1

Calculate the terminal settling velocity in 20°C air of a 45 μm diameter particle with a density of 1 g/cm³.

Solution:

Calculate K to determine the flow region:

$$K = d_p \left(\frac{g \rho_p \rho_g}{\mu_g^2} \right)^{0.33} = 45 \times 10^{-4} \text{ cm} \left[\frac{\left(980 \frac{\text{cm}}{\text{sec}^2} \right) \left(1.0 \frac{\text{g}}{\text{cm}^3} \right) \left(1.20 \times 10^{-3} \frac{\text{g}}{\text{cm}^3} \right)}{\left(1.80 \times 10^{-4} \frac{\text{g}}{\text{cm} \cdot \text{sec}} \right)^2} \right]^{0.33} = 1.41$$

Therefore, the flow region is laminar.

Calculate the terminal settling velocity:

Assume $C_c = 1.0$

$$v_t = \frac{g C_c \rho_p d_p^2}{18 \mu_g} = \frac{\left(980 \frac{\text{cm}}{\text{sec}^2} \right) (1.0) \left(1.0 \frac{\text{g}}{\text{cm}^3} \right) (45 \times 10^{-4} \text{ cm})^2}{18 \left(1.80 \times 10^{-4} \frac{\text{g}}{\text{cm} \cdot \text{sec}} \right)} = 6.13 \frac{\text{cm}}{\text{sec}}$$

Example 4-2

Calculate the terminal settling velocity in 20°C air of a 2 μm diameter particle with a density of 1 g/cm³.

Solution:

Calculate K to determine the flow region:

$$K = d_p \left(\frac{g \rho_p \rho_g}{\mu_g^2} \right)^{0.33} = 2 \times 10^{-4} \text{ cm} \left[\frac{\left(980 \frac{\text{cm}}{\text{sec}^2} \right) \left(1.0 \frac{\text{g}}{\text{cm}^3} \right) \left(1.20 \times 10^{-3} \frac{\text{g}}{\text{cm}^3} \right)}{\left(1.80 \times 10^{-4} \frac{\text{g}}{\text{cm} \cdot \text{sec}} \right)^2} \right]^{0.33} = 0.06$$

Therefore, the flow region is laminar.

Calculate the Cunningham slip correction factor:

$$C_c = 1 + \frac{6.21 \times 10^{-4} T}{d_p} = 1 + \frac{6.21 \times 10^{-4} (293 \text{ K})}{2 \mu\text{m}} = 1.09$$

Calculate the terminal settling velocity:

$$v_t = \frac{g C_c \rho_p d_p^2}{18 \mu_g} = \frac{\left(980 \frac{\text{cm}}{\text{sec}^2}\right) (1.09) \left(1.0 \frac{\text{g}}{\text{cm}^3}\right) (2 \times 10^{-4} \text{ cm})^2}{18 \left(1.80 \times 10^{-4} \frac{\text{g}}{\text{cm} \cdot \text{sec}}\right)} = 0.013 \frac{\text{cm}}{\text{sec}}$$

Summary

Equations 4-20, 4-21 and 4-22 have been used to calculate the terminal settling velocities of particles from 0.1 μm to 100,000 μm . These data (see Table 4-2) clearly indicate that the terminal settling velocities are virtually negligible for particles less than 10 μm , moderate for particles in the size range of 10-80 μm , and relatively fast only for particles larger than 80 μm .

It is for this reason that air pollution control devices that employ only gravitational settling to accomplish initial separation are limited to pre-cleaners that are designed to reduce the large-particle fraction before entering fans or the primary control device. In most systems, gravity settling is employed only for the removal of large agglomerated masses or clumps of dust (1,000 to 100,000 micrometers) that have been collected on bags, precipitator plates, or other collection surfaces. These large clumps of material have high terminal settling velocities.

Particle Size (μm)	Terminal Settling Velocity at 25°C (cm/sec)	Flow Condition
0.1	0.000087	Laminar
1.0	0.0035	Laminar
10.0	0.304	Laminar
50.0	7.5	Laminar
80.0	19.3	Laminar
100	31.2	Transitional
200	68.8	Transitional
1,000	430.7	Transitional
10,000	1,583	Turbulent
100,000	5,004	Turbulent

Centrifugal Inertial Force

Inertial force can be an effective collection mechanism when a particulate-laden gas stream is made to flow in a circular manner within a cylinder, as shown in Figure 4-5. Inertial force that is applied in a spinning gas stream is often termed *centrifugal force*.

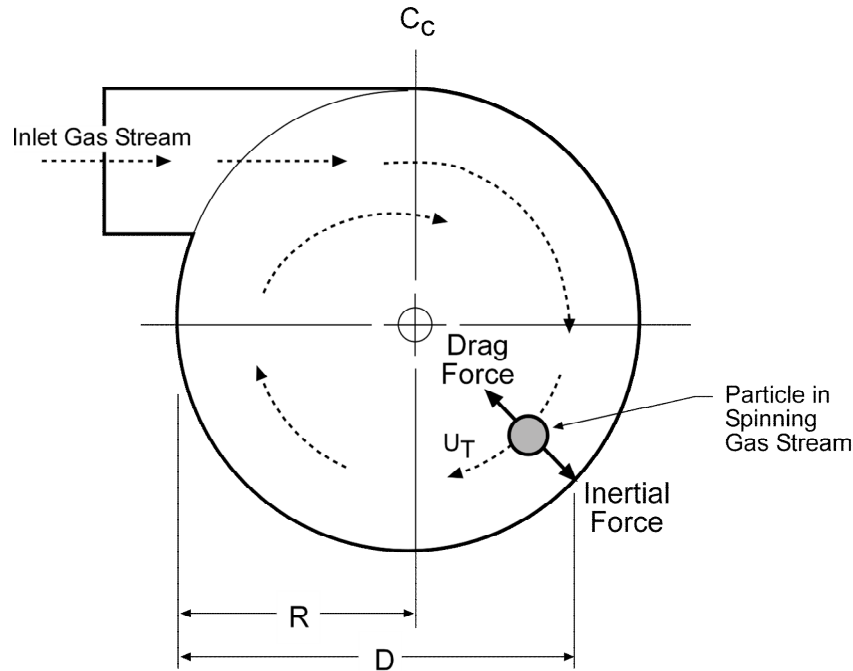


Figure 4-5. Top view of spinning gas in a cyclone

The movement of particles due to inertial force in a spinning gas stream is estimated using the same procedure described for terminal settling velocity due to gravitational force. Accordingly:

$$F_C - F_D = 0 \quad (4-24)$$

The equation for centrifugal force is:

$$F_C = \frac{m_p u_T^2}{R} \quad (4-25)$$

where

- F_C = centrifugal force ($\text{g} \cdot \text{cm}/\text{sec}^2$)
- m_p = mass of the particle (g)
- u_T = tangential velocity of the gas (cm/sec)
- R = cylinder radius (cm)

Note that for centrifugal force, the term “ u_T^2/R ” is similar to the gravitation force term “ g ” used in the discussion of gravitational settling.

Expressing the mass of the particle (m_p) in Equation 4-25 in terms of the particle density and the particle volume (see Equations 4-3 and 4-4) yields the following equation:

$$F_C = \frac{\pi d_p^3 \rho_p u_T^2}{6R} \quad (4-26)$$

where

d_p = physical particle diameter (cm)

ρ_p = particle density (g/cm^3)

For small particles that have particle Reynolds numbers in the laminar range, the drag force is (see Equation 4-15):

$$F_D = \frac{3\pi\mu_g v_p d_p}{C_c} \quad (4-27)$$

The velocity of the particle radially across the gas streamlines and toward the wall of the cyclonic chamber is then given by substituting Equations 4-26 and 4-27 into Equation 4-24 and solving for particle velocity:

$$v_c = \frac{C_c d_p^2 \rho_p u_T^2}{18\mu_g R} \quad (4-28)$$

where

v_c = radial particle velocity (cm/sec)

C_c = Cunningham slip correction factor (dimensionless)

ρ_p = particle density (g/cm^3)

μ_g = gas viscosity ($g/(cm \cdot sec)$)

d_p = physical particle diameter (cm)

u_T = tangential velocity of the gas (cm/sec)

R = cylinder radius (cm)

This equation illustrates that the velocity of the particle moving across the gas stream lines in the cyclone and toward the cyclone wall is proportional to the square of the particle size. This means that cyclones will be substantially more effective for large particles than for small particles. At any given particle size, the particle radial velocity will be proportional to the square of the gas stream tangential velocity and inversely proportional to the cyclone radius. These two parameters determine the extent to which the gas stream is spinning within the cyclone. High velocities increase the spinning action and therefore increase particle radial velocity and particle collection. A small cyclone radius makes the gas stream turn more sharply and therefore also increases cyclone efficiency.

Inertial Impaction

The inertia of a particle in motion in a gas stream can cause it to strike slow-moving or stationary obstacles in its path (see Figure 4-6). As the gas stream deflects to flow around the obstacle, the particle, because of its inertia, is displaced across the gas streamlines and toward the direction of the target. If it has sufficient inertia, the particle contacts the obstacle and is captured.

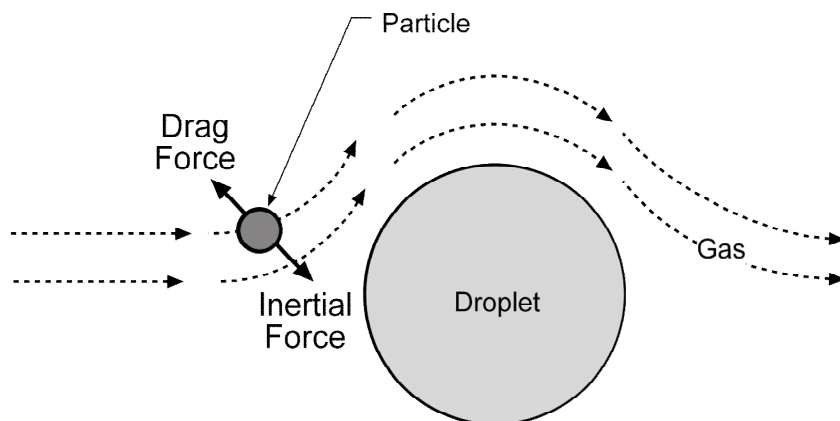


Figure 4-6. Inertial impaction

The efficiency of impaction can be evaluated using the same general procedures used to evaluate gravitational settling and centrifugal force. For particles having a Reynolds number less than 1 (drag force Equation 4-15), the effectiveness of impaction can be related to the inertial impaction parameter shown in Equation 4-29. As the value of this parameter increases, particles have a greater tendency to move radially toward the collection target. As the value of the parameter approaches zero, the particles have a tendency to remain on the gas streamlines and pass around the target.

$$\psi_I = \frac{C_c d_p^2 v_r \rho_p}{18 \mu_g D_c} \quad (4-29)$$

where

- ψ_I = inertial impaction parameter (dimensionless)
- C_c = Cunningham slip correction factor (dimensionless)
- d_p = physical particle diameter (cm)
- v_r = difference in velocity between the particle and the target (cm/sec)
- D_c = diameter of collection target (cm)
- μ_g = gas viscosity (g/(cm·sec))
- ρ_p = particle density (g/cm³)

Note that, in some texts, the inertial impaction parameter is termed the *Stokes number* and sometimes has a value that is twice that shown in Equation 4-29.

The inertial impaction parameter indicates that collection efficiency by impaction will be greatest when the particle size is large, the relative velocity is high and the collection target is small.

Brownian Motion

Very small particles (0.2 μm to 0.002 μm) deflect slightly when they are struck by gas molecules. The deflection is caused by the transfer of kinetic energy from the rapidly moving gas molecule to the small particle. An exaggerated illustration of this motion is shown in Figure 4-7.

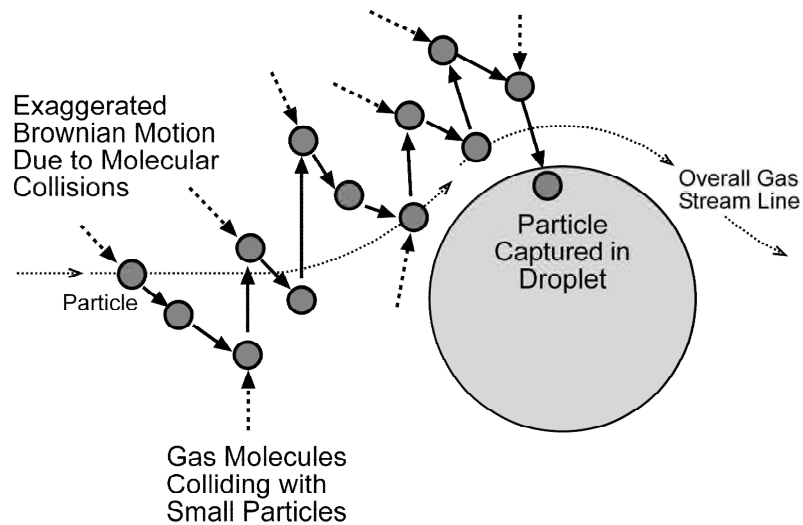


Figure 4-7. Brownian motion

The effectiveness of Brownian motion can be related to the diffusional collection parameter given in Equation 4-30. As the value of this parameter increases, particles have an increasing tendency to be collected by Brownian motion.

$$\Psi_D = \frac{\mathcal{D}_p}{D_c v_r} \quad (4-30)$$

where

Ψ_D = diffusional collection parameter (dimensionless)

\mathcal{D}_p = particle diffusivity (cm^2/sec)

D_c = diameter of collection target (cm)

v_r = relative velocity between particle and collection target (cm/sec)

Particle diffusivity is given by:

$$\mathcal{D}_p = \frac{C_c kT}{3\pi\mu_g d_p} \quad (4-31)$$

where

- k = Boltzmann constant ($\text{g}\cdot\text{cm}^2/\text{sec}^2\cdot\text{K}$)
- T = absolute temperature (K)
- C_c = Cunningham slip correction factor (dimensionless)
- μ_g = gas viscosity ($\text{g}/\text{cm}\cdot\text{sec}$)
- d_p = physical particle diameter (cm)

Substituting Equation 4-31 into Equation 4-30 gives:

$$\Psi_D = \frac{C_c kT}{3\pi\mu_g d_p D_c v_r} \quad (4-32)$$

The diffusional collection parameter indicates that collection efficiency by diffusion will be greatest when the particle size is small, the relative velocity is low and the collection target is small.

Brownian motion or diffusion is important only for particles less than $0.3\ \mu\text{m}$ and is responsible for the slight increase in the observed collection efficiencies of air pollution control devices in this size range. However, diffusion rates are low even for particles in the 0.3 to $0.01\ \mu\text{m}$ size range. Accordingly, particle diffusion is not significant in the majority of air pollution control systems.

Electrostatic Attraction

The following two particle charging mechanisms are active in air pollution control devices used to collect particulate matter:

- Diffusion charging
- Field charging

Field charging is the dominant charging mechanism for particles larger than $2\ \mu\text{m}$. It becomes progressively less important as the particle size decreases. Conversely, diffusion charging is more effective on particles smaller than $0.4\ \mu\text{m}$, and it becomes progressively more important as particle size decreases.

Diffusion or ion charging is the result of the collisions of unipolar ions with particles in a gas stream. These collisions are caused by the random Brownian motion of both the ions and the particles. Diffusion charging continues until electrical charges on the surface of the particle are sufficiently strong to repel approaching ions. The number of electrical charges that accumulate on the surface of a particle due to this mechanism is given by:

$$n_d = \frac{d_p kT}{2e^2} \ln \left(1 + \frac{\pi d_p c_i e^2 N_i t}{2kT} \right) \quad (4-33)$$

where

- n_d = number of charges deposited by diffusion charging
- d_p = particle diameter (cm)
- k = Boltzmann constant ($k = 1.4 \times 10^{-16} \text{ g} \cdot \text{cm}^2/\text{sec}^2 \cdot \text{K}$)
- T = absolute temperature (K)
- c_i = ion velocity ($c_i = 2.4 \times 10^4 \text{ cm/sec}$)
- e = charge of an electron ($e = 4.8 \times 10^{-10} \text{ statcoulomb}$)
- t = time (sec)
- N_i = ion concentration (number/cm³)

Diffusion charging does not require an electrical field. However, particles that acquire an electrical charge will be influenced by any field that exists. These particles will move along the electrical field lines to an area of lower field strength (e.g., a collection surface).

Field charging occurs when particles placed in a strong electrical field with a high concentration of unipolar ions have sufficient mass to locally disrupt the field lines. The ions move to the particle surface along electric field lines that intersect the particle. The transfer of electrical charge continues until the field strength of the particle is sufficient to repel the electrical field. This point is termed the *saturation charge*. The number of electrical charges that accumulate on the surface of a particle at saturation charge is given by:

$$n_f = \left(\frac{3\varepsilon}{\varepsilon + 2} \right) \left(\frac{Ed_p^2}{4e} \right) \quad (4-34)$$

where

- n_f = number of charges deposited by field charging
- d_p = particle diameter (cm)
- ε = dielectric constant of the particle (dimensionless)
- e = charge of an electron ($e = 4.8 \times 10^{-10} \text{ statcoulomb}$)
- E = electrical field strength (statvolts/cm)

Equation 4-34 indicates that the number of charges placed on a particle due to field charging is related to the square of the particle diameter. This level of charge is achieved extremely quickly. Once charged, the particles will be influenced by the electrical field, developing a force directed toward the collection surface.

The charge on a particle is usually expressed as the number of charges, n , times the smallest unit of charge, the charge on an electron, e ($4.8 \times 10^{-10} \text{ statcoulombs}$). The force on a particle with n units of charge in an electrical field, E , is given by:

$$F_E = neE \quad (4-35)$$

where

F_E = electrostatic force (dyne)

n = number of charges

e = charge of an electron ($e = 4.8 \times 10^{-10}$ statcoulomb)

E = electric field strength (statvolt/cm)

The forces created in an electric field can be thousands of times greater than gravity. The velocity with which particles in the electric field migrate can be determined in a manner similar to that shown for gravity settling and centrifugal force:

$$F_E - F_D = 0 \quad (4-36)$$

$$neE - \frac{3\pi\mu_g d_p v_p}{C_c} = 0 \quad (4-37)$$

$$v_p = \omega = \frac{neEC_c}{3\pi\mu_g d_p} \quad (4-38)$$

The particle velocity toward the collecting surface, ω , is called the *migration velocity* or *drift velocity*. This relationship applies to particles in the laminar region. When $Re_p > 1.0$, a more complicated procedure is required.

Example 4-3

Determine the migration velocity of a 2 μm diameter particle with a density of 1 g/cm^3 and carrying 800 units of charge in an electric field of 2 kV/cm . Assume that the gas temperature is 20°C.

Solution:

To solve this problem, the following relationships are used:

$$300 \text{ volts} = 1 \text{ statvolt}$$

$$1 \text{ statvolt} = 1 \text{ statcoulomb}/\text{cm}$$

$$1 \text{ dyne} = 1 \text{ statcoulomb}^2/\text{cm}^2 = 1 \text{ g} \cdot \text{cm}/\text{sec}^2$$

$$C_c = 1.09 \text{ (as calculated in Example 4-2)}$$

The electric field in centimeter-gram-second units is:

$$E = 2 \frac{\text{kV}}{\text{cm}} = 2,000 \frac{\text{V}}{\text{cm}} \left(\frac{\text{statvolt}}{300 \text{ volts}} \right) = 6.67 \frac{\text{statvolts}}{\text{cm}} = 6.67 \frac{\text{statcoulombs}}{\text{cm}^2}$$

$$\omega = \frac{neEC_c}{3\pi\mu_g d_p} = \frac{(800)(4.8 \times 10^{-10} \text{ statcoulombs}) \left(6.67 \frac{\text{statcoulombs}}{\text{cm}^2} \right) (1.09)}{3\pi \left(1.8 \times 10^{-4} \frac{\text{g}}{\text{cm} \cdot \text{sec}} \right) (2 \times 10^{-4} \text{ cm})} = 8.23 \frac{\text{cm}}{\text{sec}}$$

It is apparent that the migration velocity for the 2 μm particle is substantially greater than the settling velocity for the same size particle. This is due to the much greater force imposed by the electrostatic field.

Thermophoresis and Diffusiophoresis

Thermophoresis and diffusiophoresis are two relatively weak forces that can affect collection of submicrometer particles. Thermophoresis is particle movement caused by temperature differences on opposite sides of the particle. The gas molecule kinetic energies on the hot side of the particle are higher than they are on the cold side. Therefore, collisions with the particle on the hot side transfer more energy than molecular collisions on the cold side. Accordingly, the particle is deflected toward the cold area.

Diffusiophoresis is particle movement caused by concentration differences on opposite sides of the particle. When there is a strong difference in the concentration of molecules on opposite sides of the particle, there is a difference in the number of molecular collisions. The particle moves toward the area of lower concentration.

Phoretic forces can be important when the evaporation or condensation of water is involved, since these conditions create substantial temperature and concentration gradients. The normal differences in gas stream temperature and concentration are not sufficient to cause significant particle movement.

Particle Size-Collection Efficiency Relationships

Due to the combined action of the various collection mechanisms described in the previous sections, the performance of particulate control devices often has the particle size-efficiency relationship form shown in Figure 4-8. Above 100 μm , particles are collected with very high efficiency by inertial impaction, electrostatic attraction, and even gravitational settling. Efficiency remains high throughout the range of 10-100 μm due to high inertial or electrostatic forces (depending on the type of collector), both of which are proportional to the square of the particle diameter. For particles less than 10 μm , the limits of inertial forces and electrostatic forces begin to become apparent, and the efficiency drops. Efficiency of these collection mechanisms reaches low levels between 1 μm and 0.1 μm , depending on such factors as gas velocities (inertial forces) and electrical field strengths (electrostatic attraction). Below 0.3 μm , Brownian motion begins to become effective. Accordingly, the overall efficiency curve begins to rise in the very small size range.

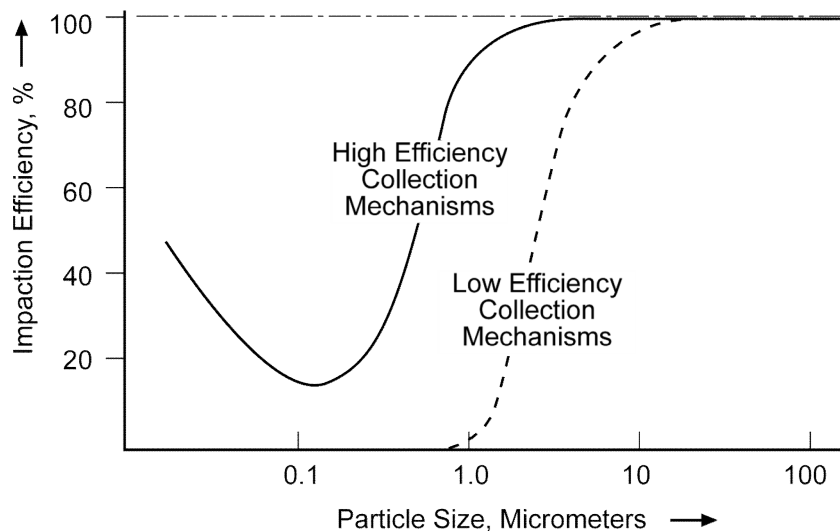


Figure 4-8. General relationship between collection efficiency and particle size

The combined result of these various collection mechanisms is a minimum collection efficiency in the particle size range of 0.1 μm to 0.5 μm . Collection mechanisms in many devices are not highly efficient for particles in this range. These particles can be classified as difficult-to-control due to the inherent limitations of the collection mechanisms. Sources generating high concentrations of particles in the 0.1 μm to 0.3 μm size range may be an especially challenging control problem.

The actual extent of this dip in particulate control capability varies substantially among the types of particulate control systems. The dip is most noticeable in wet scrubbers and electrostatic precipitators. Fabric filters generally have a minimal decrease in overall efficiency in this range due to the multiple-collection mechanisms inherently present. Cyclonic collectors generally are inefficient for particles less than 1 to 3 μm (low efficiency mechanism curve).

Operators of stationary sources that generate large fractions of the total particulate matter in the 0.1 to 0.3 μm range may need to modify the process to alter the particle size distribution or use a pretreatment system to *grow* the particles to a more easily collected size range. These options are discussed in Chapter 8.

Review Questions

1. What is the main role of gravity settling in high efficiency particulate control systems?
 - a. Initial capture of particles in the gas stream being treated
 - b. Collection of solids dislodged during the cleaning cycle
 - c. Minimization of the particulate matter in the gas stream prior to the inlet of the particulate matter control device.
 - d. None of the above.

2. How is the collection efficiency of a cyclonic collector related to the particle size?
 - a. It increases proportional to the cube of the particle diameter.
 - b. It increases proportional to the square of the particle diameter.
 - c. It increases proportional to the particle diameter.
 - d. It is independent of the particle diameter.

3. How is the collection efficiency of an air pollution control device using inertial impaction (e.g., particulate wet scrubber) related to the particle size?
 - a. It increases proportional to the cube of the particle diameter.
 - b. It increases proportional to the square of the particle diameter.
 - c. It increases proportional to the particle diameter.
 - d. It is independent of the particle diameter.

4. How does the effectiveness of Brownian motion relate to the particle size?
 - a. It increases proportional to the cube of the particle diameter.
 - b. It increases proportional to the square of the particle diameter.
 - c. It increases proportional to the inverse of the particle diameter.
 - d. It increases proportional to the inverse of the square of the particle diameter.

This page intentionally left blank.

Review Question Answers

1. What is the main role of gravity settling in high efficiency particulate control systems?
 - b. Collection of solids dislodged during the cleaning cycle
2. How is the collection efficiency of a cyclonic collector related to the particle size?
 - b. It increases proportional to the square of the particle diameter.
3. How is the collection efficiency of an air pollution control device using inertial impaction (e.g., particulate wet scrubber) related to the particle size?
 - b. It increases proportional to the square of the particle diameter.
4. How does the effectiveness of Brownian motion relate to the particle size?
 - c. It increases proportional to the inverse of the particle diameter.

This page intentionally left blank.

Review Problems

Calculate the terminal settling velocities in 20°C air of spherical particles having the following physical diameters and a density of 1 g/cm³.

- a. 1 μm
- b. 10 μm
- c. 100 μm

This page intentionally left blank.

Review Problem Solutions

Calculate the terminal settling velocities in 20°C air of spherical particles having the following physical diameters and a density of 1 g/cm³.

- 1 μm
- 10 μm
- 100 μm

Solution for Part a:

Calculate K to determine the flow region:

$$K = d_p \left(\frac{g \rho_p \rho_g}{\mu_g^2} \right)^{0.33} = 1 \times 10^{-4} \text{ cm} \left[\frac{\left(980 \frac{\text{cm}}{\text{sec}^2} \right) \left(1.0 \frac{\text{g}}{\text{cm}^3} \right) \left(1.20 \times 10^{-3} \frac{\text{g}}{\text{cm}^3} \right)}{\left(1.80 \times 10^{-4} \frac{\text{g}}{\text{cm} \cdot \text{sec}} \right)^2} \right]^{0.33} = 0.03$$

Therefore, the flow region is laminar.

Calculate the Cunningham slip correction factor:

$$C_c = 1 + \frac{6.21 \times 10^{-4} T}{d_p} = 1 + \frac{6.21 \times 10^{-4} (293 \text{ K})}{1 \mu\text{m}} = 1.18$$

Calculate the terminal settling velocity:

$$v_t = \frac{g C_c \rho_p d_p^2}{18 \mu_g} = \frac{\left(980 \frac{\text{cm}}{\text{sec}^2} \right) (1.18) \left(1.0 \frac{\text{g}}{\text{cm}^3} \right) \left(1 \times 10^{-4} \text{ cm} \right)^2}{18 \left(1.80 \times 10^{-4} \frac{\text{g}}{\text{cm} \cdot \text{sec}} \right)} = 0.0036 \frac{\text{cm}}{\text{sec}}$$

Solution for Part b:

Calculate K to determine the flow region:

$$K = d_p \left(\frac{g \rho_p \rho_g}{\mu_g^2} \right)^{0.33} = 10 \times 10^{-4} \text{ cm} \left[\frac{\left(980 \frac{\text{cm}}{\text{sec}^2} \right) \left(1.0 \frac{\text{g}}{\text{cm}^3} \right) \left(1.20 \times 10^{-3} \frac{\text{g}}{\text{cm}^3} \right)}{\left(1.80 \times 10^{-4} \frac{\text{g}}{\text{cm} \cdot \text{sec}} \right)^2} \right]^{0.33} = 0.31$$

Therefore, the flow region is laminar.

Calculate the Cunningham slip correction factor:

$$C_c = 1 + \frac{6.21 \times 10^{-4} T}{d_p} = 1 + \frac{6.21 \times 10^{-4} (293 \text{ K})}{10 \mu\text{m}} = 1.02$$

Calculate the terminal settling velocity:

$$v_t = \frac{g C_c \rho_p d_p^2}{18 \mu_g} = \frac{\left(980 \frac{\text{cm}}{\text{sec}^2}\right) (1.02) \left(1.0 \frac{\text{g}}{\text{cm}^3}\right) (10 \times 10^{-4} \text{ cm})^2}{18 \left(1.80 \times 10^{-4} \frac{\text{g}}{\text{cm} \cdot \text{sec}}\right)} = 0.3085 \frac{\text{cm}}{\text{sec}}$$

Solution for Part c:

Calculate K to determine the flow region:

$$K = d_p \left(\frac{g \rho_p \rho_g}{\mu_g^2} \right)^{0.33} = 100 \times 10^{-4} \text{ cm} \left[\frac{\left(980 \frac{\text{cm}}{\text{sec}^2}\right) \left(1.0 \frac{\text{g}}{\text{cm}^3}\right) \left(1.20 \times 10^{-3} \frac{\text{g}}{\text{cm}^3}\right)}{\left(1.80 \times 10^{-4} \frac{\text{g}}{\text{cm} \cdot \text{sec}}\right)^2} \right]^{0.33} = 3.12$$

Therefore, the flow region is transition.

Calculate the Cunningham slip correction factor:

$$C_c = 1 + \frac{6.21 \times 10^{-4} T}{d_p} = 1 + \frac{6.21 \times 10^{-4} (293 \text{ K})}{100 \mu\text{m}} = 1.00$$

Calculate the terminal settling velocity:

$$v_t = \frac{0.153 g^{0.71} \rho_p^{0.71} d_p^{1.14}}{\mu_g^{0.43} \rho_g^{0.29}} = \frac{0.153 \left(980 \frac{\text{cm}}{\text{sec}}\right)^{0.71} \left(1.0 \frac{\text{g}}{\text{cm}^3}\right)^{0.71} (100 \times 10^{-4} \text{ cm})^{1.14}}{\left(1.8 \times 10^{-4} \frac{\text{g}}{\text{cm} \cdot \text{sec}}\right)^{0.43} \left(1.2 \times 10^{-3} \frac{\text{g}}{\text{cm}^3}\right)^{0.29}} = 30.60 \frac{\text{cm}}{\text{sec}}$$

References

Beachler, D.S., and J.A. Jahnke, *Control of Particulate Emissions*, APTI Course 413 Student Manual, EPA 450/2-80-066, October 1981.

Noll, K.E., *Fundamentals of Air Quality Systems*, American Academy of Environmental Engineers, 1999.

This page intentionally left blank.

CHAPTER 5

SETTLING CHAMBERS

Long used by industry for removing solid or liquid particles from gaseous streams, settling chambers have the advantages of simple construction, low initial cost, low maintenance, low pressure drop and simple disposal of collected materials. It was one of the first devices used to control particulate emissions and is simply an expansion chamber in which gas velocity is reduced, allowing time for particles to settle out under the action of gravity. The settling chamber, however, is generally limited to the removal of particles larger than about 40-60 μm diameter. Today's demands for cleaner air and stricter emission standards have relegated the settling chamber to use as a pre-cleaner for other particle control devices.

Types and Components

There are three basic types of settling chambers: the simple expansion chamber, the multiple-tray settling chamber and the momentum separator.

Simple Expansion Chamber

A typical simple expansion settling chamber is shown in Figure 5-1. The unit is constructed in the form of a long horizontal box with a gas inlet and outlet and dust collection hoppers. The particle-laden gas stream enters the unit at the gas inlet and flows into an expansion section. Expansion of the gas stream causes the gas velocity to be reduced to the chamber velocity. As the gas flows through the chamber, particles in the gas stream are subjected to the force of gravity and settle into the dust collection hoppers. The principal parameters that control collection efficiency are the settling time of the particles and residence time in the chamber. Theoretically, a settling chamber of infinite length could collect even very small particles. The collection hoppers located at the bottom of the settler are usually designed with positively sealing valves and should be emptied as the dust is collected to avoid re-entrainment problems.

Howard Settling Chamber

The multiple-tray settling chamber, also called the Howard settling chamber, is shown in Figure 5-2. Several collection plates are introduced to shorten the settling path of the particles and to improve the collection efficiency of smaller particles. Although the trays are shown as horizontal, they are typically angled vertically upward to provide for gravity cleaning. The gas must be uniformly distributed as it flows through the passageways created by the trays. Uniform distribution is usually achieved by the use of gradual transitions, guide vanes and perforated plates or screens.

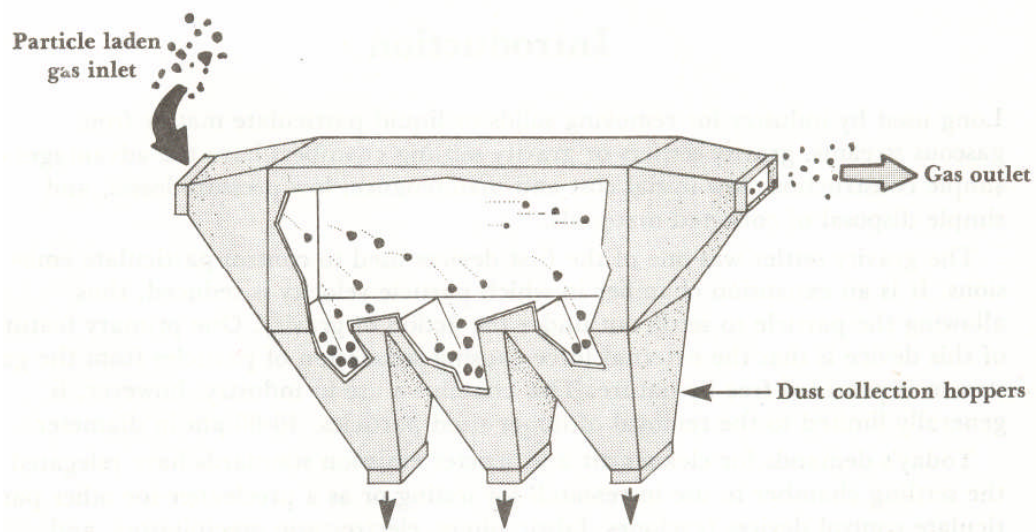


Figure 5-1. Horizontal flow settling chamber

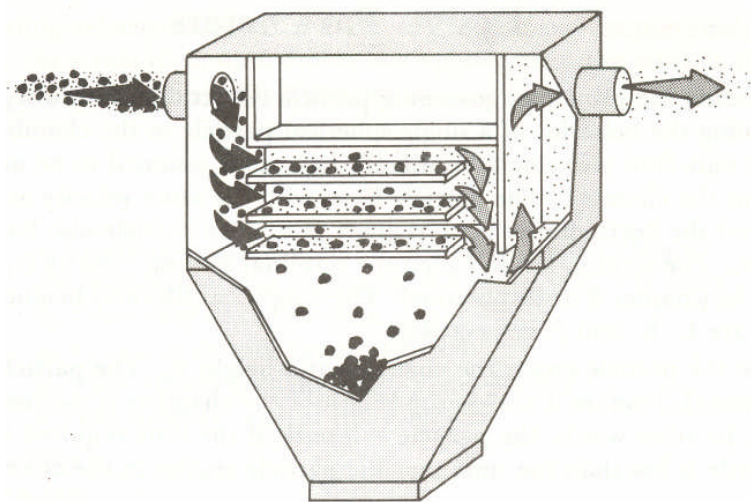


Figure 5-2. Multi-tray settling chamber

Momentum Separators

Momentum separators cause the gas to change directions and add a downward inertial force to supplement the gravitational force. Examples of momentum separators are shown in Figure 5-3

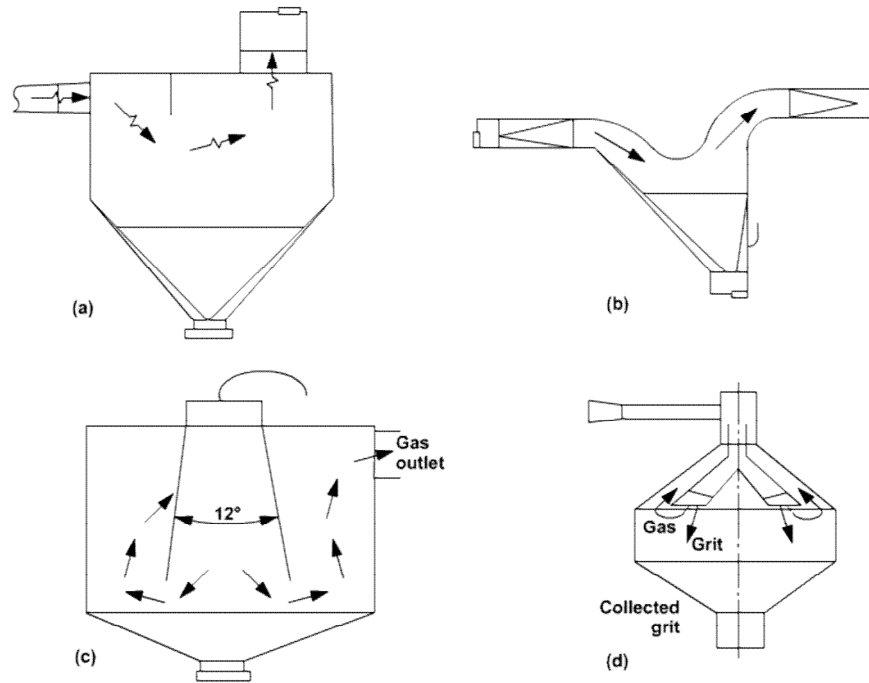


Figure 5-3. Momentum separators

Performance Evaluation

Understanding the principles governing particle collection in a settling chamber begins by examining the behavior of a single spherical particle in the chamber (see Figure 5-3). The gas velocity is assumed to be uniform throughout the chamber, and the particles move horizontally at the gas stream velocity, v_g . The particle also has a downward vertical velocity as a result of the effect of gravity. This is the terminal settling velocity, v_t , discussed in Chapter 4.

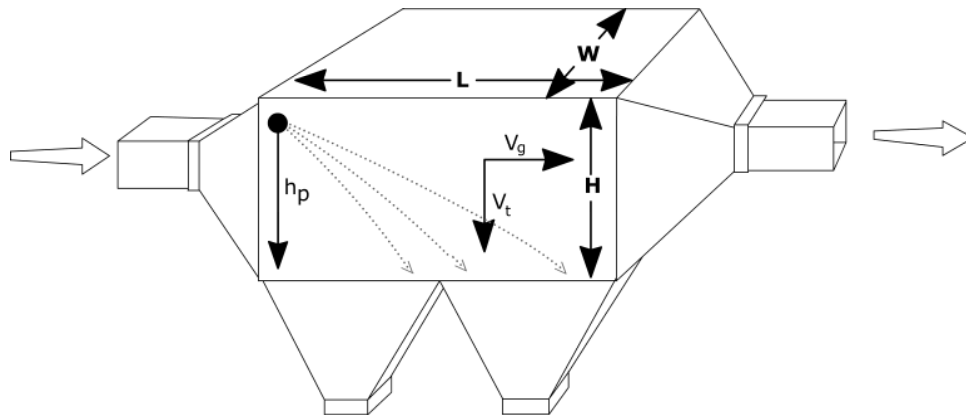


Figure 5-4. Settling chamber dimensions

Suppose a particle enters the chamber at a height, h_p . The particle must fall this distance before it travels the length of the chamber, if the particle is to be collected. In other words, the particle will be collected if the time required for the particle to settle is less than the time that the particle resides in the chamber.

Unfortunately, it is not as simple as the above scenario would suggest. The Reynolds number at chamber conditions is very high, indicating very turbulent conditions. Instead of particles settling directly into the hopper, they may settle a short distance, encounter a turbulent eddy, and be carried back upward to begin settling again as the eddy velocity decreases. The general form for determining collection efficiency when the flow is turbulent is:

$$\eta = 1 - e^{-x} \quad (5-1)$$

where

η = collection efficiency for one size particle (fractional)

For a simple settling chamber:

$$x = \frac{t_r}{t_s} \quad (5-2)$$

where

t_r = chamber residence time

t_s = particle settling time

The chamber residence time is determined from the gas velocity and the chamber length:

$$t_r = \frac{L}{v_g} \quad (5-3)$$

where

L = chamber length (ft)

v_g = gas velocity (ft/sec)

The gas velocity is determined from the gas flow rate and the width and height of the chamber:

$$v_g = \frac{Q}{WH} \quad (5-4)$$

where

Q = gas flow rate (ft^3/sec)

W = chamber width (ft)

H = chamber height (ft)

Substituting Equation 5-4 into Equation 5-3 gives:

$$t_r = \frac{LWH}{Q} \quad (5-5)$$

The particle settling time is determined from the particle terminal settling velocity and, in the worst case, the chamber height:

$$t_s = \frac{H}{v_t} \quad (5-6)$$

where

H = chamber height (ft)

v_t = particle terminal settling velocity (ft/sec)

Substituting Equations 5-5 and 5-6 into Equation 5-2 and then substituting that into Equation 5-1 gives:

$$\eta = 1 - e^{-\frac{v_t LW}{Q}} \quad (5-7)$$

To expand the applicability of Equation 5-7 to multi-tray settling chambers, we can add the parameter N_c , the number of parallel passageways through the chamber. For a simple settling chamber, N_c is one. For a multi-tray settling chamber, N_c is the number of trays plus one. The final relationship for the efficiency of a settling chamber then becomes:

$$\eta = 1 - e^{-\frac{v_t LWN_c}{Q}} \quad (5-8)$$

Recall from Chapter 4 that the terminal settling velocity of a particle in a laminar region ($Re_p < 1$) is given by (C_c is assumed to be 1):

$$v_t = \frac{g \rho_p d_p^2}{18 \mu_g} \quad (5-9)$$

where

v_t = terminal settling velocity (ft/sec)

g = acceleration of particle due to gravity (32.17 ft/sec²)

ρ_p = particle density (lb_m/ft³)

μ_g = gas viscosity (lb_m/(ft·sec))

d_p = physical particle diameter (ft)

Particles that are smaller than 100 μm generally fall into this region. However, the linear relationship for drag coefficient can be extended into the transition region, up to a particle Reynolds number of about 5-10, without introducing significant error. This allows Equation 5-9 to be approximately applied to particles considerably larger than 100 μm . The error introduced by this assumption should be checked and, if it is significant, the terminal settling velocity for the transition region should be used where appropriate.

Substituting Equation 5-9 into Equation 5-8 give the collection efficiency relationship for particles in the laminar region:

$$\eta = 1 - e^{-\left(\frac{g\rho_p L W N_c}{18\mu_g Q}\right) d_p^2} \quad (5-10)$$

Example 5-1

Estimate the collection efficiency of a 75 μm diameter particle in a simple settling chamber 10 ft wide by 10 ft high by 30 ft long when the gas velocity through the chamber is 5 ft/sec. Assume a particle density of 120 lb_m/ft^3 and gas stream conditions of 68°F and 1 atm.

Solution:

Convert particle size to feet:

$$d_p = 75 \mu\text{m} \left(\frac{\text{ft}}{0.3048 \times 10^6 \mu\text{m}} \right) = 2.46 \times 10^{-4} \text{ft}$$

Calculate volumetric flow rate:

$$Q = v_g WH = \left(5 \frac{\text{ft}}{\text{sec}} \right) (10 \text{ft})(10 \text{ft}) = 500 \frac{\text{ft}^3}{\text{sec}}$$

Calculate collection efficiency:

$$\eta = 1 - e^{-\left(\frac{g\rho_p L W N_c}{18\mu_g Q}\right) d_p^2} = 1 - e^{-\left[\frac{\left(32.17 \frac{\text{ft}}{\text{sec}^2} \right) \left(120 \frac{\text{lb}_m}{\text{ft}^3} \right) (30 \text{ft})(10 \text{ft})(1)}{18 \left(1.21 \times 10^{-5} \frac{\text{lb}_m}{\text{ft}\cdot\text{sec}} \right) \left(500 \frac{\text{ft}^3}{\text{sec}} \right)} \right] (2.46 \times 10^{-4} \text{ft})^2} = 0.475 = 47.5\%$$

The design variables for a settling chamber include the length, width and height of the chamber. These parameters are chosen by the equipment manufacturer to remove all particles above a specified size. The chamber design must provide conditions for sufficient residence time to capture the desired particle size range. This can be accomplished by keeping the velocity of the gas through the chamber as low as possible. If the velocity is too high, dust re-entrainment will occur. However, the design velocity should not be so low as to

cause the chamber volume to be exorbitant. Accordingly, units are typically designed for gas velocities in the range of 1 to 10 ft/sec.

In settling chamber designs, the velocity at which the gas moves through the chamber is usually called the *throughput velocity*. The velocity at which settled particles become re-entrained is called the *pickup velocity*. In order to avoid re-entrainment of collected dust, the throughput velocity must not exceed the pickup velocity. Pickup velocities for several materials are given in Table 5-1. If no data are available, the pickup velocity should be assumed to be 10 ft/sec. In this case, the gas velocity through the chamber must be less than 10 ft/sec.

Table 5-1. Pickup Velocities of Various Materials			
Material	Density (g/cm³)	Median Size (μm)	Pickup Velocity (ft/sec)
Aluminum chips	2.72	335	14.2
Asbestos	2.20	261	17.0
Nonferrous foundry dust	3.02	117	18.8
Lead oxide	8.26	15	25.0
Limestone	2.78	71	21.0
Starch	1.27	64	5.8
Steel shot	6.85	96	15.2
Wood chips	1.18	1,370	13.0
Sawdust	---	1,400	22.3

This page unintentionally left blank.

Review Questions

1. Identify the primary force responsible for particle collection in settling chambers.
 - a. electrostatic
 - b. impaction
 - c. centrifugal
 - d. gravity
 - e. Brownian diffusion

2. Settling chambers are normally effective for removing particles in which of the following size ranges.
 - a. less than 10 microns
 - b. between 10 and 50 microns
 - c. greater than 70 microns
 - d. submicron particles only

3. Increasing the gas volumetric feed rate to an existing settling chamber would be expected to result in
 - a. a decrease in collection efficiency
 - b. an increase in collection efficiency
 - c. no change in collection efficiency
 - d. impossible to say

This page intentionally left blank.

Review Question Answers

1. Identify the primary force responsible for particle collection in settling chambers.
 - d. gravity
2. Settling chambers are normally effective for removing particles in which of the following size ranges.
 - c. greater than 70 microns
3. Increasing the gas volumetric feed rate to an existing settling chamber would be expected to result in
 - a. a decrease in collection efficiency

This page intentionally left blank.

Review Problem

Estimate the collection efficiency of a 50 μm diameter particle in a simple settling chamber 5 meters wide by 2 meters high by 10 meters long when the gas velocity is 0.3 m/sec. Assume a particle density of 4.6 g/cm^3 and gas stream conditions of 20°C and 1 atm.

This page unintentionally left blank.

Review Problem Solution

Estimate the collection efficiency of a 50 μm diameter particle in a simple settling chamber 5 meters wide by 2 meters high by 10 meters long when the gas velocity is 0.3 m/sec. Assume a particle density of 4.6 g/cm^3 and gas stream conditions of 20°C and 1 atm.

Solution:

Calculate volumetric flow rate:

$$Q = v_g WH = \left(0.3 \frac{\text{m}}{\text{sec}}\right)(5\text{ m})(2\text{ m}) = 3.0 \frac{\text{m}^3}{\text{sec}} = 3.0 \times 10^6 \frac{\text{cm}^3}{\text{sec}}$$

Calculate collection efficiency:

$$\eta = 1 - e^{-\left(\frac{g \rho_p L W N_c}{18 \mu_g Q}\right) d_p^2} = 1 - e^{-\left[\frac{\left(\frac{980 \frac{\text{cm}}{\text{sec}^2}\right)\left(\frac{4.6 \frac{\text{g}}{\text{cm}^3}\right)(1,000\text{ cm})(500\text{ cm})(1)}{18\left(1.80 \times 10^{-4} \frac{\text{g}}{\text{cm}\cdot\text{sec}}\right)\left(3.0 \times 10^6 \frac{\text{cm}^3}{\text{sec}}\right)}\right] (50 \times 10^{-4} \text{ cm})^2} = 0.997 = 99.7\%$$

This page intentionally left blank.

References

Beachler, D.S., and J.A. Jahnke, *Control of Particulate Emissions*, APTI Course 413 Student Manual, EPA 450/2-80-066, October 1981.

This page intentionally left blank.

CHAPTER 6

CYCLONES

Cyclone collectors use inertial force to separate particles from a rotating gas stream. There are two main types of cyclones: (1) large diameter cyclones and (2) small diameter multi-cyclones. Large diameter cyclones range in size from approximately 1 foot in diameter to more than 12 feet in diameter and are used for the collection of large diameter particulate matter that would otherwise settle out near the source and create a nuisance in the immediate area. Large diameter cyclones typically have operating pressure drops of 2 in WC to 4 in WC. Multi-cyclone collectors are groups of small diameter cyclones, typically 6 inches to 12 inches in diameter, which have better particulate removal capability than large diameter cyclones. The multi-cyclone units are used as stand-alone collectors on sources generating moderate-to-large particulate matter and are also used as pre-collectors to reduce the particle loading into fabric filters and electrostatic precipitators. Multi-cyclones typically have operating pressure drops greater than 4 in WC.

Cyclone collectors are occasionally used as pre-collectors in air pollution control systems vulnerable to ember entrainment. While the embers do not damage cyclone components, the hoppers must be properly designed to prevent the accumulation of combustible material that could be ignited. Simmering fires in the hoppers could warp the tube sheet supporting the multi-cyclone tubes, crack welds and gaskets used to seal the tubes to the tube sheet, and damage the hopper casings.

Operating Principles

Cyclones use inertial force to separate particles from a gas stream. Because the inertial force is applied in a spinning gas stream, the inertial force is often termed centrifugal force. The first step in particle capture is the accumulation of particles along the inner wall of the cyclone due to centrifugal force.

For vertically oriented cyclones, settling the particles into a hopper is the second step in the overall process of particle capture. However, unlike electrostatic precipitators and fabric filters, there is little if any particle agglomeration to facilitate gravity settling, until the particles reach the cyclone tube discharge. The particles settle at a rate that is dependent partially on their terminal settling velocities. These settling rates are quite small for particles less than 10 micrometers in diameter. Fortunately, most particles in vertical cyclones also retain some momentum toward the hopper due to the motion of the gas stream passing through the cyclone. The combined effect of gravity settling and the momentum from the gas stream are sufficient to transport the particles from the cyclone wall to the cyclone tube discharge, and eventually to the hopper.

The third step in the overall particulate matter control process is the removal of accumulated solids from the hoppers. This is an especially important step because the cyclone outlets extend directly into the hoppers. The presence of high solids levels due to hopper discharge problems could block the outlets and make the cyclone entirely ineffective for particulate removal.

Several factors affect the performance of a cyclone collector. The more important ones are the size and mass of the particles, the gas velocity through the unit, the cyclone diameter, and the residence time of the gases in the cyclone (see Equation 4-28). Since inertial forces are used to separate the particles from the gas stream, collection efficiency increases as the size and mass of the particle increases and as the gas velocity through the unit increases. Centrifugal force increases as the radius of turn decreases. As a result, smaller diameter cyclones are more efficient than larger diameter cyclones. Cyclones that have bodies and cones, that are long relative to their diameter have longer residence times and higher collection efficiencies. As a result of these factors and others, a range of performance can be achieved with cyclones, as shown in Figure 6-1.

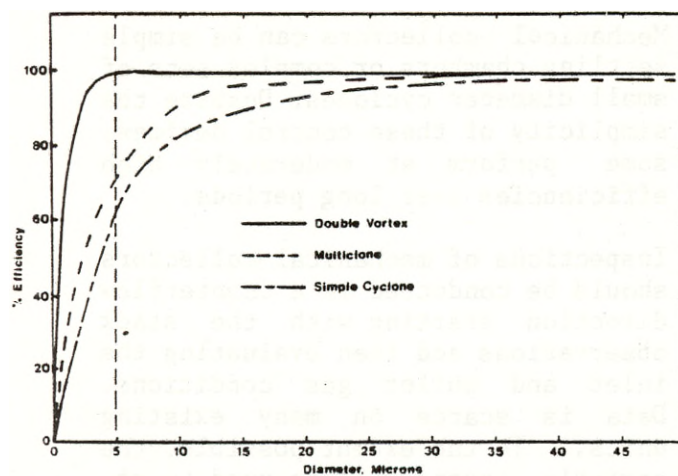


Figure 6-1. Cyclone fractional efficiency curves

In general, cyclones are not useful for the collection of sticky particulate matter. The main difficulties associated with these materials involve removal from the hoppers and build-up along the inner wall of the cyclone. Examples of hard-to-collect sticky material include partially polymerized oils, condensed high molecular weight organics, and ammonium sulfate and bisulfate particles. Sources emitting stringy material can cause build-up of material in the inlet vanes of multi-cyclone collectors. Partially blocked inlet spinner vanes do not generate the cyclonic flow patterns necessary for proper inertial separation.

Small diameter cyclones, including all multi-cyclone collectors, are vulnerable to severe erosion when treating gas streams having very large diameter particulate matter. Particles over twenty micrometers in diameter are very abrasive at the high tangential velocities achieved in the small diameter cyclones. The abrasiveness of particulate matter increases with the square of the particle diameter. Accordingly, cyclones handling particles in the

twenty to more than one hundred micrometer size range can be vulnerable to high erosion rates.

Cyclone Systems

Large Diameter Cyclones

The inlet gas stream enters the large diameter cyclone through a tangentially mounted duct that imparts a spin to the gas stream. The inlet duct is usually at the top of the cyclone body, but large diameter cyclones may also have bottom inlets. Both arrangements are shown in Figure 6-2.

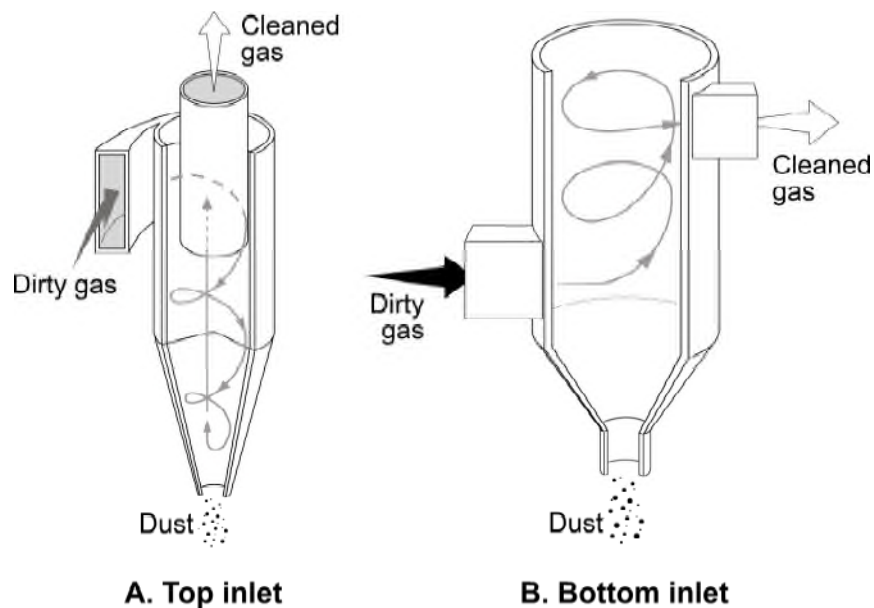


Figure 6-2. Large diameter cyclones

With the normal inlet gas stream velocity of 20 to 50 ft/sec, the gas stream spins approximately one-half to three complete rotations within the cyclone body of both types. An increase in the gas inlet velocity increases the spinning action of the gas stream, thereby improving inertial separation of the particles.

The gas flow pattern in a bottom inlet large diameter cyclone is relatively simple. The inlet gas stream begins to spin in the cyclone body because of the tangential inlet duct configuration. The gas stream forms an ascending vortex that rises up in the cyclone body to the outlet duct at the top of the unit. The particles that migrate across the gas streamlines settle by gravity when they approach the surface of the cyclone body where the gas velocity is low.

In the top inlet design, the gas stream spins in two separate vortices. The inlet stream creates an outer vortex due to the tangential location of the inlet duct and due to the presence of the

outlet tube extension that prevents gas movement into the center of the cyclone body. As the gas stream passes down the cyclone body, it turns 180° and forms an inner vortex that moves toward the gas outlet tube at the top of the cyclone. The outlet tube must extend sufficiently far into the cyclone to facilitate formation of the outer vortex and to prevent a short-circuit path for the gas stream.

The particles that have migrated toward the outer portion of the outer vortex break away from the gas stream when it turns 180° to enter the inner vortex. Due to their inertia, the particles continue to move downward toward the cyclone hopper as the gas stream turns from the outer vortex to the inner vortex. The movement of the particles toward the hopper is controlled partially by inertial forces. The force of gravity also assists in particle movement toward the hopper.

Top-inlet, large-diameter cyclones can have a number of different inlet designs, as shown in Figure 6-3. The most common design is the simple tangential inlet (A). The deflector vane (B) reduces the gas stream turbulence at the inlet and can reduce the overall pressure drop. However, the deflector vanes can also impair vortex formation and thereby reduce particulate collection. Helical inlets (C) have been used in an attempt to reduce cyclone pressure drop and to improve performance. Involute entries (D) can also reduce turbulence-related pressure drop at the inlet. However, they usually provide improved efficiency due to the manner in which the outer vortex develops.

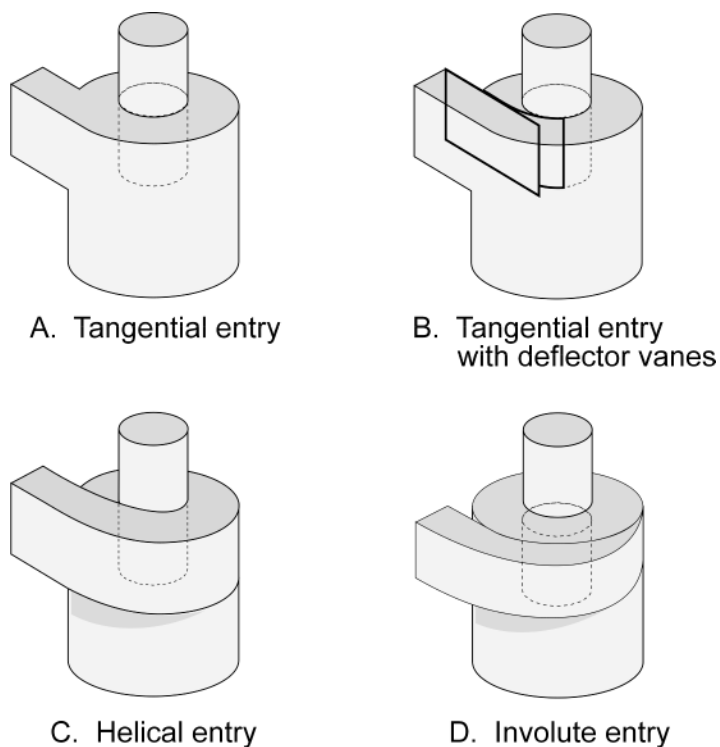


Figure 6-3. Types of cyclone inlets

The outlet gas tube is also an important consideration in the design of a large diameter cyclone. Some of the energy due to the radial motion of the ascending gases can be recovered by scroll devices (A) or outlet drums (B) placed on top of the outlet tube. These two cyclone enhancements, which are shown in Figure 6-4, are essentially flow straighteners that can effectively reduce the overall pressure drop across the unit without affecting the particulate matter removal efficiency.

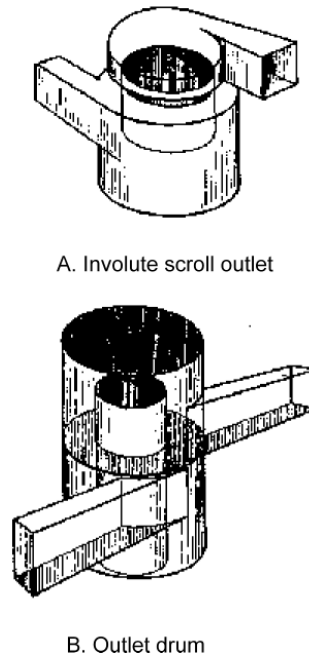


Figure 6-4. Special outlet configuration for large diameter cyclones

Large diameter cyclones can be used in series or parallel arrangements in order to increase particulate matter removal efficiency or to increase gas flow capability. A series arrangement (A) of two cyclones of equal size and a parallel arrangement (B) of four cyclones of equal size are shown in Figure 6-5.

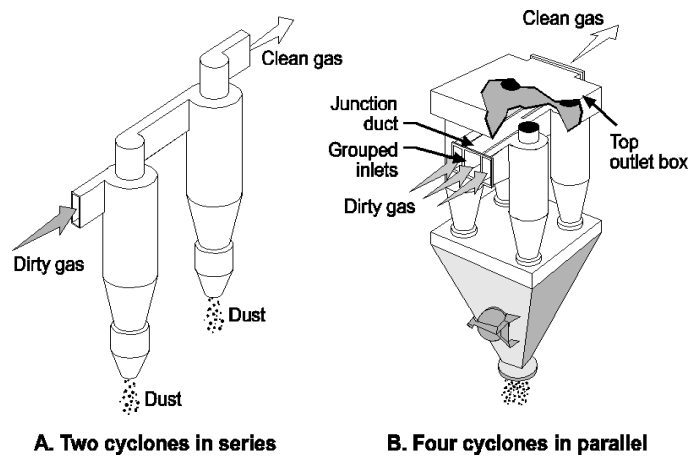


Figure 6-5. Series and parallel arrangement of cyclones

The dust discharge system for a large diameter cyclone is similar to that used in other dry particle collectors and consists of a hopper for receiving the collected solids and a solids discharge valve that allows solids to be removed from the hopper without letting air in or out of the system. Four common types of solids discharge valves are shown in Figure 6-6. The slide gate (A), the rotary discharge valve (B), and the double flapper valve (D) are all capable of providing an airtight seal. The screw conveyor arrangement (C) cannot provide an airtight seal unless a solids discharge valve is placed between the bottom of the cyclone and the screw conveyor.

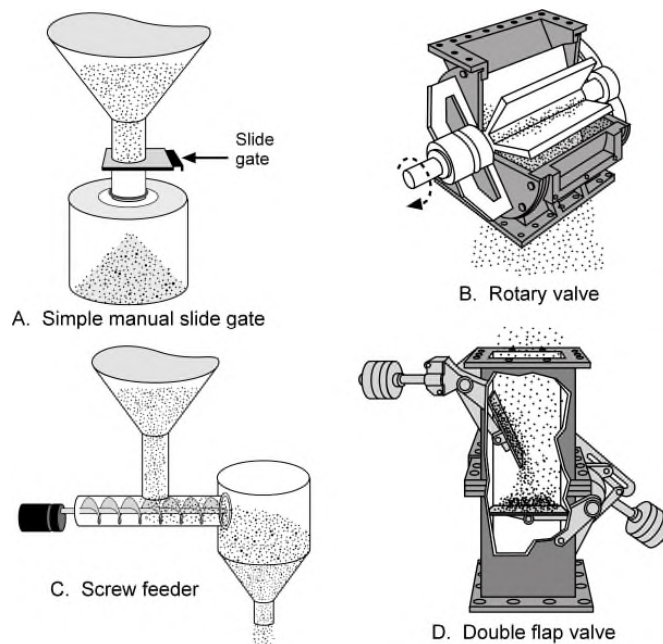


Figure 6-6. Types of solid discharge valves

Air infiltration into negative pressure cyclones, either through the solids discharge valve or through holes in the casing, can significantly reduce collection efficiency by disrupting the vortex and by entraining particles and carrying them toward the outlet flow. Also, collection of very large particles in high velocity vortices can be difficult because of the tendency for the particles to bounce off the wall.

Small Diameter Multi-Cyclones

The particulate matter removal capability of a small diameter cyclone is greater than that of a large diameter cyclone because the gas stream is forced to spin in smaller vortices, imparting greater inertial force to the particles. However, it is not possible to handle a large gas volume in a single small diameter tube. In order to treat the entire gas stream, a large number of small diameter tubes can be used in a single collector in which the tubes are in a parallel arrangement. Multi-cyclone collectors have cyclone tubes that range in size from 6 to 12 in. in diameter. A small multi-cyclone collector, such as the one shown in Figure 6-7, can have as few as 16 tubes. Large units may have several hundred tubes.

These units are divided into three separate areas by two tube sheets. The *dirty gas tube sheet* is mounted horizontally, supporting the cyclone tubes and separating the inlet gas stream from the hopper area of the unit. The *clean gas tube sheet* stair-steps down from front to back at approximately a 45° angle, dividing the inlet gas stream from the treated outlet gas stream. The outlet gas tubes from each of the cyclones pass through the clean gas tube sheet.

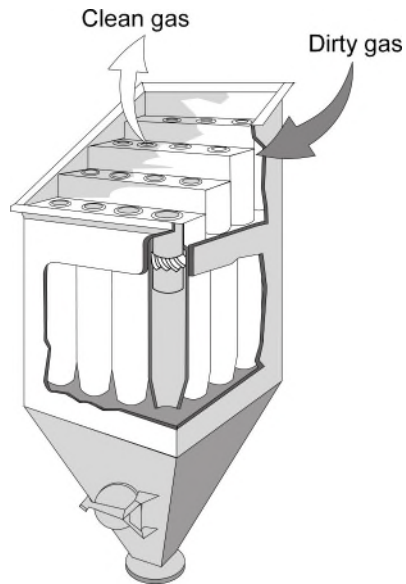


Figure 6-7. Multi-cyclone collector

Solids discharge valves are necessary under negative pressure multi-cyclone hoppers to prevent air infiltration upward through the hoppers and into each of the cyclone tubes. This air would impair cyclone particulate matter collection by disrupting the vortex of the inlet gas stream. Also, particles already in the hoppers could be entrained in the upward flowing air stream and driven out of the cyclone tube toward the outlet gas plenum.

A small diameter cyclone tube used in multi-cyclone collectors is shown in Figure 6-8. The gas stream entering the cyclone is spun as it passes over the turning vanes mounted at the inlet. The gas stream turns one-half to three times depending on the gas flow rate and the length and diameter of the cyclone. As in the case with large diameter cyclones, particles move toward the wall of the cyclone and subsequently fall by gravity. The gas stream turns 180° and passes out the center tube.

In large scale multi-cyclone collectors, the gas flow resistance of the outlet tubes can create an undesirable gas flow pattern called cross-hopper recirculation. As shown in Figure 6-9, the treated gas stream in the rows of cyclone tubes near the inlet can exit the bottom of the tube instead of the top, travel across the upper portions of the hopper, and pass upward through cyclone tubes near the back rows. This is possible due to the low gas flow resistance of the short outlet tubes for the cyclones on the back rows and the high gas flow resistance of the long outlet tubes for the inlet rows.

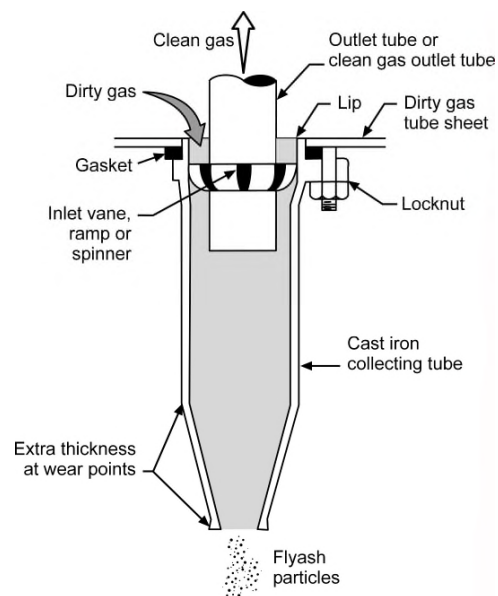


Figure 6-8. Cyclone tube used in multi-cyclone collector

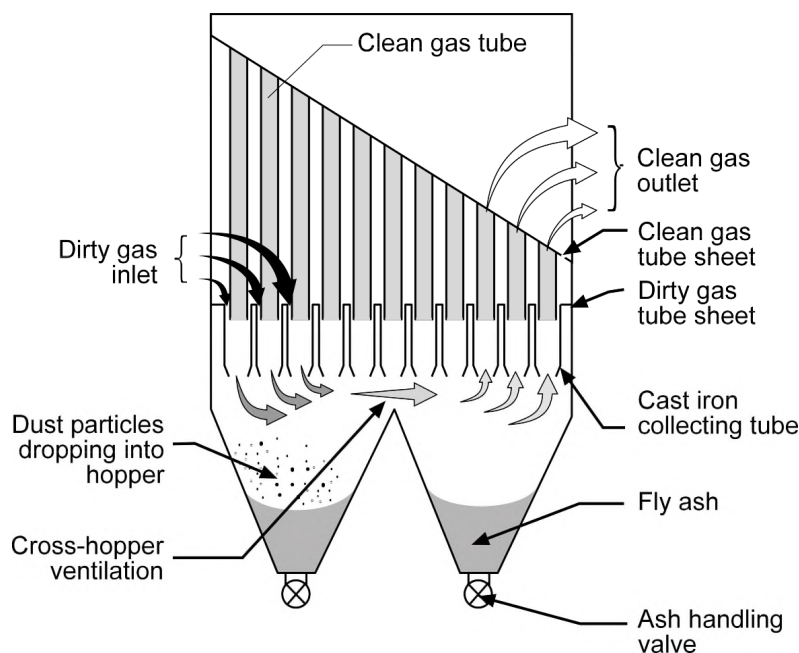


Figure 6-9. Cross hopper recirculation

Particulate matter emissions are increased substantially by cross-hopper recirculation because the gas stream passing through the hopper re-entrains dust from the hopper and because this gas disrupts the vortex in the cyclone tube it reenters. Cross-hopper recirculation can be avoided by designing the outlet tubes to be of equal length throughout the collector or by placing baffles in the hopper to prevent gas flow from the front to the back of the unit.

The hoppers of cyclone collectors should be designed to minimize solids discharge problems. Solids accumulation in the hoppers can block the cyclone tube outlets of both large diameter cyclones and small multi-cyclone tubes. Several hopper design features are used to minimize hopper solids overflow.

- Properly sealing solids discharge valve
- Adequately sized hopper throat
- Adequately sloped hopper walls
- Strike plates or vibrators
- Thermal insulation

Cyclones generally use rotary discharge valves or double flapper valves (see earlier discussion) for the discharge of solids from the hoppers. These valves must be well maintained to minimize air infiltration up through the hopper and into the cyclone tubes. It is important to note that most cyclone collectors are located on the inlet (upstream) side of the fan and operate with negative static pressures in the range of -2 to -10 in WC in the hopper area. The solids discharge valve must be in good condition to maintain an air seal with these moderately high negative static pressures.

The hopper throat must be sized to allow for adequate solids flow. Solids bridging in the hoppers might occur when the throat is undersized. The necessary size of the throat depends on the sizes of particles collected, the tendency of particles to agglomerate in the hopper, and the temperature of the solids being withdrawn from the hopper. It is common practice to use throats of at least 10 inches diameter. In some large units, the throats are in the range of 12 to 24 inches.

The hopper walls must be sloped properly to allow for solids movement toward the hopper throat. Generally hopper valley angles are at least 60 degrees. This severe slope minimizes the tendency for material to cling to the walls. It is also helpful to minimize protrusions into the hopper from the wall. Obstacles, such as U-shaped hand holds, can provide an initial site for solids accumulation and bridging even when the hopper walls are properly sloped.

Strike plates are reinforced, anvil-like plates mounted on the exterior hopper walls in an area near the hopper throat. These plates protrude through any thermal insulation and outer lagging present around the hopper wall. The purpose of these plates is to provide a site where operators can apply a moderate force to dislodge solids accumulating on the side walls or bridging over the hopper throats. Without these strike plates, operators might be tempted to use a sledge hammer on the unreinforced hopper wall. Over time, the use of a sledge hammer on the unprotected hopper wall causes it to bulge inward. The hammer-related deflections can choke off the approach to the throat and provide sites for more severe solids accumulation. Mounting a strike plate provides an inexpensive means to minimize this hopper discharge problem.

On large cyclone systems, an electric vibrator can be used in lieu of a strike plate or in combination with the strike plate. The electric vibrator is used whenever the solids discharge valves are operating in order to gently force solids in the hopper to flow toward the hopper

throat. Electrical vibrators are usually not economically reasonable for very small cyclone systems.

Thermal insulation is used around most mechanical collectors serving combustion sources. This helps to keep the solids hot and free flowing in the hoppers. It also minimizes stresses caused when the interior surface of metal is exposed to the 250°F to 600°F gas stream temperature while the exterior surface is exposed to ambient temperatures. It is common to install 2 to 4 inches of either mineral wool or fiberglass as insulating material around hoppers. In some cases, designers include an air gap and air stops under the thermal insulation to improve the insulating effect.

Performance Evaluation

Collection Efficiency

Two methods will be presented for evaluating the efficiency of a cyclone collector. The first is an older method, developed by Lapple (1951), for estimating the fractional efficiency of the average or standard cyclone. It is a relatively simple technique, but does not allow consideration of specific cyclone dimensions. Efficiencies determined with this technique should be considered only approximations. The second method was developed more recently by Leith, et al (1973). It is mathematically more complex, but allows consideration of the specific cyclone dimensions.

Lapple Technique

The first step in this procedure is the calculation of the particle size collected with 50% efficiency, termed the *cut diameter*, using the following equation:

$$[d_p]_{\text{cut}} = \sqrt{\frac{9\mu_g B_c}{2\pi n_t v_i \rho_p}} \quad (6-1)$$

where

- $[d_p]_{\text{cut}}$ = cut diameter (ft)
- μ_g = gas viscosity (lb_m/ft·sec)
- v_i = inlet gas velocity (ft/sec)
- ρ_p = particle density (lb_m/ft³)
- ρ_g = gas density (lb_m/ft³)
- B_c = cyclone inlet width (ft)
- n_t = number of turns

$$n_t = \frac{v_i t}{\pi D} \quad (6-2)$$

where

t = residence time (sec)
 D = cyclone diameter (ft)

$$t = \frac{V_{\text{cyclone}} - V_{\text{outlet core}}}{Q} \quad (6-3)$$

where

V_{cyclone} = total volume of cyclone (ft³)
 $V_{\text{outlet core}}$ = volume of outlet core [calculated from outlet pipe diameter] (ft³)
 Q = volumetric flow rate (ft³/sec)

The cut diameter is a characteristic of the cyclonic control device and should not be confused with the geometric mean particle diameter of the particle size distribution. The cut diameter takes into account the gas stream inlet velocity, the cyclone inlet width, the gas viscosity, and other factors that influence particle removal in the cyclone.

The second step is to calculate the $[d_p]_i/[d_p]_{\text{cut}}$ ratio for each particle size of interest. Finally, the fractional efficiencies, η_i , for each $[d_p]_i/[d_p]_{\text{cut}}$ ratio are read from Figure 6-10. These efficiencies may be used directly or they may be plotted against $[d_p]_i$ to form a fractional efficiency curve for a specific cyclone operation.

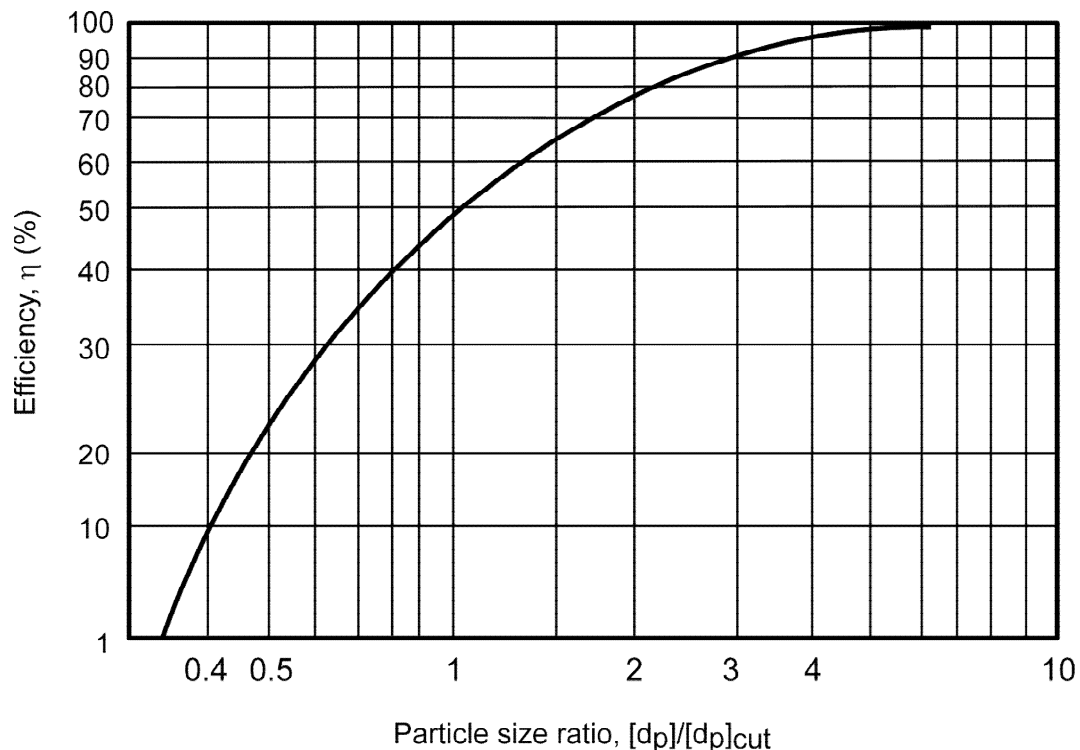


Figure 6-10. Lapple cyclone efficiency curve

These efficiency values give the estimated performance characteristics of a cyclone at the operating conditions used to estimate $[d_p]_{\text{cut}}$. Because this procedure only gives a very

approximate estimate, a range of cut diameters is often used instead of a single value. Maximum and minimum efficiency curves determined from these values will then give a range of efficiencies for evaluation purposes.

Example 6-1

A large diameter cyclone is being used for the removal of grain dust in the range of 8 to 100 μm diameter. What are collection efficiencies over this range if the cyclone has an inlet width of 1 ft, an inlet gas velocity of 50 ft/sec, and an operating temperature of 68°F? Assume $n_t = 1$ and a particle density of 80 lb_m/ft^3 .

Solution:

$$[d_p]_{\text{cut}} = \sqrt{\frac{9\mu_g B_c}{2\pi n_t v_i \rho_p}} = \sqrt{\frac{9\left(1.21 \times 10^{-5} \frac{\text{lb}_m}{\text{ft} \cdot \text{sec}}\right)(1 \text{ ft})}{2\pi(1)\left(50 \frac{\text{ft}}{\text{sec}}\right)\left(80 \frac{\text{lb}_m}{\text{ft}^3}\right)}} = 6.58 \times 10^{-5} \text{ ft} = 20 \mu\text{m}$$

Estimate efficiency of 8, 12, 20, 30, 50 and 100 μm diameter particles:

Example 6-1 Efficiency Estimates		
$[d_p]_i$ (μm)	$[d_p]_i/[d_p]_{\text{cut}}$	η_i (%)
8	0.40	9
12	0.60	28
20	1.00	50
30	1.50	65
50	2.50	85
100	5.00	98

Leith Technique

The fractional efficiency equation of Leith and Licht is similar to many equations developed for particulate control devices:

$$\eta = 1 - e^{-2(C\Psi)^{\frac{1}{2n+2}}} \quad (6-4)$$

where

- η_i = efficiency for particle diameter i (dimensionless)
- C = cyclone dimension factor (dimensionless)
- Ψ = cyclone inertial impaction parameter (dimensionless)
- n = vortex exponent (dimensionless)

The following steps are involved in the solution of Equation 6-4:

1. Calculate n from Equation 6-5, using Equation 6-6 to adjust the value from ambient to elevated temperature, if necessary:

$$n = \frac{(12D)^{0.14}}{2.5} \quad (6-5)$$

where

D = cyclone diameter (ft)

$$\frac{1 - n_1}{1 - n_2} = \left(\frac{T_1}{T_2} \right) \quad (6-6)$$

where

n_1 = vortex index at ambient temperature (dimensionless)

n_2 = vortex index at elevated temperature (dimensionless)

T_1 = ambient absolute temperature ($^{\circ}\text{R}$)

T_2 = elevated absolute temperature ($^{\circ}\text{R}$)

2. Calculate the vortex natural length, l , and compare this with the value of the dimension $(H - S)$:

$$l = 2.3D_e \left(\frac{D^2}{ab} \right)^{1/3} \quad (6-7)$$

where

l = vortex natural length (ft)

D_e = cyclone outlet diameter (ft)

D = cyclone diameter (ft)

a = cyclone inlet height (ft)

b = cyclone inlet width (ft)

$H-S$ = overall cyclone height - outlet pipe length

- A. If $l < (H - S)$, calculate V_{nl} :

$$V_{nl} = \frac{\pi D^2}{4} (h - S) + \frac{\pi D^2}{4} \left(\frac{1 + S - h}{3} \right) \left(1.0 + \frac{d}{D} + \frac{d^2}{D^2} \right) - \frac{\pi D_e^2 l}{4} \quad (6-8)$$

$$d = D - (D - B) \left(\frac{1 + S - h}{H - h} \right) \quad (6-8a)$$

where

V_{nl} = volume of cyclone at natural length (ft^3)

- D = cyclone diameter (ft)
- h = height of upper cylindrical body of cyclone (ft)
- S = outlet pipe length (ft)
- l = vortex natural length (ft)
- D_e = outlet pipe diameter (ft)
- H = overall cyclone height (ft)

B. If $l > (H - S)$, calculate V_H :

$$V_H = \frac{\pi D^2}{4}(h - S) + \frac{\pi D^2}{4} \left(\frac{H - h}{3} \right) \left(1.0 + \frac{B}{D} + \frac{B^2}{D^2} \right) - \frac{\pi D_e^2}{4}(H - S) \quad (6-9)$$

where

- V_H = volume of cyclone below end of exit pipe (ft³)
- B = dust outlet diameter (ft)

3. Calculate K_c using either V_{nl} or V_H :

$$K_c = \frac{V_s + \frac{V_{nl}}{2}}{D^3} \text{ or } K_c = \frac{V_s + \frac{V_H}{2}}{D^3} \quad (6-10)$$

$$V_s = \frac{\pi \left(S - \frac{a}{2} \right) (D^2 - D_e^2)}{4} \quad (6-10a)$$

where

- K_c = cyclone volume constant (dimensionless)
- V_s = annular shaped volume above exit duct to midlevel of entrance duct (ft³)
- V_{nl} = volume of cyclone at natural length (ft³)
- V_H = volume of cyclone below end of exit pipe (ft³)
- S = outlet pipe length (ft)
- D = cyclone diameter (ft)
- D_e = outlet pipe diameter (ft)
- a = cyclone inlet height (ft)

4. Calculate the cyclone dimension factor:

$$C = \frac{8K_c}{K_a K_b} \quad (6-11)$$

where

- C = cyclone dimension factor (dimensionless)
- K_a = cyclone inlet height divided by the cyclone diameter, a/D (dimensionless)

K_b = cyclone inlet width divided by the cyclone diameter, b/D (dimensionless)

K_c = cyclone volume constant (dimensionless)

5. Calculate the cyclone inertial impaction parameter for a single particle size:

$$\Psi = \frac{\rho_p d_p^2 u_{T_2} (n + 1)}{18 \mu_g D} \quad (6-12)$$

$$u_{T_2} = \frac{Q}{ab} \quad (6-12a)$$

where

Ψ = cyclone inertial impaction parameter (dimensionless)

ρ_p = particle density (lb_m/ft^3)

d_p = particle diameter (ft)

u_{T_2} = tangential velocity of particle at cyclone wall (ft/sec)

μ_g = gas viscosity ($\text{lb}_m/\text{ft}\cdot\text{sec}$)

D = cyclone diameter (ft)

n = vortex exponent (dimensionless)

Q = gas flow rate (ft^3/sec)

a = cyclone inlet height (ft)

b = cyclone inlet width (ft)

6. Using the values of C , Ψ and n , determine the collection efficiency using Equation 6-4.
7. Repeat the calculation of Ψ for a series of particle sizes and determine the efficiency for each size.

This technique is obviously more complex than that of Lapple. However, it allows consideration of the actual cyclone dimensions and, when compared to experimental data, gives more accurate estimates. An Excel spreadsheet is available from your instructor to ease some of the pain in using this method.

Pressure Drop

The pressure drop across a cyclone is an important parameter for the operator of the equipment. Increased pressure drop means greater costs for power to move exhaust gas through the control device. With cyclones, an increase in pressure drop usually means that there will be an improvement in collection efficiency.

One method for estimating pressure drop is based on the velocity head and the inlet and outlet dimensions of the cyclone:

$$\Delta P = 0.003K_c \rho_g v_g^2 \left(\frac{ab}{D_e^2} \right) \quad (6-13)$$

where

ΔP = static pressure drop (in WC)

K_c = 16, for tangential inlet; 7.5, for inlet vane (dimensionless)

ρ_g = gas density (lb_m/ft^3)

v_g = inlet velocity (ft/sec)

a = cyclone inlet height (ft)

b = cyclone inlet width (ft)

D_e = outlet pipe diameter (ft)

Another method is similar. It bases the pressure drop on the velocity head, but includes all other effects in a single constant:

$$\Delta P = K_p \rho_g v_g^2 \quad (6-14)$$

where

ΔP = static pressure drop (in WC)

K_p = 0.013 to 0.024 (dimensionless)

ρ_g = gas density (lb_m/ft^3)

v_g = inlet velocity (ft/sec)

Example 6-2

A single high efficiency cyclone has an inlet width of 2 ft, an inlet height of 5 ft and an outlet pipe diameter of 5 ft. Estimate the pressure drop when the inlet velocity is 50 ft/sec and the gas temperature is 68°F.

Solution:

Using Equation 6-13:

$$\Delta P = 0.003K_c \rho_g v_g^2 \left(\frac{ab}{D_e^2} \right) = 0.003(16) \left(0.075 \frac{\text{lb}_m}{\text{ft}^3} \right) \left(50 \frac{\text{ft}}{\text{sec}} \right)^2 \left[\frac{(5 \text{ ft})(2 \text{ ft})}{(5 \text{ ft})^2} \right] = 3.6 \text{ in WC}$$

Using Equation 6-14:

Since this is a high efficiency cyclone design, assume $K_p = 0.024$.

$$\Delta P = K_p \rho_g v_g^2 = 0.024 \left(0.075 \frac{\text{lb}_m}{\text{ft}^3} \right) \left(50 \frac{\text{ft}}{\text{sec}} \right)^2 = 4.5 \text{ in WC}$$

Instrumentation

There are usually few instruments on cyclone collectors, due primarily to their small size and service requirements. On moderate-to-large systems, the following instruments might be useful.

- Static pressure drop gauges
- Inlet and outlet temperature gauges

Cyclones collectors are usually not equipped with opacity monitors due to the limited light-scattering characteristics of the moderate-to-large diameter particles collected in these units.

Static Pressure Drop Gauges

The static pressure drop across the unit is dependent mainly on the inlet gas velocity and the physical conditions of the cyclonic collector. The inlet gas velocity is dependent directly on the gas flow rate, which in turn is a function of the process operating rate. At a given process operating rate, the pressure drop is dependent almost exclusively on the physical condition of the collector. This fact can be used to evaluate mechanical problems within the collector that could impair performance. An increase in the pressure drop at a given process operating rate could indicate solids plugging at the inlet to the cyclone tubes of multi-cyclone collectors. A decrease in the pressure drop at a given process operating rate could be due to a variety of problems:

- Erosion of the inlet turning vanes in multi-cyclone collectors
- Erosion of the outlet tubes in multi-cyclone collectors
- Failure of one or more of the gaskets on the clean side tube sheet of multi-cyclone collectors

The static pressure gauge provides the only data that can be used to readily identify these problems while the unit is operational. This relatively inexpensive instrument is very useful.

Inlet and Outlet Gas Temperature Gauges

Air infiltration is a common problem with multi-cyclone collectors serving combustion sources. It is caused by frequent thermal expansion and contraction as the boiler load varies, by erosion of the solid discharge valve, and by aging of the high temperature gaskets. Air leaking into the hopper area of a multi-cyclone collector can significantly reduce the particulate removal efficiency. The intruding air re-entrains particulate matter from the hopper and disrupts the vortices in the cyclone tubes as it moves upward toward the outlet tubes.

The onset of air infiltration problems can be readily identified by the gas temperature drop across the unit. The relatively cold ambient air dilutes the flue gas stream and increases the temperature drop across the unit. A multi-cyclone collector with a gas temperature drop of more than about 25°F probably has significant air infiltration, assuming that the temperature

data are correct and representative. Increases in the gas temperature drop of 5 to 10°F from the baseline range (at a given boiler load) are also indicative of significant air infiltration. The cost of the temperature gauges at the inlet and outlet is relatively small compared to the benefits provided with respect to the early identification of air infiltration problems. The temperature gauges are usually mounted in the inlet and outlet ductwork.

Review Questions

1. What is the normal range of inlet gas stream velocity for large diameter cyclones?
 - a. 5 to 10 feet per second
 - b. 20 to 50 feet per second
 - c. 5 to 10 feet per minute
 - d. 20 to 50 feet per minute

2. What is the purpose of using a solids discharge valve on the hoppers of cyclone collectors? Select all that apply.
 - a. Minimize air infiltration into the cyclone
 - b. Minimize the risk of fires
 - c. Maintain solids flow out of the hopper

3. What design feature initiates the spinning gas flow in a large diameter cyclone?
 - a. Turning vanes
 - b. Gravity
 - c. Tangential gas inlet
 - d. None of the above

4. Which type of cyclone collector has higher radial velocities?
 - a. Large diameter cyclones
 - b. Multi-cyclones

5. What is the purpose of the clean side tube sheet in a multi-cyclone collector?
 - a. Support the cyclone tubes
 - b. Separate the inlet gas stream from the outlet gas stream
 - c. Separate the outlet gas stream from the hopper
 - d. None of the above

6. What is the typical number of complete turns (360 degrees) achieved in a large diameter cyclone operating with a normal inlet gas velocity?
 - a. One-half to three
 - b. Two to five
 - c. Five to ten
 - d. Greater than ten

7. What is the typical range in the diameters of multi-cyclone tubes?
- 1 to 6 inches
 - 6 to 12 inches
 - 12 to 18 inches
 - 18 to 24 inches
8. Must multi-cyclone tubes be oriented vertically (inlet at top, cyclone discharge at bottom) in order to operate properly?
- Yes
 - No
9. Why is it important to fabricate the outlet extension tubes of multi-cyclone collectors from abrasion resistant material?
- Minimize abrasion caused by the inlet gas stream
 - Minimize abrasion caused by the outlet gas stream
 - Minimize fracturing the inlet particulate matter
 - All of the above
10. The performance of a cyclone collector is related to the _____ of the particle diameter.
- First power
 - Second power
 - Third power
 - Performance is independent of particle size
11. The performance of a cyclone collector is related to the _____ of the gas velocity.
- First power
 - Second power
 - Third power
 - Performance is independent of radial gas velocity
12. Static pressure drop across a cyclone collector is related to the _____ of the gas flow rate.
- First power
 - Second power
 - Third power
 - Static pressure drop is independent of gas flow rate

13. Typical static pressure drops in a multi-cyclone collector are _____.

- a. 1 to 3 in WC
- b. 2 to 6 in WC
- c. 1 to 3 psig
- d. 2 to 6 psig

14. Multi-cyclone collectors are capable of effectively removing particles down to approximately _____ micrometers.

- a. 0.5 micrometers
- b. 3 micrometers
- c. 10 micrometers
- d. 20 micrometers
- e. 50 micrometers

This page intentionally left blank.

Review Question Answers

1. What is the normal range of inlet gas stream velocity for large diameter cyclones?
 - b. 20 to 50 feet per second
2. What is the purpose of using a solids discharge valve on the hoppers of cyclone collectors? Select all that apply.
 - a. Minimize air infiltration into the cyclone
 - b. Minimize the risk of fires
 - c. Maintain solids flow out of the hopper
3. What design feature initiates the spinning gas flow in a large diameter cyclone?
 - c. Tangential gas inlet
4. Which type of cyclone collector has higher radial velocities?
 - b. Multi-cyclones
5. What is the purpose of the clean side tube sheet in a multi-cyclone collector?
 - b. Separate the inlet gas stream from the outlet gas stream
6. What is the typical number of complete turns (360 degrees) achieved in a large diameter cyclone operating with a normal inlet gas velocity?
 - a. One-half to three
7. What is the typical range in the diameters of multi-cyclone tubes?
 - b. 6 to 12 inches
8. Must multi-cyclone tubes be oriented vertically (inlet at top, cyclone discharge at bottom) in order to operate properly?
 - b. No
9. Why is it important to fabricate the outlet extension tubes of multi-cyclone collectors from abrasion resistant material?
 - a. Minimize abrasion caused by the inlet gas stream

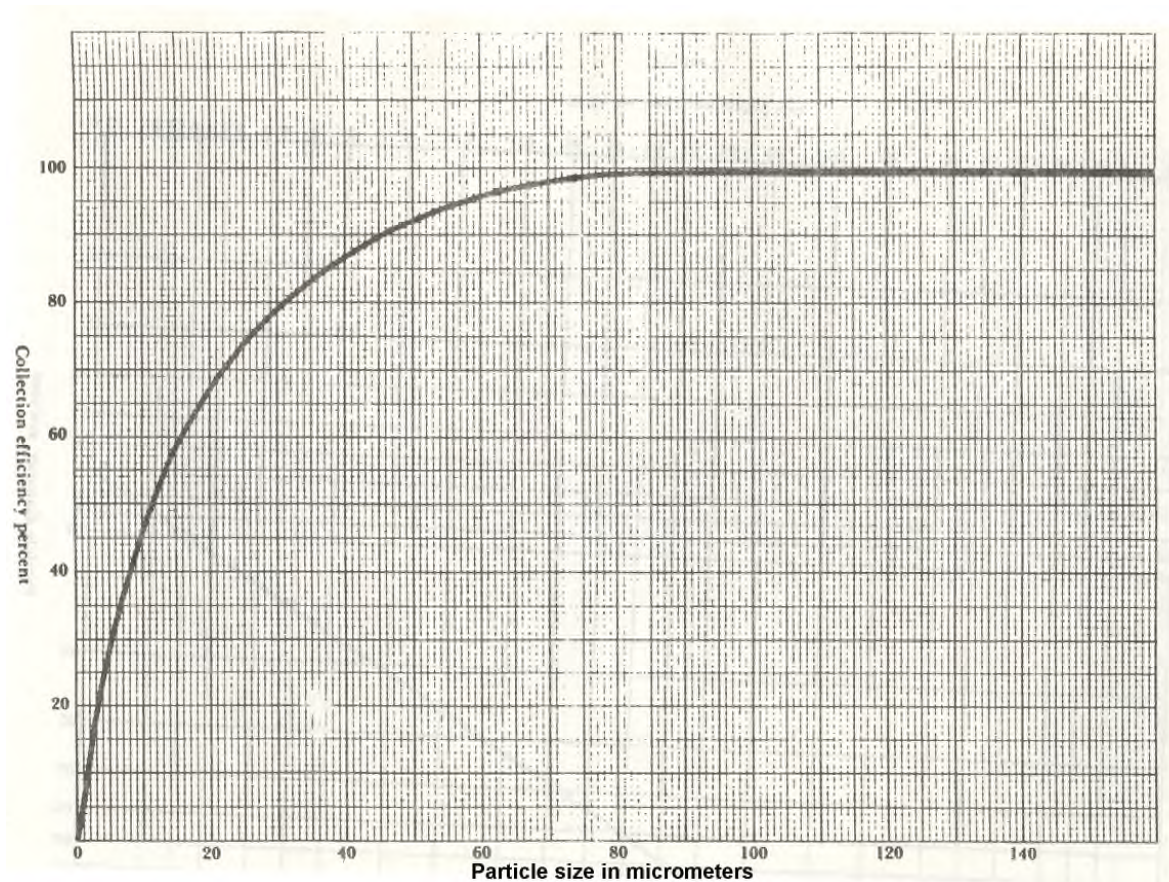
10. The performance of a cyclone collector is related to the _____ of the particle diameter.
- b. Second power
11. The performance of a cyclone collector is related to the _____ of the gas velocity.
- b. Second power
12. Static pressure drop across a cyclone collector is related to the _____ of the gas flow rate.
- b. Second power
13. Typical static pressure drops in a multi-cyclone collector are _____.
- b. 2 to 6 in WC
14. Multi-cyclone collectors are capable of effectively removing particles down to approximately _____ micrometers.
- b. 3 micrometers

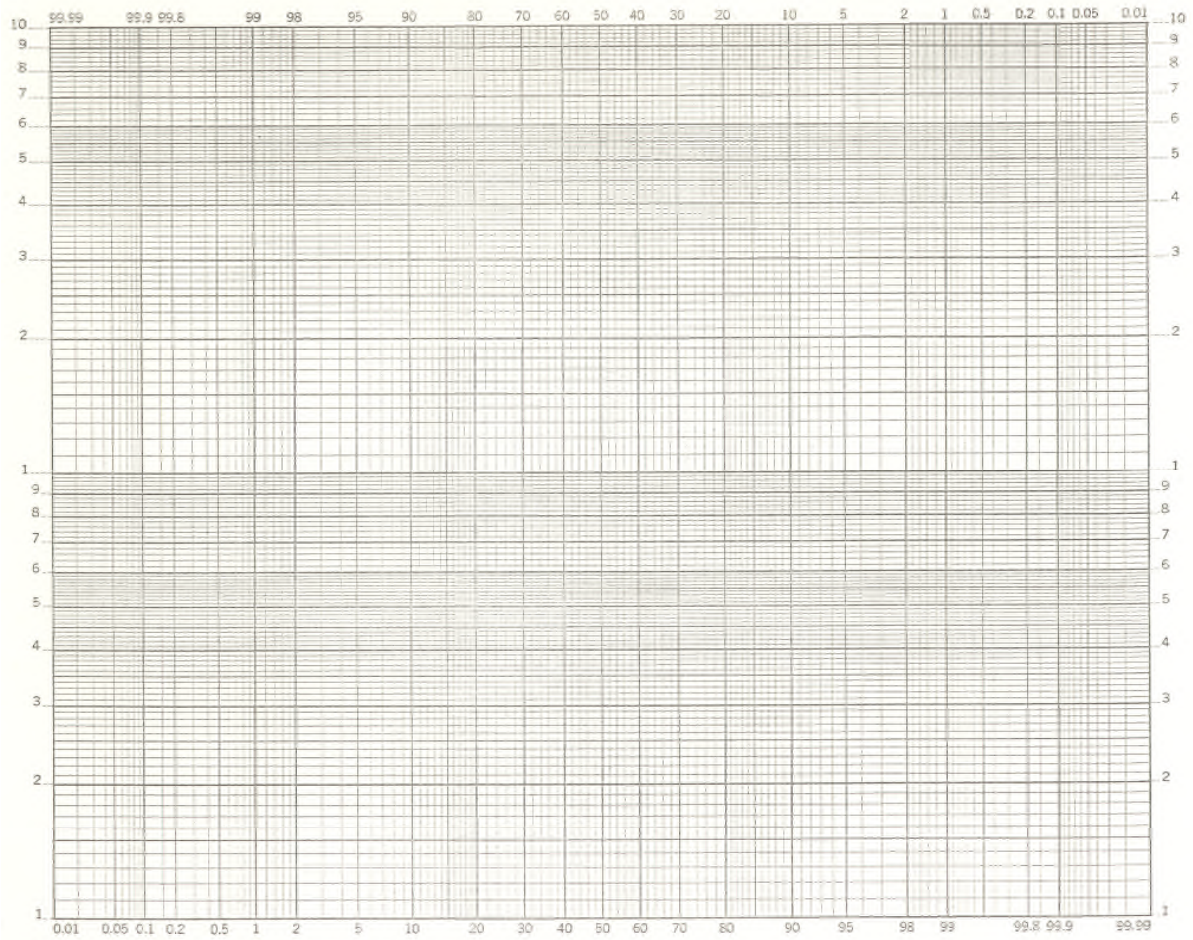
Review Problems

1. What is the overall collection efficiency for a single cyclone collecting dust with the distribution given below. The collector has an inlet width of 1 ft, an inlet gas velocity of 50 ft/sec, and an operating temperature of 200°F? The particle density is 70 lb_m/ft³. Assume the gas stream spins two complete rotations within the cyclone.

Size (μm)	% of Mass
10	1
20	3
30	9
40	13
50	24
60	29
70	15
80	4
100	2
	100%

2. A single cyclone collector has the following fractional efficiency curve. Estimate the overall collection efficiency of a dust with a d_{50} of 50 μm and a σ_g of 1.67.





Review Problem Solutions

1. What is the overall collection efficiency for a single cyclone collecting dust with the distribution given below. The collector has an inlet width of 1 ft, an inlet gas velocity of 50 ft/sec, and an operating temperature of 200°F? The particle density is 70 lb_m/ft³. Assume the gas stream spins two complete rotations within the cyclone.

Size (μm)	% of Mass
10	1
20	3
30	9
40	13
50	24
60	29
70	15
80	4
100	2
	100%

Solution:

Estimate the gas viscosity at 200°F:

$$\mu = \mu_{\text{ref}} \left(\frac{T}{T_{\text{ref}}} \right)^{0.768} = 1.21 \times 10^{-5} \frac{\text{lb}_m}{\text{ft} \cdot \text{sec}} \left(\frac{660^\circ\text{R}}{528^\circ\text{R}} \right)^{0.768} = 1.44 \times 10^{-5} \frac{\text{lb}_m}{\text{ft} \cdot \text{sec}}$$

Calculate the cut diameter:

$$[d_p]_{\text{cut}} = \sqrt{\frac{9\mu_g B_c}{2\pi n_t v_i \rho_p}} = \sqrt{\frac{9 \left(1.44 \times 10^{-5} \frac{\text{lb}_m}{\text{ft} \cdot \text{sec}} \right) (1 \text{ ft})}{2\pi (2) \left(50 \frac{\text{ft}}{\text{sec}} \right) \left(70 \frac{\text{lb}_m}{\text{ft}^3} \right)}} = 5.43 \times 10^{-5} \text{ ft} = 16.5 \mu\text{m}$$

Calculate the fractional efficiencies:

Problem 6-1 Efficiency Estimates		
$[d_p]_i$ (μm)	$[d_p]_i/[d_p]_{\text{cut}}$	η_i (%)
10	0.6	28
20	1.2	55
30	1.8	74
40	2.4	83
50	3.0	90
60	3.6	94
70	4.2	97
80	4.8	98
100	6.1	100

Calculate the overall efficiency:

Size (μm)	% of Mass	η (%)	Mass collected (%)
10	1	28	0.28
20	3	55	1.65
30	9	74	6.66
40	13	83	10.79
50	24	90	21.60
60	29	94	27.26
70	15	97	14.55
80	4	98	3.92
100	2	100	2.00
	100%		88.71%

2. A single cyclone collector has the following fractional efficiency curve. Estimate the overall collection efficiency of a dust with a d_{50} of $50 \mu\text{m}$ and a σ_g of 1.67.

Solution:

Plot cumulative distribution plot:

For a “% of mass less than size” plot--

$$\sigma_g = \frac{d_{50}}{d_{15.87}}$$

so
$$d_{15.87} = \frac{d_{50}}{\sigma_g} = \frac{50 \mu\text{m}}{1.67} = 30 \mu\text{m}$$

$$\sigma_g = \frac{d_{84.13}}{d_{50}}$$

so $d_{84.13} = \sigma_g \times d_{50} = 1.67 \times 50 \mu\text{m} = 83.5 \mu\text{m}$

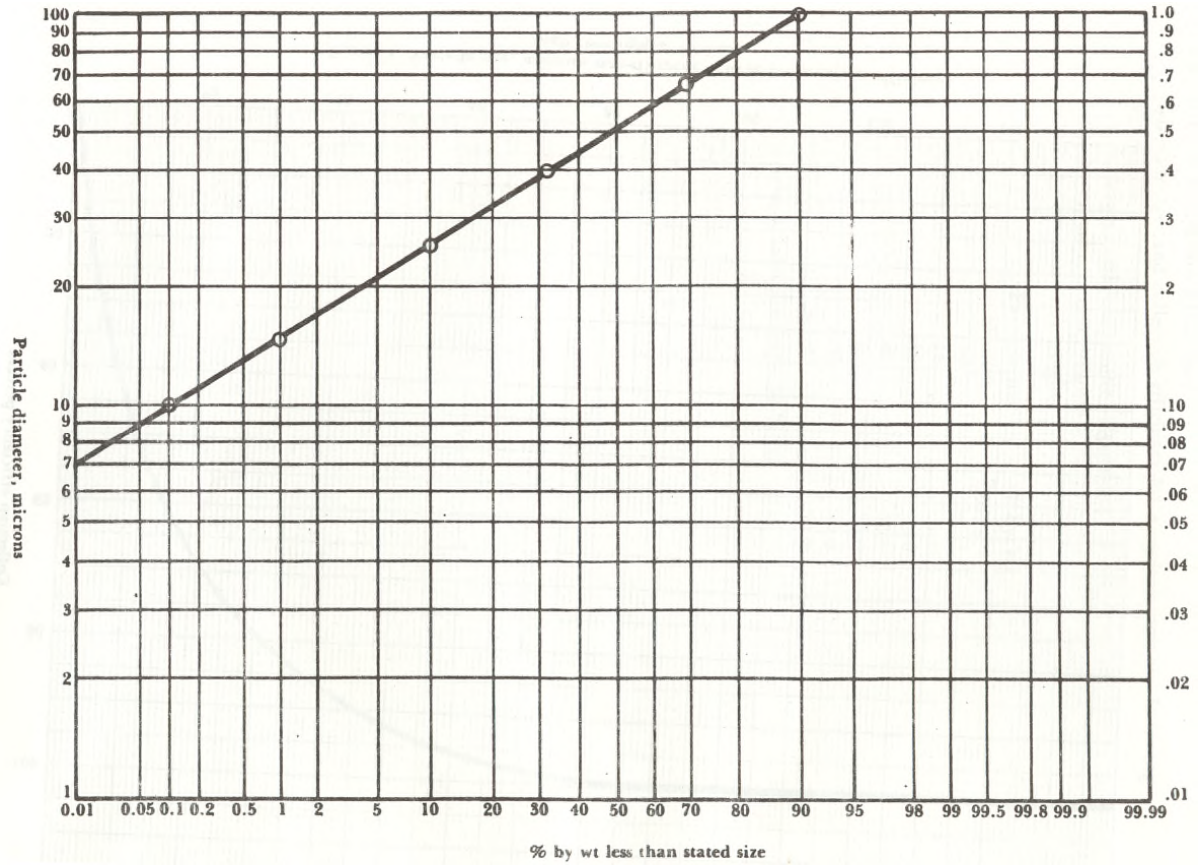
Plot the three points and draw a straight line through them.

Divide distribution into particle size ranges and determine the percent mass in each size range:

Size (μm)	% of Mass Less Than Size	Size Range (μm)	% of Mass
10	0.1	0 to 10	0.1
15	1.0	10 to 15	0.9
26	10.0	15 to 26	9.0
40	32.0	26 to 40	22.0
67	70.0	40 to 67	38.0
100	90.0	67 to 100	20.0
		>100	10.0

Calculate the overall efficiency:

Size Range (μm)	Average Size (μm)	% of Mass	η (%)	Mass Collected (%)
0 to 10	5.0	0.1	28	0.03
10 to 15	12.5	0.9	52	0.47
15 to 26	20.5	9.0	68	6.12
26 to 40	33.0	22.0	82	18.04
40 to 67	53.5	38.0	93	35.34
67 to 100	83.5	20.0	99	19.80
>100	100.0	10.0	99	9.90
		100%		89.70%



References

Lapple, C.E., “Processes use many collection types”, *Chemical Engineering*, **58**, 145 (1951).

Leith, D., and W. Licht, “The collection efficiency of cyclone type particle collectors—a new theoretical approach”, *AIChE Symposium Series*, Vol. 68, No. 126 (1973).

Shepard, C.B., and C.E. Lapple, “Flow pattern and pressure drop in cyclone dust collectors”, *Industrial and Engineering Chemistry*, **31**, 972 (1939).

This page intentionally left blank.

CHAPTER 7

FABRIC FILTERS

Fabric filters, also referred to as *baghouses*, are capable of high-efficiency particulate matter removal in a wide variety of industrial applications. Uses for fabric filters have steadily expanded since the 1960s, because of the development of new, highly effective fabrics capable of efficiently collecting particles over the size range of 0.1 μm to 1,000 μm . This particle collection efficiency, even in the difficult-to-control range of 0.2 μm to 0.5 μm , is due to the multiple opportunities for a particle to be captured as it attempts to pass through a dust cake and fabric and the multiple modes of particle capture that occur within the dust cake and fabric. These modes of capture include impaction, Brownian diffusion, and electrostatic attraction.

The conceptual simplicity of fabric filters belies the complexity of the equipment design and the operating procedures necessary to achieve and maintain high particulate removal efficiencies. Serious performance problems can develop relatively rapidly. Holes and tears in the bags can develop due to chemical attack, high temperature excursions, or abrasion and flex damage. Cleaning system problems can result in excessive static pressure drops. Particles can also seep through the dust cake and fabric due to improper design or cleaning.

This chapter emphasizes four of the major types of fabric filters: shaker, reverse air, pulse jet, and cartridge. There are many other types that are not explicitly discussed in this manual. However, the operating principles and evaluation procedures discussed are generally applicable to all types of fabric filters. All fabric filters designs typically operate with a static pressure drop of about 4-6 in. WC.

Operating Principles

Particle Collection

Multiple mechanisms are responsible for particle capture within dust layers and fabrics. Impaction is an inertial mechanism that is most effective on particles larger than about 1 μm . It is effective in fabric filters because there are many sharp changes in flow direction as the gas stream moves around the various particles and fibers. Unlike some types of particulate collection devices, there are multiple opportunities for particle impaction due to the numbers of individual dust cake particles and fabric fibers in the gas stream path.

Brownian diffusion is moderately effective for collecting submicrometer particles because of the close contact between the gas stream and the dust cake. The particle does not have to be displaced a long distance in order to come into contact with a dust cake particle or fiber.

Furthermore, the displacement of submicrometer particles can occur over a relatively long time as the gas stream moves through the dust cake and fabric.

Electrostatic attraction is another particle collection mechanism. Particles can be attracted to the dust layer and fabric due to the moderate electrical charges that accumulate on the fabrics, the dust layers, and the particles. Both positive and negative charges can be generated, depending on the chemical make-up of the materials. Particles are attracted to the dust layer particles or fabric fibers when there is a difference in charge polarity or when the particle has no electrical charge.

Sieving of particulate matter can occur after the dust cake is fully established. The net result of the various types of collection mechanisms is shown in Figure 7-1, which indicates relatively high removal efficiency levels even in the difficult-to-control particle size range of 0.2 μm to 0.5 μm .

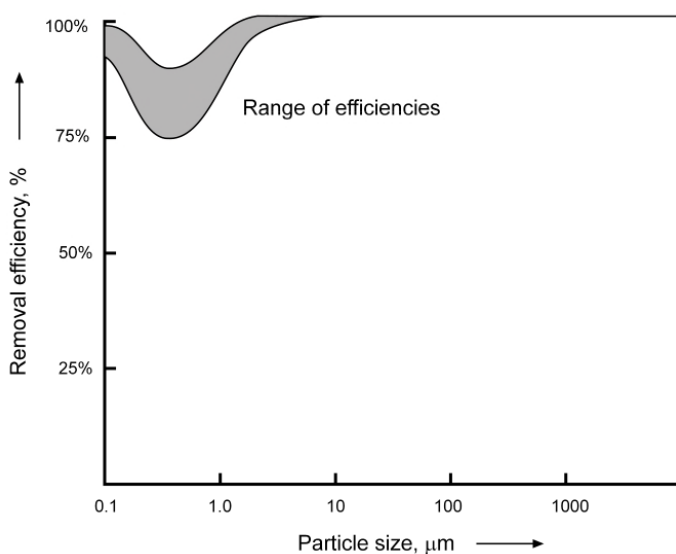


Figure 7-1. Fabric filter fractional efficiency curve

For new bags, the initial particle removal efficiency is not nearly as high as suggested in Figure 7-1. Time is needed to establish residual dust cakes on the surfaces of the fabric. These particles provide the foundation for the accumulation of the operating mode dust cake, which is ultimately responsible for the high efficiency particulate matter removal. The particles on the fabric surface are termed the *residual dust cake* because they remain after normal cleaning of the bag.

The fractional efficiency curve shown in Figure 7-1 applies only when an adequate dust cake has been established. Immediately after cleaning, patchy areas of the fabric surface may be exposed. Only the residual dust cake remains in these patchy areas. Depending on the particulate matter concentration, it may take several seconds to a minute for the dust cake to repair over these patchy areas and thereby reduce emissions. During the time that the dust cake is being reestablished, particle removal efficiency can be low, especially for small

particles. For this reason, excessive cleaning intensity, frequency, or duration can increase particulate emissions.

Particulate matter emissions can be increased dramatically by related phenomena such as particle seepage and pore collapse. Both phenomena are related to the quantity of gas passing through a given area of the cloth. This gas flow rate is normally expressed as the air-to-cloth ratio, as defined in Equation 7-1:

$$A / C \text{ Ratio} \left(\frac{\text{ft}}{\text{min}} \right) = \frac{\text{Actual Gas Flow Rate} \left(\frac{\text{ft}^3}{\text{min}} \right)}{\text{Fabric Surface Area} \left(\text{ft}^2 \right)} \quad (7-1)$$

As the air-to-cloth ratio increases, the localized gas velocities through the dust cake and fabric increase. At high air-to-cloth values, some particles, especially small particles, can gradually migrate through the dust layer and fabric. This is possible because dust particles within the cake are retained relatively weakly. After passing through the dust cake and fabric, these particles are re-entrained in the clean gas stream leaving the bag. Some of the factors that increase the tendencies for particle bleed-through include the following:

- Small particle size distribution
- Fabric flexing and movement
- Small dust cake quantities

Pore collapse in woven fabrics is also caused by high air-to-cloth ratios. At high air-to-cloth ratios, the forces on the particle bridges that span the holes in the fabric weave can be too large. Once a bridge is shattered and pushed through the fabric, an uncovered hole is created. The gas stream channels through this low resistance path through the bag.

The net result of seepage and pore collapse is increased particulate matter emissions at high air-to-cloth ratios. The general nature of the relationship is shown in Figure 7-2. The effect is relatively minor until a threshold air-to-cloth ratio is reached. Above this value, emissions can increase rapidly. A baghouse that is severely undersized for the gas flow being treated (high air-to-cloth ratio) can have abnormally low removal efficiency.

Pressure Drop

The static pressure drop across a fabric filter system is important for several reasons. Lower-than-normal static pressure drop indicates that there may be insufficient dust cake thickness, resulting in reduced collection efficiency. Higher-than-expected static pressure drop increases the overall system resistance to gas flow. Decreased gas flow from the process area will result if the centrifugal fan and damper system cannot compensate for this increased resistance. Fugitive emissions can occur when the gas flow rate at the hood is too low. High static pressure drop also increases the electrical energy needed for the centrifugal fan, increasing the operating costs for the system.

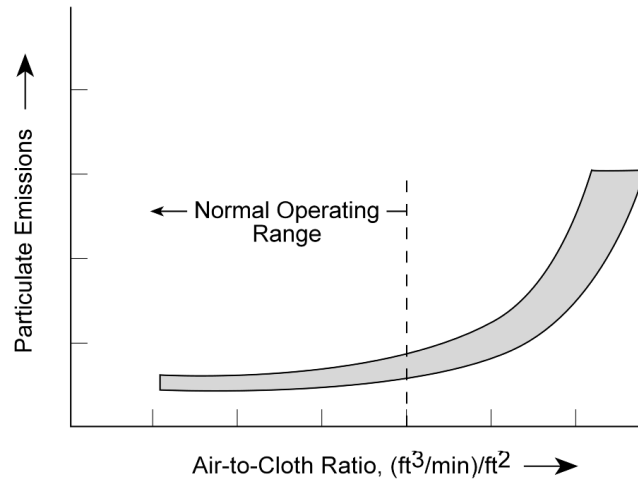


Figure 7-2. Emissions as a function of air-to-cloth ratio

There are two alternative locations for monitoring the static pressure drop of a fabric filter. As indicated in Figure 7-3, the gauge can be mounted across the tube sheet that supports the bag and separates the clean side from the dirty or unfiltered side of the unit. An instrument in this location is termed the *media static pressure drop gauge* because it indicates the resistance to gas flow caused only by the filter media and the dust cake on the filter media. A gauge that monitors the static pressure drop from the inlet duct to the outlet duct, also shown in Figure 7-3, is termed the *overall static pressure drop gauge*. In this location, the static pressure drop gauge monitors the frictional losses at the inlet of the fabric filter, the pressure drop across the media and the dust cake on the media, the frictional losses at the entrance of the outlet duct, and the acceleration losses at the entrance of the outlet duct. The overall static pressure drop value is usually 1 to 3 in. WC higher than the media static pressure drop value. This difference is due primarily to the acceleration losses and frictional losses at the entrance of the outlet duct.

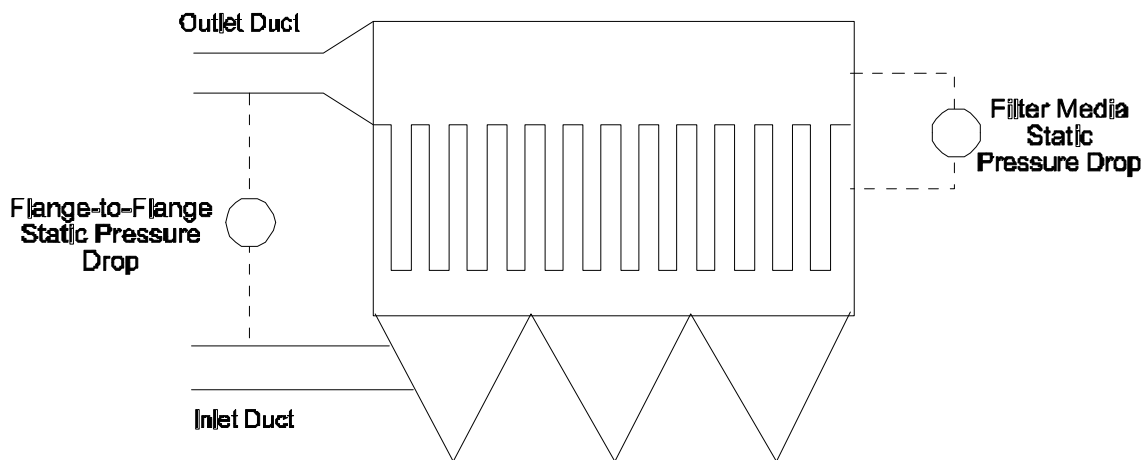


Figure 7-3. Flange-to-flange and filter media static pressure drops

One simple model for the media static pressure drop is to express it as the sum of the pressure drop across the filter media and the pressure drop across the dust cake, as shown in Equation 7-2.

$$\Delta P_{\text{total}} = \Delta P_{\text{media}} + \Delta P_{\text{dust cake}} \quad (7-2)$$

The static pressure drop across filter media can then be approximated by Equation 7-3 and the pressure drop across the dust cake by Equation 7-4.

$$\Delta P_{\text{media}} = k_1 v_f \quad (7-3)$$

where:

- ΔP_{media} = pressure drop across filter media (in. WC)
- k_1 = filter media resistance constant (in. WC/(ft/min))
- v_f = velocity through filter (ft/min)

$$\Delta P_{\text{dust cake}} = k_2 c_i v_f^2 t \quad (7-4)$$

where:

- $\Delta P_{\text{dust cake}}$ = pressure drop across dust cake (in. WC)
- k_2 = dust cake resistance constant (in. WC/(ft/min)(lb_m/ft²))
- v_f = velocity through filter (ft/min)
- c_i = particulate concentration (lb_m/ft³)
- t = filtration time (min)

Substituting Equation 7-3 and 7-4 into Equation 7-2 give:

$$\Delta P_{\text{total}} = k_1 v_f + k_2 c_i v_f^2 t \quad (7-5)$$

Dividing both sides of Equation 7-5 by v_f , the velocity through the filter, gives:

$$S_f = \frac{\Delta P_{\text{total}}}{v_f} = k_1 + k_2 c_i v_f t \quad (7-6)$$

where:

- S_f = filter drag (in. WC/(ft/min))

Equation 7-6 gives a straight line when S_f is plotted against $c_i v_f t$, the dust loading on the filter surface in lb_m/ft². The slope of this straight line is k_2 and the intercept (the value at zero dust loading) is k_1 .

Unfortunately, the behavior of the static pressure drop is not quite this simple. First, during normal bag cleaning, not all of the dust cake is removed. As noted previously, a residual dust cake remains that serves as the foundation for the accumulation of the operating mode dust cake. Secondly, the repair of the dust cake that occurs after cleaning results in non-linear behavior. Accordingly, the profile for the filter drag is better represented by Figure 7-4.

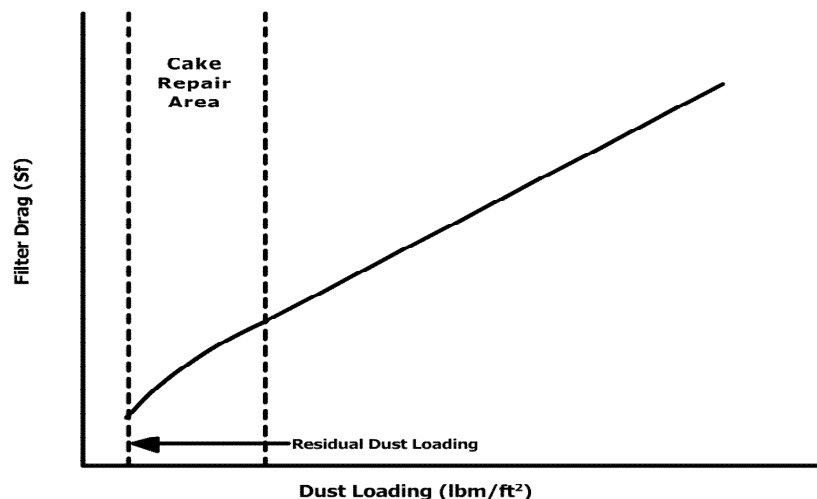


Figure 7-4. Filter drag as a function of dust loading

Certainly, the pressure drop across the dust cake will increase steadily over time, as indicated by Equation 7-4. It will become necessary to clean the bags when the static pressure drop reaches the design maximum value, which is generally in the range of 5 to 6 in. WC. During cleaning, a portion of the dust cake is removed, and the overall pressure drop is reduced. This results in the sawtooth-type pressure drop profile illustrated in Figure 7-5. The degree of variation in the static pressure drop profile depends on the frequency of cleaning, the intensity of cleaning, and the fraction of bags cleaned at any given time.

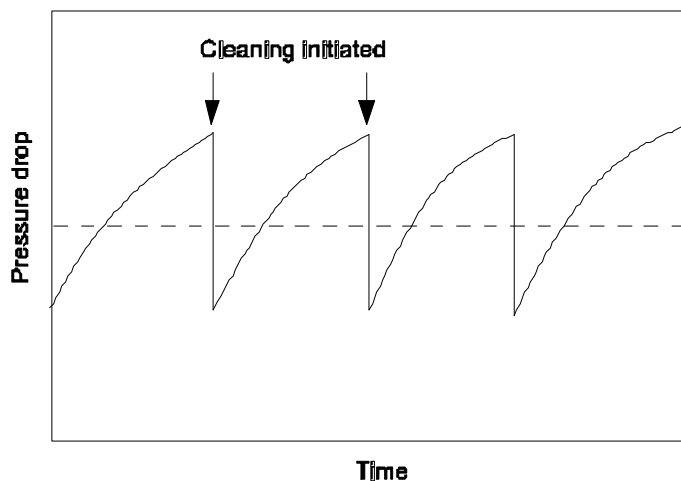


Figure 7-5. Static pressure drop profile

It should be noted that the particulate removal efficiency does not vary significantly despite these static pressure drop fluctuations. The high efficiency performance characteristics of fabrics are reestablished very soon after dust cake repair. Unlike some other devices, particulate matter removal efficiency does not increase as the static pressure drop across the baghouse increases. For example, a fabric filter operating at 9 in. WC pressure drop does not necessarily have a higher particulate matter removal efficiency than a unit operating at 4 in.

WC pressure drop. In fact, quite the opposite can be true. Because of the bleed-through and pore collapse modes of emission, particulate matter removal efficiency is often lower when the pressure drop is in the high range.

Filter Media Blinding and Bag Blockage

Water droplets in the dust cake can severely increase the resistance to gas flow. At the very least, the water can fill the voids in the dust cake where the gas would normally flow. If the quantity of water is high, the dust cake can be packed tightly together or even form a muddy layer. At this point, the affected portion of the bag is essentially impervious to gas flow. This is termed *fabric blinding*.

Water is not the only substance that can cause blinding, but it is one of the most common. Condensed water droplets can be entrained from the process being treated, or they can be carried in with the compressed air in pulse jet fabric filters. Excessive gas cooling in baghouses serving combustion sources and other sources generating high vapor concentrations can cause water condensation in the dust cakes.

Another common blinding agent is the lubricating oil often present in pulse jet fabric filter compressed air supplies. The oil droplets can deposit in the upper, clean side surfaces of the bags and prevent gas flow. The entire inlet gas stream must, therefore, be filtered in the unaffected lower portions of the pulse jet bag.

Wet materials are not the only blinding agents. Submicrometer particles can be driven deep into the fabric if the bag is exposed to a high velocity particulate-laden gas stream before a protective residual dust layer is present. This type of blinding often occurs when a new bag is installed in a compartment with a large number of seasoned bags. Due to the resistance caused by the seasoned bags' residual dust cakes, the gas velocities through the new bag are excessively high. Submicrometer particle blinding can also occur following the installation of new bags at sources that generate high concentrations of submicrometer particulate matter. In these cases, the new bags can be conditioned prior to service by exposing them to resuspended large diameter particles.

Hopper overflow or solids bridging in hoppers can cause high dust levels. A portion of the filtering area will be inadvertently isolated if these solids block some of the bag inlets in shaker or reverse air baghouses. This occurs most often around the exterior walls of the hoppers where cooling of the solids is most severe. If moisture is present, these deposits can become crusty and remain even after the solids in the hopper have been removed. Proper hopper design and frequent emptying are important in minimizing the occurrence of this condition.

The net effect of these operating problems is to remove fabric area from service. This increases the air-to-cloth ratio in the unaffected fabric and can lead to seepage or pore collapse problems. The higher air-to-cloth ratios will also result in increased pressure drop across the baghouse.

Fabric Filter Applicability Limitations

There are several limitations that should be considered when working with fabric filters. Clogging or blinding of the fabric can occur when the particulate is sticky or if moisture is present. Blinding can also occur when large quantities of small particles (0.1 μm to approximately 2 μm) pass through new bags that are not protected by a dust cake. Fabric filters can be designed to operate with moderate blinding conditions. However, they may not be appropriate for very sticky conditions.

Excessive quantities of large particles moving at high velocities can be abrasive and cause erosion of the fabric, especially near the bottoms of the bags. The gas velocities are usually highest near the bottom because of the way the particulate-laden gas stream enters the baghouse. Large particles are the most abrasive and can strike exposed fabric yarns and fibers with considerable force.

Fires and explosions can occur in fabric filters due to the high concentration of dust on the bags and in the upper elevations of the hoppers. These fires and explosions can be ignited by embers from process equipment and even by static electricity generated inside the baghouse. Baghouses can be designed to minimize the risks of fires and explosions. However, when the risk is very high, alternative particulate control systems or combinations of control systems may be necessary.

There are gas temperature limits to the application of fabric filters because of the limits of the fabric itself. At high temperatures, the fabric can thermally degrade, or the protective finishes can volatilize. Accordingly, fabric filters have usually been limited to gas temperatures below approximately 500°F, which is the maximum long-term temperature of the most temperature-tolerant fabric. Recently commercialized fabrics can tolerate much higher temperatures.

Fabric Filter Systems

One way of distinguishing between different types of fabric filter collectors is the method used to clean the filter material. As dust builds up on the filter surface, the pressure drop across the filter increases. In order to avoid excessively high pressure drops, the filter material is cleaned periodically. The most common methods of cleaning are shaking, reverse air, and reverse pulse or pulse jet.

Another way of distinguishing between different types of fabric filter collectors is based on the way they operate. The three modes of operation are intermittent, periodic and continuous. Intermittent collectors are used on processes that operate intermittently. When the process shuts down, the collector goes through a cleaning cycle and then shuts down and waits for the next processing cycle before starting up. Most intermittent collectors clean by shaking, but could also clean by reverse pulse.

Periodic collectors are used on processes that operate continuously. The total fabric is divided between several modules or compartments. This allows a compartment to be taken off line and cleaned, while the remaining compartments stay on line to provide filtration. Most periodic collectors clean by shaking or reverse air, but could also clean by reverse pulse.

Continuous collectors are also used on processes that operate continuously, but they do not have compartments that shut down for cleaning. Instead, individual rows of bags in the collector are cleaned, while the remaining bags continue to provide filtration. Continuous collectors usually clean by reverse pulse, but could also clean by reverse air.

Shaker Fabric Filters

Figure 7-6 shows the typical components of a shaker cleaned fabric filter. The tube sheet or cell plate provides the seal which separates the bags in the upper portion of the collector from the hoppers. The open bottoms of the bags are attached to the tube sheet by a clamp-and-thimble arrangement (as shown in Figure 7-7) or by a snap-ring arrangement (as shown in Figure 7-8). The closed tops are attached to the shaker mechanism. The dust laden gases enter through the hopper, where some of the larger particles in the gas stream settle out. Most of the dust will be carried by the gas stream as it passes up through the filter bag and will be deposited on the inside of the bag. The cleaned gases then exit the collector through an outlet duct or through louvers, if the collector is operating under positive pressure. Shaker collectors use woven fabrics and generally operate with an air-to-cloth ratio of 2-4 ft/min.

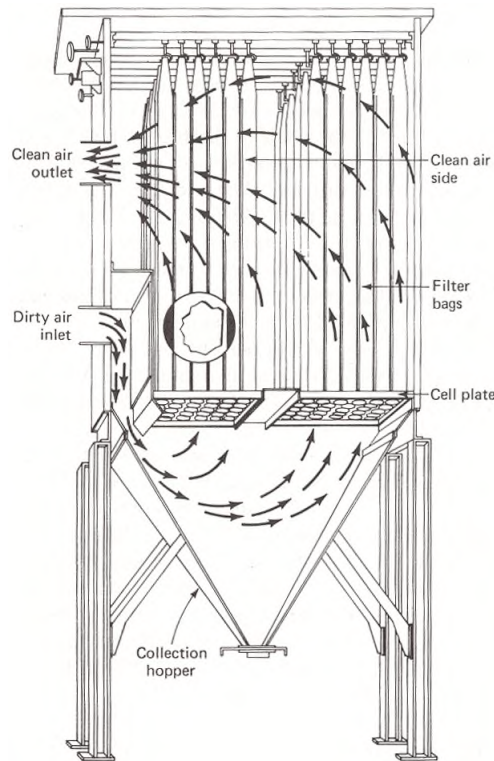


Figure 7-6. Shaker fabric filter

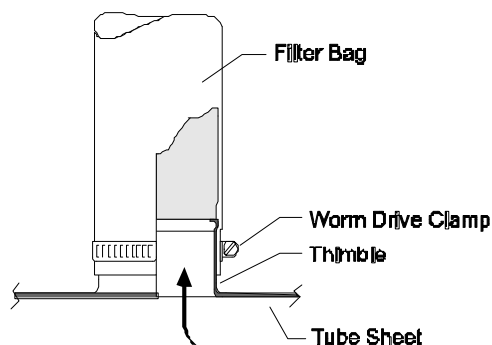


Figure 7-7. Clamp-and-thimble-type bag attachment

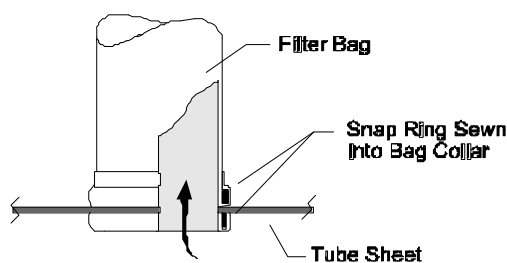


Figure 7-8. Snap-ring-type bag attachment

During the cleaning cycle, gas flow to the collector is stopped. In compartmentalized collectors, this is accomplished with a shut-off damper in the inlet duct, for a positive pressure unit, or in the outlet duct, for a negative pressure unit. It is critically important that this damper seals effectively, so that there is no air flow through the compartment during cleaning. A leaking damper will cause the bag to remain inflated during shaking and will significantly reduce the cleaning effectiveness. It may also cause particles to be driven through the fabric and carried out of the collector.

After a null period of 15-30 seconds to allow the bags to relax, the bags are mechanically shaken, and the dislodged dust cake falls into the hopper. This type of cleaning usually involves the use of a rocker-arm lever assembly to produce a motion at the top of the filter bag that is roughly horizontal. However, other shaker mechanisms may impart vertical motion or may follow an arc. The bags are usually installed slightly slack to be able to accommodate the shaking motion without tearing or pulling loose from the tube sheet. Typically, the bags are shaken from 10 to 100 cycles at a rate of 1 to 5 cycles per second with an amplitude of up to 2 inches. After shaking is completed, a second null period of 1-2 minutes is provided to allow the dust to settle before the collector or compartment is returned to service. In compartmentalized collectors, the cleaning interval for each compartment is typically 30 minutes to 2 hours.

Reverse Air Fabric Filters

The construction and operation of reverse air fabric filters is very similar to shaker collectors. There is a tube sheet that separates the bags in the upper portion of the collector from the hoppers. The open bottoms of the bags are attached to the tube sheet and the closed tops are attached to an upper support structure (see Figure 7-9). The dust laden gases enter through the hopper and pass up through the filter bag, depositing the dust cake on the inside of the bag. The cleaned gases then exit the collector through an outlet duct. Reverse air collectors usually use woven fabrics; however, membrane bags and felted bags may be used in some applications. They typically operate with an air-to-cloth ratio of 1½-3½ ft/min.



Figure 7-9. Reverse air collector hangers and tube sheet attachment

Reverse air fabric filters must be compartmentalized. During cleaning, the gas flow through a compartment is stopped, and filtered gas is passed in a reverse direction through the bags in the compartment. This cleaning procedure is the basis for the name *reverse air*. The main components of the cleaning system are shown in Figure 7-10. The system consists of one or more reverse air fans, a set of dampers to control gas flow to each compartment, and instrumentation to monitor compartment conditions before and after cleaning.

The cleaning cycle is initiated by closing the outlet damper on the compartment to be cleaned, stopping the gas flow into the compartment. After a null period of 15-30 seconds to allow the bags to relax, the reverse air damper is opened to allow filtered gas from the baghouse outlet to enter the compartment. For a period of 30 seconds to a few minutes, this filtered gas is passed from the outside of the bags to the inside in order to remove some of the dust cake. The dislodged dust cake drops into the hopper, and the reverse gas passes through the open inlet damper and enters the gas stream inlet duct leading to other compartments that are in the filtering mode. To prevent the bag from collapsing during the reverse air flow, it is held under a tension of 60-120 pounds of force and has anti-collapse rings sewn into it every 4-6 feet, as shown in Figure 7-11. After cleaning is completed, there is a second null period of 1-2 minutes to allow time for particles to settle before the compartment is returned to

filtering service. As with shaker collectors, the cleaning interval for each compartment is typically 30 minutes to 2 hours.

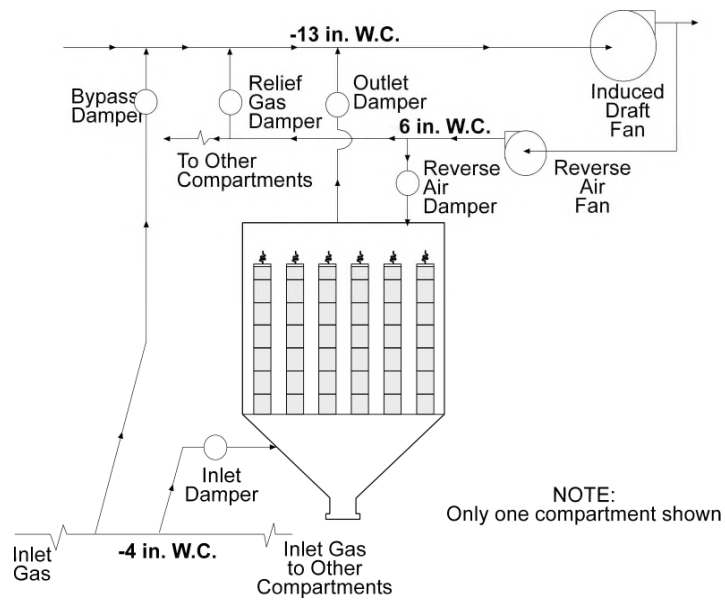


Figure 7-10. Reverse air cleaning system

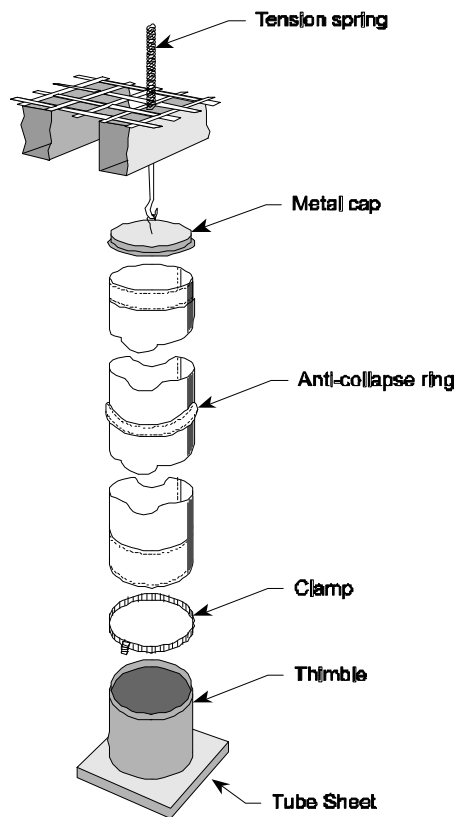


Figure 7-11. Reverse air bag

The reverse air fans are sized considerably smaller than the main system fan. The reverse air fan needs only to supply sufficient gas flow to clean a single compartment at a time. The gas flow needed to dislodge the dust cake from the interior of the bags and to carry the particulate matter into the hopper is usually less than 1/3 to 1/2 the gas flow rate that passes through the compartment during filtration. Specific sizing criteria for a given system are site specific because they depend on factors such as (1) the difficulty in dislodging dust from the bags, (2) the bag dust cake retention characteristics, (3) the residual dust cake characteristics, (4) the particulate mass loading at the inlet of the fabric filter, and (5) the anticipated frequency of cleaning.

The design of the dampers used to control gas flow in and out of the compartment is very important in ensuring that the reverse air fabric filter will perform properly. A typical poppet damper is illustrated in Figure 7-12. This consists of a damper seat, a damper plate, the support rod, an actuator, and limit switches. The poppet damper can be oriented to use either the upper or lower surface of the damper plate for sealing against the damper seat. The damper shown in part A of Figure 7-12 uses the lower surface for sealing. When the damper is closed, the damper sealing plate often deflects slightly. The maximum gap around the circumference of the sealing surface is minimized to prevent improper gas movement through the closed damper. When it is necessary to open the damper, the actuator lifts the support rod until the limit switch indicates that the damper plate is fully lifted. A second limit switch is used during closing of the damper to shut off the actuator when the damper has returned to the closed position.

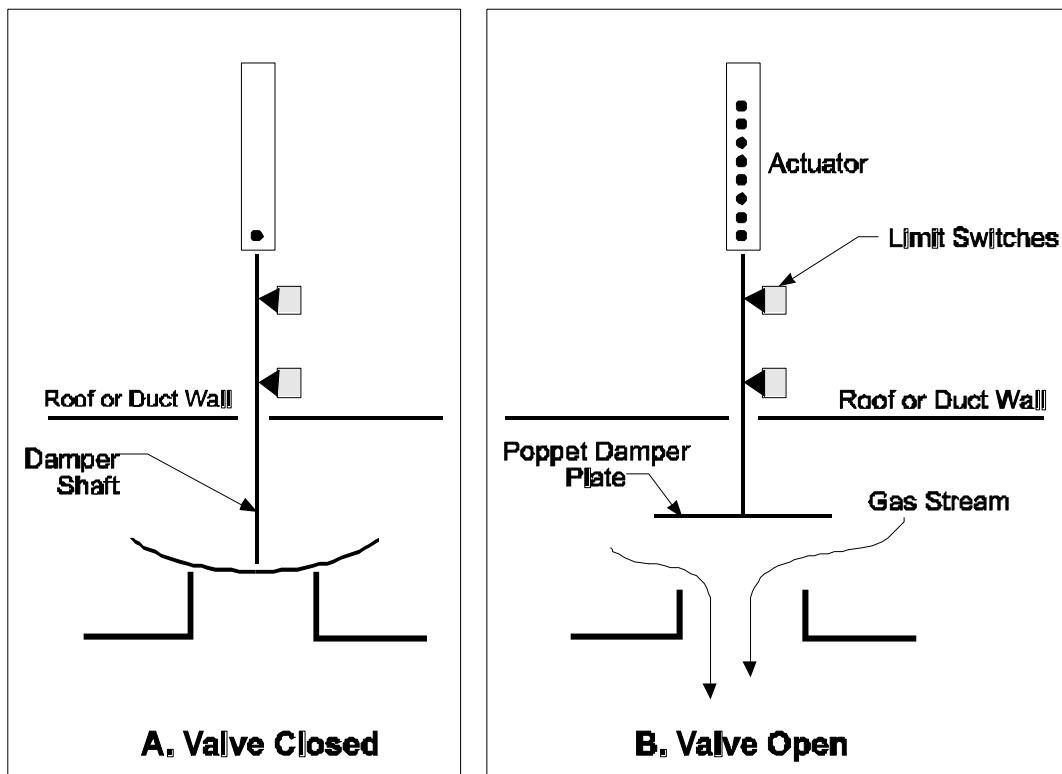


Figure 7-12. Poppet valve in open and closed positions

Sealing the outlet and reverse air dampers is critical to the performance of the baghouse. If the reverse air dampers do not seal properly, the cleaning air supplied by the reverse air fan can be lost to compartments in filtering service. If the outlet dampers do not seal properly, the cleaning gas short-circuits through these openings rather than passing through the bags to be cleaned.

Pulse Jet Fabric Filters

There are two major types of pulse jet collectors: top access and side access. The more common top access design has a number of large hatches across the top of the baghouse for bag replacement and maintenance. The side access design has one large hatch on the side for access to the bags. The side access units often have a single small hatch on the top of the baghouse for routine inspection.

A cutaway drawing of a typical top access type pulse jet fabric filter is shown in Figure 7-13. In pulse jet collectors, the tube sheet is located near the top of the unit and the bags are suspended from it. There are no frames or attachments at the bottom of the pulse jet bags. This free-hanging design is necessary in order to facilitate bag replacement, to allow gas stream movement upward, and to eliminate any abrasive surfaces near the bottom of the bags.

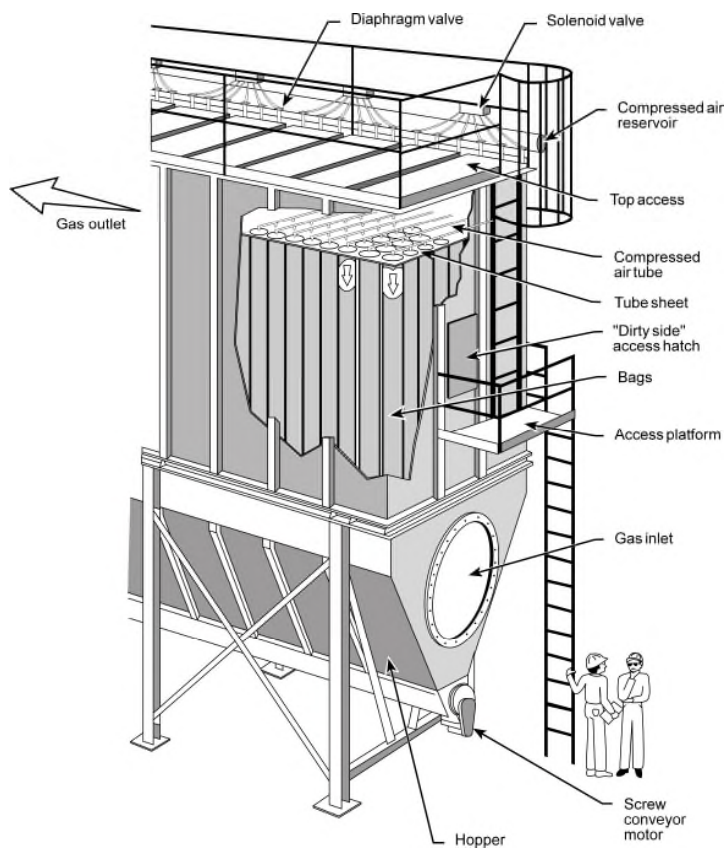


Figure 7-13. Pulse jet fabric filter

In top access designs, the bags are clamped and sealed to the top of the tube sheet to allow for bag removal and replacement from the top of the unit. Two of the many techniques for bag attachment are shown in Figures 7-14 and 7-15. A proper bag seal is very important to prevent dust-laden gases from short-circuiting to the clean side of the baghouse without passing through the dust cake and bag. Even small leak sites can cause significant particulate emissions due to the static pressure drop across the bags.

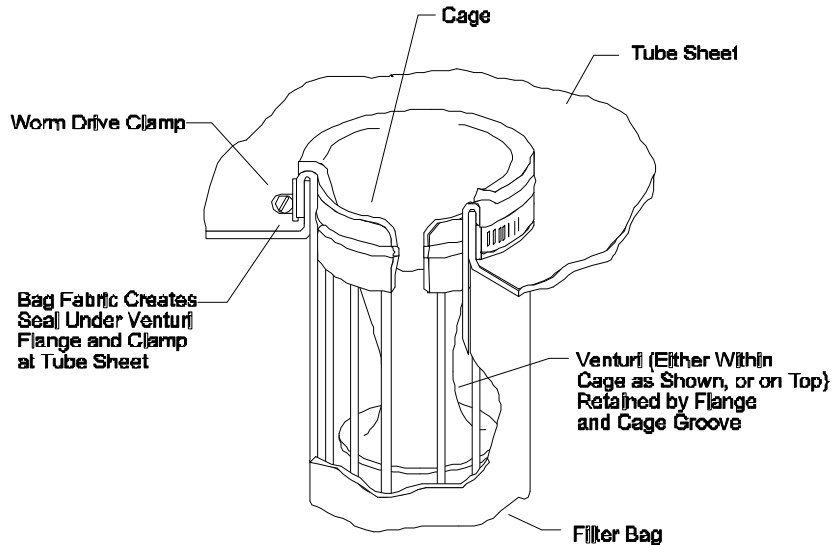


Figure 7-14. Worm-drive-clamp-type bag attachment

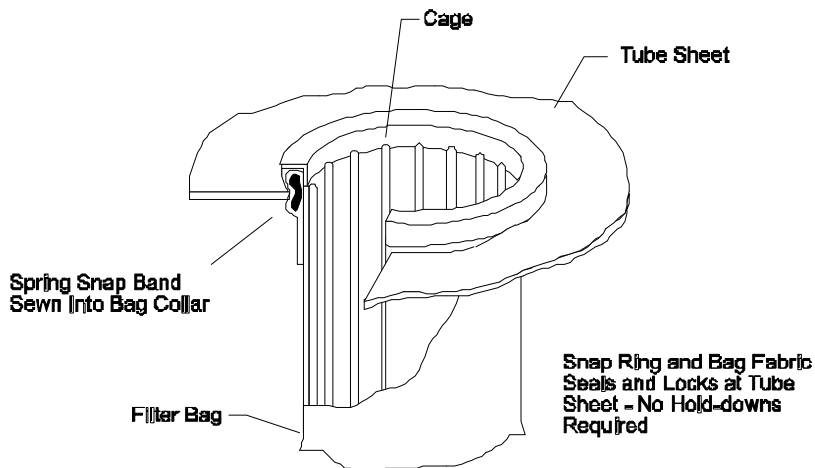


Figure 7-15. Snap-ring-type bag attachment

The gas stream enters either into the side of the casing or into the hopper. The gas flows into the bags and moves upward into the clean gas outlet plenum at the top, leaving the dust cake on the outside of the bag. The bags are supported on metal cages to prevent them from collapsing. Because the fabric tends to wrap around the cage wires during filtering, as shown in Figure 7-16, some fabric wear is possible. To minimize this potential problem, cages with closely-spaced wires are used for fabrics that are especially vulnerable to flex-type wear. More economical cages are used for fabrics that are very tolerant of flex. Pulse jet collectors use felted fabrics and generally operate with an air-to-cloth ratio of 3-10 ft/min.



Figure 7-16. View of the bottoms of pulse jet bags

A portion of the dust must occasionally be removed from the bags in order to avoid excessively high pressure drops. The bags are cleaned by introducing a high-pressure pulse of compressed air at the top of each bag. The sudden pulse of air generates a pressure wave that travels down inside the bag. The pressure wave also induces some filtered gas to flow downward into the bag. Because of the combined action of the pressure wave and the induced gas flow, the bags are briefly deflected outward. This cracks the dust cake on the outside of the bags and causes some of the dust to fall into the hopper. Cleaning is normally performed on a row-by-row basis while the baghouse is operating. However, with this operating practice, dust released from one row of bags can either return to the bag because of settling problems or be recaptured on a bag in an adjacent row that remains in filtering service. Both problems can be avoided by using off-line cleaning. This is accomplished by dividing the pulse jet baghouse into compartments and isolating the compartment being cleaned to prevent gas flow through it.

Excessive cleaning of pulse jet bags can simultaneously cause increased emissions, increased static pressure drop, and accelerated bag wear. If there is insufficient dust cake on the bag when it is cleaned, particles or small agglomerates of particles can be dispersed. These particles do not settle by gravity and simply return to the bag at an area where the dust cake is thin. Here, they can accumulate as a low porosity cake, increasing the pressure drop. Over time, these fine particles can seep through the bag and cause opacity spiking after each

cleaning pulse. This seeping of emissions is caused, in part, by the deceleration shock occurring when the just-pulsed bag snaps back against the cage as the bag returns to filtering service. Insufficient cleaning of pulse jet bags can cause high static pressure drops and reduced air flow from the source. The frequency of cleaning should be set by balancing the limits on high static pressure drop with the need to allow a moderate dust cake to accumulate on the bags between each cleaning cycle.

The main components of the pulse jet cleaning system are illustrated in Figure 7-17. The major components include (1) a source of compressed air, (2) a drier, (3) a coalescing oil filter, (4) a compressed air header, (5) diaphragm and solenoid valves, (6) a solenoid valve controller, (7) compressed air delivery tubes, and (8) instrumentation.

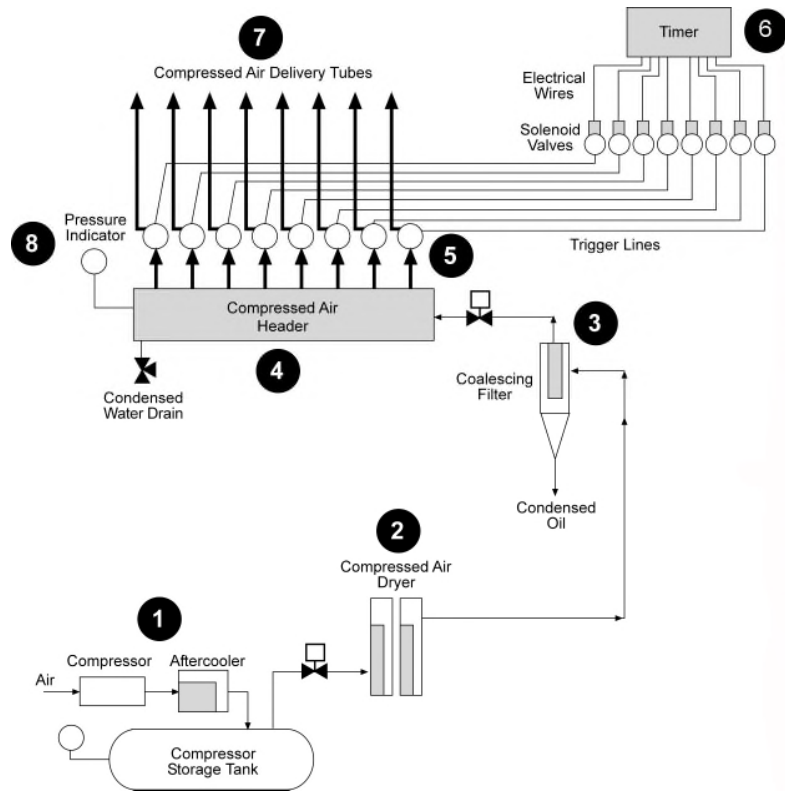


Figure 7-17. Components of a pulse jet cleaning system

The source of compressed air for bag cleaning can be an air compressor dedicated to the specific baghouse or the plant air system. Dedicated compressors usually include an aftercooler to reduce the high temperature caused by compression, a pressure regulator to control the compressor, and a compressed air storage tank. The compressed air is piped from the storage tank to the compressed air header mounted on the side wall of the pulse jet unit.

A drier is sometimes used on a compressed air supply to reduce the water content. Ambient moisture compressed along with the air can condense once the compressed air stream begins to cool. This moisture can accumulate in the compressed air header and be entrained in the cleaning air injected into the bags. Water entering the bags can cause blinding of the filter

due to the formation of muddy deposits. The types of driers used on compressed air supplies include refrigerant and desiccant driers. These driers usually reduce the dewpoint of the gas stream to levels 20°F to 30°F below the lowest ambient wintertime temperature. These low dewpoints mean that the water vapor levels are less than 5% of the levels of untreated compressed air. For baghouses that do not have driers on the compressed air supply, the compressed air header is usually mounted below the elevation of the diaphragm valves to prevent condensed water carryover into the bags.

A coalescing filter is often used after the compressor to remove entrained oil droplets. The oil is introduced into the compressed air stream by the vaporization of lubricating oil used in certain types of compressors. After the compressed air cools, the oil vapor can condense to form oil droplets. If they are not removed, the oil droplets can accumulate on the bag surface and eventually cause blinding. In dedicated systems, oil-less or oil-free compressors are typically used to significantly reduce the amount of oil introduced into the compressed air stream.

A typical compressed air header is shown in Figure 7-18. This provides a reservoir of compressed air to support the operation of the diaphragm valves during a cleaning cycle. There is a connection to each diaphragm valve serving each row of the baghouse. It is important that these connections and the header itself be leak free to ensure that the header remains at the necessary air pressure. In most systems, the compressed air pressure is in the range of 60 to 90 psig.

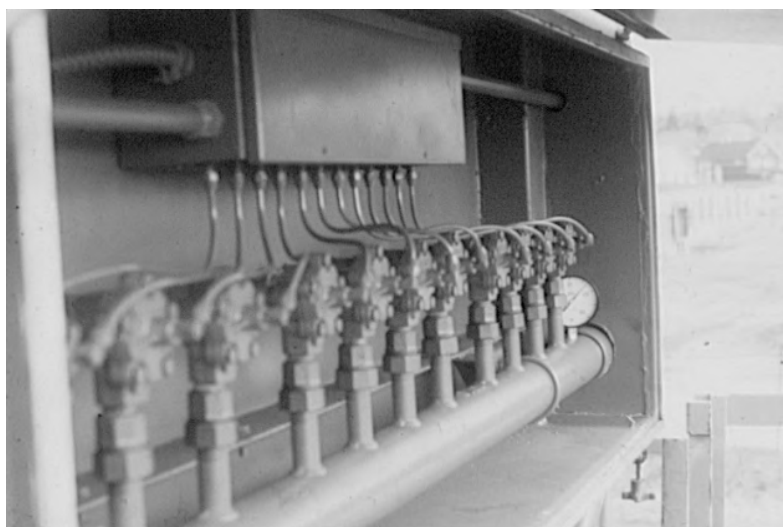


Figure 7-18. Pulse jet compressed air manifold and valves

The cleaning cycle can be regulated by either a standard timing board or with a differential pressure transmitter and controller. The timing board simply activates the cleaning cycle on a frequency set by the operator. The differential pressure transmitter and controller monitors the media static pressure drop and activates the cleaning cycle whenever the static pressure drop exceeds the maximum level set by the operator. In either case, bags are cleaned on a relatively frequent basis, with each row being cleaned from once every five minutes to once

every several hours. Cleaning usually starts with the first row of bags and continues through the remaining rows in the order the bags are mounted.

The opening and closing of the diaphragm valve serving each row of bags is controlled by a solenoid valve. When the solenoid valve is closed, compressed air fills the small tube, called a *trigger line*, running between the solenoid valve and the back of the diaphragm valve. This pressure keeps the diaphragm valve closed. When it is necessary to activate the diaphragm valve, the cleaning cycle controller sends an electrical signal to the solenoid to open the valve and the compressed air in the trigger line is exhausted to the atmosphere. The release of compressed air from the back of the diaphragm valve causes the diaphragm valve to open, allowing the compressed air to enter the delivery tube passing above the row of bags.

The compressed air delivery tube, usually called a *lateral* or *blow tube*, transports the compressed air from the discharge side of the diaphragm valve to the inlet of each bag in the row (see Figure 7-19). These tubes have either a small orifice or an extension tube on the lower side. This hole or extension tube directs the compressed air into the center of the bag. After a period of 0.1-0.2 seconds, the cleaning cycle controller sends a signal to close the solenoid valve. The trigger line again fills with compressed air and the diaphragm valve closes. If the trigger line is broken, the diaphragm valve cannot be closed, and compressed air continues to flow through the affected valve.



Figure 7-19. Compressed air delivery tubes

It is important that the delivery tube be oriented so that the orifice or extension tube points straight into the bag. Rotation of the delivery tube causes the compressed air pulse to strike the side of the bag near the top and holes are created. It is also important to securely fasten the compressed air delivery tube. This tube experiences a pressure rise from ambient pressure to more than 60 psig in a time period of 10 to 50 milliseconds. If this tube is not firmly secured, it can break free. Most baghouses have a fastener on the end of the delivery tube to ensure that it does not move. This same fastener is often used to ensure that the delivery tube is properly rotated. The use of the clamps and other fasteners is important because baghouse operators must remove and reinstall the delivery tubes each time it is necessary to change one or more bags.

Diaphragm valve freezing is a problem that can occur when the baghouse is located outside in cold climates. Diaphragm valve freezing can be minimized by one or more of the following actions:

- Using a compressed air drier
- Relocating the compressed air manifold below the elevation of the diaphragm valves
- Enclosing the diaphragm valves, manifold, and solenoid valves in a weatherproof enclosure and, if necessary, providing heat
- Using drains on manifolds to remove accumulated water on a routine basis

The instrumentation for the compressed air pulsing system is usually quite limited. There is usually a compressed air pressure gauge on the storage tank of the compressor and on the compressed air header serving the baghouse. The compressed air pressure data can be used in conjunction with the overall static pressure drop data for the baghouse to confirm that the baghouse cleaning system is performing properly.

Cartridge Filters

Cartridge filter systems are similar to pulse jet fabric filter systems. The filter elements are supported on a tube sheet that is usually mounted near the top of the filter housing. The gas stream to be filtered passes from the outside of the filter element to the inside. Filtering is performed by the filter media and the dust cake supported on the exterior of the filter media. The filter media is usually a felted material composed of cellulose, polypropylene, or other flex-resistant material.

The unique feature of a cartridge filter is the design of the filter element. Essentially all cartridges are shorter than pulse jet bags. Some cartridges have simple cylindrical designs. Others can have a large number of pleats as shown in Figure 7-20 or other complex shapes as shown in Figure 7-21 in order to increase the filtering surface area. Due to the shortness of the cartridge filter elements, they are usually less vulnerable to abrasion caused by the inlet gas stream. The shorter length also facilitates cleaning by a conventional compressed air pulsing system identical to those used on pulse jet collectors.

Cartridge filter elements are used in a wide variety of industrial applications. Due to their inherently compact design, they can be used in small collectors located close to the point of particulate matter generation. They are generally used on gas streams less than approximately 400°F. This temperature limit is due to the capabilities of the flex resistant, high temperature fabrics and by the limitation of the gasket material used to seal the cartridge filter element to the tube sheet.

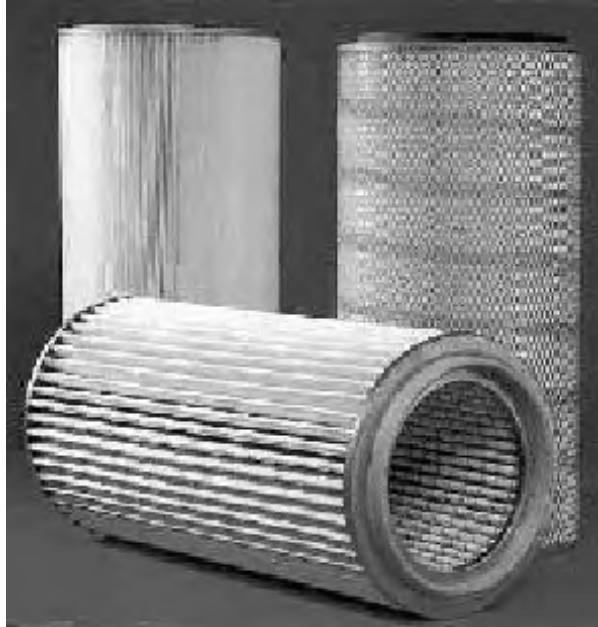


Figure 7-20. Pleated cartridge filter element

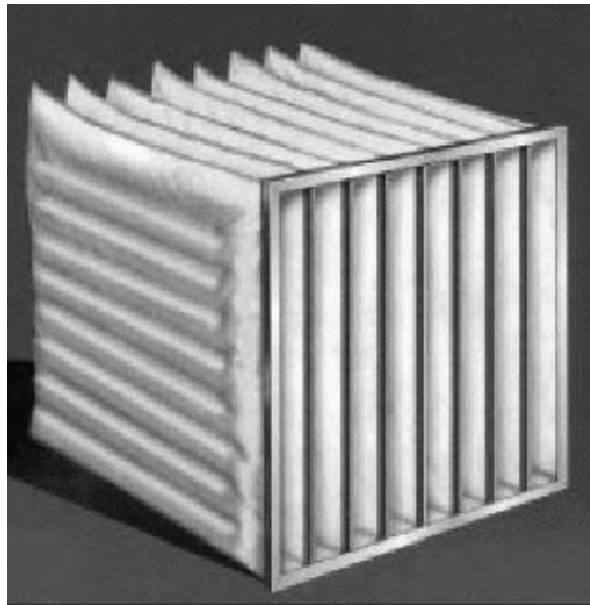


Figure 7-21. Flat cartridge filter element

Fabrics

There is a wide variety of commercially available filtration media. These can be categorized into five different groups:

- Woven fabric
- Felted fabric

- Membrane fabric
- Sintered metal fiber
- Ceramic cartridge

A **woven fabric** is composed of interlaced yarns, as shown in Figure 7-22. The yarns in the warp direction provide strength to the fabric, and the yarns in the fill direction determine the characteristics of the fabric. The pores, which are the gaps between the yarns, can be more than 50 μm in size. Small particles can easily pass through these pores until particles are captured on the sides of the yarns and bridge over the openings. The dust cake is critical for proper filtration by woven fabrics.

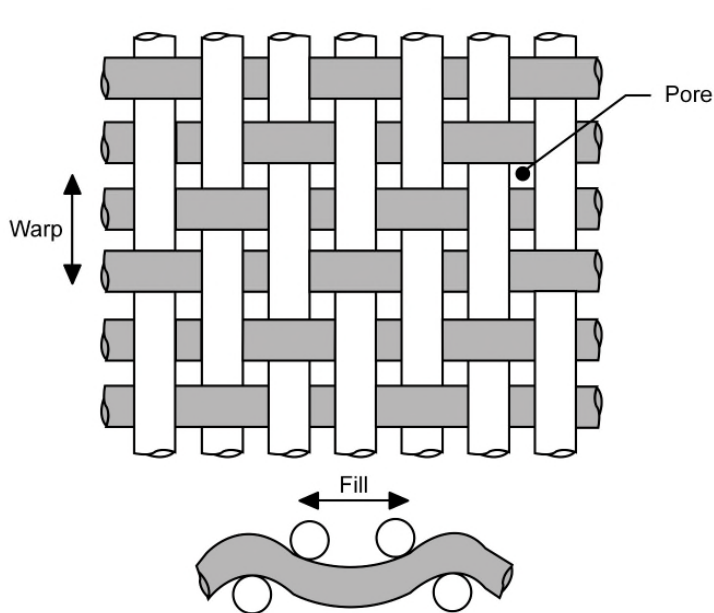


Figure 7-22. Woven fabric

There are a variety of weave types used to modify the characteristics of the fabric. For example, the twill weave shown in Figure 7-22 is less vulnerable than other weaves to fabric blinding due to the penetration of fine particles into the fabric. Overall, the weave characteristics influence the strength of the cloth, the difficulty of dust cake release during cleaning, and the resistance to gas flow.

Felted fabrics are composed of randomly oriented fibers attached to a very open weave termed the *scrim*. The felted fabrics are usually much thicker than woven cloths because of the layer of fibers on both sides of the scrim. With this type of fabric construction, there are no pores as indicated in Figure 7-23. The fibers on the filtering side provide a large number of targets for particle impactation, Brownian diffusion, and electrostatic attraction. However, even with felted fabrics, the dust cake that accumulates on the surface is primarily responsible for particle capture.

Membranes are another major category of fabrics used in air pollution control. These are composed of a polytetrafluoroethylene (PTFE) membrane that is laminated to either a woven

or felted support fabric. The membrane is placed on the filtering side of the fabric. Particle collection occurs primarily due to the sieving action of the membrane's very small pores (less than 5 μm). In membrane fabrics, the dust layer is not especially important in particulate removal. Furthermore, static pressure drop is relatively low due to the good dust cake release properties.

Sintered metal fiber bags are composed of small metal fibers randomly oriented on a cylindrical surface. The bags are heated to high temperatures to bond the fibers together. The bags are rigid and require specially designed pulse jet type cleaning systems. Sintered metal fiber bags can be used for hot gas streams. They can also be aggressively cleaned if they become blinded by sticky or moist dust.

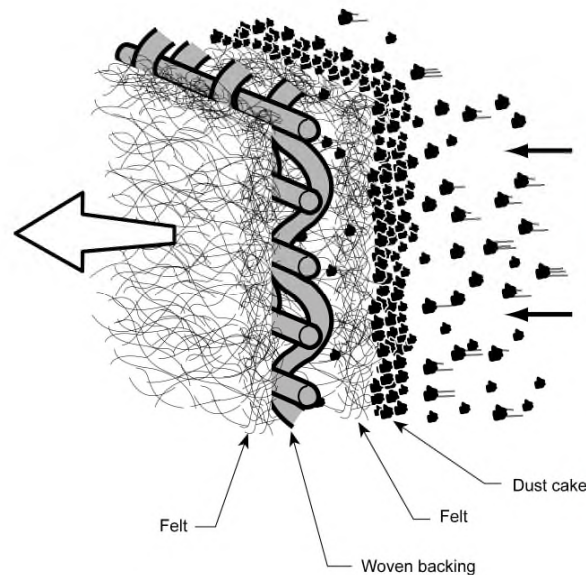


Figure 7-23. Felted fabric

Ceramic cartridge filters are fabricated in cylindrical candle or honeycomb forms. Particle capture occurs as the dust passes through the dust cake on the exterior surface and through the pores through the ceramic media. These filters are designed for applications where the gas temperatures are extremely hot.

The fabrics used for baghouses can be composed of a variety of synthetic and natural materials. Selection of the fabric material is based primarily on three criteria:

- Maximum gas temperatures of the gas stream
- Corrosive chemical concentrations in the gas stream
- Physical abrasion and fabric flex conditions

The various fabrics differ substantially with respect to their ability to tolerate temperature, chemical attack, and physical abrasion and flex. The temperature and acid-resistant capabilities of some of the commercially available types of fabrics are summarized in Table

7-1. The continuous temperature rating shown in the table is intended only as a general indicator of the fabric's capability. To optimize bag life, the normal operating temperatures should be slightly below this limit. The resistance to acids primarily involves inorganic acids such as sulfuric acid and hydrochloric acid.

The ability to handle temperature surges is a function mainly of the fabric's dimensional stability and protective coatings. For example, the limiting maximum surge temperature for fiberglass fabrics is due, in part, to the need to avoid volatilization of lubricants on the fiber surfaces. These lubricants are necessary to prevent fiber-fiber abrasion during cleaning. Also, the ability of the fabric to withstand short-term temperature spikes depends on the quantity of dust cake present. The dust can absorb some of the heat and thereby moderate the maximum temperature while slightly extending the time period that the fabric is exposed to elevated temperature.

Table 7-1. Temperature and Acid Resistance Characteristics				
Generic	Common or	Maximum Temperature, °F		Acid
		Name	Trade Name	
Natural Fiber, Cellulose	Cotton	180	225	Poor
Polyolefin	Polyolefin	190	200	Good to Excellent
Polypropylene	Polypropylene	200	225	Excellent
Polyamide	Nylon®	200	225	Excellent
Acrylic	Orlon®	240	260	Good
Polyester	Dacron®	275	325	Good
Aromatic Polyamide	Nomex®	400	425	Fair
Polyphenylene Sulfide	Ryton®	400	425	Good
Polyimide	P-84®	400	425	Good
Fiberglass	Fiberglass	500	550	Fair
Fluorocarbon	Teflon®	400	500	Excellent
Stainless Steel	Stainless Steel	750	900	Good
Ceramic	Nextel®	1300	1400	Good

The ability of fabrics to withstand physical abrasion and flex is summarized in Table 7-2. Fabrics listed as fair must be cleaned gently, and the bags must be handled carefully during installation. Most of the fabrics have good to excellent capability with respect to abrasion

and flex. The three main exceptions are fiberglass, Teflon[®], and ceramic fabrics which are often used for moderate-to-high gas temperature applications.

Some of the fabrics are coated to improve their ability to withstand acid attack and abrasion and flex type physical damage. All fiberglass fabrics must have coatings to protect the relatively brittle fibers that can easily be broken by fiber-to-fiber abrasion. Silicone-graphite finishes for fiberglass fabrics have been used for more than 40 years. Other coatings that have been developed and used successfully over the last 20 years include Teflon-B[®] coating, I-625[®], Blue Max[®], and Chemflex[®]. Some of these newer coatings also protect the fabric from acid attack.

Table 7-2. Fabric Resistance to Abrasion and Flex

Generic Name	Common or Trade Name	Resistance to Abrasion and Flex
Natural Fiber, Cellulose	Cotton	Good
Polyolefin	Polyolefin	Excellent
Polypropylene	Polypropylene	Excellent
Polyamide	Nylon [®]	Excellent
Acrylic	Orlon [®]	Good
Polyester	Dacron [®]	Excellent
Aromatic Polyamide	Nomex [®]	Excellent
Polyphenylene Sulfide	Ryton [®]	Excellent
Polyimide	P-84 [®]	Excellent
Fiberglass	Fiberglass	Fair
Fluorocarbon	Teflon [®]	Fair
Stainless Steel	Stainless Steel	Excellent
Ceramic	Nextel [®]	Fair

Performance Evaluation

Unlike other particle control devices, we do not have mathematical relationships for estimating the collection efficiency of fabric filters. Instead, we evaluate a number of factors to assess whether the device has been properly designed. These factors include:

- Fabric selection
- Air-to-cloth ratio
- Approach velocity
- Bag spacing and length
- Bag accessibility

- Cleaning system design
- Hopper design
- Bypass dampers
- Instrumentation

The cleaning system design parameters were discussed earlier for each type of cleaning system. The remaining evaluation factors will be discussed in this section. A well designed, properly operated, and well maintained fabric filter system should achieve overall collection efficiencies in excess of 99 percent.

Air-to-Cloth Ratio

The air-to-cloth ratio is the main sizing parameter used for fabric filters. Low values of the air-to-cloth ratio indicate that the velocity of gas passing through a given area of the fabric is relatively low. This favors proper particulate matter capture and moderate static pressure drops.

The gross air-to-cloth ratio is defined as the actual gas flow rate at maximum operating conditions divided by the total fabric area in the baghouse. This is summarized in Equation 7-7.

$$(A/C)_{\text{gross}} = \frac{Q_{\text{maximum}}}{A_{\text{total}}} \quad (7-7)$$

where:

$$\begin{aligned} (A/C)_{\text{gross}} &= \text{gross air-to-cloth ratio } ((\text{ft}^3/\text{min})/\text{ft}^2) \\ Q_{\text{maximum}} &= \text{maximum actual gas flow rate } (\text{ft}^3/\text{min}) \\ A_{\text{total}} &= \text{total fabric area } (\text{ft}^2) \end{aligned}$$

The net air-to-cloth ratio is often used for multi-compartment fabric filters where one or more of the compartments is isolated from the gas flow due to cleaning or maintenance. This sizing parameter is defined in Equation 7-8.

$$(A/C)_{\text{net}} = \frac{Q_{\text{maximum}}}{A_{\text{net}}} \quad (7-8)$$

where:

$$\begin{aligned} (A/C)_{\text{net}} &= \text{net air-to-cloth ratio } ((\text{ft}^3/\text{min})/\text{ft}^2) \\ Q_{\text{maximum}} &= \text{maximum actual gas flow rate } (\text{ft}^3/\text{min}) \\ A_{\text{net}} &= \text{fabric area in filtering service } (\text{ft}^2) \end{aligned}$$

The gross and net air-to-cloth ratios can be calculated using basic information concerning the number of bags, the dimensions of the bags, and the actual gas flow rate at maximum process operating conditions. The bag areas for cylindrical shaker, reverse air and pulse jet bags are calculated with the formula shown in Equation 7-9.

$$A = \pi DL \quad (7-9)$$

where:

A= bag surface area (ft²)

D= bag diameter (ft)

L= bag length (ft)

Equation 7-9 is the formula for the area of the side of a cylinder. In using this equation, it is assumed that filtration occurs only on the side of the bag, not on the circular top (shaker and reverse air) or bottom (pulse jet). This is a reasonable approach because reverse air and pulse jet bags usually have a solid cup across the circular area and shaker bags usually taper to a sewn closure.

The formula for calculating the fabric area of a pleated cylindrical cartridge filter (Figure 7-20) is provided in Equation 7-10.

$$A=2ndh \quad (7-10)$$

where:

A = cartridge surface area (ft²)

n = number of pleats

d = depth of pleat (ft)

h = pleat height (ft)

For other types of cartridges, the filter area should be calculated by applying standard geometrical relationships to the shape of the filter surfaces.

Example 7-1 illustrates the calculation of the gross and net air-to-cloth ratios for a reverse air baghouse. Example 7-2 illustrates procedures for calculating the gross and net air-to-cloth ratios for a cartridge baghouse.

Example 7-1

Calculate the gross and net air-to-cloth ratios for a reverse air baghouse with 20 compartments, 360 bags per compartment, a bag length of 30 ft, and a bag diameter of 11 inches. Use an actual gas flow rate of 1.2×10^6 ft³/min. Assume that two compartments are out of service when calculating the net air-to-cloth ratio.

Solution:

$$\text{Bag area} = \pi DL$$

$$\text{Area/bag} = \pi (11 \text{ inches})(\text{ft}/12 \text{ in.}) 30 \text{ ft} = 86.35 \text{ ft}^2/\text{bag}$$

The gross air-to-cloth ratio is calculated assuming that all the bags are in service.

$$\text{Total number of bags} = (360 \text{ bags/compartment})(20 \text{ compartments}) = 7,200 \text{ bags}$$

$$\text{Total fabric area} = (7,200 \text{ bags})(86.35 \text{ ft}^2/\text{bag}) = 621,720 \text{ ft}^2$$

$$(A/C)_{\text{gross}} = \frac{1.2 \times 10^6 \text{ ft}^3 / \text{min}}{621,720 \text{ ft}^2} = 1.93 (\text{ft}^3 / \text{min}) / \text{ft}^2$$

The net air-to-cloth ratio is calculated by subtracting the compartments that are not in filtering service.

$$\text{Total number of bags} = (360 \text{ bags/compartment})(18 \text{ compartments}) = 6,480 \text{ bags}$$

$$\text{Total fabric area} = (6,480 \text{ bags})(86.35 \text{ ft}^2/\text{bag}) = 559,548 \text{ ft}^2$$

$$(A/C)_{\text{net}} = \frac{1.2 \times 10^6 \text{ ft}^3 / \text{min}}{559,548 \text{ ft}^2} = 2.14 (\text{ft}^3 / \text{min}) / \text{ft}^2$$

Example 7-2

Calculate the gross and net air-to-cloth ratios for a cartridge baghouse with 4 compartments, 16 cartridges per compartment, a cartridge length of 2 ft, and a cartridge diameter of 8 inches. Use a pleat depth of 1.5 inches and a total of 36 pleats in the cartridge. Use an actual gas flow rate of 4,000 ft³/min. Assume one compartment is out of service when calculating the net air-to-cloth ratio.

Solution:

$$\text{Cartridge area} = 2\pi dh$$

$$\text{Area/cartridge} = 2(36 \text{ pleats})(1.5 \text{ in.}/(12 \text{ in. per ft}))(2 \text{ ft}) = 18 \text{ ft}^2$$

The gross air-to-cloth ratio is calculated assuming that all the bags are in service.

$$\begin{aligned} \text{Total number of cartridges} &= (16 \text{ cartridges/compartment})(4 \text{ compartments}) \\ &= 64 \text{ cartridges} \end{aligned}$$

$$\text{Total fabric area} = (64 \text{ cartridges})(18 \text{ ft}^2/\text{cartridge}) = 1,152 \text{ ft}^2$$

$$(A/C)_{\text{gross}} = \frac{4,000 \text{ ft}^3 / \text{min}}{1,152 \text{ ft}^2} = 3.47 (\text{ft}^3 / \text{min}) / \text{ft}^2$$

The net air-to-cloth ratio is calculated by subtracting the compartments that are not in filtering service.

$$\text{Total number of cartridges} = (16 \text{ cartridges/compartment})(3 \text{ compartments})$$

$$= 48 \text{ cartridges}$$

$$\text{Total fabric area} = (48 \text{ cartridges})(18 \text{ ft}^2/\text{cartridge}) = 864 \text{ ft}^2$$

$$(A/C)_{\text{net}} = \frac{4,000 \text{ ft}^3 / \text{min}}{864 \text{ ft}^2} = 4.62 \text{ (ft}^3 / \text{min) / ft}^2$$

The appropriate air-to-cloth ratio for a given application depends on the particle size distribution, fabric characteristics, particulate matter loadings, and gas stream conditions. Low values for a design air-to-cloth ratio are generally used when the particle size distribution includes a significant fraction of submicrometer particulate matter or when the particulate loading is high. The air-to-cloth ratios for cartridge filters are usually maintained at values less than approximately 4 (ft³/min)/ft². A summary of air-to-cloth ratio values for shaker, reverse air and pulse jet fabric filters in a variety of industries is provided in Table 7-3. Some caution is warranted in reviewing any table of this type, because the design air-to-cloth ratios were gradually decreased over the past 20 years, and there can be significant site-to-site differences in the particle size distributions, particulate loadings, and fabric characteristics. Furthermore, the regulations based on the Clean Air Act Amendments of 1990 place even greater demands on fabric filter performance. Accordingly, historical design data may not be strictly applicable to a specific application.

Industry	Shaker	Reverse Air	Pulse Jet
Basic oxygen furnaces	2.5-3.0	1.5-2.0	6-8
Brick manufacturers	2.5-3.2	1.5-2.0	9-10
Coal-fired boilers	1.5-2.5	1.0-2.0	3-5
Electric arc furnaces	2.5-3.0	1.5-2.0	6-8
Ferroalloy plants	2.0	2.0	9
Grey iron foundries	2.5-3.0	1.5-2.0	7-8
Lime kilns	2.5-3.0	1.5-2.0	8-9
Municipal incinerators	1.5-2.5	1.0-2.0	2.5-4.0
Phosphate fertilizer	3.0-3.5	1.8-2.0	8-9
Portland cement kilns	2.0-3.0	1.2-1.5	7-10

Source: EPA 450/3-76-014

Approach Velocity

Gravity settling of dust cake agglomerates, sheets, and particles released during bag cleaning is a critical step in the fabric filtration process. If fine particles with inherently poor terminal settling velocities return to the bag-dust cake surface, there can be adverse effects on both collection efficiency and static pressure drop. This can occur in off-line cleaning systems (shaker and reverse air) if insufficient null time is provided after cleaning to allow the particles to settle. In on-line cleaning systems (pulse jet), gas flow entering into the hopper of the collector, rather than the side, can produce an upward velocity that may prohibit some

particles and particle agglomerates from settling. Using a side entry significantly reduces this problem.

In pulse jet units with gas entry into the hopper, the point of maximum velocity is the area around the bottoms of the bags. As shown in Figure 7-24, all the particulate-laden gas to be filtered by the bags must pass through this area in order to reach the bag surfaces, and the dust released during cleaning must fall through this area as it settles by gravity. If the upward velocity of the inlet gas stream exceeds the downward terminal settling velocity, the particles will be caught and returned to the bag surface.

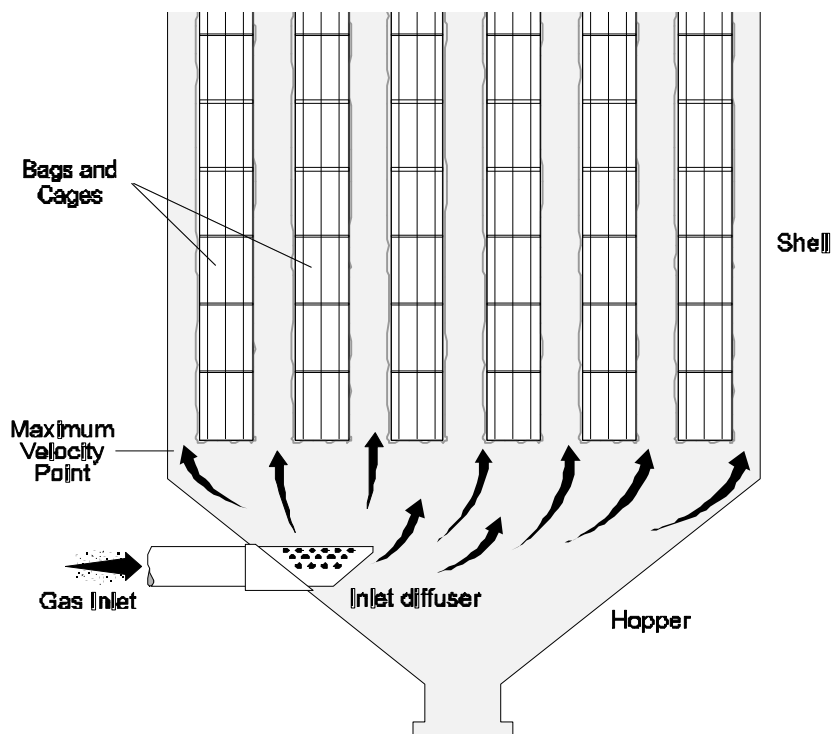


Figure 7-24. Gas approach velocity for pulse jet baghouse

The air-to-cloth ratio is one factor that affects the severity of gravity settling problems in pulse jet fabric filters with hopper entry. The gas approach velocity is directly proportional to the air-to-cloth ratio, as illustrated in Example 7-3. A comparison of the calculated approach velocity indicates that even 100 μm particles released from the dust cake will not settle by gravity. Accordingly, it is important that large dust agglomerates or sheets be released, not small agglomerates or individual particles.

Gravity settling problems can also occur in shaker and reverse air fabric filters. If the compartment isolation damper does not seal properly, settling may be opposed by a modest inlet gas flow into the bags during the cleaning cycle. In reverse air units, small particle removal may not be aided by the downward movement of the reverse air if the flow rates are inadequate.

Example 7-3

What is the difference in gas approach velocities for two identical pulse jet fabric filters with the following design characteristics?

Characteristic	Unit A	Unit B
Compartment area, ft ²	130	130
Number of bags	300	300
Bag diameter, in.	6	6
Bag height, ft	10	10
Air-to-cloth ratio, (ft ³ /min)/ft ²	5	8

Solution:

The bag area for both units is identical. It is calculated using the circumference of the bag times the length.

$$\begin{aligned} \text{Bag area} &= \pi DL = \pi(6 \text{ in.})(1 \text{ ft}/12 \text{ in.})(10 \text{ ft}) = 15.7 \text{ ft}^2/\text{bag} \\ \text{Total bag area} &= (300 \text{ bags})(15.7 \text{ ft}^2/\text{bag}) = 4,710 \text{ ft}^2 \end{aligned}$$

$$\text{Total gas flow rate, Unit A} = \frac{5(\text{ft}^3/\text{min})}{\text{ft}^2}(4,710 \text{ ft}^2) = 23,550 \text{ ft}^3/\text{min}$$

$$\text{Total gas flow rate, Unit B} = \frac{8(\text{ft}^3/\text{min})}{\text{ft}^2}(4,710 \text{ ft}^2) = 37,680 \text{ ft}^3/\text{min}$$

The area for gas flow at the bottom of the pulse jet bags is identical in both units.

$$\begin{aligned} \text{Area for flow} &= \text{total area} - \text{bag projected area} \\ &= \text{total area} - (\text{number of bags})(\text{circular area of bag at bottom}) \\ &= 130 \text{ ft}^2 - (300)(\pi D^2/4) \\ &= 130 \text{ ft}^2 - 58.9 \text{ ft}^2 \\ &= 71.1 \text{ ft}^2 \end{aligned}$$

$$\text{Gas approach velocity for Unit A} = \frac{23,550 \text{ ft}^3/\text{min}}{71.1 \text{ ft}^2} = 331 \text{ ft}/\text{min}$$

$$\text{Gas approach velocity for Unit B} = \frac{37,680 \text{ ft}^3/\text{min}}{71.1 \text{ ft}^2} = 530 \text{ ft}/\text{min}$$

Bag Spacing and Length

In pulse jet baghouses, the approach velocity is directly proportional to the length of the bag. For example, an increase in the bag length to 16 ft from 10 ft in Unit B (Example 7-3) would

increase the approach velocity to approximately 850 ft/min, as long as the air-to-cloth ratio remained constant. Furthermore, particles and small dust cake agglomerates would have a longer distance to travel with the taller bag. Both factors increase the susceptibility to gravity settling-related problems.

Approach velocities are also a function of bag spacing. Units that crowd the bags close together have high approach velocities because there is very little area between the bags for the inlet gas stream to pass through. For example, the velocities calculated in Example 7-3 were based on a unit having bags on 8-inch centers (8 inches from center of bag to center of adjacent bag). If the bags were spaced on 7-inch centers, the approach velocities for Units A and B would be 571 and 913 ft/min, respectively.

Gravity settling and bag cleaning in general would be significantly more difficult at these higher velocities. It is usually preferable to space the bags far apart to minimize this potential problem. However, there are practical limits to the bag spacing because wide spacing increases the size of the baghouse shell and the area needed for the baghouse.

Pulse jet bag length and spacing are important for other reasons, as well. Bag-to-bag abrasion can occur at the bottoms of the bags because they hang freely from the tube sheet. Slight bows in the pulse jet bag support cages or slight warpage of the supporting tube sheet can cause bag-to-bag contact at the bottom, as illustrated in Figure 7-25. Abrasion damage can occur due to the slight movement of the fabric and cage during each pulse cycle. Holes can develop within several weeks to several months of routine operation, depending on the abrasion sensitivity of the fabric being used. Pulse jet units with relatively short bags are less vulnerable to this mode of bag failure.

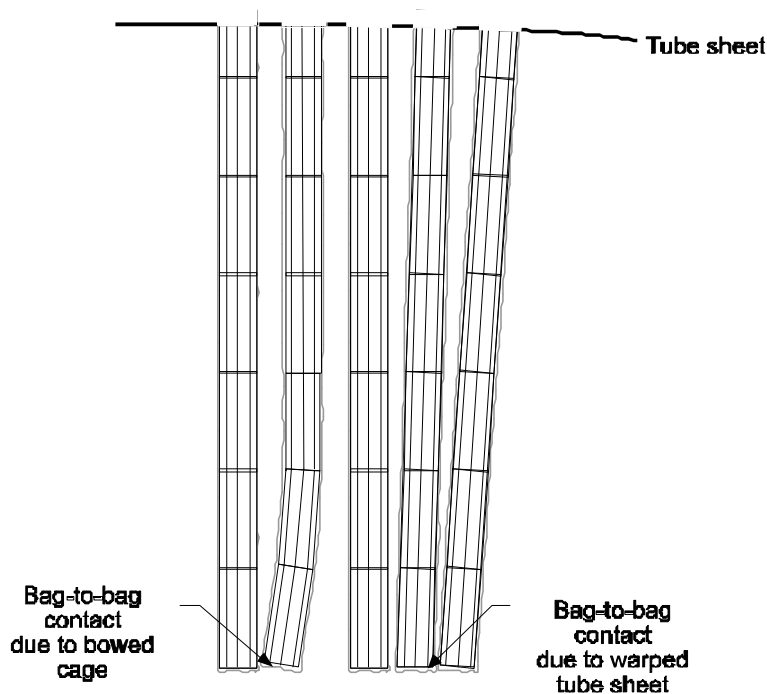


Figure 7-25. Possible problems with tall pulse jet bags

A variety of other practical problems limit bag length. Very tall bags are often difficult to install in a pulse jet baghouse when there is limited overhead clearance to remove the failed bag mounted on the rigid cage. In some cases, failed bags partially fill with solids and, in the case of tall bags, the weight can be substantial. For all these reasons, relatively short bags of 8 to 14 ft are preferable to tall bags, which can be as long as 20 ft.

Bag length and spacing are also important for shaker and reverse air fabric filters. However, the problems with length are less severe because the bags are fixed at both the top and the bottom. Tall reverse air bags are vulnerable to bag tension problems caused by the weight of dust on the bag. This can lead to bag sagging if the support springs become overloaded. Once this happens, bag abrasion can be rapid because the folds of sagging fabric are usually in the direct path of the bag inlet gas stream. Reverse air bags are usually less than 32 ft in length. Shaker bags are usually less than 20 ft long because of the difficulty of maintaining effective shaking movement over longer distances.

Bag Accessibility

Access for bag inspection and replacement is important. In the case of shaker and reverse air baghouses, sufficient space should be allowed so that each bag can be checked visually and either capped off (bag opening sealed) or replaced, if necessary. One measure of the accessibility provided for the maintenance staff is termed the *bag reach*. This is simply the maximum number of rows of bags from the nearest access walkway. For example, the baghouse compartment shown in Figure 7-26 has a reach of 1-1/2. Each row of bags in the compartment is no more than 1-1/2 rows from the nearest walkway. Accordingly, it is possible for plant maintenance staff to find and correct bag problems. Units with less accessible bags are difficult to service. Furthermore, it is possible to damage bags in the outer rows while attempting to work on bags in rows far from the access walkways. There is no single value for bag reach that is considered appropriate for shaker and reverse air baghouses; however, it should certainly be less than one arm's length. Units with a minimum bag reach are easier to maintain.

Hopper Design

A variety of solids-handling systems are used to empty hoppers and transport the solids. Large shaker and reverse air baghouses usually have either pneumatic or pressurized solids-handling systems, both of which empty one hopper at a time. The solids-handling system often cycles continuously between the hoppers in order to minimize solids build-up problems. Smaller baghouses often have screw conveyors with either rotary discharge valves or double flapper valves to prevent air infiltration. As discussed in Chapter 6, rotary valves use either metal blades or flexible wipers on metal blades to maintain an air seal, while the sections of the double flapper valve move in an alternating fashion so that one is always in place to provide an air seal.

Hoppers must be designed to facilitate proper solids discharge. High solids levels due to blockage in the baghouse hoppers are very undesirable. The solids can be reentrained by the

inlet gas stream and contribute to abrasion damage at the lower portions of both pulse jet and shaker and reverse air bags. Additionally, the inlets of shaker and reverse air bags can be blocked as the solids levels increase. As discussed in Chapter 6, several hopper design features are used to minimize solids overflow. Some of these features are shown in Figure 7-27 and include:

- Properly sealing solids discharge valve
- Adequately sized hopper throat
- Adequately sloped hopper walls
- Strike plates or vibrators
- Thermal insulation

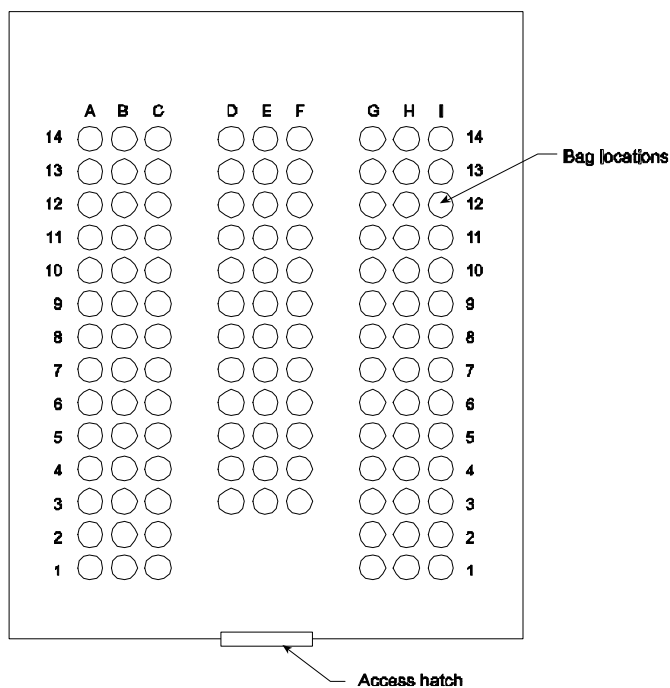


Figure 7-26. Baghouse plan view

Bypass Dampers

Bypass dampers are sometimes mounted in short connecting ductwork that leads from the baghouse inlet duct to the outlet duct. These dampers provide important protection for the baghouse during periods of adverse gas temperatures or other conditions that could severely damage the bags. For example, dampers are usually open during start-up and shut down of solid-fuel combustion processes because the gas stream temperature is below the acid dew point and the particulate matter can be sticky, prompting bag blinding.

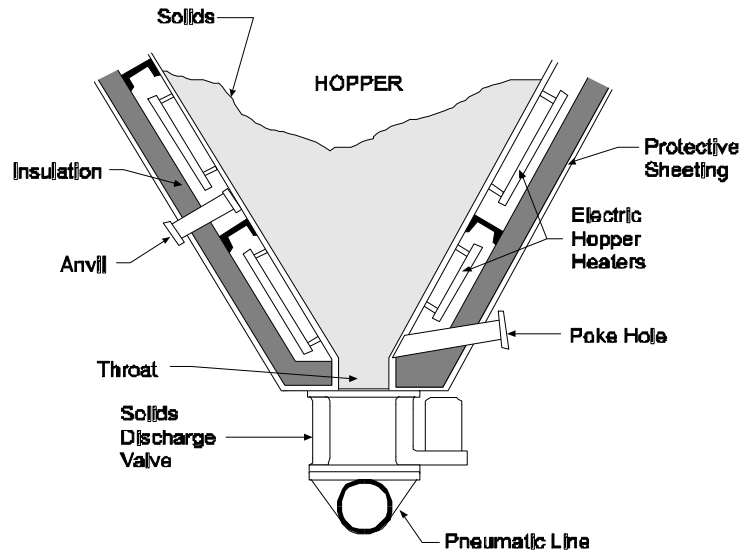


Figure 7-27. Hopper design features

During routine operation, it is important that these dampers seal tightly. They are subjected to a static pressure differential that is equivalent to the overall static pressure drop across the entire baghouse. Slight gaps in the poppet or louvered dampers can allow relatively large quantities of unfiltered air to short circuit around the baghouse. This problem is often indicated by a constant opacity of several percent.

Instrumentation

Fabric filters are sophisticated devices that are often applied to sources generating small diameter particulate matter. Instrumentation that is useful in evaluating their performance include:

- Static pressure drop gauges
- Inlet and outlet gas temperature gauges
- Opacity monitors

Static Pressure Drop Gauges

Many of the problems that can occur during the operation of a fabric filter system usually result in a change in the static pressure drop. If the baghouse static pressure drop is high, undercleaning may be occurring and gas flow rates through the system may have decreased because of high flow resistance. This can result in fugitive emissions from the process. If the baghouse static pressure drop is low, overcleaning could be occurring, resulting in increased stack emissions. Accordingly, it is important to have static pressure drop gauges to monitor the overall resistance across the entire fabric filter.

For shaker and reverse air collectors, and any other collector that cleans off line, there is a normal cycle in the static pressure drop of individual compartments. In order to evaluate

isolation during off-line cleaning and the effectiveness of reverse air flow, static pressure drop gauges are also needed on individual compartments.

Inlet and Outlet Gas Temperature Gauges

Filter bags are not tolerant of either very high or very low gas temperatures. Short term excursions of more than approximately 25°F above the filter media temperature limits can cause volatilization of protective coatings, yarn degradation, fabric shrinkage, or fabric stretching. All these conditions lead to premature bag failure. Acid attack occurs when the gas temperature drops below the acid vapor dewpoint, also resulting in yarn degradation and premature bag failure.

Air infiltration into fabric filters may cause damage because of localized temperatures that are below the acid or moisture dewpoints. It may also reduce the air flow at the source, contribution to fugitive emission losses. One of the most useful ways to evaluate air infiltration into negative pressure collectors is to compare the difference between the inlet and outlet gas temperatures to the baseline difference. If the temperature difference is significantly higher than during the baseline condition, excessive air infiltration may be occurring. If baseline data are not available, excessive air infiltration may be indicated by an inlet and outlet temperature difference that is greater than about 25°F.

Opacity Monitors

Some fabric filter systems have bag break indicator systems to provide an early warning of increased particulate emissions. The types of instruments used for bag break monitoring include Triboflow®, single pass light scattering, and scintillation instruments.

The Triboflow® instrument (Figure 7-28) uses a probe inserted in the outlet duct of a compartment or of the overall fabric filter. The transfer of electrical charge from the particulate emitted from the fabric filter to the probe provides an indication of the particulate matter concentration in the outlet gas stream. An increase in the instrument signal provides a qualitative indication of increased emissions.

In the single pass light scattering detectors, a visible light source is mounted on one side of the outlet duct, and a light detector is mounted on the opposite side. A decrease in light intensity due to the presence of particulate matter in the gas stream provides an indication of a failed bag. These instruments often have an output scale expressed in terms of opacity. However, these instruments do not satisfy a number of the performance specifications applying to opacity monitors, and the output value is intended to be qualitative.

A scintillation type bag break indicator is also a light scattering, cross-stack monitor. The frequency of the light is varied to provide a means to evaluate the particulate mass concentration. This instrument provides data in the form of mass concentration values rather than opacity; however, these data are considered qualitative.

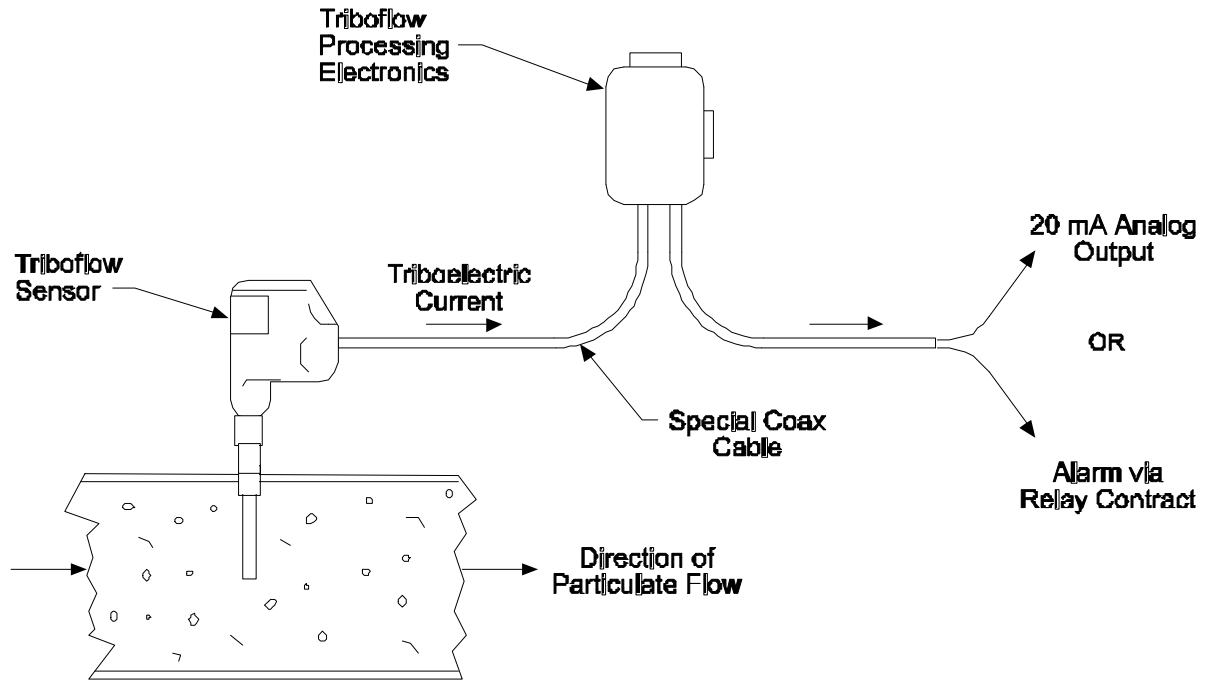


Figure 7-28. Triboflow® bag break detector

On large fabric filter systems, a double-pass transmissometer is often used to continuously monitor the effluent gas stream opacity. These systems use visible light that is projected across the stack, reflected off the surface of a mirror, and returned to a detector. The loss in light due to absorption and scattering during this double pass across the stack is measured as percent transmittance and is mathematically converted to opacity. These instruments are designed and installed in accordance with U.S. EPA Performance Specification 1 (40 CFR Part 60, Appendix A). They are usually located in either an outlet duct or the stack serving the fabric filter system.

This page intentionally left blank.

Review Questions

1. What types of fabric filter systems collect the dust cake on the exterior surface of the filter media? Select all that apply.
 - a. Pulse jet
 - b. Cartridge
 - c. Reverse air

2. What is the purpose of using offline cleaning in a multi-compartment pulse jet collector? Select all that apply.
 - a. Minimize solids build-up problems in hoppers
 - b. Minimize gravity settling problems during cleaning of the bags
 - c. Minimize high static pressure drop problems
 - d. Minimize variability of the overall static pressure drop across the baghouse during the cleaning cycle

3. What fabrics have a long term temperature limitation above 400°F? Select all that apply.
 - a. Fiberglass
 - b. Cellulose
 - c. Nomex
 - d. P84
 - e. Stainless steel
 - f. Ceramic
 - g. Teflon

4. A static pressure drop gauge is mounted on the side wall of a pulse jet baghouse. One side of the gauge is connected to the side wall of the baghouse at a location just below the tube sheet. The other side of the gauge is located just above the tube sheet. The data provided by this instrument is termed the _____.
 - a. Overall baghouse static pressure drop
 - b. Filter media static pressure drop
 - c. Compressor discharge static pressure
 - d. Compressor header static pressure

5. What types of contaminants can be present in untreated compressed air used to clean pulse jet fabric filters and cartridge fabric filters? Select all that apply.
 - a. Condensed water droplets
 - b. Sulfur dioxide
 - c. Carbon monoxide
 - d. Condensed oil droplets

6. What problem or problems are created if a pulse jet bag does not seal properly to the tube sheet? Select all that apply.
 - a. Unfiltered gas could leak around the bag into the clean gas plenum
 - b. The bags could fall into the hoppers due to inadequate support
 - c. The filter media static pressure drop would decrease

7. A reverse bag constructed of fiberglass has very low tension and is sagging severely at the connection to the tube sheet thimble. What problem or problems could be created by this condition? Select all that apply.
 - a. The bag could develop holes due to its vulnerability to flex failure
 - b. The bag could be abraded by the high velocity inlet gas stream
 - c. The sagging bag could choke off flow of unfiltered air into the bag

8. What forces are used to remove particles in woven and felted bags? Select all that apply.
 - a. Inertial impaction
 - b. Brownian diffusion
 - c. Electrostatic attraction
 - d. Sieving

9. What forces are used to remove particles in a membrane bag? Select all that apply.
 - a. Inertial impaction
 - b. Brownian diffusion
 - c. Electrostatic attraction
 - d. Sieving

10. What problem occurs at excessive air-to-cloth ratios?
 - a. Accelerated bag failure
 - b. Decreased static pressure drop
 - c. Increased particulate emissions through the filter media
 - d. All of the above

Review Question Answers

1. What types of fabric filter systems collect the dust cake on the exterior surface of the filter media? Select all that apply.
 - a. Pulse jet
 - b. Cartridge
2. What is the purpose of using offline cleaning in a multi-compartment pulse jet collector? Select all that apply.
 - b. Minimize gravity settling problems during cleaning of the bags
 - c. Minimize high static pressure drop problems
3. What fabrics have a long term temperature limitation above 400°F? Select all that apply.
 - a. Fiberglass
 - e. Stainless steel
 - f. Ceramic
4. A static pressure drop gauge is mounted on the side wall of a pulse jet baghouse. One side of the gauge is connected to the side wall of the baghouse at a location just below the tube sheet. The other side of the gauge is located just above the tube sheet. The data provided by this instrument is termed the _____.
 - b. Filter media static pressure drop
5. What types of contaminants can be present in untreated compressed air used to clean pulse jet fabric filters and cartridge fabric filters? Select all that apply.
 - a. Condensed water droplets
 - d. Condensed oil droplets
6. What problem or problems are created if a pulse jet bag does not seal properly to the tube sheet? Select all that apply.
 - a. Unfiltered gas could leak around the bag into the clean gas plenum
7. A reverse bag constructed of fiberglass has very low tension and is sagging severely at the connection to the tube sheet thimble. What problem or problems could be created by this condition? Select all that apply.
 - a. The bag could develop holes due to its vulnerability to flex failure
 - b. The bag could be abraded by the high velocity inlet gas stream
 - c. The sagging bag could choke off flow of unfiltered air into the bag

8. What forces are used to remove particles in woven and felted bags? Select all that apply.
- a. Inertial impaction
 - b. Brownian diffusion
 - c. Electrostatic attraction
9. What forces are used to remove particles in a membrane bag? Select all that apply.
- a. Inertial impaction
 - b. Brownian diffusion
 - c. Electrostatic attraction
 - d. Sieving
10. What problem occurs at excessive air-to-cloth ratios?
- c. Increased particulate emissions through the filter media

Review Problems

1. Calculate the net air-to-cloth ratio for a reverse air baghouse with 12 compartments containing 276 bags each. The diameter of each bag is 11 in, and the bag height is 28 ft. One of the compartments is always off-line for cleaning, and another is off-line for maintenance. Use a gas flow rate of 350,000 acfm.
2. Calculate the gas approach velocity for a pulse jet baghouse having a single compartment, 60 rows of bags with 10 bags each, and a bag diameter of 6 in. Assume that the internal dimensions of the compartment are 6.5 ft x 40 ft. Use a gas flow rate of 66,000 acfm.
3. Would a 150 μm size particle or particle agglomerate successfully settle by gravity in the pulse jet baghouse described in Problem 2? Assume a temperature of 20°C, a particle density of 1.0 g/cm^3 , and that the transitional region terminal settling velocity equation is appropriate for this particle size.
4. Calculate the static pressure difference between the clean gas plenum of a top access type pulse jet baghouse and the ambient air. Assume that the inlet static pressure to the baghouse is - 4 in WC and the static pressure drop across the baghouse is 5 in WC.
5. It is proposed to install a pulse jet fabric filter with an air-to-cloth ratio of 2.5 ft/min to clean a 10,000 scfm air stream at 250°F. Determine the filtering area required for this operation and, using the information below, choose an appropriate filter bag and determine how many will be needed.

Filter bag	A	B	C	D
Tensile strength	Excellent	Very good	Fair	Excellent
Maximum temperature (°F)	260	275	260	220
Relative cost per bag	2.6	3.8	1.0	2.0
Size	4¾" x 10'	6" x 10'	6" x 14'	6" x 14'

This page intentionally left blank.

Review Problem Solutions

1. Calculate the net air-to-cloth ratio for a reverse air baghouse with 12 compartments containing 276 bags each. The diameter of each bag is 11 in, and the bag height is 28 ft. One of the compartments is always off-line for cleaning, and another is off-line for maintenance. Use a gas flow rate of 350,000 acfm.

Solution:

$$\text{Individual bag area} = \pi Dh = \pi \left[11 \text{ in} \left(\frac{1 \text{ ft}}{12 \text{ in}} \right) \right] (28 \text{ ft}) = 80.6 \frac{\text{ft}^2}{\text{bag}}$$

$$\text{Total net bag area} = 80.6 \frac{\text{ft}^2}{\text{bag}} \left(276 \frac{\text{bags}}{\text{compartment}} \right) (10 \text{ compartments}) = 222,456 \text{ ft}^2$$

$$\text{Net air-to-cloth ratio} = \frac{Q}{A} = \frac{350,000 \frac{\text{ft}^3}{\text{min}}}{222,456 \text{ ft}^2} = 1.57 \frac{\text{ft}}{\text{min}}$$

2. Calculate the gas approach velocity for a pulse jet baghouse having a single compartment, 60 rows of bags with 10 bags each, and a bag diameter of 6 in. Assume that the internal dimensions of the compartment are 6.5 ft x 40 ft. Use a gas flow rate of 66,000 acfm.

Solution:

$$\text{Total baghouse shell area} = (6.5 \text{ ft})(40 \text{ ft}) = 260 \text{ ft}^2$$

$$\text{Bottom area of bag} = \frac{\pi D^2}{4} = \frac{\pi \left[6 \text{ in} \left(\frac{1 \text{ ft}}{12 \text{ in}} \right) \right]^2}{4} = 0.196 \frac{\text{ft}^2}{\text{bag}}$$

$$\text{Total bottom area} = 0.196 \frac{\text{ft}^2}{\text{bag}} \left(10 \frac{\text{bags}}{\text{row}} \right) (60 \text{ rows}) = 118 \text{ ft}^2$$

$$\text{Open area} = \text{total shell area} - \text{total bottom area} = 260 \text{ ft}^2 - 118 \text{ ft}^2 = 142 \text{ ft}^2$$

$$\text{Gas approach velocity} = \frac{Q}{A} = \frac{66,000 \frac{\text{ft}^3}{\text{min}}}{142 \text{ ft}^2} = 465 \frac{\text{ft}}{\text{min}} = 7.75 \frac{\text{ft}}{\text{sec}}$$

3. Would a 150 μm size particle or particle agglomerate successfully settle by gravity in the pulse jet baghouse described in Problem 2? Assume a temperature of 20°C, a particle density of 1.0 g/cm^3 , and that the transitional region terminal settling velocity equation is appropriate for this particle size.

Solution:

$$v_t = \frac{0.153 g^{0.71} \rho_p^{0.71} d_p^{1.14}}{\mu_g^{0.43} \rho_g^{0.29}} = \frac{0.153 \left(980 \frac{\text{cm}}{\text{sec}^2} \right)^{0.71} \left(1 \frac{\text{g}}{\text{cm}^3} \right)^{0.71} \left(150 \times 10^{-4} \text{cm} \right)^{1.14}}{\left(1.8 \times 10^{-4} \frac{\text{g}}{\text{cm} \cdot \text{sec}} \right)^{0.43} \left(1.2 \times 10^{-3} \frac{\text{g}}{\text{cm}^3} \right)^{0.29}} = 48.58 \frac{\text{cm}}{\text{sec}} = 1.59 \frac{\text{ft}}{\text{sec}}$$

The 150 μm particle will not settle. The upward velocity of the gas stream is much higher than the terminal settling velocity.

4. Calculate the static pressure difference between the clean gas plenum of a top access type pulse jet baghouse and the ambient air. Assume that the inlet static pressure to the baghouse is -4 in WC and the static pressure drop across the baghouse is 5 in WC.

Solution:

$$\text{Static pressure in the clean gas plenum} = -4 \text{ in WC} - (5 \text{ in WC}) = -9 \text{ in WC}$$

Since the ambient gauge pressure is 0 in WC, the static pressure difference between the clean gas plenum and the ambient air is 9 in WC.

5. It is proposed to install a pulse jet fabric filter with an air-to-cloth ratio of 2.5 ft/min to clean a 10,000 scfm air stream at 250°F. Determine the filtering area required for this operation and, using the information below, choose an appropriate filter bag and determine how many will be needed.

Filter bag	A	B	C	D
Tensile strength	Excellent	Very good	Fair	Excellent
Maximum temperature (°F)	260	275	260	220
Relative cost per bag	2.6	3.8	1.0	2.0
Size	4¾" x 10'	6" x 10'	6" x 14'	6" x 14'

Solution:

Calculate actual flow rate:

$$Q = 10,000 \frac{\text{ft}^3}{\text{min}} \left(\frac{250^\circ\text{F} + 460}{68^\circ\text{F} + 460} \right) = 13,447 \frac{\text{ft}^3}{\text{min}}$$

Calculate filtering area:

$$\text{Filter area} = \frac{Q}{A/C\text{Ratio}} = \frac{13,447 \frac{\text{ft}^3}{\text{min}}}{2.5 \frac{\text{ft}}{\text{min}}} = 5,379 \text{ft}^2$$

Bag D can be eliminated because its maximum temperature is too low. Bag C can be eliminated because it has only fair tensile strength. Only Bags A and B will be considered further.

For Bag A:

$$\text{Bag area} = \pi Dh = \pi \left[4.75 \text{in} \left(\frac{1 \text{ft}}{12 \text{in}} \right) \right] (10 \text{ft}) = 12.44 \frac{\text{ft}^2}{\text{bag}}$$

$$\text{Number of bags} = \frac{5,379 \text{ft}^2}{12.44 \frac{\text{ft}^2}{\text{bag}}} = 432 \text{bags}$$

$$\text{Relative cost} = \left(\frac{2.6}{\text{bag}} \right) 432 \text{bags} = 1,123$$

For Bag B:

$$\text{Bag area} = \pi Dh = \pi \left[6 \text{in} \left(\frac{1 \text{ft}}{12 \text{in}} \right) \right] (10 \text{ft}) = 15.71 \frac{\text{ft}^2}{\text{bag}}$$

$$\text{Number of bags} = \frac{5,379 \text{ft}^2}{15.71 \frac{\text{ft}^2}{\text{bag}}} = 342 \text{bags}$$

$$\text{Relative cost} = \left(\frac{3.8}{\text{bag}} \right) 342 \text{bags} = 1,300$$

Bag A should be chosen because of its lower relative cost.

This page intentionally left blank.

References

Bundy, R.P., "Operation and maintenance of fabric filters", *Proceedings, Operating and Maintenance Procedures for Gas Cleaning*, Air Pollution Control Association Specialty Conference, pp. 139-152, 1980.

Campbell, P.R., "Make fiberglass filter bags last longer by maintaining proper tension", *Power*, pp. 92-93, March 1980.

Carr, R.C., "Second Conference on Fabric Filter Technology for Coal-Fired Power Plants, Conference Summary", *Journal of the Air Pollution Control Association*, **33**, 949 (1983).

Dennis, R., R.W. Cass and R.R. Hall, "Dust dislodgement from woven fabrics versus filter performance", *Journal of the Air Pollution Control Association*, **28**, 47 (1978).

Makansi, J., "Match bag material for your fabric filter to type of service", *Power*, pp. 115-118, October 1983.

Perkins, R.P., "State-of-the-art of baghouses for industrial boilers", Presented at the Industrial Fuel Conference, West Lafayette, Indiana, October 5-6, 1972.

Perkins, R.P., and J.F. Imbalzano, "Factors affecting bag life performance in coal-fired boilers", *Proceedings, The User and Fabric Filtration Equipment III*, Air Pollution Control Association Specialty Conference, pp. 120-144, 1978.

Turner, J.H., A.S. Viner, J.D. McKenna, R.E. Jenkins and W.M. Vatavuk, "Sizing and costing of fabric filters", *Journal of the Air Pollution Control Association*, **37**, 749 (1987).

Viner, A.S., R.P. Donovan, D.S. Ensor and L.S. Hovis, "Comparison of baghouse test results with the GCA/EPA design model", *Journal of the Air Pollution Control Association*, **34**, 872 (1984).

Weber, G. F., and G.L. Schelkoph, "Performance/durability evaluation of 3M Company's high-temperature Nextel filter bags", Presented at the Eighth Symposium on the Transfer and Utilization of Particulate Control Technology, San Diego, California, March 30-23, 1990.

This page intentionally left blank.

CHAPTER 8

WET SCRUBBERS

Wet scrubbers are a diverse set of control devices that can be used to collect both particles and gases, but usually not simultaneously at high efficiency for both. This is because particulate scrubbers are designed to generate high inertial forces or electrostatic forces on particles to drive them into droplets or sheets of liquid. Gas absorbers are designed to have high liquid surface areas and relatively long residence times to maximize the absorption of contaminants into liquid droplets or sheets. Despite the fundamental operating differences, most particulate scrubbers have at least modest efficiencies for gaseous contaminant removal, and most gaseous absorbers have modest efficiencies for the removal of particulate larger than approximately 3 micrometers. In this chapter we will focus on wet scrubbers used for particle collection.

Wet scrubbers use a three-step process for the treatment of particulate-laden gas streams:

- Particle capture in either droplets, liquid sheets, or liquid jets
- Capture of the liquid droplets entrained in the gas stream
- Treatment of the contaminated liquid prior to reuse or discharge

Particle capture is accomplished in a contacting vessel, such as a venturi scrubber, a tray tower scrubber, or a spray tower scrubber. Mist eliminators built into the scrubber vessel, or provided as a separate vessel, are used to collect the entrained water droplets after the scrubber. Clarifiers, vacuum filters, or settling ponds are used to treat the wastewater stream from the scrubber. Particle size is an important factor in all types of scrubbing systems. This is because they all use the same basic collection mechanism--inertial impaction, which is highly dependent on particle size.

Operating Principles

Collection Mechanisms

The mechanisms involved in collecting particulate matter in various wet scrubber designs include:

- Impaction
- Brownian motion
- Electrostatic attraction
- Thermophoresis
- Diffusiophoresis

The primary mechanism by which particles are collected in wet scrubbers is impaction. Because of the limited residence time in most scrubbers, Brownian motion is typically not significant. Those collectors, like the venturi scrubber, that can collect submicron particles at high efficiency, make up for the lack of particle mass by using impaction at high velocities.

Some wet scrubbers use enhancements to improve their ability to collect small particles without incurring higher pressure drops. One of these enhancements is electrostatic charging. By creating particles and droplets of opposite polarities, the collection efficiency is improved by electrostatic attraction. Scrubber performance can also be enhanced by promoting condensation. The not only results in the growth of submicron particles, but also sweeps them toward condensing surfaces by the mechanisms of thermophoresis and diffusiphoresis.

Inertial Impaction

Recalling the discussion in Chapter 4, impaction occurs when a particle has too much inertia to avoid a target that it is approaching. It crashes into the target instead of flowing around it on the gas streamlines. If the particle is retained by the target (in this case, a droplet), a successful impaction has occurred. The efficiency of particle collection by impaction is proportional to the inertial impaction parameter shown in Equation 4-1.

$$\Psi_I = \frac{C_c d_p^2 \rho_p V_r}{18 \mu_g d_d} \quad (8-1)$$

where:

- Ψ_I = inertial impaction parameter (dimensionless)
- C_c = Cunningham slip correction factor (dimensionless)
- d_p = physical particle diameter (cm)
- ρ_p = particle density (gm/cm³)
- V_r = relative velocity between particle and droplet (cm/sec)
- d_d = droplet diameter (cm)
- μ_g = gas viscosity (gm/cm sec)

This equation indicates that impaction effectiveness is related to the square of the particle diameter. Impaction is much more efficient for large particles than for small particles, especially those particles less than 0.5 μm . Impaction rapidly becomes less efficient as the particle size decreases into the submicron range. To overcome this inherent limitation, the differences in droplet and particle velocities must be high when most of the particulate matter is in the submicron range.

The impaction parameter indicates that impaction is directly proportional to the difference in the velocities of the particle and the droplet or liquid sheet target. There are substantial differences among the various types of scrubbers with respect to this relative velocity term. Furthermore, the difference in velocity does not remain constant throughout some types of scrubbers.

For example, in venturi scrubbers there is a very large difference between particle velocity and droplet velocity at the inlet to the throat. However, a fraction of a second later, when the gas stream reaches the throat outlet, the droplets have accelerated to a velocity approaching that of the particles in the gas stream. Accordingly, impaction is most efficient at the inlet to the throat, before the droplets have accelerated. In packed bed scrubbers, the difference in particle and target velocities is very low due to the low gas velocity. This difference remains relatively constant throughout the bed. As a result, impaction is very limited and is dependent partially on the height of the bed.

The effectiveness of impaction is inversely related to the diameter of the target. Small water droplets serve as better targets than large droplets. The formation of small droplets is favored by droplet atomization in high-velocity gas streams and droplet atomization in high-pressure nozzles. Low surface tension conditions in the liquid also favor small droplet size distributions.

Brownian Motion

Brownian motion, or diffusion, is the particle movement caused by the impact of gas molecules on the particle. Only very small particles are affected by the molecular collisions, since they possess little mass and, therefore, little inertial tendency. Brownian motion begins to be effective as a capture mechanism for particles less than approximately 0.3 μm , and it is significant for particles less than 0.1 μm . Most industrial sources of concern in the air pollution field do not generate large quantities of particulate matter in the less than 0.1 μm size range. Therefore, in most cases, Brownian motion is not a major factor influencing overall scrubber collection efficiencies.

Static Pressure Drop

The static pressure drop across scrubbers is due to the frictional losses of the gas stream moving through the ductwork and the scrubber, the energy required to accelerate the gas, and the energy required to accelerate and atomize (if applicable) the liquid stream. The energy losses for all of these are related to the square of the gas velocity, as indicated in Equation 8-2.

$$\Delta P \propto v^2 \quad (8-2)$$

where:

$$\begin{aligned} \Delta P &= \text{static pressure drop} \\ v &= \text{gas velocity in scrubber} \end{aligned}$$

For scrubber systems using primarily impaction for particle capture, there is a logical relationship between the efficiency and the static pressure drop. The efficiency should increase as the static pressure drop increases. This is because the effectiveness of impaction is directly proportional to the difference in the velocities of the rapidly moving particles and the slow-moving liquid droplets or sheets. High static pressure drop values are associated with high gas velocities through the scrubber. Due to the logical association between static pressure drop and efficiency, the easily measured static pressure drop has been used as an indirect indicator and predictor of performance for a number of years.

A number of correlations have been published that relate emissions to the static pressure drop across the scrubber. Three of these correlations are reproduced in Figures 8-1, 8-2 and 8-3 in order to demonstrate their characteristics.

Emissions data for flooded disc scrubbers (a type of adjustable throat venturi that is no longer manufactured) serving lime kilns at four separate kraft pulp mills are shown in Figure 8-1. The data scatter is evident. A 90% confidence interval would demonstrate considerable variability, even near the mean pressure drop value of approximately 9 in. WC. It is difficult to use correlations of this nature to make accurate estimates of performance.

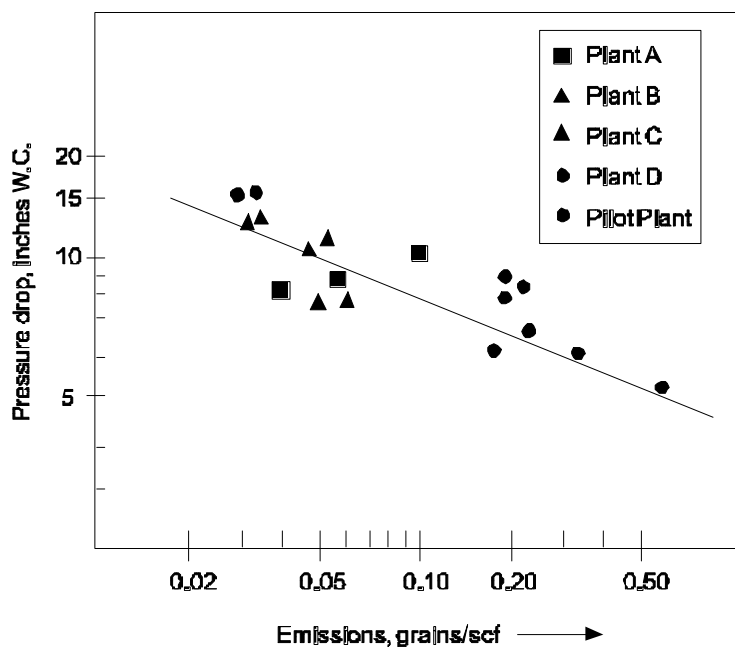


Figure 8-1. Emissions versus pressure drop for flooded disc scrubbers serving lime kilns (Walker and Hall, 1968)

Figure 8-2 is a plot of the emissions versus the static pressure drops of conventional venturi scrubbers serving a number of different coal thermal dryers. There is no apparent correlation in these data.

Only the data shown in Figure 8-3 appear to have a correlation with a minimum amount of variability. These data were taken at three side-by-side venturi scrubber systems serving similar metallurgical furnaces. Furthermore, the tests used to compile the data were performed over a short time period, thereby avoiding variations due to changes in scrubber operating conditions.

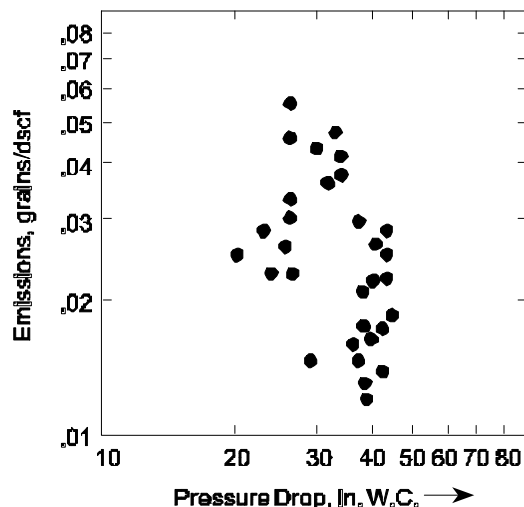


Figure 8-2. Emissions versus pressure drop for venturi scrubbers serving coal driers (Engineering Science, 1979)

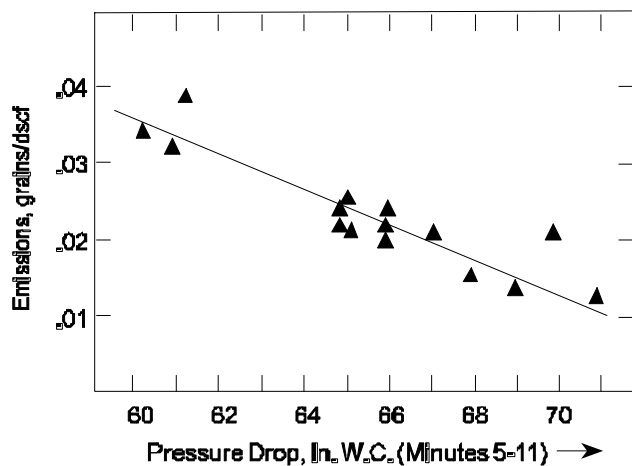


Figure 8-3. Emissions versus pressure drop for venturi scrubbers serving Q-BOF processes

The underlying cause of the data scatter apparent in Figures 8-1 and 8-2 is differences in the particle size distribution from plant-to-plant over time. The correlation of emissions with static pressure drop is based on the assumption that the particle size distribution is a constant. This is rarely accurate when data from different plants or processing units are combined into a single correlation. The acceptable correlation shown in Figure 8-3 appears to be one of the few cases in which data from different units can be combined into a single correlation. Overall, the inability to account for possible variations in the inlet particle size distribution to the scrubber is the major limitation of these types of correlations.

Some variations in particle size distribution are common in all processes due to slight changes in raw materials, operating conditions, and process loads. However, problems such as vapor

nucleation and solids release during droplet evaporation can cause major changes in the quantity of particulate matter in the difficult-to-control size range of 0.1 to 1 μm .

Certain operating problems in wet scrubbers can also increase emissions without affecting the static pressure drop across the unit. For example, gas-liquid maldistribution in the throat of a venturi scrubber can cause dramatically increased emissions with little, if any, change in the observed static pressure drop. Changes in the effectiveness of particle impaction into the droplet targets can also affect performance. Reduced capture effectiveness can be caused by changes in the surface tension of the droplets or by the presence of non-wettable materials coating the surfaces of the particles.

Correlations based on scrubber static pressure drop must be used with caution due to the possible shifts in particle size distribution and changes in emissions that can occur without significant changes in the static pressure drop. Caution is also warranted with correlations for devices that enhance their performance with other mechanisms besides impaction.

Gas Cooling

Process gases that are at elevated temperature are usually passed through an evaporative cooler before entering the scrubber. The primary purpose of the evaporative cooler is to reduce the gas temperature to protect temperature-sensitive components in the scrubber vessel, mist eliminators and other components. For example, it is common for the scrubber vessels to have corrosion-resistant liners that can volatilize at temperatures exceeding 400°F to 1,000°F. Some scrubber vessels and many mist eliminators are fabricated with fiberglass reinforced plastics (FRP) that have temperature limitations of 180°F to 250°F. The evaporative cooler is provided to ensure that the gas temperatures in the scrubber vessel, mist eliminator, and other portions of the system do not exceed their design limitations even if the liquid recirculation system in the scrubber fails.

The evaporative cooler provides a secondary benefit in particulate matter control systems. By cooling the gas stream prior to particulate matter removal, the evaporation of droplets in the scrubber vessel is significantly reduced. The mass flux of water vapor away from evaporating droplets impedes particle capture by the droplets. Accordingly, the minimization of evaporation has a beneficial impact on the particulate matter collection efficiency.

Liquid Recirculation

The scrubbing liquid is recirculated to minimize the amount of liquid that must be treated and discharged. The scrubbing liquid is collected in the sump of the scrubber and mist eliminator delivered by gravity to a recirculation tank having a liquid residence time of several minutes. This provides sufficient time to introduce alkali additives, if necessary, to adjust the pH back to the proper range. The recirculation pump recirculates the liquid back to the scrubber vessel from this tank. Centrifugal pumps are used almost exclusively.

Some scrubber systems use spray nozzles to atomize the scrubbing liquid. The full cone nozzle is used most frequently because it projects droplets across an entire circular area. This is necessary in many types of scrubbers to obtain effective gas-liquid contact. The droplets

produced by full cone nozzles usually have mean diameters of 100 to 1,000 micrometers and are typically log-normally distributed.

Liquid-to-Gas Ratio

The rate of liquid flow to a scrubber is often expressed in terms of the liquid-to-gas ratio, with units of gallons of liquid per 1,000 actual cubic feet of gas flow. In some performance relationships, the liquid and gas rates are expressed in the same units, giving a dimensionless liquid-to-gas ratio. Most wet scrubber systems for particle collection operate with liquid-to-gas ratios between 4 and 20 gal/1,000 acf. Higher values do not usually improve performance, and they may have a slightly adverse impact due to changes in the droplet size distribution formed in the scrubber. Low values can have a highly adverse impact because there are simply too few impaction targets available. At low liquid-to-gas ratio conditions, a portion of the particle-containing gas stream may pass through the collection zone without encountering a liquid target.

The liquid-to-gas ratio can be defined based either on the inlet or outlet gas flow rates. It can also be defined based on either actual or standard gas flow rates. In this course, the liquid-to-gas ratio is defined as:

$$\frac{L}{G} = \frac{\text{Inlet liquid flow (gpm)}}{\text{Outlet gas flow rate (1,000 acfm)}} \quad (8-3)$$

The outlet gas flow rate is used because this value is readily measured as part of an emission test program. It is considerably easier to obtain an accurate flow measurement at the scrubber outlet, where particulate matter loading in the gas stream is reduced and good sampling ports are available. Most scrubber inlet ducts are not well suited for gas flow rate testing.

It is helpful to confirm that the liquid-to-gas ratio to be used on a scrubber system is above the minimum level necessary to ensure proper gas-liquid distribution. As noted above, in most gas-atomized scrubbers, this minimum value is approximately 4 gal/1,000 acf. In other type of scrubbers, the value is as low as 2 gal/1,000 acf. Calculation of the liquid-to-gas ratio is illustrated in the following example.

Example 8-1

What is the design liquid-to-gas ratio for a scrubber system that has an outlet gas flow rate of 15,000 acfm, a pump discharge rate of 100 gpm, and a liquid purge rate of 10 gpm? The purge stream is withdrawn from the pump discharge side.

Solution

$$\frac{L}{G} = \frac{\text{Inlet liquid flow (gpm)}}{\text{Outlet gas flow rate (1,000 acfm)}}$$

$$\text{Inlet liquid flow} = 100 \text{ gpm} - 10 \text{ gpm} = 90 \text{ gpm}$$

$$\frac{L}{G} = \frac{90 \text{ gpm}}{15,000 \text{ acfm}} = 0.006 \frac{\text{gal}}{\text{acf}} = 6.0 \frac{\text{gal}}{1,000 \text{ acf}}$$

Liquid Purge Rates

A small portion of the recirculating liquid in a scrubber system must be purged for treatment. The treated liquid can then be returned to the system or replaced with make-up water. The liquid purge rate necessary to ensure long term proper performance of a system depends on one or more of the following factors.

- The rate of particulate matter capture
- The maximum concentration of suspended solids acceptable in the scrubber system
- The rate of dissolved solids precipitation in the recirculated liquid due to the accumulation of calcium and/or magnesium ions
- The rate of chloride or fluoride ion accumulation in the scrubber liquid

Example 8-2 illustrates the calculations involved in evaluating the necessary liquid purge rate based on the particulate matter capture rates and maximum suspended solids levels.

Example 8-2

Estimate the liquid purge rate and recirculation pump flow rate for a scrubber system treating a gas stream of 30,000 acfm (inlet flow) with a particulate matter loading of 0.8 grains per acf. Assume that the scrubber particulate matter removal efficiency is 95% and the maximum suspended solids level desirable in the scrubber is 2% by weight. Use a liquid-to-gas ratio of 8 gallons (inlet) per thousand acf (outlet) and an outlet gas flow rate of 23,000 acfm.

Solution:

Calculate the inlet particulate mass:

$$\text{Inlet mass} = 30,000 \frac{\text{ft}^3}{\text{min}} \left(\frac{0.8 \text{ grains}}{\text{ft}^3} \right) \left(\frac{\text{lb}}{7,000 \text{ grains}} \right) = 3.43 \frac{\text{lb}}{\text{min}}$$

$$\text{Collected mass} = 0.95 (\text{Inlet mass}) = 3.26 \frac{\text{lb}}{\text{min}}$$

Purge solids of 3.26 lb/min are 2% of the total purge stream, therefore:

$$\text{Purge stream} = \frac{3.26 \frac{\text{lb}}{\text{min}}}{0.02} = 163.0 \frac{\text{lb}}{\text{min}}$$

A stream with 2% suspended solids has a specific gravity of about 1.02, therefore:

$$\text{Purge stream density} = \left(8.34 \frac{\text{lb water}}{\text{gal}} \right) (1.02) = 8.51 \frac{\text{lb}}{\text{gal}}$$

$$\text{Purge stream flow rate} = \frac{163.0 \frac{\text{lb}}{\text{min}}}{8.51 \frac{\text{lb}}{\text{gal}}} = 19.2 \frac{\text{gal}}{\text{min}}$$

$$\text{Inlet liquid flow rate} = \left(23,000 \frac{\text{ft}^3}{\text{min}} \right) \left(8 \frac{\text{gal}}{1,000 \text{ft}^3} \right) = 184.0 \frac{\text{gal}}{\text{min}}$$

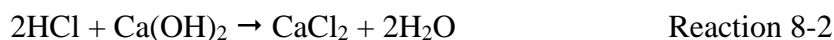
$$\text{Pump flow rate} = 184.0 \frac{\text{gal}}{\text{min}} + 19.2 \frac{\text{gal}}{\text{min}} = 203.2 \frac{\text{gal}}{\text{min}}$$

Alkali Addition

An alkali addition system is used on wet scrubber systems that collect acidic particulate matter or treat gas streams that have acidic gases or vapors that could absorb in the liquid stream. The most common acid gases include sulfur dioxide, hydrogen chloride, and hydrogen fluoride. Carbon dioxide formed in most combustion processes is also mildly acidic.

The most common alkalis used for neutralization of acidic material in scrubbers include lime, soda ash, and sodium hydroxide. In some cases, limestone and nahcolite are used. With the exception of sodium hydroxide, all of these materials are typically stored and fed to the recirculation tank in a powder form. Sodium hydroxide is usually fed in solution. The rate of addition of alkali is controlled by a pH meter that is usually mounted in the scrubber recirculation tank or the recirculation pipe leading to the scrubber vessel.

The alkali requirements are usually calculated based on the quantities of acidic gases captured and the molar ratios necessary for the following reactions:



Example 8-3

Calculate the amount of calcium hydroxide (lime) needed to neutralize the HCl absorbed from a gas stream having 50 ppmv HCl and a flow rate of 10,000 scfm. Assume an HCl removal efficiency of 95%.

Solution:

Calculate HCl absorbed in the scrubbing liquid:

$$50 \text{ ppmv} = \frac{50 \text{ ft}^3 \text{ HCl}}{10^6 \text{ ft}^3 \text{ total}} = 0.00005 \frac{\text{ft}^3 \text{ HCl}}{\text{ft total}} = 0.00005 \frac{\text{lb - mole HCl}}{\text{lb - mole total}}$$

$$\begin{aligned} \text{HCl absorbed} &= 10,000 \text{ scfm} \left(\frac{\text{lb - mole}}{385.4 \text{ scf}} \right) \left(0.00005 \frac{\text{lb - mole HCl}}{\text{lb - mole total}} \right) (0.95) \\ &= 0.00123 \frac{\text{lb - mole}}{\text{min}} \end{aligned}$$

$$\begin{aligned} \text{Ca(OH)}_2 \text{ required} &= \left(\frac{1 \text{ lb - mole Ca(OH)}_2}{2 \text{ lb - mole HCl}} \right) \left(0.00123 \frac{\text{lb - mole HCl}}{\text{min}} \right) \\ &= 0.00062 \frac{\text{lb - mole}}{\text{min}} \left(74 \frac{\text{lb Ca(OH)}_2}{\text{lb - mole}} \right) \left(60 \frac{\text{min}}{\text{hr}} \right) \\ &= 2.75 \frac{\text{lb}}{\text{hr}} \end{aligned}$$

Wastewater Treatment

There are a wide variety of wastewater treatment systems for particulate matter wet scrubbers. Some small scrubbers at large industrial facilities discharge directly to the plant wastewater system, rather than using a dedicated system. Small scrubbers collecting nontoxic particulate matter, such as those at asphalt plants, sometimes use a small two-zone settling pond for wastewater treatment. In these cases, the effluent overflowing the second zone of the pond is returned to the scrubber system.

A small wastewater treatment system is usually installed for large wet scrubber systems. A clarifier is used for removal of the suspended solids that will settle by gravity. The overflow from the clarifier is returned to the scrubber recirculation tank. The clarifier underflow containing the concentrated solids is often sent to a rotary vacuum filter for removal of the suspended solids. The sludge from the rotary vacuum filter is sent to a landfill for disposal.

In some cases, a flocculent is added to the clarifier to optimize solids removal. However, addition of flocculates must not exceed the levels that cause an increase in the liquid surface tension. This can have an unintended detrimental effect on particulate removal efficiency of the scrubber by decreasing the effectiveness of particle impaction into the liquid droplets and by changing the droplet size distribution formed in the scrubber.

Mist Elimination

Essentially all scrubber vessels generate relatively large water droplets that are entrained in the gas stream. Most of these droplets contain captured particles and must be removed from the gas stream prior to discharge to the atmosphere. A mist eliminator is used for this purpose. In addition to minimizing the carry-over of solids-containing droplets to the atmosphere, mist eliminators also protect downstream equipment, such as fans, from solids-containing droplets and minimize the amount of water lost from the system. Mist eliminators are usually equipped with one or more sets of spray nozzles to remove accumulated solids. Solids build-up is due to impaction of solids-containing water droplets and due to the chemical precipitation of dissolved solids from the scrubbing liquid. The four most common types of mist eliminators are chevrons, mesh or woven pads, tube banks and cyclones. Static pressure drops across them range from 0.5 in. WC to more than 4 in. WC.

Chevrons

Chevrons are simply zig-zag baffles that force the gas to turn sharply several times while passing through. As the gas stream turns to pass through the baffles, droplets impact on the baffles and run together to form large droplets that drain back into the scrubber. Chevrons are usually designed with one to four changes in gas stream direction, termed a *pass*. Separation efficiency increases with the number of passes. A three-pass chevron mist eliminator is shown in Figure 8-4. Other common types of chevrons have two- and four-pass arrangements. Each manufacturer has a variety of designs for the chevron blades to minimize reentrainment and optimize the gas flow range.

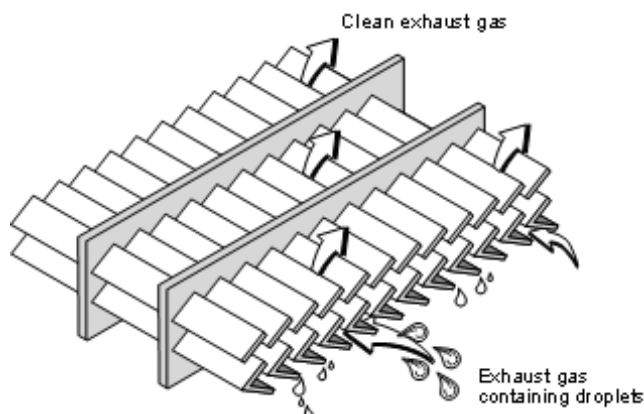


Figure 8-4. Chevron mist eliminator

Chevron mist eliminators can be installed in either a vertical or horizontal outlet arrangement. In the vertical outlet design, liquid draining from the chevron blades is opposed by the upward moving gas stream. In the horizontal outlet arrangement, the liquid drains in a direction 90 degrees from the gas stream; therefore, less reentrainment of collected droplets occurs.

Essentially all of the chevron mist eliminator designs are limited to gas velocities of less than approximately 20 ft/sec. Many of the chevrons have optimum performance in the 5 to 15 ft/sec range. At higher velocities, liquid on the blades can be driven toward the outlet side of the chevron where it can be reentrained into the gas stream. Higher velocities can occur in an operating system because of solids accumulation on the blades.

Solids accumulation on the chevron mist eliminators can create high velocities by restricting the amount of area open for gas flow. In applications where solids accumulation is possible, mist eliminator sprays are installed to clean the chevrons on a frequent basis. These sprays are activated on an hourly or shift basis, as necessary to maintain the static pressure drop across the mist eliminator in the design range. In most cases, the sprays are mounted on the inlet side. However, in cases especially prone to solids accumulation, sprays are mounted on both the leading and trailing sides. The sprays can be activated either by timers or by static pressure sensors. Clean water is used for mist eliminator cleaning. The necessary water pressures depend on the placement of the spray nozzles. Values of 5 to 20 psig are common.

Mesh and Woven Pads

Mesh pads are composed of randomly interlaced metal fibers and can be up to 6 inches thick. As the gas stream turns to pass by the elements of the mesh, droplets impact on the baffles and run together to form large droplets that drain back into the scrubber. As in the case with the chevrons, there is a maximum gas velocity above which reentrainment is possible. That maximum velocity is usually in the range of 10-23 ft/sec. A mesh pad mist eliminator pad is shown in Figure 8-5.

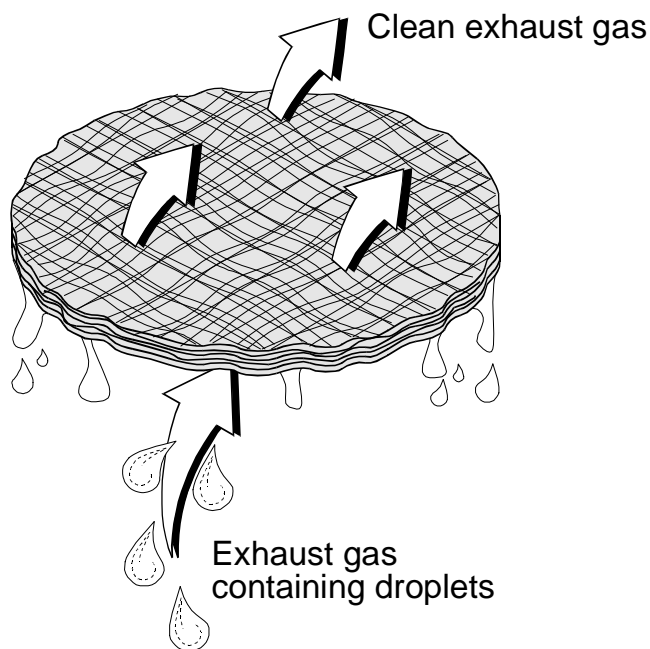


Figure 8.5. Mesh pad mist eliminator

Woven pads have complex, interlaced synthetic fibers that serve as impaction targets. Mist eliminators composed of these materials are often layered. The inlet side layers are open weaves that are capable of removing large quantities of large-diameter material without overloading. The middle and outlet side layers have more compact weaves, which have high removal efficiencies for the small liquid droplets. These units have maximum velocities of 8 to 15 ft/sec, depending on the pad construction characteristics.

Tube Bank

A tube bank mist eliminator is made of vertical or horizontal layers of offset cylindrical tubes. As the gas stream turns to pass by each layer, droplets impact on the tubes and run together to form large droplets that drain back into the scrubber. As in the case with the chevrons and mesh and woven pads, there is a maximum gas velocity above which reentrainment is possible. That maximum velocity is usually in the range of 12-23 ft/sec. A tube bank mist eliminator is shown in cross-section in Figure 8-6.

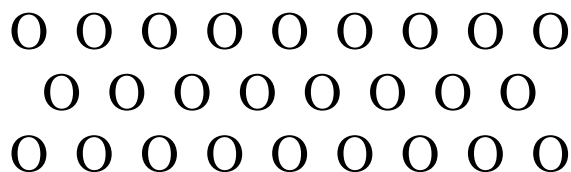


Figure 8-6. Tube bank mist eliminator

Cyclones

The smaller droplet size distributions created in venturi scrubbers are usually collected in a separate large diameter cyclone. As illustrated in Figure 8-7, the gas stream enters tangentially at the bottom of the vessel and, depending on the gas velocity, turns one-half to two revolutions prior to discharge. They have reasonable efficiency when operated at close to the design inlet gas velocity. However, droplet removal decreases rapidly at gas flow rates less than 80% or more than 120% of the design value.

The gas flow rate sensitivity is the main disadvantage of cyclonic mist eliminators. The cost of a stand-alone vessel is another major disadvantage. All of the other types of mist eliminators can be installed in the outlet portion of the scrubber vessel and, therefore, do not require their own vessel. The main advantage of the cyclonic mist eliminator is its openness. As long as the cyclonic vessel drain is properly sized and remains open, the mist eliminator is not vulnerable to plugging caused by excessive carryover of solids-containing droplets from the scrubber vessel.

Due to the spinning action of the gas stream, it is often necessary to install anti-vortex baffles in the stack in order to eliminate cyclonic flow conditions at emission testing locations. It is also common to install liquid flow deflectors to prevent liquid collected on the inner cyclone wall from flowing across the tangential inlet duct and being reentrained into the gas stream.

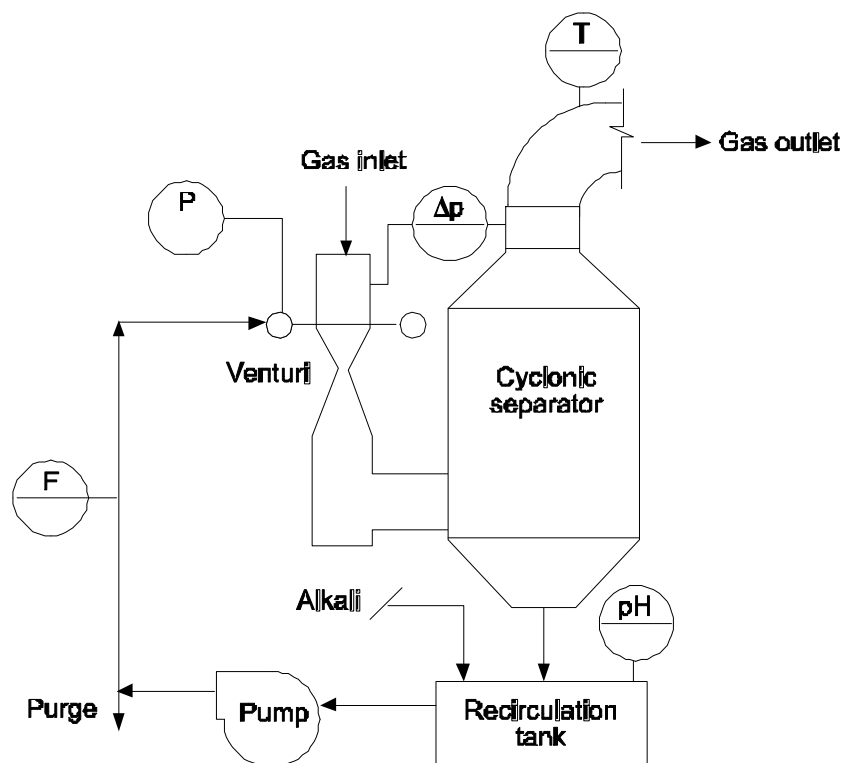


Figure 8-7. Cyclonic mist eliminator in a venturi scrubber system

There are definite limits to the gas velocity through the different types of mist eliminators. As noted, at high gas velocities liquid can be forced toward the trailing edge of the mist eliminator elements and reentrained in the gas stream. General guidelines concerning the maximum velocities are presented in Table 8-1.

Table 8-1. Gas Velocities Through Mist Eliminators		
Mist Eliminator Type	Orientation	Maximum Gas Velocity ft/sec
Chevron	Horizontal	15 – 20
Chevron	Vertical	12 – 15
Mesh Pad	Horizontal	15 – 23
Mesh Pad	Vertical	10 – 12
Woven Pad ¹	Vertical	8 – 15
Tube Bank	Horizontal	18 – 23
Tube Bank	Vertical	12 – 16

Source: Shiffner and Hesketh (1983)

1. Kimre Inc.

The actual maximum velocities that apply to the specific type of mist eliminator should be determined from the manufacturer's specification sheets. These data can then be used to confirm that the mist eliminator is located in an area with gas velocities below the maximum levels. The average gas velocity through the mist eliminator can be calculated simply by dividing the actual

gas flow rate by the cross-sectional area of the mist eliminator, as shown in Equation 8-4. The calculation of the mist eliminator velocity is illustrated in Example 8-4.

$$\text{Velocity} = \frac{\text{Gas flow rate (acfm)} \left(\frac{\text{min}}{60 \text{ sec}} \right)}{\text{Cross - sectional area (ft}^2\text{)}} \quad (8.4)$$

Example 8-4

Estimate the gas velocity through a mist eliminator having a diameter of 6.5 feet, an average gas flow rate of 4,000 dscfm, and a peak gas flow rate of 4,760 dscfm. The peak gas stream temperature is 130°F, the static pressure during peak flow in the vessel is -30 in. WC, and the barometric pressure is 29.4 in. Hg. The moisture content of the gas stream is 6% by volume.

Solution:

The gas velocity should be evaluated under peak flow conditions because this is the time when reentrainment is most probable.

Convert the gas flow rate to actual conditions:

$$\text{scfm} = \frac{\text{dscfm}}{\left(\frac{100 - \% \text{H}_2\text{O}}{100} \right)} = \frac{4,760 \text{ dscfm}}{\left(\frac{100 - 6}{100} \right)} = 5,064 \text{ scfm}$$

$$\text{Absolute pressure} = 29.4 \text{ in. Hg} + \left[-30 \text{ in. WC} \left(\frac{1 \text{ in. Hg}}{13.6 \text{ in. WC}} \right) \right] = 27.19 \text{ in. Hg}$$

$$\text{Absolute temperature} = 130^\circ\text{F} + 460^\circ = 590^\circ\text{R}$$

$$\text{acfm} = 5,064 \left(\frac{590^\circ\text{R}}{528^\circ\text{R}} \right) \left(\frac{29.92 \text{ in. Hg}}{27.19 \text{ in. Hg}} \right) = 6,227 \text{ acfm}$$

$$\text{Area} = \frac{\pi d^2}{4} = \frac{\pi (6.5 \text{ ft})^2}{4} = 33.2 \text{ ft}^2$$

$$\text{Velocity} = \frac{6,227 \frac{\text{ft}^3}{\text{min}} \left(\frac{\text{min}}{60 \text{ sec}} \right)}{33.2 \text{ ft}^2} = 3.13 \text{ ft/sec}$$

Note that the amount of area blocked by mist eliminator blades or any support frames is not taken into account in estimating the average velocity. Accordingly, the velocity estimated is lower than the actual velocity through the mist eliminator. However, this is taken into account when manufacturers publish their maximum velocity guidelines.

Fans, Ductwork and Stacks

The gas handling components of a particulate matter wet scrubber system must be designed for the high negative static pressures that are present during routine operating periods. These components must also be designed for the high levels of entrained droplets, low pH levels, and highly corrosive gas concentrations that can be present during scrubber and/or process upsets.

Fans

The fans used on particulate matter wet scrubbers are usually larger and require more energy than fans for other comparably sized air pollution control systems because of the considerably higher static pressures that must be generated to overcome the flow resistance of the scrubber. Because of their ability to generate these higher static pressures and because of their ability to withstand moderate solids and droplet loadings in the gas stream, radial blade fans are the most commonly used. The fan wheel and fan housing materials of construction are selected based on information concerning the expected gas stream temperatures and the peak concentrations of potentially corrosive materials. Drains are usually provided at the bottom of the fan housing to allow for the removal of moisture accumulating due to droplet entrainment in the gas stream or due to condensation of water vapor from the gas stream.

Ductwork

Ductwork requirements for high energy particulate wet scrubbers are also more demanding than for other types of air pollution control systems. The ductwork must be reinforced to prevent deflection and collapse if the static pressure is lower than -20 in. WC. Failure to adequately reinforce the ductwork could result in damage to welds. Air infiltration through damaged welds could become severe due to the high negative pressures. Severe air infiltration reduces the amount of gas captured at the process, potentially resulting in fugitive emissions.

Stacks

Particulate matter wet scrubbers can have one or two stacks. The main stack is used to disperse the effluent stream of the scrubber system. This stack must be fabricated from materials that can withstand the contaminants that are emitted when scrubber or process upsets occur. Bypass stacks are used upstream of the scrubber vessel when the gas stream being treated is very hot. The bypass stack is usually sealed by a butterfly damper or louver damper. These dampers must provide a tight gas seal to prevent air infiltration into the scrubber system during routine operating periods. The bypass damper is opened when there is a loss of liquid flow. Without liquid flow, the temperatures in the scrubber vessel could exceed the design limitations of the scrubber shell, mist eliminator, or corrosion resistant liners.

Wet Scrubber Capabilities and Limitations

Particulate matter wet scrubbers can provide high efficiency control in a wide variety of industrial applications. Certain types of scrubber systems can provide simultaneous control of both particulate matter and gaseous contaminants. Wet scrubbers are often the control device of choice if there is the potential for embers or explosive gases and vapors in the gas stream to be treated.

The main limitation that must be considered in a specific type of wet scrubber is the particle control capability in the submicrometer size range. Many types of wet scrubbers have very limited efficiencies when the inlet gas stream has particles that are mostly in the difficult-to-control size range of 0.1 to 1.0 μm . A typical fractional efficiency curve illustrating the range for performance for the various types of wet scrubbers is shown in Figure 8-8.

The extent of the efficiency decrease in this size range depends primarily on the intensity of the gas liquid contact in the scrubber vessel. Scrubber vessel types that use high energies to develop large differences in the velocities of the particles and the liquid targets have excellent inertial impaction efficiencies in the difficult to control size range. Those scrubbers designed primarily for gaseous contaminant control have low differences in particle-liquid velocities and little or no particle collection in the difficult-to-control size range.

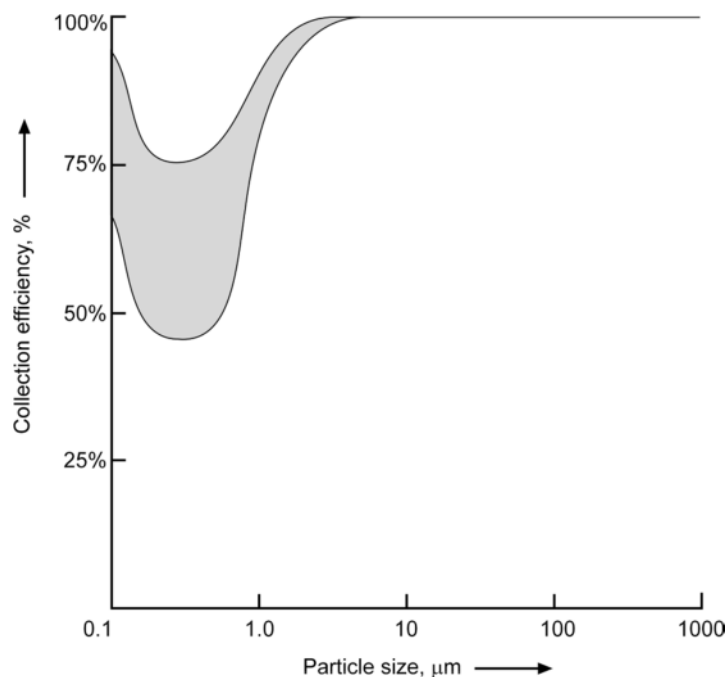


Figure 8-8. Wet scrubber fractional efficiency curve

Another limitation of wet scrubbers is the availability of water. Make-up water is needed to replace water evaporated with the effluent gas stream, water lost as part of the discharged wastewater, and water lost as part of sludge from rotary vacuum filters or similar processing units. In arid climates, there might be insufficient water to use a wet scrubber.

The ability to economically dispose of the wastewater stream in an environmentally sound manner is another limitation of wet scrubbers in some locations. The purge stream from the scrubber recirculation liquid stream might contain dissolved species that have poor leachability characteristics in disposal ponds.

Wet scrubbers usually generate very visible plumes composed of condensed water droplets. The highly visible water droplet plumes that can be quite persistent in cold weather and high humidity conditions can cause visibility problems for nearby roads and airports. Water droplet fallout from the plumes can, in unusual cases, cause freezing problems on walking surfaces and roadways near the facility.

Wet Scrubber Systems

There are many equipment designs for contacting the liquid with the contaminated gas stream. The capability of a particular design can be approximated from the gas stream pressure drop across the scrubber. In general, higher pressure drops indicate more aggressive contact between the liquid and the gas stream, causing smaller particles to be collected with greater efficiency.

Scrubbers with static pressure drops less than about 5 in. WC are capable of efficiently removing particles greater than about 5-10 μm in diameter. These are referred to as *low energy wet scrubbers*. *Medium energy wet scrubbers* have pressure drops from 5 to 25 in. WC. These collectors are capable of removing micrometer-sized particles, but are not very efficient on submicrometer particles. Removal of submicrometer particles requires significant energy input, ranging from 25 to over 100 in. WC, depending on the particle size. These collectors are referred to as *high energy wet scrubbers*. Not all scrubber designs will conform to these generalized categories. Collectors that may collect smaller particles than their pressure drop would indicate include electrostatically enhanced scrubbers and condensation growth scrubbers.

Spray Tower Scrubbers

The spray tower scrubber shown in Figure 8-9 is an example of a low energy wet scrubber. It is the simplest and least expensive type of wet scrubber. The scrubber consists of an open vessel with an array of spray nozzles mounted on multiple headers that are usually spaced about three feet apart. Full cone spray nozzles are used to generate droplets with a mean size of several hundred micrometers. These type nozzles provide complete coverage of the intended target area, which is necessary to ensure maximum particle capture. As the droplets fall downward, they are contacted with the particle-laden gas stream passing upward. The particles are collected by impaction onto the droplets. Because of the inherent limitations in the relative velocity between the droplets and the particles, spray tower scrubbers are effective only for particles greater than about 5 μm in diameter. Despite this limitation, spray tower scrubbers are very useful for treating gas streams having high concentrations of large diameter particulate matter. They are also useful when it is necessary to control both particulate matter and gaseous pollutants.

Spray scrubbers operate with a flange-to-flange static pressure drop of 1 to 3 in. WC. The static pressure drop is due to the normal flow resistance associated with the inlet ductwork, the mist eliminator (if present) and the outlet ductwork. The static pressure drop is not directly related to the particulate matter removal efficiency of the scrubber. Also, because of the relatively low volume occupied by the droplets, changes in the liquid flow rate do not significantly change the pressure drop.

Because of the large size of the droplets produced in the spray tower, mist eliminators may not be used. Instead, sufficient space is provided above the last spray header to allow any droplets carried upward by a turbulent eddy the time to drop downward.

Mechanically Aided Scrubbers

A mechanically aided scrubber uses mechanical energy to accelerate the gas stream to create conditions favorable for particle impaction. The fan-type mechanically aided scrubber shown in Figure 8-10 has a single spray nozzle in the inlet gas duct. This generates the liquid droplets that serve as the initial particle impaction targets. These droplets also wet the fan blades that provide for additional impaction as the gas stream is accelerated through the fan. The centrifugal force of the fan wheel moves the liquid to the outside of the housing, providing mist elimination. The liquid is typically drained from a sump in the outlet air discharge.

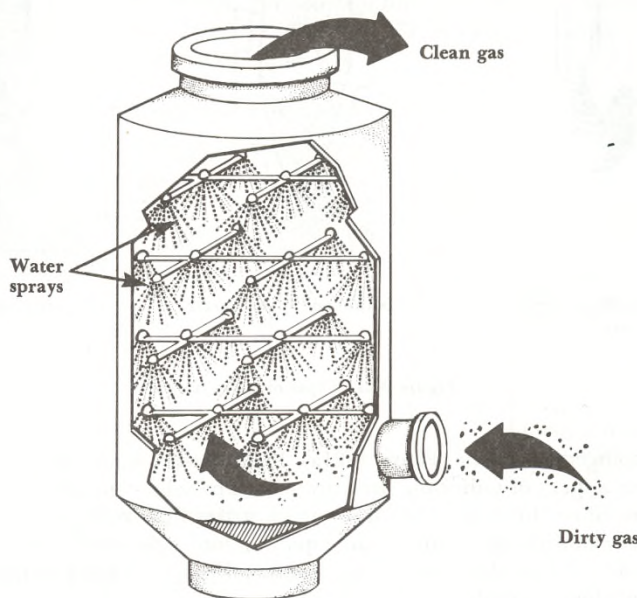


Figure 8-9. Spray tower scrubber

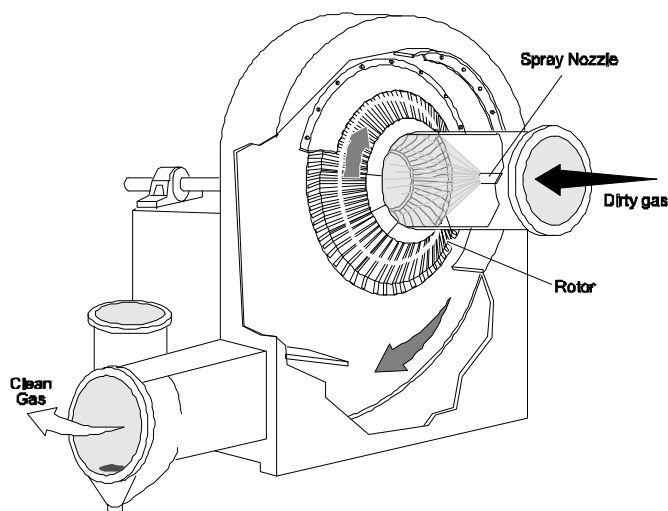


Figure 8-10. Mechanically aided scrubber

A mechanically aided scrubber is limited to a particle size range greater than approximately $1\ \mu\text{m}$, giving it lower medium energy performance. This limit is due partially to the maximum differences in particle and droplet velocities that can be obtained in the co-current (liquid and gas streams move in the same direction) type of scrubbing system. Because of the potential for plugging the closely-spaced fan blades, application is further limited to gas streams with low particle concentrations.

Orifice Scrubbers

Another device that exhibits lower medium energy performance is the orifice scrubber shown in Figure 8-11. In orifice scrubbers, the gas stream is forced through a pool of scrubbing liquid using inlets of different designs. As the gas stream exits the pool it entrains and atomizes the scrubbing liquid. Impaction of the particles on the entrained droplets occurs as the gas stream continues to turn through the section above the inlet. Additional turns of the gas stream provides for mist elimination before the gas stream is discharged. Orifice scrubbers are usually less vulnerable to gas-liquid distribution problems; however, it is more difficult to achieve high gas velocities in this type of system, limiting their collection efficiency.

Packed Bed Scrubbers

The packed bed scrubber is an example of a medium energy wet scrubber. In a typical packed bed scrubber, scrubbing liquid is introduced above the bed and trickles down over packing contained in one or more beds arranged in series. The beds can be in either a vertical tower or in a horizontal vessel. The packing materials are designed to provide the largest possible exposed liquid surface area per unit volume of bed, while maintaining a reasonable pressure drop. Some common types of packing materials are shown in Figure 8-12. Packings come in a variety of sizes and are constructed of different materials. Although ceramic and metal packings are available, plastic packings are used almost exclusively in air pollution applications.

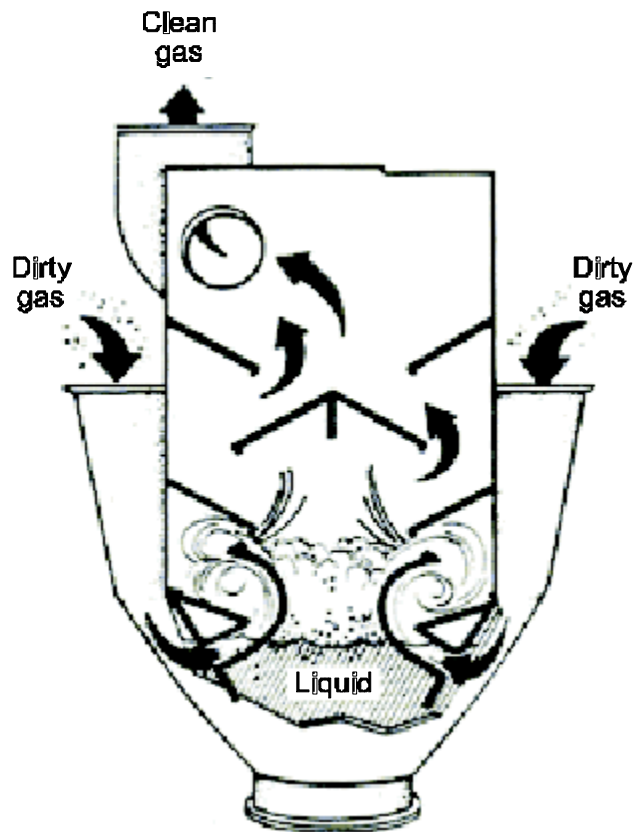


Figure 8-11. Orifice scrubber
(Reprinted courtesy of Joy Energy Systems)

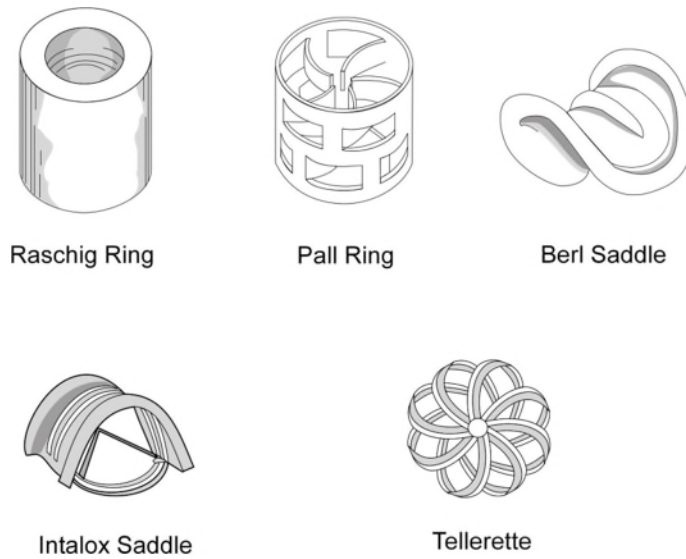


Figure 8-12. Common types of packing materials

In the vertical packed bed scrubber shown in Figure 8-13, the contaminated gas stream moves upward through the irrigated packing. This arrangement provides the best collection of gases and vapors, but has the lowest collection efficiency for particles. Because of hydrostatic limitations, there is a limit on the upward velocity that can be used for a given quantity of liquid. This limit results in reduced impaction efficiency. Removal efficiencies for particulate matter less than approximately 3 μm are very low. In addition, a portion of the bed can become plugged if the particulate matter concentration is high. The scrubbing liquid flowing downward over the packing moves too slowly to purge out large quantities of particulate matter.

Somewhat better particle removal performance can be achieved in the crossflow packed bed scrubber shown in Figure 8-14. In the crossflow scrubber, the gas stream passes horizontally through the bed, while the scrubbing liquid is distributed on the top of the packing and passes downward. Since the hydrostatic limitations of the vertical arrangement are not present, larger quantities of liquid and higher gas velocities can be used. This provides a modest increase in collection efficiency and helps reduce plugging problems. The bed is usually slanted, as shown, to account for the deflection of the liquid by the gas stream and to reduce liquid entrainment as the gas exits the lower portion of the packing.

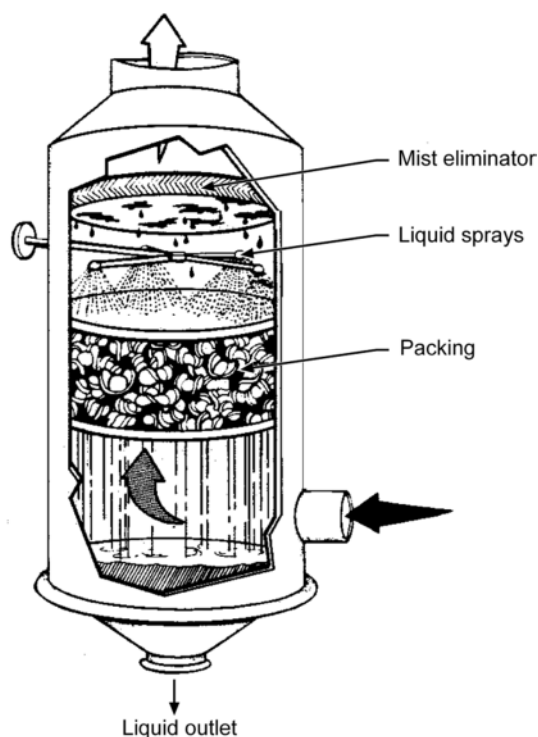


Figure 8-13. Vertical packed bed scrubber

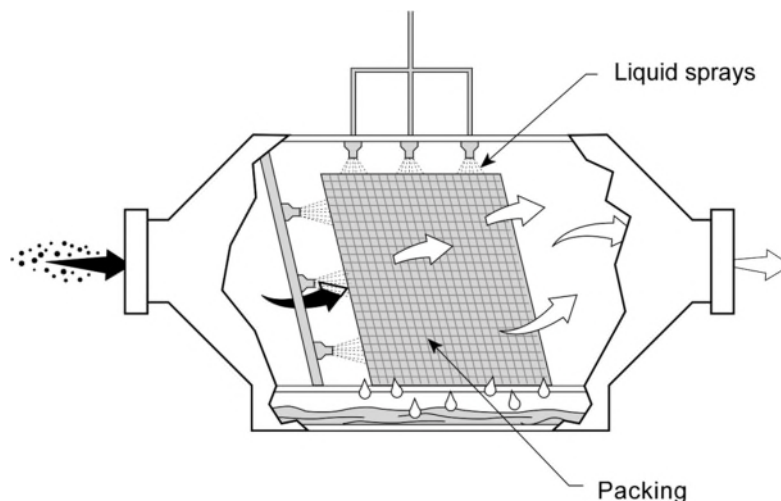


Figure 8-14. Horizontal packed bed scrubber

The most effective use of the scrubbing liquid is to have it spread out as a thin film on the surface of the packing. As long as this condition is maintained, increasing the liquid flow rate does not significantly affect pressure drop. However, if the liquid begins to accumulate in the spaces within the packing, the pressure drop will increase. This condition generally results in reduced collection efficiency.

Ionizing Wet Scrubbers

The ionizing wet scrubber, shown in Figure 8-15, is the only type of scrubber that uses electrostatic attraction as the primary technique for particle capture. Accordingly, it achieves better performance on submicrometer particulate matter than its medium pressure drop would indicate. The inlet gas stream passes through a short ionizer section composed of a number of high voltage discharge electrodes separated by small, grounded collection plates. The ionizer section is conceptually similar to a conventional negative corona electrostatic precipitator field; however, it is designed to impart a high negative electrical charge to the particles and not to collect them. The ionizer section usually operates at secondary voltages of 20 to 30 kilovolts DC.

Following the ionizer section, the gas stream passes through a crossflow packed bed section. Scrubbing liquid is distributed by means of a set of nozzles on the top and front of the bed. The particles are captured in the liquid layers surrounding the packing material due to the induced static charge in the liquid layers caused by the highly charged particles. While these units are capable of removing particles extending into the submicrometer range, they are not intended for sources generating high concentrations of submicrometer particulate matter. When necessary, scrubber modules can be arranged in series. This provides multiple opportunities to capture the particulate matter and minimizes problems caused by gas flow distribution at the inlet of the scrubber.

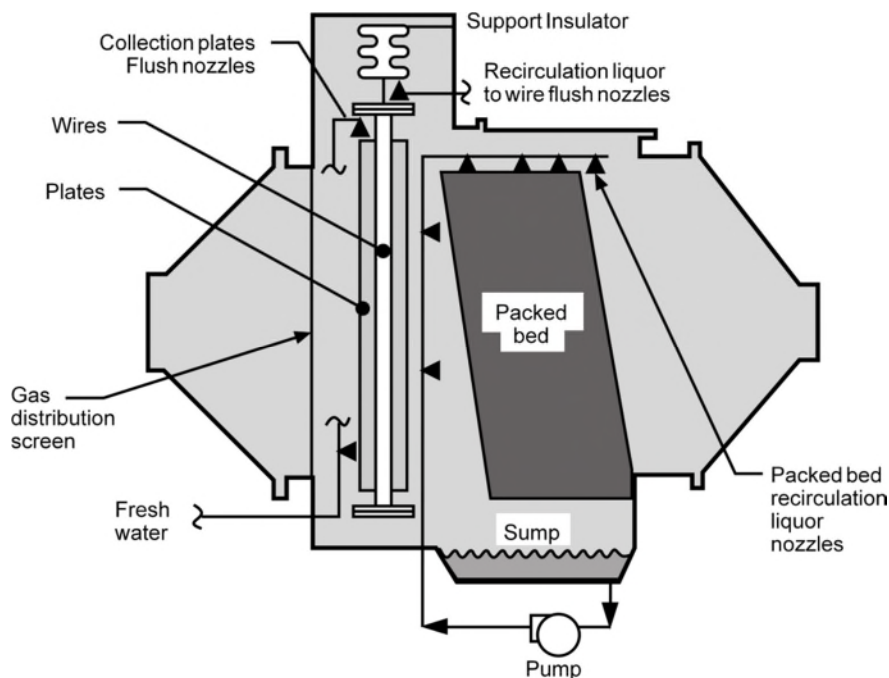


Figure 8-15. Ionizing wet scrubber

Fiber Bed Scrubbers

Another lower medium energy device is the fiber bed scrubber. Fiber bed scrubbers collect liquid particles using one or more vertical mesh pads composed of interlaced synthetic fibers. Often, composite mesh pads are constructed using mesh of different fiber diameters and densities. These scrubbers are designed exclusively in a crossflow orientation, as shown in Figure 8-16. In the illustration, the number before each slash is the fiber diameter in mils (thousandths of an inch) and the number after the slash is the percent of open space in the pad. There are usually two to four separate beds in series. An open weave pre-collector bed is used in applications where heavy droplet loadings or large diameter droplets are expected in the gas stream. This type of scrubber is capable of efficient particle removal down to sizes approaching 1 micrometer. It is frequently used for the control of mists that can coalesce and drain from the mesh pad. Scrubbing liquid can be sprayed either continuously or intermittently on the inlet side of each of the mesh pads.

The gas velocities through the fiber pad are usually maintained in the range of 5 to 12 feet per second, depending on the fiber diameters and fiber pad design characteristics. The static pressure drop across each of the stages ranges from 0.5 in. WC to approximately 2 in. WC, depending on the gas velocities and the fiber pad characteristics.

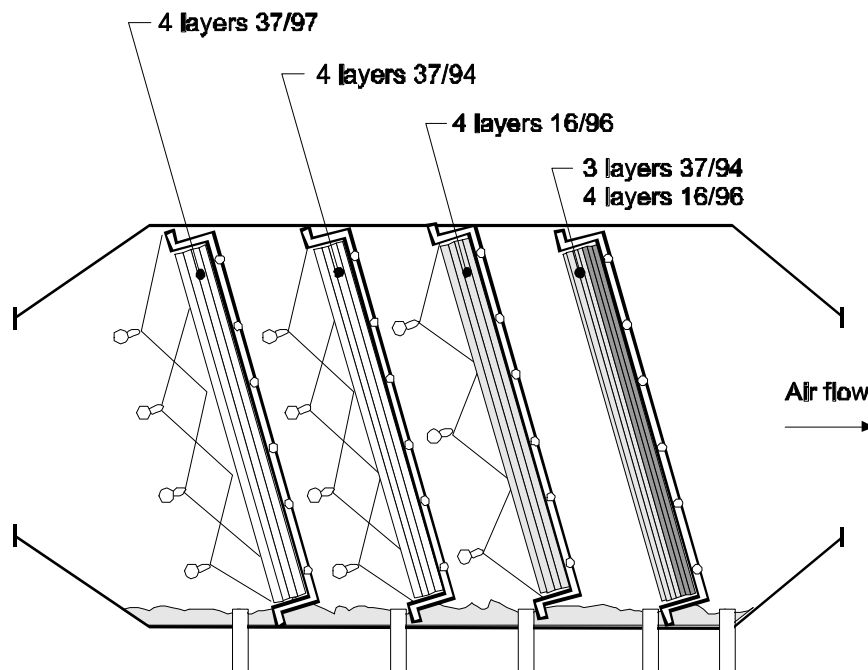


Figure 8-16. Four-stage fiber bed scrubber
(Reprinted courtesy of Kimre, Inc.)

Moving Bed Scrubbers

Moving bed scrubbers are another type of medium energy contactor. Spherical, hollow packing approximately the diameter of a ping-pong ball is used in a moving bed scrubber. About half of the volume between two open supporting grids is filled with this packing. As the gas flows upward through the packing, it fluidizes it. Liquid is distributed across the top of the fluidized bed by spray nozzles. Highly turbulent mixing occurs due to the motion of the packing material, aiding the formation of droplets and liquid sheets that can serve as impaction targets.

Moving bed scrubbers were originally designed to control sources of very sticky particulate matter; specifically, the organic aerosols emitted by Soderberg-type primary aluminum electrolytic cells. Because of the turbulent movement of the packing, sticky material deposited on the surface is continually removed. Moving bed scrubbers are also tolerant of high suspended solids levels in the recirculation liquid that can cause scaling problems on stationary packing. The turbulent contact between gases and liquids created by the movement of the packing also facilitates gas absorption into the scrubber liquid. Accordingly, reactive slurries of lime and limestone can be used if there is a need to simultaneously control acid gases.

Moving bed scrubbers often have two or three beds in series in the same scrubber vessel. In some cases, an additional bed is used at the top of the tower for mist elimination. A conventional mist eliminator can also be used. There is no need for an enlarged mist eliminator section, because the optimum velocity for the moving bed scrubber is similar to the optimum velocity range for conventional mist eliminators.

Tray Scrubbers

Another example of a medium energy scrubber is the tray scrubber. Tray scrubbers are vertical towers with multiple trays for contacting the gas and liquid streams. The liquid stream enters from the top, flows across the tray and then down to the next tray, until it reaches the bottom of the column. The gas moves upward through holes in the tray, creating a bubbling action that provides for particle collection by impaction. Tray scrubbers are usually selected for applications involving particulate matter greater than approximately $1\ \mu\text{m}$. They have limited efficiency below $1\ \mu\text{m}$ due to the limits to the gas stream velocities through the openings in the trays.

There are several tray designs to contact the gas with the liquid. A typical impingement tray scrubber is shown in Figure 8-17. The trays are metallic plates with numerous holes approximately $3/16$ inches in diameter. Small baffle plates are mounted directly above each of the holes. Scrubbing liquid enters as a stream at the top of the unit. Overflow weirs set the height of the liquid on each tray to approximately 1 to 1.5 inches. After passing across the tray, the liquid passes down a vertical passage called the *downcomer*. A liquid seal at the bottom of each downcomer allows the liquid to flow freely to the next tray while preventing the gas stream from short-circuiting up the downcomer.

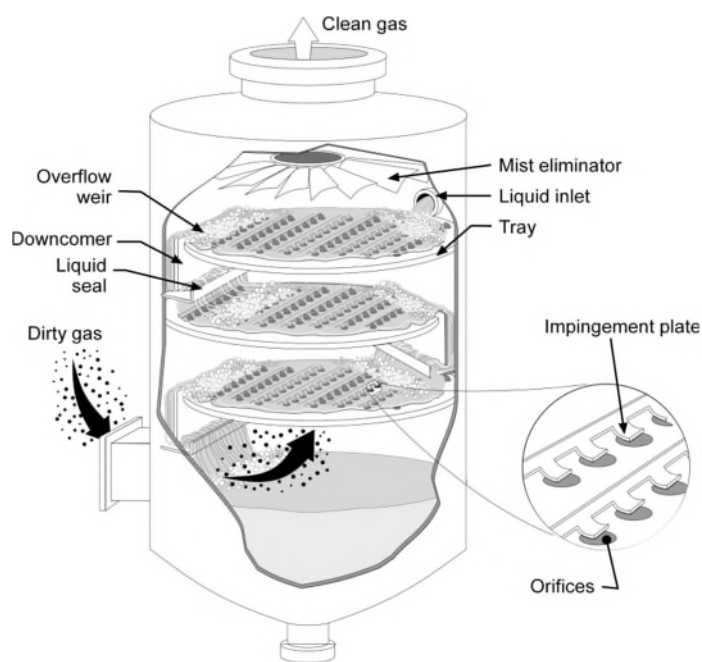


Figure 8-17. Impingement plate scrubber

The gas stream is accelerated as it passes through the impingement tray holes. The gas jets atomize a portion of the liquid above the tray, creating droplets that serve as the impaction targets. The gas velocity through the holes must be high enough to provide for efficient atomization of the liquid and must have sufficient force to prevent liquid from dripping through the holes. Excessive liquid dripping, termed *weepage*, reduces collection efficiency, particularly

for gases and vapors, and may limit the flexibility of tray scrubbers to operate over a wide range of gas flows.

Sieve tray scrubbers are conceptually similar to impingement tray scrubbers, but do not have baffle plates over the holes. These trays have larger holes, ranging from 0.25 to 1.0 inch in diameter, and are, therefore, less vulnerable to pluggage. However, the gas velocities are slightly lower than impingement tray scrubbers, reducing the collection efficiency.

Other designs include the float valve and bubble cap trays shown in Figure 8-18. These designs are better able to handle variations in flow rate while reducing or eliminating weepage problems. With valve trays, the gas stream flows up through small holes in the tray and lifts up metal discs that cover the openings. These discs are restrained by legs that limit vertical movement. The liftable discs act as variable orifices and adjust the opening for gas flow proportional to the gas flow rate through the scrubber. The gas stream in bubble cap trays enters through short vertical risers, turns 180° inside the cap and then exits the cap through the liquid layer. This type of tray can handle wide ranges of gas and liquid rates without adversely affecting efficiency.

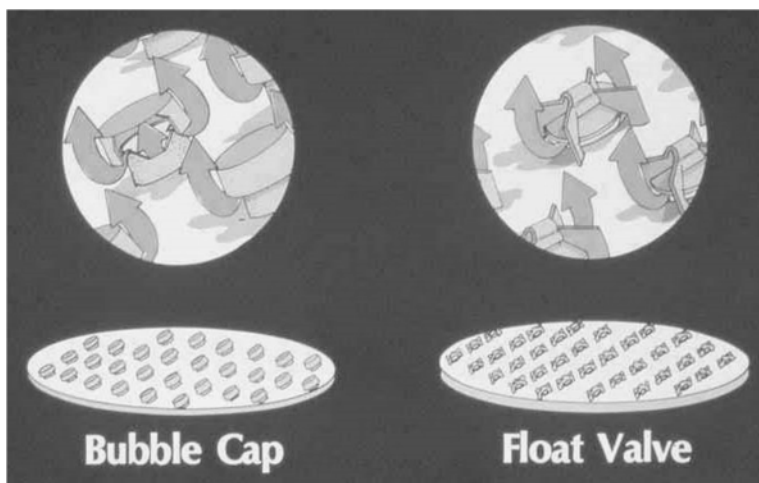


Figure 8-18. Bubble cap and float valve trays

The performance of tray scrubbers is dependent on the physical condition of the tray and the holes in the tray. Bowed or sloped trays will imbalance the height of the scrubbing liquid. The gas stream will preferentially pass through the holes with the lowest liquid height, because this is the low resistance path. The portion of the gas stream that continues to pass through the holes with high liquid levels will be slow and have reduced collection efficiency.

Plugging the holes in the tray must be avoided. Tray scrubbers are vulnerable to plugging due to the small diameters of the holes. Suspended solids can accumulate in these holes and harden, making it necessary to drill or rod them out. Due to the vulnerability to solids accumulation, the liquor recirculation system and treatment system are especially important. The suspended solids must be restricted to low levels by use of clean scrubbing liquid, to the extent possible, and by effective treatment of the recirculated liquor.

Catenary Grid Scrubbers

Catenary grid scrubbers, shown in Figure 8-19, are medium energy devices that have a set of catenary or saucer-shaped wire mesh grids across a vertical tower scrubber. The liquid is introduced above the top grid and flows downward from stage to stage without the need for the side-mounted downcomers used on other types of tray tower scrubbers. The mixing action of the gas stream and the liquid on the trays creates a highly turbulent zone, causing droplet atomization. Particle impaction occurs on the droplets.

The superficial gas velocity through a catenary grid scrubber ranges from 12 to 20 feet per second. The upper end of this range is slightly higher than most other types of tray tower scrubbers. The static pressure drop ranges from as low as 4 in. WC to more than 40 in. WC, depending on the gas velocity and the liquid-to-gas ratio. Catenary grid systems are more tolerant of high suspended solids levels in the recirculation liquid than other types of tray tower scrubbers, and the relatively open wire mesh stages are not highly prone to pluggage.

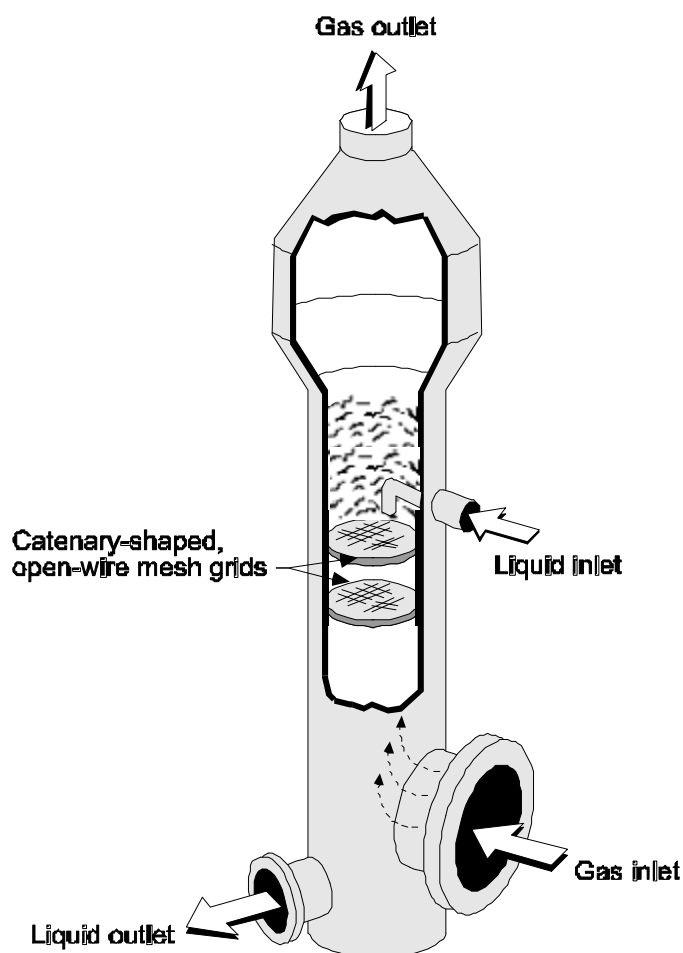


Figure 8-19. Catenary grid scrubber
(Reprinted courtesy of CECO Filters, Inc.)

A conventional mist eliminator is used at the top of the catenary grid for the removal of entrained water droplets. An expanded area must often be provided to ensure that the gas stream velocities are slowed prior to entering the mist eliminator.

Condensation Growth Scrubbers

Condensation growth scrubbers are designed to improve particulate matter removal efficiencies in the submicrometer particle size range. Large quantities of water vapor are introduced into the gas stream and then cooled. Some of this water vapor condenses on the surfaces of the submicrometer particles, increasing their size. The particles are then collected in conventional scrubber downstream of the vessel used for condensation growth.

Figure 8-20 is a simplified flowchart for a condensation growth scrubbing system. In this system, water vapor is introduced by evaporating clean water injected into a very hot gas stream. This approach can be used for incinerators and other processes operating with inlet gas temperatures in excess of 1,800°F. For other processes, it is necessary to inject low pressure steam to provide the necessary water vapor.

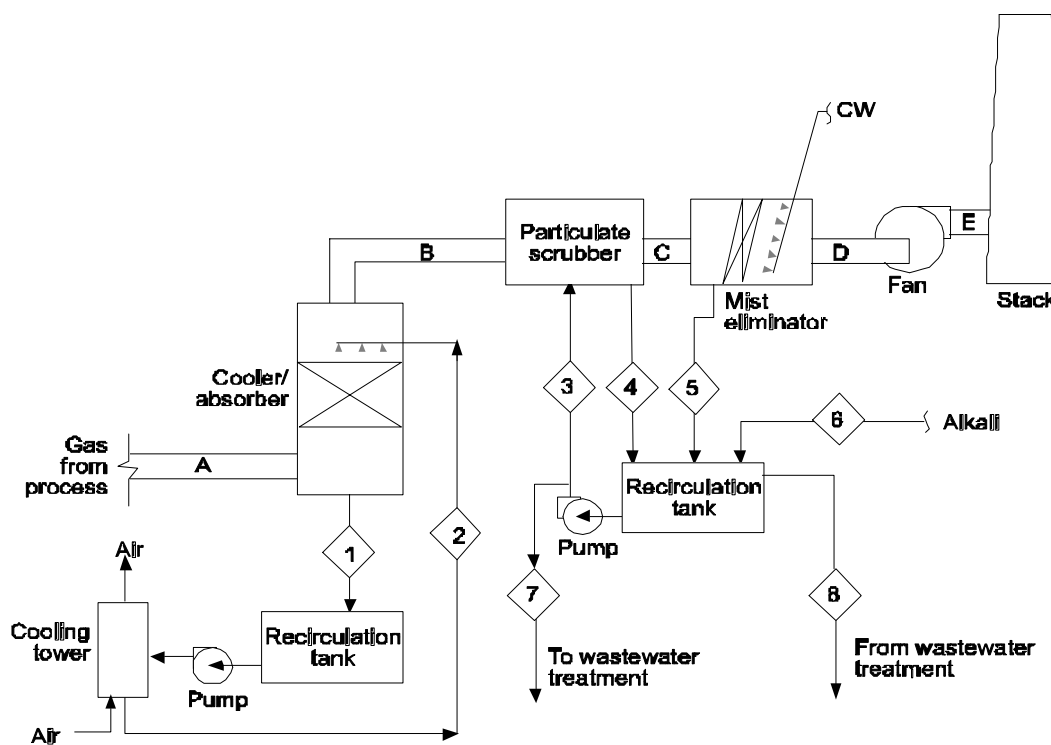


Figure 8-20. Condensation growth scrubber system

Following the evaporative cooling or steam injection step, the water vapor content can range from 40% to 60% by volume. This water vapor is condensed in a vessel upstream of the particle collection device. The amount of condensation is maximized by cooling the scrubbing liquor recirculating through the system. Sensible heat can be removed from the scrubber water by means of a small indirect heat exchanger or a small cooling tower.

The grown particulate matter is typically removed in a medium energy scrubber, such as a tray tower. However, depending on the resulting particle size distribution and on the removal efficiencies required, a venturi or other type of scrubber capable of high efficiency removal of small particulate matter may be necessary.

Venturi Scrubbers

The venturi scrubber is an example of a high energy wet scrubber, although it can also be operated as a medium energy scrubber. The fixed throat venturi, shown in Figure 8-21, is one of the most common designs. The gas stream entering the converging section of the venturi is accelerated to a velocity between 200 and 600 feet per second at the throat inlet. Liquid is injected into the throat and atomized into droplets with a mean size of 50 to 75 micrometers by the impact of the gas stream. The size of the droplets produced depends on the throat gas velocity and the liquid-to-gas ratio. These droplets are initially moving relatively slowly, and it takes time for them to accelerate to the same velocity as the particles entrained in the gas stream. Impaction occurs on the droplets due to the large difference in the gas stream velocity and the velocity of the accelerating droplets. The gas stream leaving the throat enters the diverging section. Here, the velocity of the gas stream is gradually reduced and the velocities of the particles and the droplets approach one another. Impaction does not occur efficiently in this section because the particles and droplets are moving at similar velocities and in the same direction.

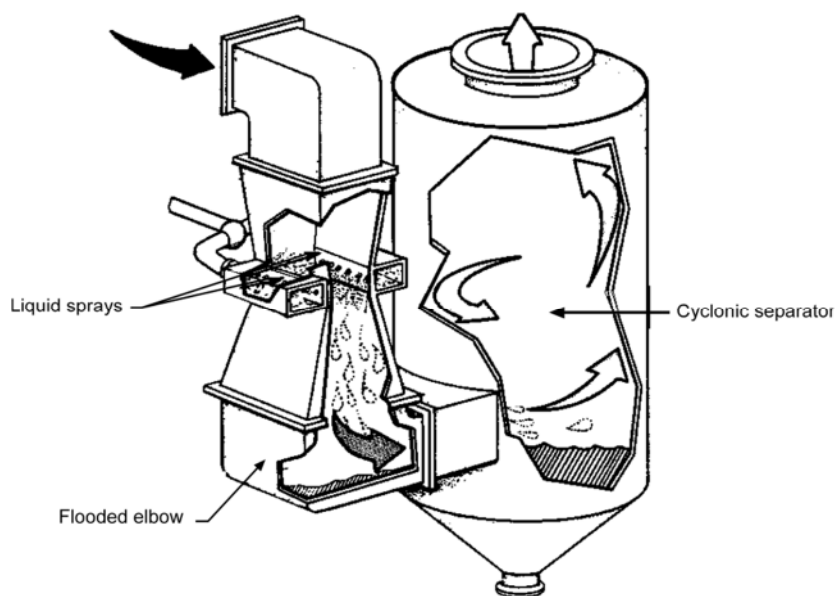


Figure 8-21. Fixed throat venturi scrubber

The effectiveness of a venturi scrubber is related to the maximum difference in the droplet and gas stream velocities. Because the fixed throat has a constant open area, the actual gas velocity achieved in the throat section depends on the gas flow rate. Particle collection efficiency is, therefore, gas flow rate dependent. Fixed throat venturi scrubbers are used on sources where the

gas flow rate is relatively constant or where the particle size distribution is sufficiently large that some variation in gas velocity is tolerable.

Proper liquid distribution is essential in obtaining optimum performance in a venturi scrubber. Because of the high gas velocities, the residence time of the gas stream in the venturi throat, where most collection occurs, is only 0.001 to 0.005 sec. Most of the particles that penetrate the throat will pass through the remainder of the scrubbing system uncollected. Obviously, portions of the venturi throat without any atomized scrubbing liquid will have no capability for collecting particulate matter.

The venturi scrubber system shown in Figure 8-21 includes a flooded section in the elbow directly below the venturi. This elbow leads from the diverging section to the mist eliminator. This 6 to 12 inch deep section is termed a *flooded elbow* and provides abrasion protection. Droplets that have accelerated to a high velocity in the venturi will erode the bottom of this duct if it is not protected.

One option for dealing with varying gas flow rate while maintaining good efficiency is the adjustable throat venturi shown in Figure 8-22. In this type of unit, moveable dampers are used to vary the throat area in order to control the gas velocity. The position of the dampers is usually set automatically to maintain a set pressure drop across the unit, although in some units they are positioned manually. These damper blades, and other types of flow restrictors, must be made of abrasion resistant materials because of the high velocities through the throat.

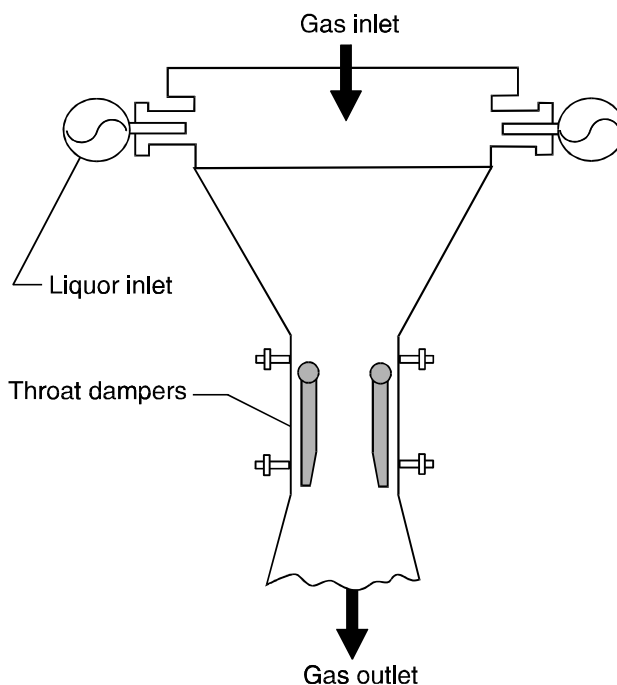


Figure 8-22. Adjustable throat venturi scrubber

There is a wide variety of adjustable throat mechanisms. The simplest is a metal plate that enters from one side of the venturi and extends across part of the throat. These simple plates are usually manually operated. Another style of adjustable throat has a flow restrictor that enters from the bottom of the throat as shown in Figure 8-22. As this flow restrictor advances, the annular area is reduced, increasing the gas velocity. The flow restrictor is raised or lowered by a hydraulic actuator.

It should be recognized that, if the flow rate is varying, so is the liquid-to-gas ratio. If the variation in flow rate is large, the liquid-to-gas ratios at the extreme ranges of operation may result in reduced collection efficiency. Systems with large flow rate variation must also modulate the liquid flow in order to keep the liquid-to-gas ratio in an acceptable range for optimum performance.

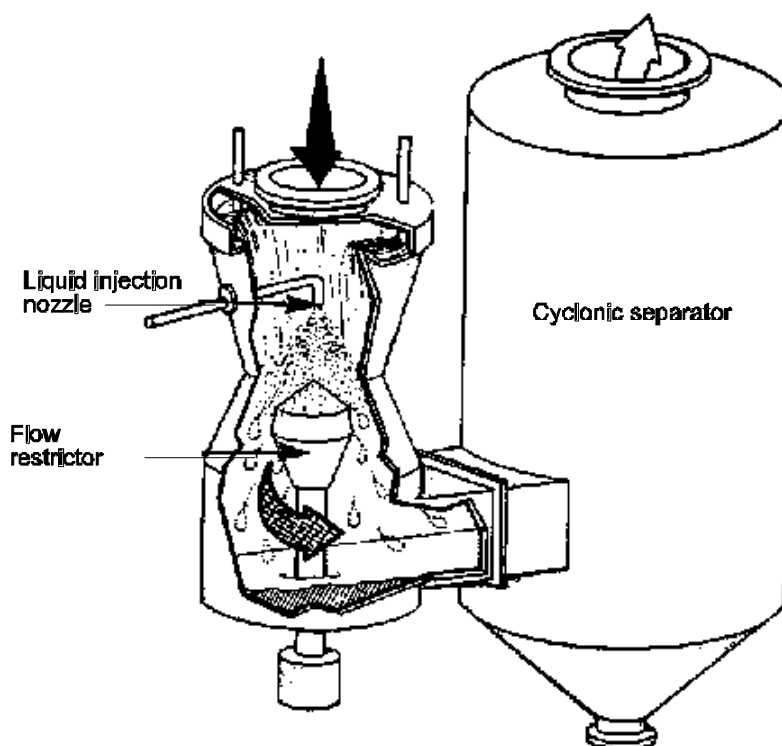


Figure 8-23. Flow restrictor type adjustable throat venturi scrubber

The venturi shown in Figure 8-22 uses spray headers at the inlet to the converging section to distribute the liquid, resulting in the wetting of the walls. This technique is called *wetted approach* and serves to protect the section from abrasion by the entering particles. The liquid is sheared off the side walls and entrained in the gas stream as it enters the throat. Alternatively, the liquid can be swirled down the converging section, as shown in Figure 8-23, until the liquid is entrained. In addition, a centrally mounted nozzle (not shown in Figure 8-22) is used in both designs to distribute liquid to the center of the throat. Because of the very high gas velocities in the throat, it is difficult for liquid droplets entrained from the wall to penetrate to the center.

The typical static pressure drop across a venturi scrubber varies from a low of 5 in. WC to values exceeding 100 in. WC. High static pressure drops are used only in situations demanding high efficiency removal of very small particulate matter. The static pressure drop is related to the gas velocities in the throat and the quantity of scrubbing liquid used. Because the energy for atomization comes from the gas stream, changes in the liquid flow rate will cause significant changes in the pressure drop.

Rod Deck Scrubbers

Rod deck scrubbers are similar to venturi scrubbers in that they use high velocity gas streams to atomize liquid droplets and to impact particulate matter. A gas stream entering a rod deck scrubber is accelerated as it passes between the closely spaced rods shown in Figure 8-24. The liquid is supplied by a set of spray nozzles above the rod deck, positioned to fully irrigate the gas flow area. The high-velocity gases in the open area between the rods further atomize the sprayed water droplets. After the rod deck, the gas stream decelerates, turns, and passes into a mist eliminator vessel to remove the entrained water droplets.

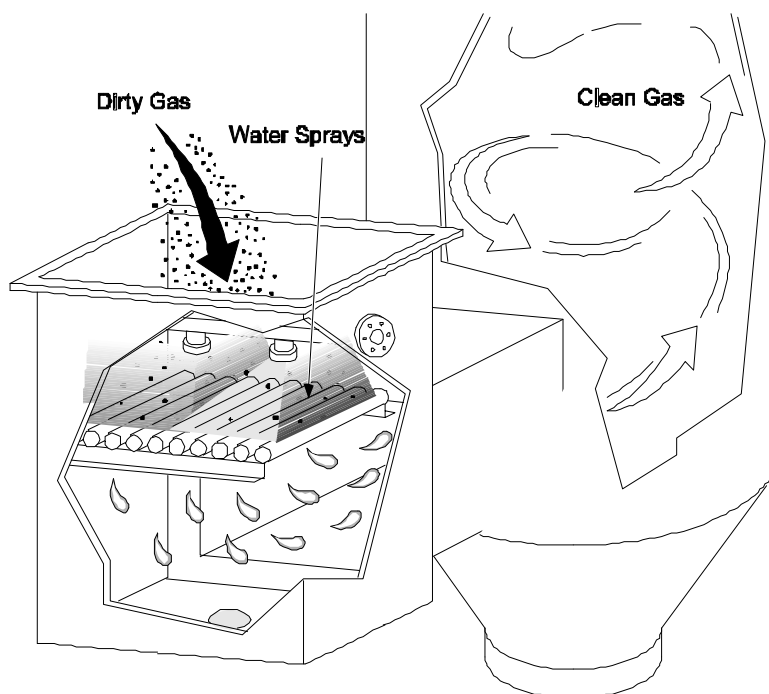


Figure 8-24. Rod deck scrubber

Multiple decks of rods can be used to improve particulate removal capability. The decks can be equipped with actuators to modify the spacing between the decks and, thereby, adjust the static pressure drop across the unit. The rods must be fabricated from abrasion resistant materials due to the high-velocity conditions, and they must be replaced when they have significantly eroded.

Collision Scrubbers

As noted above, the collection efficiency in a venturi scrubber is relatively low after the throat section because the particles and droplets are moving at similar velocities. The collision scrubber shown in Figure 8-25 avoids this by splitting the gas stream into two separate streams. Each stream enters a venturi-like section for contacting the injected scrubbing liquid. These two sections are arranged in an opposed manner so that gas streams exiting each section collide. Within the collision zone, the droplets and particles continue to impact due to the large difference in velocity. Collision scrubbers use a gas recirculation system to deal with varying gas flow rate in order to ensure adequate gas velocity in the venturi contactors.

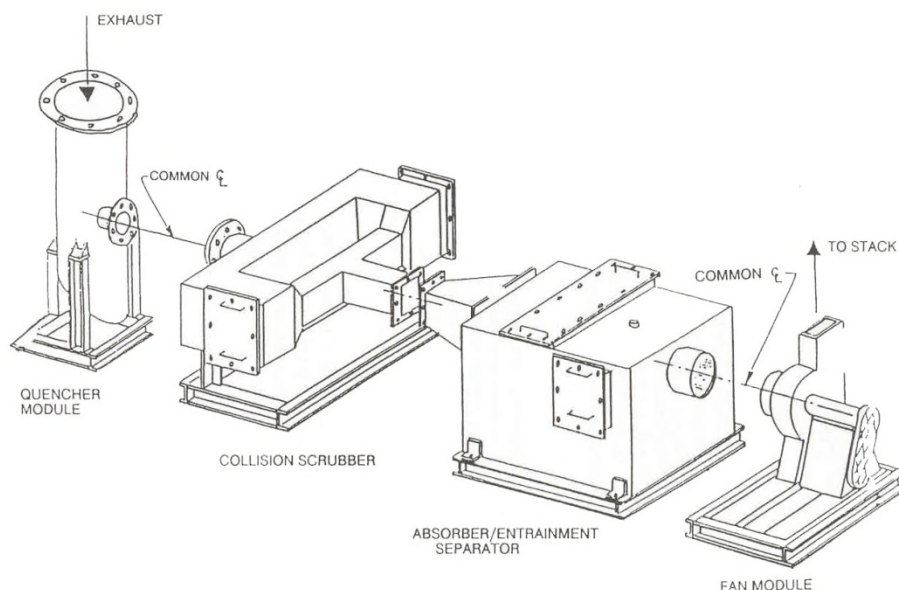


Figure 8-25. Collision scrubber system

Ejector Scrubbers

The ejector scrubber shown in Figure 8-26 uses a single high-pressure spray nozzle to inject liquid or steam into a venturi-shaped vessel. The reduced pressure created behind the high-pressure jet is sufficient to induce a gas flow from the process being controlled. The gas moving principles used in ejector scrubbers are identical to those used in a laboratory aspirator. All the energy needed to operate the scrubbing system is supplied by the liquid stream, rather than using energy supplied by a fan.

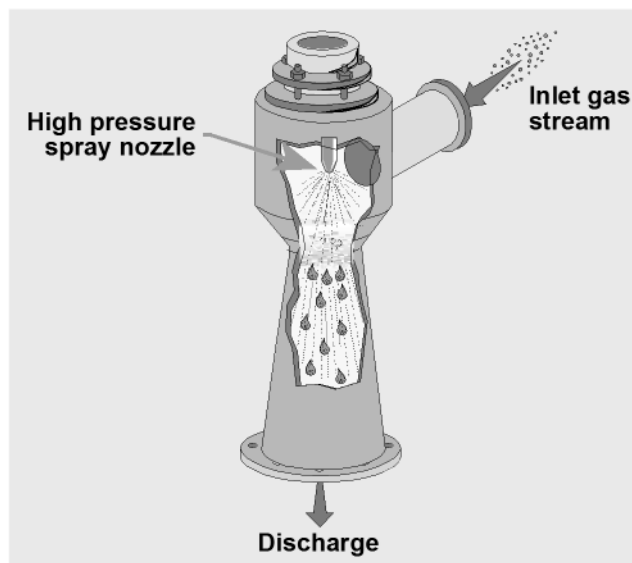


Figure 8-26. Ejector scrubber

Although it has a pressure rise, rather than a pressure drop, it gives performance comparable to a high energy venturi scrubber. Particulate matter is impacted in the droplets generated in the high-pressure nozzle. The differences in particle and droplet velocities, necessary for impaction, are due to the high-velocity droplets in the relatively slow-moving air stream. High energy ejector scrubbers can be used for both particulate matter control and gaseous absorption and are often arranged in series in order to generate the necessary static pressures for gas movement and to increase pollutant removal efficiencies.

Performance Evaluation

There are three general approaches to evaluating the capability of a scrubber system: (1) empirical evaluations based on previously installed scrubbers on similar sources, (2) pilot scale tests, and (3) mathematical models.

Empirical Evaluation

Most scrubber manufacturers have extensive databases describing the performance of their various commercial brands of scrubbers on different types of industrial sources. These data provide a starting point in determining if a given type of scrubber system will be able to meet the performance requirements specified by the purchaser. In addition, site-specific information is considered. The most important site-specific data is the inlet particle size distribution. Unfortunately, these data are often not available. Accordingly, the design review is typically limited to the following factors:

- Average and maximum gas flow rates
- Average and maximum inlet gas temperatures
- Concentrations of corrosive materials present in the inlet gas stream

- Concentrations of potentially explosive materials present in the inlet gas stream
- Availability of make-up water
- Purge liquid treatment and disposal requirements
- Process type, raw materials, and fuels
- Source operating schedule
- Area available for scrubber and waste water treatment
- Alkali supply requirements
- Particle size distribution (when available)
- Emission test data (when available)

This site-specific information is used in conjunction with the historical data base to determine if the scrubber is applicable to the process. The data also provide a basis for the design of the scrubber system components and for estimating the necessary static pressure drop.

The primary advantage of this approach is that scrubber system evaluation is based on actual emissions data obtained using test procedures identical to those to be applied to the new scrubber system. The disadvantage is the inability, in many cases, to take into account site-specific factors that could affect the particle size distribution. There can be significant process-to-process differences in the generated quantities of particulate matter in the difficult-to-control size range of 0.1 to 1 μm .

Pilot Scale Tests

Pilot scale performance tests can be conducted when there is uncertainty concerning the applicability of a scrubber or the necessary operating conditions of a scrubber. These tests are preferably conducted on the specific source to be controlled, so that the actual particle size distribution and particle characteristics are inherently taken into account. If this is an entirely new application that has not yet been built, a similar existing unit can be tested. The tests are normally conducted using a small skid-mounted scrubber system capable of handling a 500 to 2,000 acfm slip-stream that is taken from the discharge of the process source. The performance of the pilot scale scrubber system is typically determined using conventional USEPA reference method emission tests.

The primary advantage of this approach is that the performance of a scrubber very similar to the proposed unit can be evaluated on the actual gas stream. Furthermore, a series of tests can be conducted relatively quickly to identify the optimal operating conditions, such as liquid-to-gas ratio and static pressure drop. The main disadvantage is that the tests are expensive. Pilot scale tests usually indicate slightly higher particulate matter removal efficiencies than can be achieved by the full scale system because a variety of non-ideal gas flow conditions are more significant on the larger systems. Also, the particle size distribution in the pilot scale scrubber may be different than in the actual effluent gas stream due to errors in the way the slip-stream is withdrawn from the main duct or due to changes in the gas stream while passing down the temporary ductwork to the pilot scrubber.

Mathematical Models

Mathematical models provide a means of estimating performance when empirical data or pilot scale tests are not available. They also provide the permit reviewer with tools for evaluating designs proposed by the source. Some of these are empirical models that have been developed from experimental data. Others have been developed from basic principles and are based on the particle and droplet movements expected in that type of scrubber.

Counter-Current Spray Tower Scrubbers

An equation for estimating the collection efficiency of a single size particle has been developed by Calvert et al for counter-current spray tower scrubbers:

$$\eta_i = 1 - e^{-\left[\frac{1.5v_t \eta_I z}{d_d(v_t - v_g)} \right] \left(\frac{L}{G} \right)} \quad (8-5)$$

where:

- η_i = collection efficiency for particle size i
- v_t = droplet terminal settling velocity (cm/sec)
- η_I = single droplet collection efficiency due to impaction (dimensionless)
- z = scrubber height (cm)
- d_d = droplet diameter (cm)
- v_g = gas velocity (cm/sec)
- L/G = liquid to gas ratio (dimensionless; i.e., liters/min per liters/min)

The collection efficiency of a single droplet due to impaction, η_I , is given by:

$$\eta_I = \left(\frac{\Psi_I}{\Psi_I + 0.35} \right)^2 \quad (8-6)$$

where Ψ_I is the inertial impaction parameter for particle size i , defined by Equation 8-1:

$$\Psi_I = \frac{C_c d_p^2 \rho_p V_r}{18\mu_g d_d} \quad (8-1)$$

where:

- Ψ_I = inertial impaction parameter (dimensionless)
- C_c = Cunningham slip correction factor (dimensionless)
- d_p = physical particle diameter (cm)
- ρ_p = particle density (gm/cm^3)
- V_r = relative velocity between particle and droplet (cm/sec)

$$d_d = \text{droplet diameter (cm)}$$

$$\mu_g = \text{gas viscosity (gm/cm sec)}$$

Data concerning the droplet diameter can be obtained from the spray nozzle manufacturers, and the droplet terminal settling velocity can be calculated using the procedures in Chapter 4. The remainder of the parameters necessary to perform this calculation are based on readily available design data for the scrubber being analyzed.

Example 8-5

Estimate the collection efficiency of 4 μm diameter particles with a density of 1.1 g/cm^3 in a counter-current spray tower 3 meters high. The gas flow rate is 140 m^3/min at 20°C, the water flow rate is 115 l/min , and the gas velocity is 100 cm/sec . The mean droplet diameter is 500 μm , and the droplet terminal settling velocity is 200 cm/sec . Assume a Cunningham correction of 1.0.

Solution:

Calculate the inertial impaction parameter:

$$\Psi_I = \frac{C_c d_p^2 \rho_p V_r}{18 \mu_g d_d}$$

$$= \frac{(1.0)(4 \times 10^{-4} \text{ cm})^2 \left(1.1 \frac{\text{g}}{\text{cm}^3}\right) \left(200 \frac{\text{cm}}{\text{sec}} - 100 \frac{\text{cm}}{\text{sec}}\right)}{18 \left(1.8 \times 10^{-4} \frac{\text{g}}{\text{cm} \cdot \text{sec}}\right) (500 \times 10^{-4} \text{ cm})} = 0.109$$

Calculate the single droplet collection efficiency:

$$\eta_I = \left(\frac{\Psi_I}{\Psi_I + 0.35} \right)^2$$

$$= \left(\frac{0.109}{0.109 + 0.35} \right)^2 = 0.056$$

Calculate the particle collection efficiency:

$$\eta_i = 1 - e^{-\left[\frac{1.5 v_t \eta_I z}{d_d (v_t - v_g)} \right] \left(\frac{L}{G} \right)}$$

$$= 1 - e^{-\left[\frac{1.5 \left(\frac{200 \text{ cm}}{\text{sec}} \right) (0.056) (300 \text{ cm})}{(500 \times 10^{-4} \text{ cm}) \left(\frac{200 \text{ cm}}{\text{sec}} - 100 \frac{\text{cm}}{\text{sec}} \right)} \right] \left[\frac{\left(\frac{115 \frac{1}{\text{min}} \right) \left(1 \times 10^{-3} \frac{\text{m}^3}{1} \right)}{140 \frac{\text{m}^3}{\text{min}}} \right]} = 0.563 = 56.3\%$$

Packed Bed Scrubbers

Calvert et al also developed an equation for estimating the collection efficiency of a single size particle in a packed bed scrubber:

$$\eta_i = 1 - e^{-\left[\frac{\pi z \Psi_i}{(j+j^2)(\varepsilon - Hd)d_c} \right]} \quad (8-7)$$

where:

- η_i = collection efficiency for particle size i
- z = scrubber height (cm)
- Ψ_i = inertial impaction parameter (dimensionless)
- j = channel width as a fraction of packing diameter (dimensionless)
- ε = bed porosity (dimensionless)
- Hd = liquid holdup (dimensionless)
- d_c = packing diameter (cm)

Here, the inertial impaction parameter is calculated using packing diameter instead of droplet diameter. The channel width as a fraction of packing diameter, j , varies with packing type but typically ranges from 0.165 to 0.192. Bed porosity, ε , can be obtained from packing manufacturers and typically ranges from 0.57 to 0.94, depending on the type of packing. Liquid holdup, Hd , is usually assumed to be zero.

Example 8-6

Estimate the collection efficiency of 4 μm diameter particles with a density of 1.1 g/cm^3 in a 3 meter deep packed bed containing 5 cm diameter Raschig rings. The gas flow rate is 140 m^3/min at 20°C, the water flow rate is 115 l/min , and the gas velocity is 100 cm/sec . Assume $j = 0.165$, $\varepsilon = 0.75$, and $Hd = 0$, and a Cunningham correction of 1.0.

Solution:

Calculate the inertial impaction parameter:

$$\Psi_i = \frac{C_c d_p^2 \rho_p V_r}{18 \mu_g d_c}$$

$$= \frac{(1.0)(4 \times 10^{-4} \text{ cm})^2 \left(1.1 \frac{\text{g}}{\text{cm}^3}\right) \left(100 \frac{\text{cm}}{\text{sec}}\right)}{18 \left(1.8 \times 10^{-4} \frac{\text{g}}{\text{cm} \cdot \text{sec}}\right) (5.0 \text{ cm})} = 1.09 \times 10^{-3}$$

Calculate the particle collection efficiency:

$$\eta_i = 1 - e^{-\left[\frac{\pi z \Psi_1}{(j+j^2)(\epsilon - Hd)d_c}\right]}$$

$$= 1 - e^{-\left\{\frac{\pi(300 \text{ cm})(1.09 \times 10^{-3})}{[0.165 + (0.165)^2](0.75 - 0)(5.0 \text{ cm})}\right\}} = 0.759 = 75.9\%$$

Tray Scrubbers

An equation for estimating the collection efficiency of a single size particle in a tray scrubber has also been developed by Calvert et al:

$$\eta_i = 1 - \left[e^{-80F^2 \Psi_1} \right]^n \quad (8-8)$$

where:

- η_i = collection efficiency for particle size i
- F = foam density fraction (dimensionless)
- Ψ_1 = inertial impaction parameter (dimensionless)
- n = number of trays (dimensionless)

For this device, the inertial impaction parameter is calculated using the gas velocity through the holes in the plate and the diameter of the holes, rather than the diameter of the drops. The foam density fraction typically ranges from 0.38 to 0.65

Example 8-7

Estimate the collection efficiency of 4 μm diameter particles with a density of 1.1 g/cm^3 in a tray scrubber having 3 trays with 10 mm diameter holes. The gas flow rate is 140 m^3/min at 20°C, the water flow rate is 115 l/min, and the gas velocity through the holes is 1,800 cm/sec. Assume $F = 0.50$ and a Cunningham correction of 1.0.

Solution:

Calculate the inertial impaction parameter:

$$\Psi_1 = \frac{C_c d_p^2 \rho_p V_r}{18 \mu_g d_c}$$

$$= \frac{(1.0)(4 \times 10^{-4} \text{ cm})^2 \left(1.1 \frac{\text{g}}{\text{cm}^3}\right) \left(1,800 \frac{\text{cm}}{\text{sec}}\right)}{18 \left(1.8 \times 10^{-4} \frac{\text{g}}{\text{cm} \cdot \text{sec}}\right) (1.0 \text{ cm})} = 0.098$$

Calculate the particle collection efficiency:

$$\eta_i = 1 - \left[e^{-80 F^2 \Psi_1} \right]^n$$

$$= 1 - \left[e^{-80(0.50)^2(0.098)} \right]^3 = 0.997 = 99.7\%$$

Venturi scrubbers

The venturi scrubber is referred to as a gas atomizing scrubber, meaning that the energy for atomizing the liquid comes from the gas stream. Accordingly, the droplet diameter produced in the atomization process depends on the throat gas velocity and the liquid to gas ratio. A number of relationships have been developed to predict mean droplet size. The relationship that has found the widest application in venturi scrubbing, despite its dimensional inconsistency, is that of Nukiyama and Tanasawa, which estimates the Sauter mean diameter. The Sauter mean diameter is the diameter of a drop having the same volume/surface area ratio as the entire distribution. For an air-water system, this droplet diameter is given by:

$$d_d = \frac{16,400}{v_g} + 1.45 \left(\frac{Q_l}{Q_g} \right)^{1.5} \quad (8-9)$$

where:

$$d_d = \text{mean droplet diameter (micrometers)}$$

$$v_g = \text{gas velocity (ft/sec)}$$

$$Q_l/Q_g = \text{liquid to gas ratio (gal/1,000 ft}^3\text{)}$$

A relatively simple relationship for estimating the collection efficiency for a single size particle has been developed by Johnstone et al:

$$\eta_i = 1 - e^{-k \sqrt{\Psi_1} \frac{Q_l}{Q_g}} \quad 8-10$$

where:

- η_i = collection efficiency for particle size i
 k = constant (1,000 ft³/gal)
 Ψ_I = inertial impaction parameter (dimensionless)
 Q_l/Q_g = liquid to gas ratio (gal/1,000 ft³)

In this relationship, the inertial impaction parameter is calculated using the gas velocity in the throat. The constant, k , is typically 0.1-0.2 1,000 ft³/gal.

Example 8-8

Estimate the collection efficiency of a 1 μm diameter particle with a density of 1.5 g/cm³ in a venturi scrubber having a throat gas velocity of 300 ft/sec and a liquid to gas ratio of 8.0 gal/1,000 ft³. Assume a temperature of 68°F and a k of 0.15 1,000 ft³/gal.

Solution:

Calculate the mean droplet diameter:

$$\begin{aligned}
 d_d &= \frac{16,400}{v_g} + 1.45 \left(\frac{Q_l}{Q_g} \right)^{1.5} \\
 &= \frac{16,400}{300} + 1.45(8.0)^{1.5} = 87.5 \mu\text{m}
 \end{aligned}$$

Calculate the Cunningham correction factor:

$$C_c = 1 + \frac{6.21 \times 10^{-4} T}{d_p} = 1 + \frac{6.21 \times 10^{-4} (293 \text{ K})}{1 \mu\text{m}} = 1.18$$

Calculate the inertial impaction parameter:

$$\begin{aligned}
 \Psi_I &= \frac{C_c d_p^2 \rho_p V_r}{18 \mu_g d_d} \\
 &= \frac{(1.18)(1 \times 10^{-4} \text{ cm})^2 \left(1.5 \frac{\text{g}}{\text{cm}^3} \right) \left(300 \frac{\text{ft}}{\text{sec}} \times 30.48 \frac{\text{cm}}{\text{ft}} \right)}{18 \left(1.8 \times 10^{-4} \frac{\text{g}}{\text{cm} \cdot \text{sec}} \right) (87.5 \times 10^{-4} \text{ cm})} = 5.709
 \end{aligned}$$

Calculate the particle collection efficiency:

$$\eta_i = 1 - e^{-k\sqrt{\Psi_1} \frac{Q_l}{Q_g}}$$

$$= 1 - e^{-0.15 \frac{1,000 \text{ ft}^3}{\text{gal}} \sqrt{5.709} \left(8.0 \frac{\text{gal}}{1,000 \text{ ft}^3} \right)} = 0.943 = 94.3\%$$

A more sophisticated model of venturi scrubber performance has been developed by Yung et al. A simplified version of this model is based on the assumption that the droplets accelerate to the velocity of the gas stream prior to leaving the throat and is termed the infinite throat model.

$$\eta_i = 1 - e^{-B \left[\frac{4K_{po} + 4.2 - 5.02K_{po}^{0.5} \left(1 + \frac{0.7}{K_{po}} \right) \tan^{-1} \sqrt{\frac{K_{po}}{0.7}}}{K_{po} + 0.7} \right]} \quad (8-11)$$

where:

- η_i = collection efficiency for particle size i
- B = liquid to gas flow rate ratio parameter (dimensionless)
- K_{po} = $2\Psi_1$ = inertial impaction parameter at throat velocity (dimensionless)

$$B = \left(\frac{L}{G} \right) \left(\frac{\rho_l}{\rho_g} \right) \frac{1}{C_{Do}} \quad (8-12)$$

where:

- L/G = liquid to gas ratio (dimensionless)
- ρ_l = liquid density (gm/cm^3)
- ρ_g = gas density (gm/cm^3)
- C_{Do} = droplet drag coefficient at throat conditions (dimensionless)

$$C_{Do} = 0.22 + \frac{24}{\text{Re}_d} \left(1 + 0.15 \text{Re}_d^{0.6} \right) \quad (8-13)$$

where:

- Re_d = Reynolds number of the droplet at the throat inlet (dimensionless)

This technique is obviously more complex than that of Johnstone et al. However, it is based on fundamental calculations that do not involve any loosely defined constants and, when compared to experimental data, gives more accurate estimates. An Excel spreadsheet is available from your instructor to ease some of the pain in using this method.

Instrumentation

The selection and location of instrumentation is important in ensuring that the particulate control system operates at its maximum capability. The types of instruments that are used include static pressure gauges, temperature gauges, liquid flow rate gauges, liquid pressure gauges, and pH gauges. Opacity monitoring instruments are not used on particulate matter wet scrubber systems because the condensed water droplets often present in the gas stream scatter light. It is not possible to differentiate between light scattering due to particulate matter or due to water droplets.

The types of instruments that are necessary for a particulate matter wet scrubber system depend, in part, on the size of the unit, the toxicity of the pollutants being collected, the variability of operating conditions, and the susceptibility to performance problems. Instruments in particulate matter wet scrubber systems usually include one or more of the following monitors.

- Scrubber vessel static pressure drop
- Mist eliminator static pressure drop
- Inlet and outlet gas temperature
- Recirculation liquid flow rate
- Recirculation liquid pH

Static pressure gauges should be mounted in both the inlet and outlet ductwork of the scrubber system. In these positions, the gauges can be used to determine the flange-to-flange static pressure drop across the scrubber system. This value takes into account the energy losses in the scrubbing section, the mist eliminator and in entering the exit ductwork from the scrubber vessel. It may also be possible to install a static pressure drop gauge across the scrubbing section, allowing the pressure drop of the scrubbing section to be evaluated separately for the static pressure drop across the mist eliminator. However, the presence of high levels of entrained liquid exiting the scrubbing section can affect both the accuracy and reliability of these measurements.

The static pressure drop across the mist eliminator provides an excellent indicator of the physical condition of the mist eliminator. The static pressure drop is strictly a function of the geometry of the mist eliminator, the gas flow rate through the mist eliminator, and the gas density. Accordingly, the static pressure drop should be a relatively constant value, provided the flow rate is constant. If an increase in the pressure drop occurs, it is likely due to the buildup of particulate matter or chemical scale on the surface of the mist eliminator. Values well below the baseline range suggest that part of the mist eliminator has fallen apart or otherwise been damaged. Structural failure of the mist eliminator is possible because of the forces that can be imposed on the surface when it is significantly blinded or because of corrosion-related weakening of the supporting frame. Mist eliminators constructed of fiberglass-reinforced plastics (FRP) and other synthetic materials can also suffer adhesive failure if there is a gas temperature spike.

Temperature information is a useful indicator of gas-liquid distribution problems. If the liquid distribution is not adequate, collection efficiency will be reduced. When the gas-liquid distribution is good, the outlet gas stream temperature will be at the adiabatic saturation

temperature. This simply means that the gas stream will be saturated with water vapor. The adiabatic saturation temperature can be easily determined with a psychometric chart, if the inlet gas stream dry bulb temperature and absolute humidity are known. Unfortunately, the absolute humidity of the entering gas stream is rarely available. While it could be estimated, errors can significantly affect the value of the saturation temperature determined from the psychometric chart, possibly leading to erroneous conclusions. A more direct way to evaluate liquid distribution problems is to look at the difference between the inlet and outlet gas temperatures. If that temperature difference has decreased, liquid distribution problems are likely. It should be noted that temperature difference is not an especially sensitive indicator of maldistribution in venturi scrubbers. Impaction virtually ceases after the venturi throat; however, heat transfer between the gas and liquid streams can continue until the gas stream passes through the mist eliminator.

Monitoring the liquid flow rate is required by some New Source Performance Standards (NSPS) and is also included in many operating permits for existing sources. The rationale for these requirements is that scrubber performance is impaired when the liquid recirculation rate is low. On moderate-to-large scrubbers, the liquid flow rate is usually monitored continuously. The types of flowmeters include the following:

- Magnetic flowmeters
- Ultrasonic flowmeters
- Swinging vane flowmeters
- Rotameters
- Orifice meters

Smaller scrubbers may not have liquid flow rate gauges, but will typically monitor supply header pressures. Supply headers are the pipes that deliver recirculated liquid to nozzles in the scrubber. Unfortunately, supply header pressures are influenced by both changes in liquid flow rate and by changes in the resistance of the delivery system, making interpretation of the indications difficult. An increase in pressure can result from an increase in flow rate or from solids build-up in the pipes or nozzles. Likewise, a decrease in pressure can result from a decrease in flow rate or because the nozzle orifices have eroded.

The recirculation liquid pH monitor provides essential information for scrubbers handling acidic gas streams or collecting acidic particulate matter. The pH must usually be maintained above approximately 5 to minimize vulnerability to corrosion damage. If the pH exceeds levels of approximately 9, there is some vulnerability to chemical precipitation (often termed scaling) of calcium and magnesium compounds. These solids can build-up in spray nozzles and in the scrubbing vessels and mist eliminators and disrupt gas-liquid distribution. pH monitors are often mounted in areas shielded from high velocity, swirling liquid currents in the recirculation tank. They are also mounted at an elevation and position in the tank where there is a minimal risk of encapsulation in precipitated and settled solids.

Review Questions

1. What is the average residence time of the gas stream in the throat of a venturi scrubber throat?
 - a. 0.1 to 0.5 seconds
 - b. 1 to 10 seconds
 - c. 10 to 50 seconds
 - d. 0.001 to 0.005 seconds

2. What is the typical static pressure drop across a mist eliminator?
 - a. 0.1 to 0.4 in. WC
 - b. 0.5 to 4 in. WC
 - c. 4 to 8 psia
 - d. 4 to 8 kPa

3. There are more than fifteen categories of particulate matter scrubber designs. What is one of the features that can be used to determine which categories are more efficient for particles in the difficult-to-control size range?
 - a. Relative difference in velocities of the particles in the gas stream and the liquid targets used for collection
 - b. Liquid-to-gas ratio
 - c. Droplet size distribution generated by the scrubber
 - d. Liquid surface tension maintained by use of flocculants

4. What is the purpose of the evaporative cooler or presaturator often used upstream of a particulate wet scrubber? Select all that apply.
 - a. Protection of heat sensitive components in the scrubber vessel
 - b. Optimize inertial impaction into droplet targets
 - c. Increase the gas velocity through the scrubber
 - d. All of the above

5. What is the normal pH range in a particulate matter wet scrubber?
 - a. 1 to 5
 - b. 5 to 9
 - c. 9 to 11
 - d. 11 to 14

6. Select the factor(s) that often affect the necessary purge rate in a wet scrubber system. Select all that apply.
 - a. Particulate loading in the gas stream being treated
 - b. Hydrogen chloride concentration in the gas stream being treated
 - c. Maximum suspended solids levels in the recirculated liquid stream
 - d. All of the above

7. What size of droplets are usually controlled by a mist eliminator?
 - a. 0.1 to 1 micrometer
 - b. 1 to 50 micrometers
 - c. 20 to 1000 micrometers
 - d. 1,000 to 10,000 micrometers

8. What type of wet scrubber is primarily designed for the removal of gaseous air contaminants? Select all that apply.
 - a. Packed bed scrubbers
 - b. Collision scrubbers
 - c. Mechanically aided scrubbers
 - d. Crossflow packed bed scrubbers

9. What type of wet scrubber is primarily designed for the removal of mists? Select all that apply.
 - a. Fiber bed scrubber
 - b. Mesh bed scrubbers
 - c. Spray tower scrubbers
 - d. Impingement tray tower scrubbers

10. What is the most important factor affecting the ability of a particulate matter wet scrubber to achieve high removal efficiencies?
 - a. Particle size
 - b. Static pressure drop
 - c. Droplet size distribution
 - d. Droplet surface tension

11. What is the difficult-to-control particle size range?
 - a. 0.1 to 1.0 micrometers
 - b. 1 to 5 micrometers
 - c. 5 to 20 micrometers
 - d. 20 to 50 micrometers

12. What is the main particle collection mechanism used in particulate matter wet scrubbers?

- a. Brownian motion
- b. Electrostatic attraction
- c. Inertial impaction
- d. Coagulation

13. What variables can affect the adequacy of a correlation between scrubber static pressure drop and the particulate matter removal efficiency? Select all that apply.

- a. Particle size distribution
- b. Adequacy of gas-liquid maldistribution
- c. Droplet surface tension
- d. Condensation of vapors in the scrubber
- e. All of the above

14. What is the most difficult-to-collect particle size range for a venturi scrubber?

- a. 0.01 to 0.1 μm
- b. 0.1 to 1 μm
- c. 1 to 10 μm
- d. 10 to 100 μm

This page intentionally left blank.

Review Question Answers

1. What is the average residence time of the gas stream in the throat of a venturi scrubber throat?
 - d. 0.001 to 0.005 seconds
2. What is the typical static pressure drop across a mist eliminator?
 - b. 0.5 to 4 in. WC
3. There are more than fifteen categories of particulate matter scrubber designs. What is one of the features that can be used to determine which categories are more efficient for particles in the difficult-to-control size range?
 - a. Relative difference in velocities of the particles in the gas stream and the liquid targets used for collection
4. What is the purpose of the evaporative cooler or presaturator often used upstream of a particulate wet scrubber? Select all that apply.
 - a. Protection of heat sensitive components in the scrubber vessel
 - b. Optimize inertial impaction into droplet targets
5. What is the normal pH range in a particulate matter wet scrubber?
 - b. 5 to 9
6. Select the factor(s) that often affect the necessary purge rate in a wet scrubber system. Select all that apply.
 - d. All of the above
7. What size of droplets are usually controlled by a mist eliminator?
 - c. 20 to 1000 micrometers
8. What type of wet scrubber is primarily designed for the removal of gaseous air contaminants? Select all that apply.
 - a. Packed bed scrubbers
 - d. Crossflow packed bed scrubbers

9. What type of wet scrubber is primarily designed for the removal of mists? Select all that apply.
 - a. Fiber bed scrubber
 - b. Mesh bed scrubbers

10. What is the most important factor affecting the ability of a particulate matter wet scrubber to achieve high removal efficiencies?
 - a. Particle size

11. What is the difficult-to-control particle size range?
 - a. 0.1 to 1.0 micrometers

12. What is the main particle collection mechanism used in particulate matter wet scrubbers?
 - c. Inertial impaction

13. What variables can affect the adequacy of a correlation between scrubber static pressure drop and the particulate matter removal efficiency? Select all that apply.
 - e. All of the above

14. What is the most difficult-to-collect particle size range for a venturi scrubber?
 - b. 0.1 to 1 μm

Review Problems

1. Calculate the liquid-to-gas ratio for a scrubber system with a gas flow rate of 4,000 ft³/sec and a recirculation liquor flow rate of 2,000 gal/min. Is this value in the normal range for a particulate matter wet scrubber?
2. Estimate the liquid purge rate for a scrubber system treating a gas stream of 25,000 scfm with a particulate matter loading of 1.0 grains per scf. Assume that the scrubber particulate matter removal efficiency is 97% and the maximum suspended solids level desirable in the scrubber is 3% by weight.
3. A chevron mist eliminator is 8 ft in diameter. The gas flow rate through the scrubber system has been measured at 60,500 acfm.
 - a. What is the average velocity through the mist eliminator?
 - b. What is the average velocity if 40% of the mist eliminator is completely blocked due to solids accumulation? Is this velocity within the normal operating range of a vertically mounted chevron mist eliminator?
4. Estimate the collection efficiency of 5 μm diameter particles with a density of 2.0 g/cm³ in a counter-current spray tower 2.5 meters high. The gas velocity is 100 cm/sec and the mean droplet diameter is 800 μm. Assume a Cunningham correction of 1.0.
5. Using the relationship of Johnstone et al, estimate the collection efficiency of a 0.5 μm diameter particle with a density of 1.5 g/cm³ in a venturi scrubber having a throat gas velocity of 500 ft/sec and a liquid to gas ratio of 10.0 gal/1,000 ft³. Assume a temperature of 68°F and a k of 0.15 1,000 ft³/gal.

This page intentionally left blank.

Review Problem Solutions

1. Calculate the liquid-to-gas ratio for a scrubber system with a gas flow rate of 4,000 ft³/sec and a recirculation liquor flow rate of 2,000 gal/min. Is this value in the normal range for a particulate matter wet scrubber?

Solution:

$$\text{Gas flow rate} = \left(4,000 \frac{\text{ft}^3}{\text{sec}}\right) \left(60 \frac{\text{sec}}{\text{min}}\right) = 240,000 \frac{\text{ft}^3}{\text{min}}$$

$$\text{Liquid-to-gas ratio} = \frac{2,000 \frac{\text{gal}}{\text{min}}}{240 \frac{1,000 \text{ ft}^3}{\text{min}}} = 8.33 \frac{\text{gal}}{1,000 \text{ ft}^3}$$

This is within the normal range of 4-20 gal/1,000 acf.

2. Estimate the liquid purge rate for a scrubber system treating a gas stream of 25,000 scfm with a particulate matter loading of 1.0 grains per scf. Assume that the scrubber particulate matter removal efficiency is 97% and the maximum suspended solids level desirable in the scrubber is 3% by weight.

Solution:

Calculate the inlet particulate mass:

$$\text{Inlet mass} = 25,000 \frac{\text{ft}^3}{\text{min}} \left(\frac{1.0 \text{ grains}}{\text{ft}^3}\right) \left(\frac{\text{lb}}{7,000 \text{ grains}}\right) = 3.57 \frac{\text{lb}}{\text{min}}$$

$$\text{Collected mass} = 0.97 (\text{Inlet mass}) = 3.46 \frac{\text{lb}}{\text{min}}$$

Purge solids of 3.46 lb/min are 3% of the total purge stream, therefore:

$$\text{Purge stream} = \frac{3.46 \frac{\text{lb}}{\text{min}}}{0.03} = 115.3 \frac{\text{lb}}{\text{min}}$$

A stream with 3% suspended solids has a specific gravity of about 1.03, therefore:

$$\text{Purge stream density} = \left(8.34 \frac{\text{lb water}}{\text{gal}} \right) (1.03) = 8.59 \frac{\text{lb}}{\text{gal}}$$

$$\text{Purge stream flow rate} = \frac{115.3 \frac{\text{lb}}{\text{min}}}{8.59 \frac{\text{lb}}{\text{gal}}} = 13.4 \frac{\text{gal}}{\text{min}}$$

3. A chevron mist eliminator is 8 ft in diameter. The gas flow rate through the scrubber system has been measured at 60,500 acfm.
- What is the average velocity through the mist eliminator?
 - What is the average velocity if 40% of the mist eliminator is completely blocked due to solids accumulation? Is this velocity within the normal operating range of a vertically mounted chevron mist eliminator?

Solution for Part a:

$$V = \frac{Q}{A}$$

$$A = \frac{\pi D^2}{4} = \frac{\pi (8 \text{ ft})^2}{4} = 50.3 \text{ ft}^2$$

$$V = \frac{\left(60,500 \frac{\text{ft}^3}{\text{min}} \right) \left(\frac{\text{min}}{60 \text{ sec}} \right)}{50.3 \text{ ft}^2} = 20.0 \frac{\text{ft}}{\text{sec}}$$

Solution for Part b:

$$A_{\text{open}} = 0.6A = 0.6(50.3) = 30.2 \text{ ft}^2$$

$$V = \frac{\left(60,500 \frac{\text{ft}^3}{\text{min}} \right) \left(\frac{\text{min}}{60 \text{ sec}} \right)}{30.2 \text{ ft}^2} = 33.4 \frac{\text{ft}}{\text{sec}}$$

This is not within normal operating range.

4. Estimate the collection efficiency of 5 μm diameter particles with a density of 2.0 g/cm^3 in a counter-current spray tower 2.5 meters high. The gas flow rate is 200 m^3/min , the water flow rate is 150 l/min , the gas velocity is 100 cm/sec , and the mean droplet diameter is 800 μm . Assume a temperature of 20°C and a Cunningham correction of 1.0.

Solution:

Calculate the droplet terminal settling velocity:

Determine the flow region:

$$K = d_p \left(\frac{g \rho_p \rho_g}{\mu_g^2} \right)^{0.33}$$

$$= 800 \times 10^{-4} \text{ cm} \left[\frac{\left(980 \frac{\text{cm}}{\text{sec}^2} \right) \left(1.0 \frac{\text{g}}{\text{cm}^3} \right) \left(1.2 \times 10^{-3} \frac{\text{g}}{\text{cm}^3} \right)}{\left(1.8 \times 10^{-4} \frac{\text{g}}{\text{cm} \cdot \text{sec}} \right)^2} \right]^{0.33} = 25.0$$

Therefore, the flow region is transition.

$$v_t = \frac{0.153 g^{0.71} \rho_p^{0.71} d_p^{1.14}}{\mu_g^{0.43} \rho_g^{0.29}}$$

$$= \frac{0.153 \left(980 \frac{\text{cm}}{\text{sec}} \right)^{0.71} \left(1.0 \frac{\text{g}}{\text{cm}^3} \right)^{0.71} \left(800 \times 10^{-4} \text{ cm} \right)^{1.14}}{\left(1.8 \times 10^{-4} \frac{\text{g}}{\text{cm} \cdot \text{sec}} \right)^{0.43} \left(1.2 \times 10^{-3} \frac{\text{g}}{\text{cm}^3} \right)^{0.29}} = 327.5 \frac{\text{cm}}{\text{sec}}$$

Calculate the inertial impaction parameter:

$$\Psi_I = \frac{C_c d_p^2 \rho_p V_t}{18 \mu_g d_d}$$

$$= \frac{(1.0) (5 \times 10^{-4} \text{ cm})^2 \left(2.0 \frac{\text{g}}{\text{cm}^3} \right) \left(327.5 \frac{\text{cm}}{\text{sec}} - 100 \frac{\text{cm}}{\text{sec}} \right)}{18 \left(1.8 \times 10^{-4} \frac{\text{g}}{\text{cm} \cdot \text{sec}} \right) (800 \times 10^{-4} \text{ cm})} = 0.439$$

Calculate the single droplet collection efficiency:

$$\eta_I = \left(\frac{\Psi_I}{\Psi_I + 0.35} \right)^2$$

$$= \left(\frac{0.439}{0.439 + 0.35} \right)^2 = 0.310$$

Calculate the particle collection efficiency:

$$\eta_i = 1 - e^{-\left[\frac{1.5v_t\eta_i z}{d_d(v_t - v_g)} \right] \left(\frac{L}{G} \right)}$$

$$= 1 - e^{-\left[\frac{1.5 \left(327.5 \frac{\text{cm}}{\text{sec}} \right) (0.310) (250 \text{ cm})}{(800 \times 10^{-4} \text{ cm}) \left(327.5 \frac{\text{cm}}{\text{sec}} - 100 \frac{\text{cm}}{\text{sec}} \right)} \right] \left[\frac{\left(150 \frac{1}{\text{min}} \right) \left(1 \times 10^{-3} \frac{\text{m}^3}{1} \right)}{200 \frac{\text{m}^3}{\text{min}}} \right]} = 0.792 = 79.2\%$$

5. Using the relationship of Johnstone et al, estimate the collection efficiency of a $0.5 \mu\text{m}$ diameter particle with a density of 1.5 g/cm^3 in a venturi scrubber having a throat gas velocity of 500 ft/sec and a liquid to gas ratio of $10.0 \text{ gal}/1,000 \text{ ft}^3$. Assume a temperature of 68°F and a k of $0.15 \text{ 1,000 ft}^3/\text{gal}$.

Solution:

Calculate the mean droplet diameter:

$$d_d = \frac{16,400}{v_g} + 1.45 \left(\frac{Q_l}{Q_g} \right)^{1.5}$$

$$= \frac{16,400}{500} + 1.45(10.0)^{1.5} = 78.7 \mu\text{m}$$

Calculate the Cunningham correction factor:

$$C_c = 1 + \frac{6.21 \times 10^{-4} T}{d_p} = 1 + \frac{6.21 \times 10^{-4} (293 \text{ K})}{0.5 \mu\text{m}} = 1.36$$

Calculate the inertial impaction parameter:

$$\Psi_I = \frac{C_c d_p^2 \rho_p V_r}{18 \mu_g d_d}$$

$$= \frac{(1.36)(0.5 \times 10^{-4} \text{ cm})^2 \left(1.5 \frac{\text{g}}{\text{cm}^3}\right) \left(500 \frac{\text{ft}}{\text{sec}} \times 30.48 \frac{\text{cm}}{\text{ft}}\right)}{18 \left(1.8 \times 10^{-4} \frac{\text{g}}{\text{cm} \cdot \text{sec}}\right) (78.7 \times 10^{-4} \text{ cm})} = 3.048$$

Calculate the particle collection efficiency:

$$\eta_i = 1 - e^{-k\sqrt{\Psi_1} \frac{Q_l}{Q_g}}$$

$$= 1 - e^{-0.15 \frac{1,000 \text{ ft}^3}{\text{gal}} \sqrt{3.048} \left(10.0 \frac{\text{gal}}{1,000 \text{ ft}^3}\right)} = 0.927 = 92.7\%$$

References

Calvert, S., J. Goldschmid, D. Leith, and D. Mehta. *Scrubber Handbook*. Vol. 1, *Wet Scrubber System Study*. EPA-R2-72-118a. 1972.

Engineering Science. *Scrubber Emissions Correlation Final Report*. U.S. EPA Contract 68-01-4146, Task Order 49. 1979.

Ensor, D.S. *Ceilcote Ionizing Wet Scrubber Evaluation*. EPA 600/7-79-246. 1979.

Johnstone, H.F., R.B. Field and M.C. Tassler, I. & E.C., **46**, 1601 (1954).

Myers, J.R., and D. McIntosh. *The Dynawave Scrubber: a Highly Efficient Gas Cleaning*. Paper presented at the American Institute of Chemical Engineers Midwest Regional Meeting. St. Louis, MO. February, 1991.

Nukiyama, S., and Y. Tanasawa, *Trans. Soc. Mech. Engrs. (Japan)*, **4**, 86, 138 (1938); **5**, 63, 68 (1939); **6**, II-7, II-8 (1940).

Radian Corporation. *Economic and Technical Evaluation of a Hydro-Sonic Free-Jet Scrubber for a Hazardous Waste Incinerator*. Report DCN 87-213-071-05. 1987.

Richards, J. *Wet Scrubber Inspection and Evaluation Manual*. PA 340/1-83-022. 1983.

Schiffner, K. *Flux Force Condensation Scrubbers for Utilization on Municipal Solid Waste Incinerators*. Paper presented at the Joint American Society of Mechanical Engineers/IEEE Power Generation Conference. Dallas, TX. October, 1989.

Schiffner, K.C., and H.E. Hesketh. *Wet Scrubbers*. Ann Arbor Science. Ann Arbor, MI. 1983.

Schiffner, K.C., and R.G. Patterson. *Engineering Efficient Hospital Waste Incinerator Scrubbers*. Paper presented at the First National Symposium on Incineration of Infectious Wastes. Washington, D.C. May, 1988.

U.S. Environmental Protection Agency. 1982. *Control Techniques for Particulate Emissions from Stationary Sources*. Vol. 1, *Wet Scrubbers*. EPA 450/3-81-005a.

Walker, A.B., and R.M. Hall. *Operating Experience with a Flooded Disc Scrubber: a New Variable Throat Orifice Contactor*. *Journal of the Air Pollution Control Association* 18:319-323. 1968.

Yung, S., S. Calvert, and H.F. Barbarika. *Venturi Scrubber Performance Model*. EPA 600/2-77-172. 1977.

This page intentionally left blank.

CHAPTER 9

ELECTROSTATIC PRECIPITATORS

Electrostatic precipitators are used in many industries for the high efficiency collection of particulate matter. They were originally developed in the early 1900s for acid mist control. During the 1940s, precipitators began to be used for particulate matter control at coal-fired boilers, cement kilns, and kraft recovery boilers. The applications of precipitators have steadily increased since the 1940s due to their ability to impart large electrostatic forces for particle separation without imposing gas flow resistance. Electrostatic precipitator efficiency and reliability have improved steadily since the 1970s as a result of research and development programs sponsored by equipment manufacturers, trade associations, and the USEPA.

Operating Principles

In all types of electrostatic precipitators, there are three basic steps to particulate matter collection:

- ***Step 1*** is the electrical charging and migration of particles toward a vertical collection surface.
- ***Step 2*** involves the gravity settling (or draining in the case of liquids) of the collected material from the vertical collection surfaces.
- ***Step 3*** is the removal of the accumulated solids or liquids from the hopper or sump below the electrically energized zone.

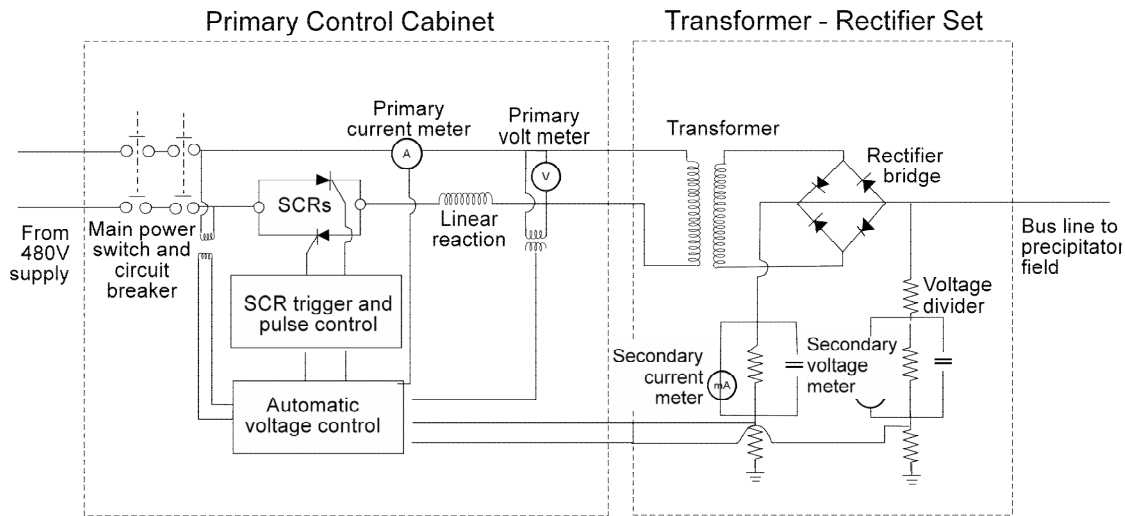
Precipitator Energization

The purpose of the high voltage equipment of an electrostatic precipitator is to cause particle-charging and migration (Step 1). A simplified drawing of the circuitry from the primary control cabinet to the precipitator field is shown in Figure 9-1.

The alternating power supplied to the primary control cabinet is at a constant 480 volts and 60 cycles per second. This electrical power is supplied to the transformer-rectifier (T-R) set when the main switch and the circuit breaker in the primary control cabinet are both on. If an electrical problem is sensed in the power supply or the precipitator field, the circuit breaker automatically opens. This is called *tripping* the field.

In the primary control cabinet, the automatic voltage controller, the silicon controlled rectifiers (SCRs) and the SCR trigger and pulse controller alter the A.C. line voltage and adjust the waveform of the voltage to control electrical conditions on the primary side of the

transformer in the T-R set. The result is a primary voltage that can range from zero to more than 400 volts.



Basic Steps in Energizing a Precipitator Field

- Open/close 480 volt A.C. power supply to the primary control cabinet
- Control voltage and adjust voltage and current waveforms in primary line to the transformer
- Control current flow during sparking
- Increase voltage
- Convert electricity to direct current form

Components

- Main power switch and circuit breaker
- Automatic voltage controller, silicon controlled rectifiers (SCRs), trigger/pulse control for SCRs
- Linear reactor (located adjacent to primary control cabinet)
- Transformer
- Rectifier bridge

Figure 9-1. Precipitator field energization

The primary alternating power is converted to a secondary pulse-type direct power in the T-R set. The relatively low primary voltage is stepped up to a secondary voltage of more than 50,000 volts. The voltage applied to the discharge electrodes is called the secondary voltage because the electrical line is on the secondary side (high voltage generating side) of the transformer. For convenience, the secondary voltage gauges are usually located on the primary control cabinets.

As the primary voltage applied to the transformer increases, the secondary voltage applied to the discharge electrodes increases. Stable electrical discharges begin to occur when the secondary voltage exceeds the onset voltage, which can be between 15,000 and 25,000 volts depending partially on the *sharpness* or extent of curvature of the discharge electrode. The relationship between the secondary voltage and the secondary current is shown in Figure 9-2.

The automatic voltage controller in the primary control cabinet is designed to increase the primary voltage applied to the T-R set to the maximum point possible at any given time. One of the following six factors will always limit the maximum secondary voltage:

- Primary voltage limit

- Primary current limit
- Secondary voltage limit
- Secondary current limit
- Spark rate limit
- SCR conduction angle

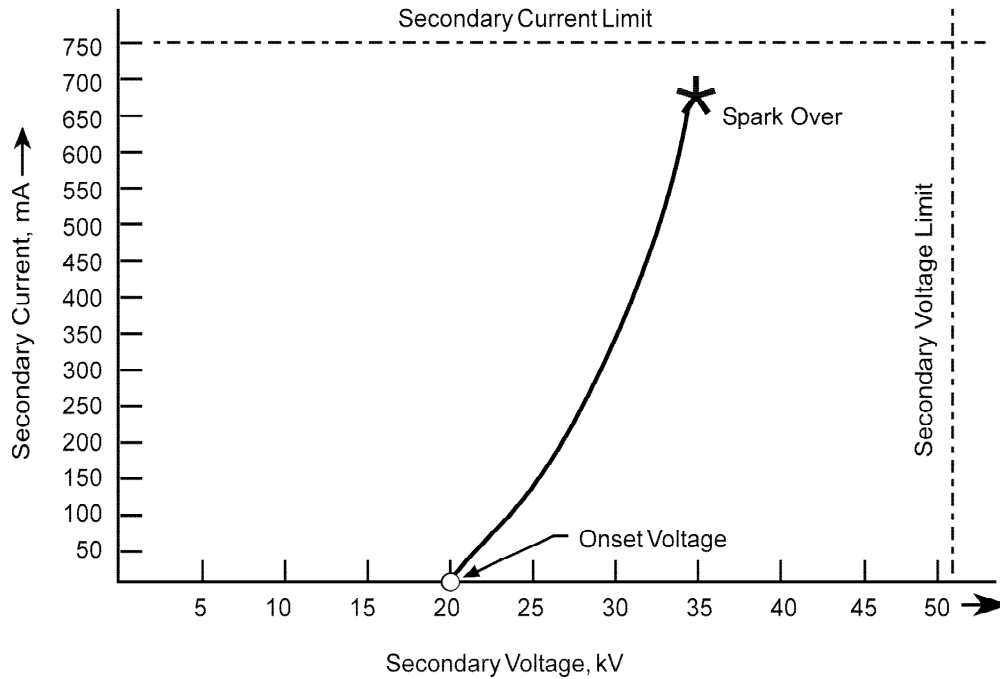


Figure 9-2. Voltage-current curve

The upper limit of the primary voltage is set by the 480 volt power line leading to the primary control cabinet. The primary current limit is set by the operator at a level below the current value that could damage the primary control cabinet components. The secondary voltage and current limits are also set at levels necessary to protect the T-R set components.

The spark rate limit is an arbitrary limit selected by the operator to optimize performance. Some electrical sparking is generally indicative of good operation. Excessive sparking can cause premature component failure. Whenever any one of these limits is reached, the automatic voltage controller decreases the applied primary voltage to protect the electrical circuitry. The applied primary voltage moves up the voltage-current curve until one of the limits is reached.

Operating conditions at any given time are determined by one of the six operating limits. The primary voltage, primary current, secondary voltage, secondary current, and spark rate are indicated by gauges mounted on the front of the primary control cabinet. Most of the new installations also have indicator lights to show the operating limit that is presently limiting the secondary voltage. The electrical conditions and the limiting factor vary at any one field over time, and they vary substantially from field-to-field. This information is very useful for

evaluating precipitator performance and is, therefore, discussed in more detail later in this chapter.

If there is no electrical sparking in a field, the electrical conditions in the field will remain very stable until dust loadings or other changes affect the electrical conditions. If electrical sparking occurs, there will be short-term variations in these indicated operating conditions. After each spark in a precipitator field, the automatic voltage controller shuts off the primary voltage for a short period of time (milliseconds) to prevent the short-term spark from becoming a sustained, damaging power arc (see Figure 9-3). Once this quench period is over, the voltage is ramped up quickly to a voltage very close to the previous point at which the spark occurred. The voltage is then gradually increased to the point where another spark occurs. Generally, these variations appear as very brief fluctuations in the secondary voltage meter.

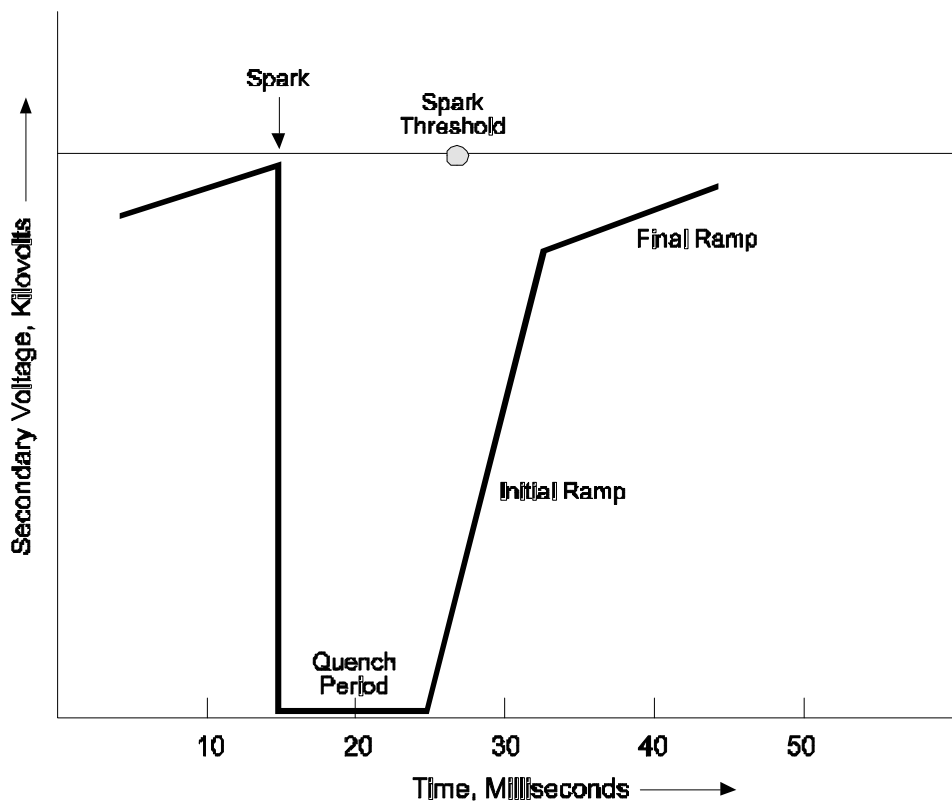


Figure 9-3. Secondary voltage before and after a spark

Protective equipment is included in the primary control cabinet. If a problem is sensed in the power supply of the precipitator field, this protective circuitry trips the power supply and the T-R set off-line. For example, a short circuit across the surface of a high voltage frame support insulator would create very low voltages and high currents. The under-voltage sensors would detect this condition and shut down the field to prevent damage to the insulator or to the power supply itself.

Particle Charging and Migration

The electrical discharges from the precipitator discharge electrodes are termed *corona discharges* and are needed to electrostatically charge the particles. Within the negative corona discharge, electrons are accelerated by the very strong electrical field and strike and ionize gas molecules (Figure 9-4a). Each collision of a fast-moving electron and a gas molecule generates an additional electron and a positively charged gas ion. The corona discharges are often described as an *electron avalanche* since large numbers of electrons are generated during multiple electron-gas molecule collisions.

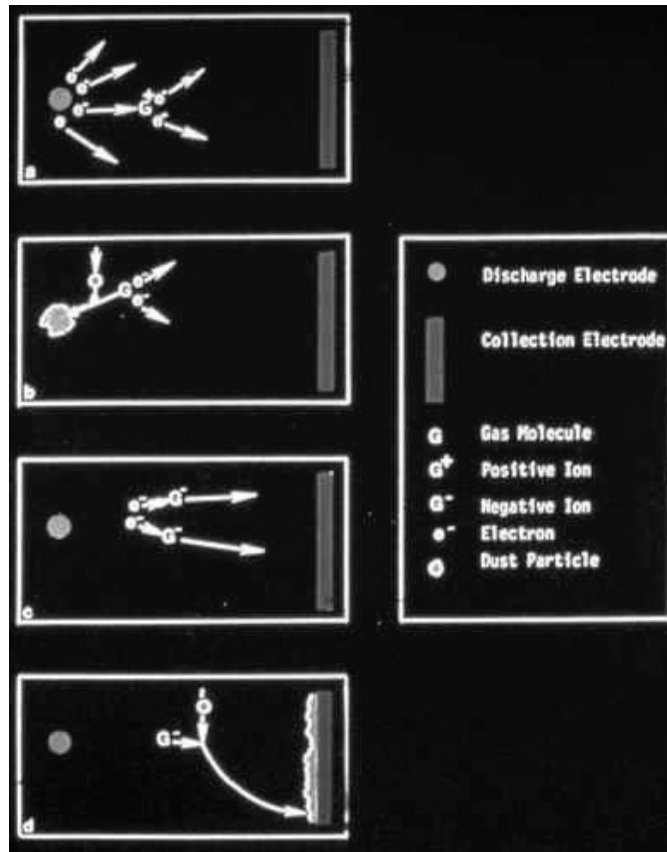


Figure 9-4. Negative corona particle charging

The positive gas ions generated in the ionization process move back toward the discharge electrode. Some of these positive gas ions will deposit on particles inside the corona and charge them positively (Figure 9-4b). These positively charged particles deposit on the negative discharge electrodes, requiring them to be cleaned periodically.

Slightly farther away from the discharge electrode, where the electrical field strength is lower, electrons released in the corona discharges are captured by gas molecules. These negatively-charged gas ions move rapidly toward the grounded collection plates (Figure 9-4c). Some of these gas ions are captured by particles, charging them negatively (Figure 9-4d). The particles quickly reach a maximum charge called the *saturation charge*. This is the

charge at which the electrostatic field created by the captured ions is strong enough to deflect additional gas ions that are approaching the particle.

The magnitude of the saturation charge is dependent on the particle size, as indicated by Equation 9-1. Small particles have a low saturation charge, since the gas ions have only a small surface on which to deposit. The saturation charge increases with surface area or with the square of the particle diameter. Large particles accumulate higher electrical charges on their surface and, therefore, are more strongly affected by the applied electrical field.

$$q = (3\pi\epsilon_0 E_0)d_p^2 \quad (9-1)$$

where:

- q = charge on particle
- ϵ_0 = permittivity of free space = 8.85×10^{-12} farads/m
- E_0 = electric field strength = volts/m
- d_p = particle diameter

Particle larger than about 1.0 μm diameter, accumulate charged gas ions by locally disrupting the electrical field, causing the gas ions to be momentarily directed to the particle surface rather than the collection plate. This mechanism is termed *contact charging*. Particle less than 0.1 μm diameter do not have sufficient mass to disrupt the electrical field. Instead, they accumulate charges as they randomly diffuse through the gas ions. This mechanism is termed *diffusional or ion charging*.

Once the particles have attached ions, they are influenced by the strong, nonuniform electrical field between the discharge electrode and the grounded collection plate. Accordingly, the charged particles begin to migrate toward the grounded plates at a velocity given by Equation 9-2. At the same time, drag forces, which depend on the particle mass or the cube of the particle diameter, are trying to move the particles straight through the precipitator. As a result, the smaller micrometer-sized particles are deposited near the inlet and progressively larger particles are deposited farther into the precipitator. Usually, particles larger than about 30 μm diameter are removed in a precleaner in order to avoid having an excessively long precipitator. Submicrometer-sized particles charge more slowly but, once charged, move rapidly to the collection plate.

$$\omega = \frac{qE_p C_c}{3\pi d_p \mu} \quad (9-2)$$

where:

- ω = migration velocity
- q = charge on particle
- E_p = electric field near collection plate
- C_c = Cunningham slip correction factor
- μ = gas viscosity

d_p = particle diameter

The combined effect of contact and diffusion charging creates a particle size-collection efficiency relationship similar to Figure 9-5. There are very high collection efficiencies above 1.0 μm due to the increasing effectiveness of contact charging for large particles. Increased diffusion charging causes collection efficiency to increase for particles smaller than 0.1 μm . There is a difficult-to-control range between 0.1 to 1.0 μm due to the size dependent limitations of both of these charging mechanisms. The precipitator is least effective for the particles in this size range.

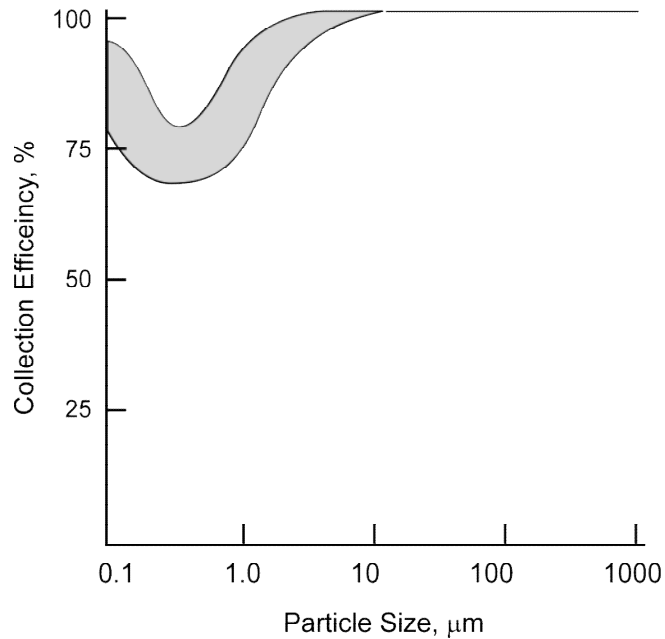


Figure 9-5. Typical particle size efficiency relationship for electrostatic precipitators

The extent of the efficiency limit in the difficult-to-control size range is related to the size of the precipitator, the extent of sectionalization, the operating conditions, and the physical conditions. Well designed and operated precipitators can have size-efficiency relationships with only a slight efficiency decrease in the difficult-to-control size range. Undersized precipitators or units in poor condition can have a more pronounced efficiency decrease in this size range.

Dust Layer Resistivity

The gas ions arriving on the surfaces of particles and arriving as uncaptured ions must pass through the dust layers on the collection plates. At the metal surface of the collection plate, the voltage is zero, since the plate is electrically grounded. At the outer surface of the dust layer where new particles and ions are arriving, the electrostatic voltage caused by the gas ions can be more than 10,000 volts.

It is this electrostatic voltage difference across the dust layer that holds the dust layer on the vertical surface of the collection plate. The same type of voltage difference is created when a child rubs a balloon on his or her hair and then sticks the balloon on a wall. It does not fall because of the very slight charge difference between the side of the balloon and the wall. Eventually, however, the balloon falls off the wall. The electrons that were initially on the balloon find a path for reaching the wall. As the electrons flow off the balloon, the force holding it to the wall becomes weak.

Essentially the same phenomenon occurs in the dust layers on precipitator collection plates. When the electrical charges from the gas ions can readily move through the dust layer to the plate, the charge difference across the dust layer is relatively low (i.e., several thousand volts). This means that the dust layer can be easily dislodged. When the electrical charges move very slowly through the dust layer, there are a large number of electrical charges on the outer surface, and the voltage difference can be very high (more than 10,000 volts). This means that the dust layer is held very tenaciously.

The ability of the electrical charges to move through the dust layer is measured in terms of the dust layer resistivity. When the resistivity is very low, the electrons are conducted very readily, and there is only a slight charge difference across the dust layer. When the resistivity is very high, the electrons have difficulty moving through the dust layer and create very high forces as they accumulate on the outer surface of the dust layer.

Very high and very low resistivity conditions are harmful to electrostatic precipitator performance. Electrostatic precipitators work best when the dust layer resistivity is in the moderate range: not too high and not too low. This is because of the various ways that the dust layer electrostatic field affects both dust layer rapping and particle charging migration.

During rapping of weakly held low resistivity dust layers, many of the particles are released back into the gas stream as individual particles or small agglomerates that do not settle fast enough to reach one of the hoppers before the gas stream leaves the precipitator. Even large particles of 100 μm diameter do not fall sufficiently fast to reach the hoppers. Accordingly, it is very important that the particles agglomerate in the dust layer and settle as large clumps or sheets rather than as discrete particles.

If the resistivity is too low and particles are redispersed during rapping, there can be a short term emission spike, called a puff. As the resistivity increases into the moderate range, the voltage drop across the dust layer increases, and the dust cake is dislodged as cohesive sheets or clumps that are large enough to fall rapidly and be collected in the hoppers of the precipitator.

If the voltage drop across the dust layers becomes too high (high resistivity), there can be a number of adverse effects. First, as the dust layer builds up and the electrical charges accumulate on the surface, the voltage difference between the discharge electrode and the dust layer decreases, reducing the electrostatic field strength used to drive the gas ion-carrying particles over to the dust layer. The migration velocities of small particles are

especially affected by the reduced field strength. The general impact of high resistivity on the migration velocity is illustrated in Figure 9-6.

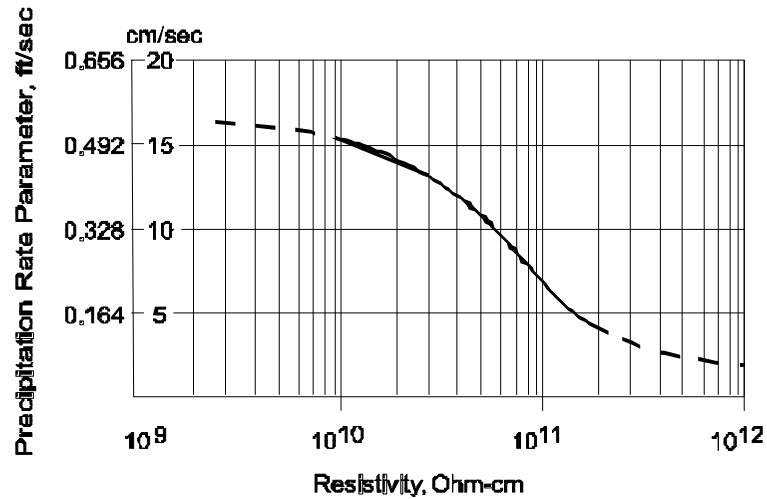


Figure 9-6. Effect of dust layer resistivity on migration velocity

Another adverse impact of high resistivity dust layers is called *back corona*. This occurs when the electrostatic voltage across the dust layer is so great that corona discharges begin to appear in the gas trapped within the dust layer. When the voltage in the dust layer reaches sufficient levels, electrons are accelerated and ionization begins. Positive gas ions formed by the electron collisions stream toward the negatively charged discharge electrode. Along the way, these positive ions neutralize some of the negative charges on the dust layer particles. They also neutralize some of the negative ions on the particles approaching the dust layer and reduce the space charge near the dust layer surface. The net result of back corona is severely impaired particulate matter removal efficiency.

The third and generally most common adverse impact of high resistivity dust layers is increased electrical sparking. Once the sparking reaches the arbitrarily set spark rate limit, the automatic controllers limit the operating voltages of the field. This causes reduced particle charging effectiveness and reduced particle migration velocities toward the collection plates. High resistivity-related sparking is due primarily to the concentration of electrical field lines in localized portions of the dust layer on the collection plates. Any misalignment problems or protrusions of the collection plate surface make those areas especially vulnerable to sparking. This is why proper alignment of precipitator collection plates and discharge electrodes is so important when the resistivity is high.

There is another adverse characteristic of high resistivity dust layers. Since the dust layers are so strongly held by the electrostatic fields, it is hard to dislodge the dust. As more charged dust continues to arrive, the depth of the dust layer increases, and it becomes even harder for electrons to pass through to the collection plates. There can be some temptation to rap the collection plates frequently and severely to reduce the dust layer quantities. In severe cases, this practice can have very little beneficial impact on the dust layer depths, and it can

lead to rapid mechanical failure of the rappers or misalignment of the collection plates. If this practice causes misalignment, the problems caused by high resistivity become even greater.

As previously noted, electrostatic precipitators work best when the dust layer resistivity is in the moderate range. It should resist current flow a little, but not too much. It is helpful to describe the dust layer resistivity based on units of ohm-centimeters. This is simply the ohms of resistance created by each centimeter of dust in the dust layer. High resistivity is generally considered to be equal to or above 5×10^{10} ohm-cm. Low resistivity is generally considered to be equal to or below 5×10^8 ohm-cm. The region between 5×10^8 and 5×10^{10} ohm-cm is, therefore, the moderate or preferred range.

There are actually two basic paths that electrons can take in passing through the dust layer to the collection plate surface. They can pass directly through each particle until they reach the metal surface. This is called bulk conduction and occurs only when there are one or more constituents in the particles that can conduct electricity. Conversely, the electrons can pass over the surfaces of various particles until they reach the metal surface. This is called surface conduction and occurs when vapor phase compounds that can conduct electricity adsorb onto the surfaces of the particles. Both paths of current dissipation are illustrated in Figure 9-7.

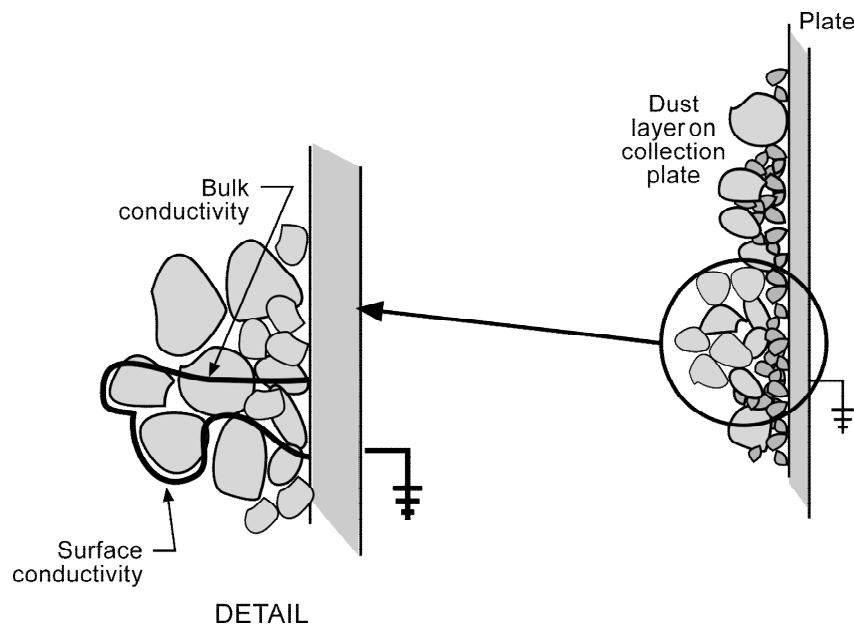


Figure 9-7. Conductivity paths through dust layer

One of the most common electrical conductors responsible for bulk conduction in particles is carbonaceous material. If the concentration of this material is sufficiently high, the electrons can pass from particle to particle to reach the collection plate. Electrical conduction through the inorganic oxides and other compounds that comprise the majority of ash particles from combustion sources and other industrial sources is sufficiently rapid when the temperatures

are above 400°F and preferably in the range of 500°F and 700°F. This resistivity-temperature relationship is indicated in Figure 9-8.

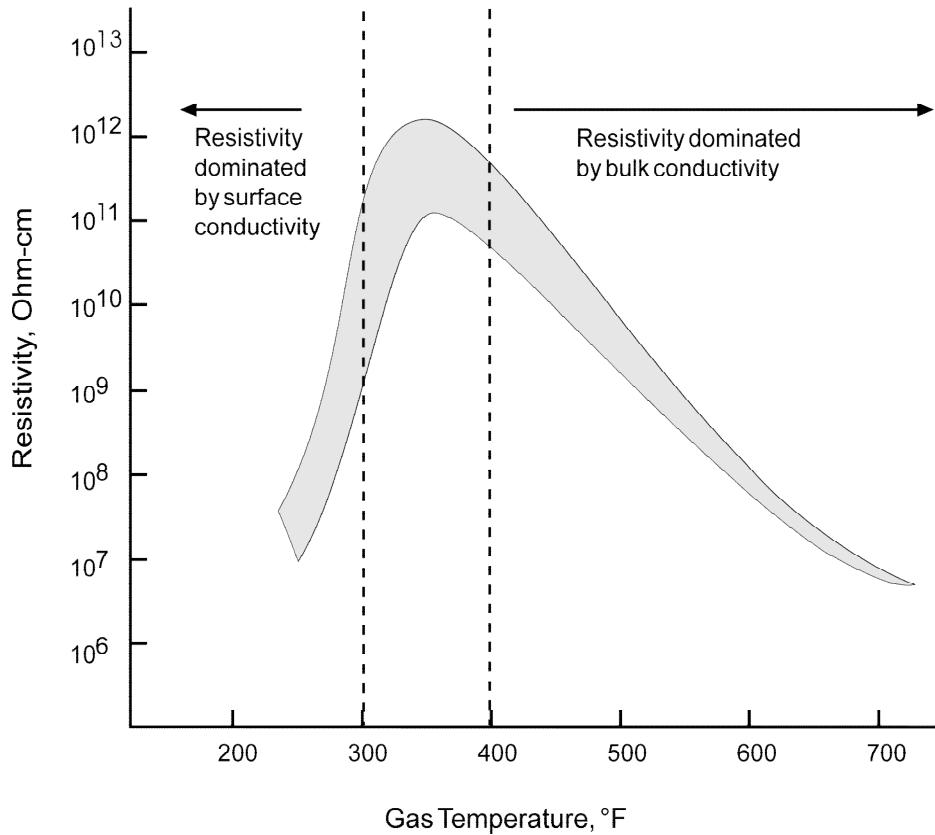


Figure 9-8. Resistivity-temperature relationship

On the low temperature side of the typical resistivity curve, the resistivity can decrease dramatically as the gas temperature drops slightly. This is due to the increased adsorption of electrically conductive vapors present in the gas stream. One of the most common compounds responsible for surface conduction is sulfuric acid. It adsorbs to particle surfaces very readily, even at gas temperatures of 250°F to 350°F. Even vapor phase concentrations of only 5 to 10 ppm are often sufficient to affect the dust layer resistivity. The ability of sulfuric acid to electrically condition the particle surfaces is due, in part, to its hygroscopic tendencies. Each sulfuric acid molecule can be attached to a cluster of water molecules, which can also be electrically conductive.

Many air pollution sources using electrostatic precipitators generate enough sulfuric acid or other particle surface conditioning agents to reduce the dust layer resistivities into the moderate range at operating temperatures of 250°F to 350°F. However, if they generate too much sulfuric acid vapor, or if the gas temperature drops too much, the resistivity can be too low. If, for some reason, enough sulfuric acid is not generated, or the gas temperature is relatively high, the resistivity can be very high.

In sources that do not inherently generate enough vapor phase compounds for surface conditioning, it is necessary to inject the materials into the precipitator inlet. The most common material used to condition precipitators is sulfur trioxide, which quickly forms vapor phase sulfuric acid upon entering the inlet gas stream. Ammonia is also used either alone or in combination with sulfur trioxide. These materials adsorb on the surfaces of the particles as they enter the precipitator and are being collected. Once the particle is in the dust layer, electrons pass through these adsorbed molecules.

The very strong temperature dependence of surface conditioning can create some very non-uniform dust layer resistivities in different portions of the unit. It is common for portions of the precipitator to be 30 to 50°F different from the average temperature indicated by the plant instrumentation. In the hot areas, very little vapor phase material adsorbs, and the resistivity can be relatively high. In the cold areas, too much conductive material can be on the particle surfaces, and the resistivity can be relatively low. Spatial differences of more than three orders of magnitude in dust layer resistivity have been found.

Applicability Limitations

Electrostatic precipitators can provide high efficiency, reliable particulate matter control in a wide variety of industrial applications. However, there are a few conditions that limit their industrial applicability:

- Extremely low fly ash resistivities
- Potential fire and explosion hazards
- Sticky particulate matter
- Ozone formation

In industrial sources that generate highly carbonaceous particulate matter, the fly ash resistivities can be extremely low due to the high bulk conductivity of this material at all temperatures. These resistivities can be below the levels where good performance can be obtained by flue gas conditioning. Severe rapping reentrainment problems can persist during routine operation due to the weak electrical forces bonding the dust layer to the collection plate and the ease of particle dispersion during rapping. Electrostatic precipitators are not an ideal choice for particulate matter control in these applications due to the probable emission problems.

Applications involving the routine or intermittent presence of highly carbonaceous particulate matter or other easily combusted material should be approached with caution. Fires can occur in dust layers on the collection plates or in the accumulated solids in a hopper. These fires can create high temperature areas in the affected part of the unit, which can result in severe warpage and misalignment of the collection plates. Electrostatic precipitators are not appropriate for sources that have potentially explosive concentrations of gases or vapors. The routine electrical sparking in the fields provides numerous opportunities to ignite the explosive materials. For these reasons, electrostatic precipitators are rarely used for sources generating highly combustible or potentially explosive contaminants in the gas streams.

The presence of highly sticky material, such as some oils and compounds like ammonium bisulfate, can present major operating problems in dry, negative corona precipitators. Rapping of the solids from the collection plates must be readily possible. The accumulation of sticky material on the collection plates and other components in the precipitator would soon cause collection plate-to-discharge electrode clearance problems that would adversely affect the electrical conditions in the affected field. For this reason, dry, negative corona precipitators are rarely used on sources that generate high concentrations of sticky particulate matter. Wet, negative corona precipitators and wet, positive corona precipitators can operate very well with moderately sticky material. However, it must be possible to remove the contaminants either by normal drainage or by occasional cleaning sprays.

Dry, negative corona and wet, negative corona precipitators generate very small quantities of ozone due to the characteristics of the corona discharge. Generally, the concentration of ozone is limited by the relatively low oxygen levels in the gas stream being treated. Due to the presence of ozone, these types of electrostatic precipitators are not used for standard air cleaning operations where the oxygen concentrations are at ambient levels, and it is necessary to recirculate the treated air stream to an occupied work area.

Precipitator Systems

There are three categories of electrostatic precipitators (ESPs). These units serve entirely different industrial applications.

- Dry, negative corona
- Wet, negative corona
- Wet, positive corona

General operating characteristics and components of these three ESPs as well as operating procedures and performance problems, are discussed in this section. The emphasis is on dry, negative corona units since this type is used on the largest systems and these are the most common type of units presently in service.

Dry, negative corona units are used in large industrial facilities such as cement kilns, kraft pulp mills, and coal-fired utility boilers. They are termed dry because the collected solids are removed from the collection plates as a dry material. The term negative corona means that the particles are collected by forcing them to move from a high negatively charged area to an electrically grounded collection plate.

Wet, negative corona units use water on the collection plates to remove the collected solids. This approach eliminates several of the major problems that can affect dry, negative corona units. However, with the use of water in close proximity to high voltage insulators, it adds to the system complexity and it increases the potential problems associated with corrosion. Most wet, negative corona units are used for small-to-moderately-sized industrial sources that

produce particulate matter that is sticky or that is too carbonaceous for a dry, negative corona application.

Wet, positive corona units are sometimes termed two-stage precipitators. Particle charging occurs in a pre-ionizer section, and particle collection occurs in a downstream collection plate section. The pre-ionizer operates at a high positive voltage. The wet, positive corona units are used to remove organic compound droplets and mists. The collected material drains from the vertical collection plates. These precipitators are used on small sources.

Dry, Negative Corona Precipitators

A dry, negative corona electrostatic precipitator consists of a large number of parallel gas passages with discharge electrodes mounted in the center and grounded collection surfaces called plates on either side. The discharge electrodes are spaced 4.5 to 6 in. away from each of the collection plates as shown in Figure 9-9. A high negative voltage is applied to the discharge electrodes. The voltage difference between the discharge electrodes and plates creates continuous electrical discharges termed *coronas*.



Figure 9-9. Gas passage between collection plates

Negatively charged gas ions formed in and near the corona discharge impart an electrical charge to the particles and cause them to move toward the electrically grounded collection plates. Mechanical hammers called *rappers* are used to remove a portion of the dust layer accumulating on these plates and the small quantities of dust that also collect on the discharge electrodes. Particle agglomerates and dust layer sheets fall by gravity into the hoppers during rapping.

The dry, negative corona electrostatic precipitator shown in Figure 9-10 is typical of units used on large-scale processes such as coal-fired utility boilers, coal-fired industrial boilers, kraft pulp mill recovery boilers, cement kilns, and municipal incinerators. They are generally quite large and are often designed for gas flow rates from 100,000 acfm to more than 3,000,000 acfm.

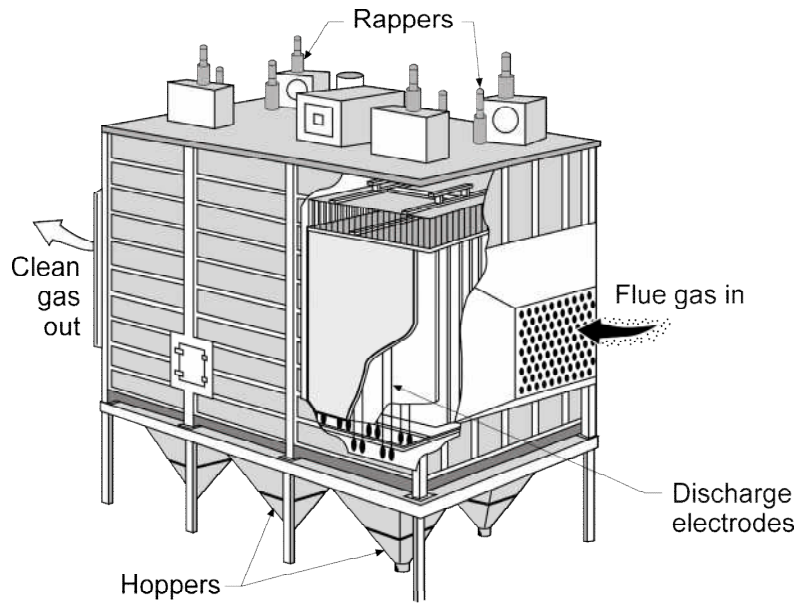


Figure 9-10. Typical dry, negative corona type electrostatic precipitator

The gas stream passing through the duct toward the precipitator is moving too fast for effective treatment. Deceleration occurs by expanding the gas flow area in the inlet transition section immediately upstream of the precipitator. The gas velocity decreases by a factor of approximately 10 so that the average velocity through the precipitator is usually between 3 to 6 feet per second.

In addition to slowing down the gas stream, the inlet transition is used to distribute the gas flow as uniformly as possible so that there are no significant cross-sectional variations in the gas velocities at the entrance of the precipitator. Proper gas distribution is achieved by proper inlet transition design, by proper inlet ductwork design, by the use of turning vanes in the inlet ductwork, and by a series of gas distribution screens mounted in the inlet transition. Perforated plate gas distribution screens are shown in Figure 9-11.



Figure 9-11. Gas distribution screens at the precipitator inlet

As the gas stream enters the precipitator, it goes through passages formed by the large, parallel collection plates. High voltage discharge electrodes are centered between each of the plates. The side walls of the precipitator have anti-sneakage baffles to prevent untreated gas from passing along the side walls, where it is impossible to mount discharge electrodes. In the precipitators shown in the figures, small diameter wires serve as the discharge electrodes. In other precipitator designs, rigid masts or wires in rigid frames are used. The high voltages applied to the discharge electrodes create a negative corona that ultimately charges most of the particles negatively. The charged particles migrate to the collection plates and build-up as dust layers on the plate surfaces. A small fraction of the particulate matter also accumulates on the discharge electrodes.

The discharge electrodes are divided into fields. These are portions of the precipitator energized by a single transformer-rectifier (T-R) set power supply. Most units have three to four fields in series as shown in Figure 9-12. However, some especially large units have as many as fourteen fields in series. The precipitator can also be divided into separate chambers that are separated by a solid wall. Chambers may also be designed as separate precipitator shells.

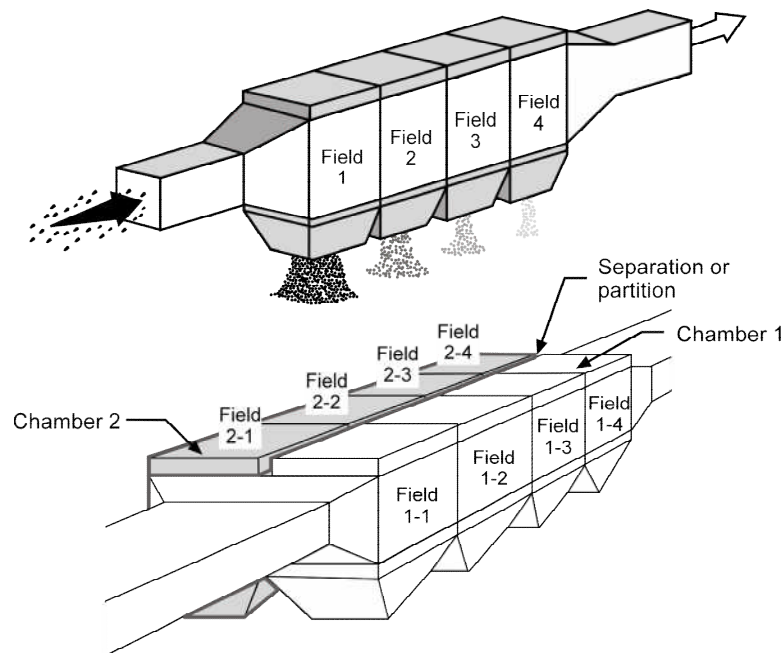


Figure 9-12. Arrangement of fields and chambers

Each of the fields is energized by a T-R set (Figure 9-13). The primary control cabinet circuitry controls the voltage in the alternating current power line applied to one side of the transformer in the T-R set. The high voltage generated in the transformer is converted into direct current in the rectifier and is then sent to the precipitator field.

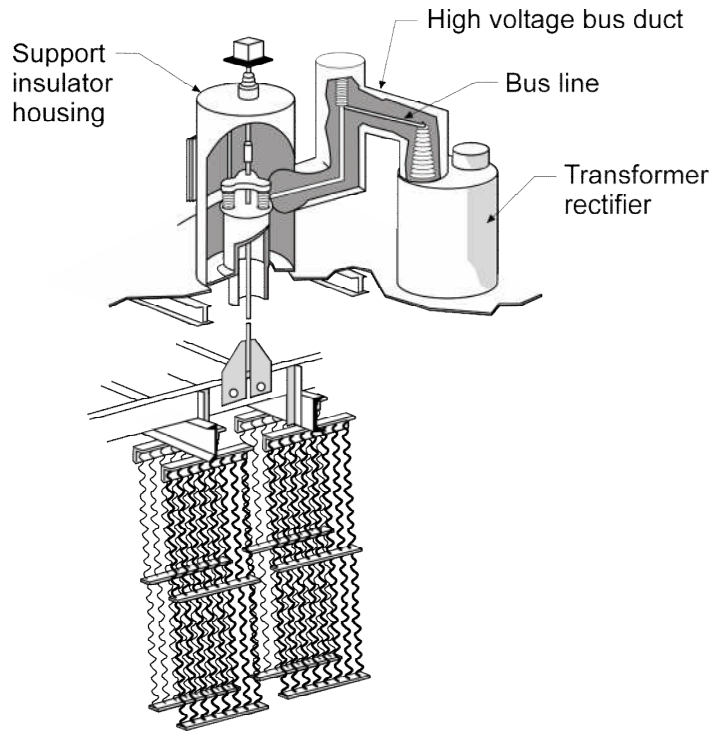


Figure 9-13. T-R set, support insulator, discharge electrode frame, discharge electrodes

The gauges on the control cabinet for each T-R set provide much of the data necessary to evaluate performance. Figure 9-14 illustrates the analog gauges common in many older units. Some new precipitators have digital gauges used alone or in combination with the analog gauges.

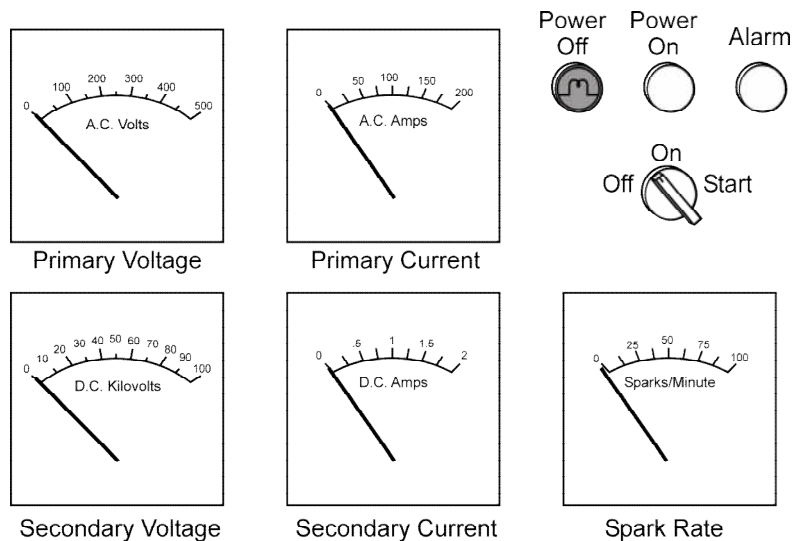


Figure 9-14. Gauges present on the control cabinet for each precipitator field

The distance between the high voltage discharge electrodes and the grounded collection plates affects the electrical charging and migration of the particles. If some portions of the discharge electrodes and collection plates are closer than others, a spark will occur frequently at the close approach point. The automatic voltage controller will respond to this condition by reducing the applied voltage. This reduces the affected field's ability to electrically charge and collect particles. For example, if the designers intended discharge electrode spacing to the collection plates is 4.5 in., it is usually necessary to maintain all the discharge electrodes with an allowable spacing deviation of only ± 0.5 in. In other words, all discharge electrodes in this unit must be between 4 and 5 in. away from all portions of the adjacent collection plates. This is not easy to maintain.

The discharge wires are suspended between the grounded collection plates using insulators called high voltage frame support insulators. There are usually at least two high voltage frame support insulators for each bus section in a field. The location of these insulators is shown in Figure 9-15.

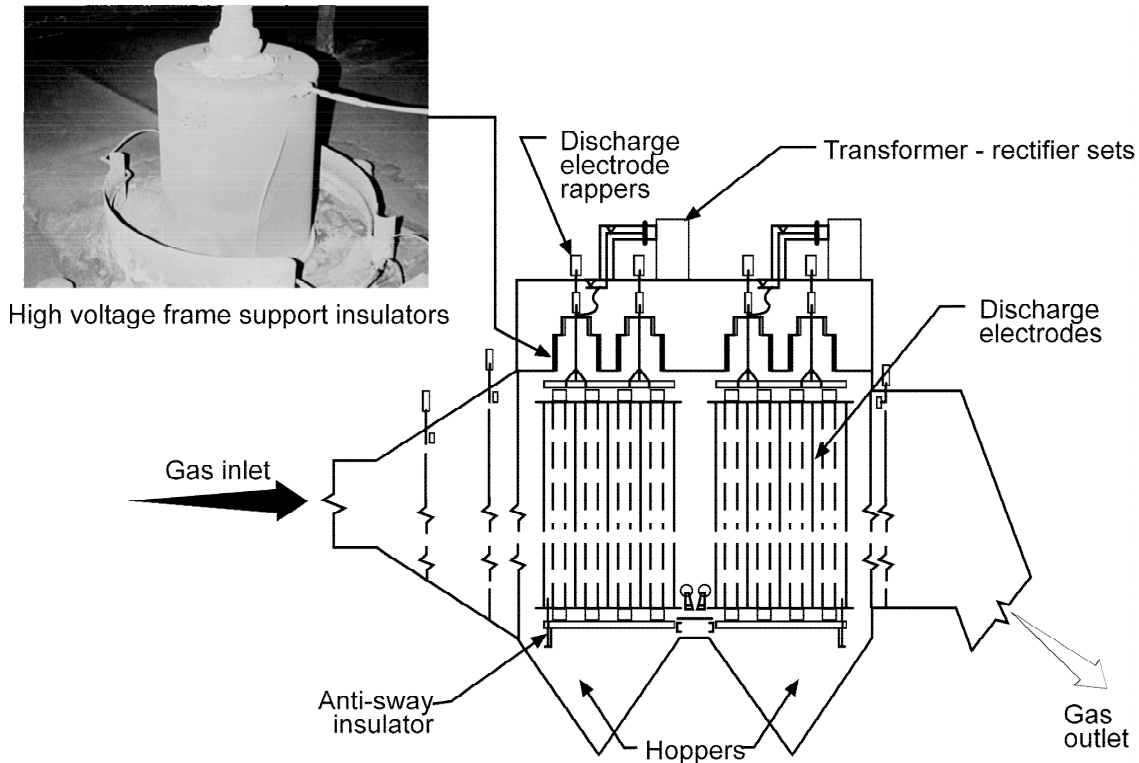


Figure 9-15. High voltage frame support insulators

The accumulation of moisture or dust on the surfaces of support insulators can cause a short circuit. These shorts start as a small current and are identified by reduced voltage in the field and reduced spark rates. As the current flow increases, it heats the surface of the insulator and can cause it to shatter. The development of a short circuit across the insulator surface can also cause the field to automatically shut down. The high voltage frame support insulator must be kept clean at all times to prevent these problems.

There are a variety of design approaches for minimizing the failure of high voltage frame support insulators. Most of these involve minimizing the quantities of moisture and solids that deposit on the inner and outer surfaces. Purge air blowers are used to provide a constant flow of hot air into the insulator penthouse or compartment. This hot air flows through holes in the insulator top cover, keeping the inner surface hot and reducing the particulate matter flowing upward into this area. In some units, unheated purge air is used with electrical resistance heaters around the high voltage frame support insulators to prevent moisture accumulation on the exterior surface. Purge air is usually supplied at a rate of 50 to 100 acfm per insulator. This purge air flow also helps prevent untreated gas from evading the electrically energized zone by passing through the upper regions of the precipitator.

Movement of the wire-type discharge electrodes is minimized by hanging bottle weights on each wire, as shown in Figure 9-16. These provide 25 to 30 pounds of tension on the wire so that it does not move excessively. In other precipitator designs, the discharge electrodes are mounted in rigid frames or are constructed as rigid masts. In these designs, there are usually several anti-sway insulators at the bottom of each high voltage frame to prevent a pendulum action that would reduce clearances between the high voltage electrodes and the grounded plates.

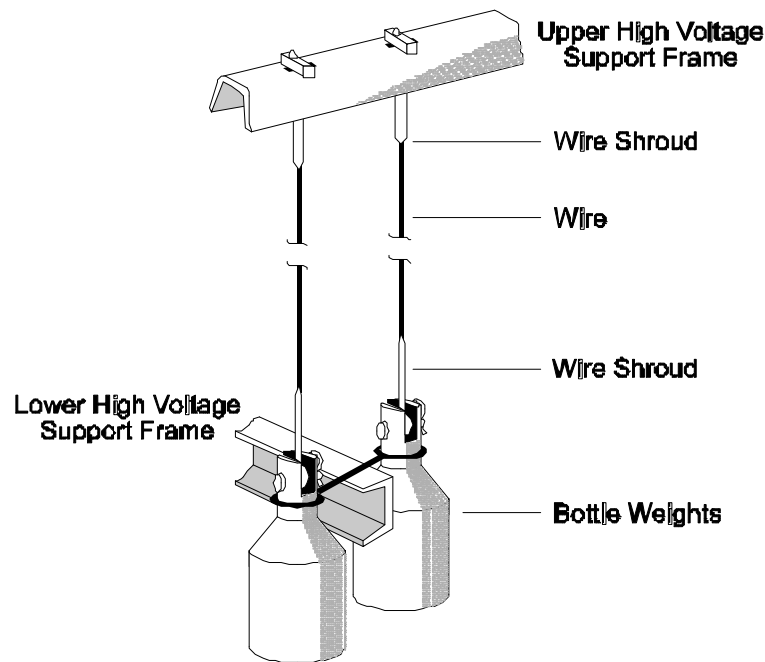


Figure 9-16. Wire-type discharge electrodes

The anti-sway insulators must inherently be located in the hopper area where it is difficult to provide supplemental heat or hot purge air. Accordingly, these insulators are vulnerable to electrical leakage and failure. For example, the anti-sway insulator shown in Figure 9-17 has electrical short-circuiting lines (leakage current) across the surface, which disabled the precipitator field. Short-circuits are normally minimized by using relatively long anti-sway

insulators. In some designs, the anti-sway insulators have been eliminated by designing more rigid discharge electrode frame supports.

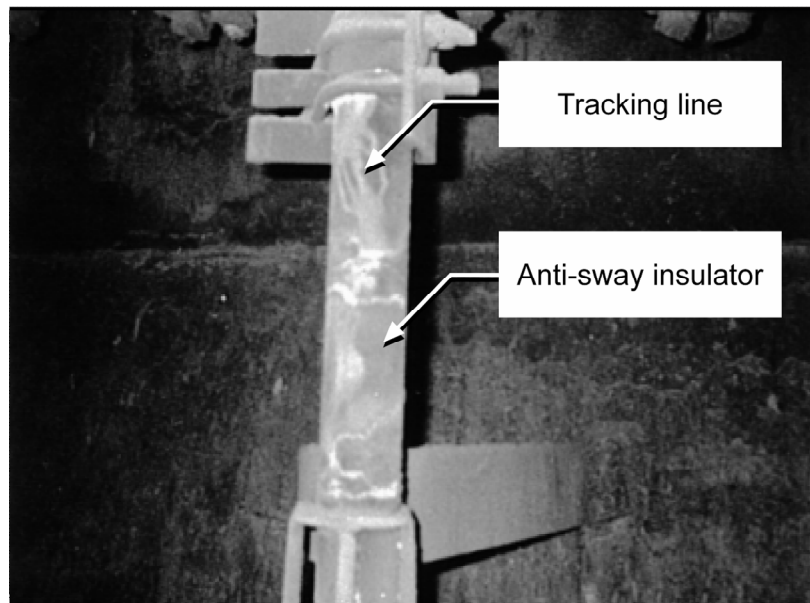


Figure 9-17. Anti-sway insulator with short-circuiting across the surface

The collection of particulate matter is not complete once the particles are removed from the gas stream and accumulate on the collection plates. The solid material must be dislodged from the plates and fall by gravity into the hopper. This important second step often significantly influences the particulate emission rates from the precipitator.

Rapping intensities and frequencies must be adjusted for the approximate resistivity range that exists in the precipitator. If the resistivity is too low, the dust is weakly held and can be easily redispersed into the gas stream by excessive intensity or frequency of rapping. This is often indicated by routinely occurring puffs from the stack. If the resistivity is high, relatively high intensity and frequent rapping is needed. However, the mechanical limits of the rappers, rapper rods, and collection plates must be considered in maintaining this type of rapping practice.

The rapping frequency is not constant throughout the precipitator. The inlet fields should be rapped much more frequently, since they collect large quantities of particulate matter, than the middle and outlet fields. If the rapping is too frequent in the outlet fields, the accumulated dust layer between rapping cycles will be very thin. During rapping, these thin dust layers can be easily redispersed since they are not very cohesive.

Separate groups of rappers are used to clean the collection plates, discharge electrodes, and gas distribution plates. There are two basic types of rappers: (1) roof-mounted rappers and (2) side-mounted rappers. Roof-mounted rapper designs incorporate a large number of individual rappers, each connected to a single high voltage discharge electrode support frame

or a section of collection plates. For collection plate rappers, the energy of roof-mounted rappers (Figure 9-18), commonly referred to as MIGIs (magnetic impulse, gravity impact), is transmitted down a metallic rod. For discharge electrodes, the energy must be transmitted through an insulator rod to prevent carrying high voltage to the rapper and the accessible areas on the roof of the precipitator.



Figure 9-18. Roof-mounted rapper

A side-mounted rapper system is shown in Figure 9-19. Motors are mounted on the exterior of the precipitator and turn shafts that run across the precipitator. A set of hammers is mounted on these rotating shafts in order to rap each individual collection plate and discharge electrode frame.

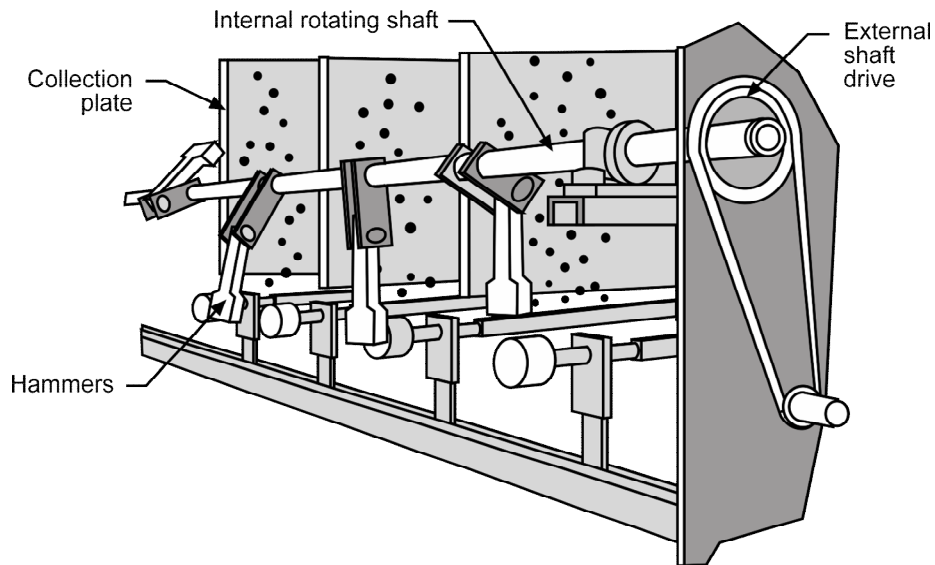


Figure 9-19. Side-mounted rapper

For both types of rapper designs, the frequency and intensity of rapping must be carefully controlled in order to achieve proper precipitator removal efficiency. The frequency of rapping must take into account that approximately 50-80% of the particulate is removed in each separate field. Accordingly, the inlet fields remove much greater quantities of dust than the outlet fields. For example, assume that the field-by-field efficiencies in a four-field unit are 80%, 70%, 60%, and 50%, respectively, from inlet to outlet. If the inlet particulate loading is 10,000 lb/hr, the quantities of dust removed in each field would be the following:

- Inlet 8,000 lb/hr (80% of inlet quantity)
- Second 1,400 lb/hr (70% of inlet field effluent)
- Third 360 lb/hr (60% of second field effluent)
- Outlet 120 lb/hr (50% of third field effluent)

This simplistic example illustrates the need to rap the inlet field collection plates and discharge electrodes much more frequently than the middle and outlet fields.

The hoppers have very steep slopes to facilitate solids movement into the solids discharge valves leading out of the hoppers. A center division plate is used in each hopper to prevent untreated gas from evading the electrically energized zone by passing through the upper regions of the hopper. This is termed the *anti-sneakage baffle*. The components of a typical hopper are illustrated in Figure 9-20.

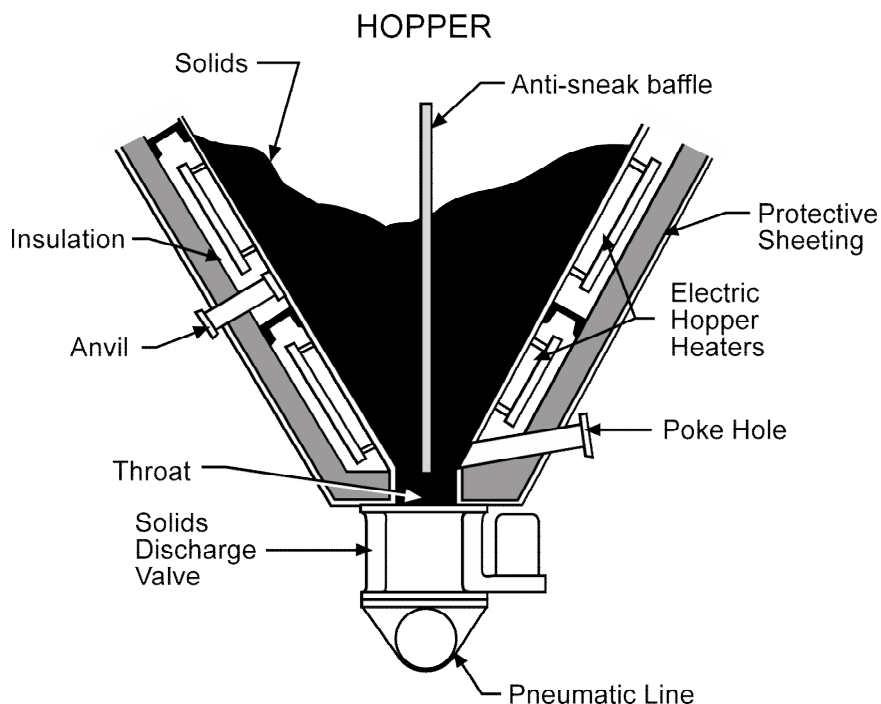


Figure 9-20. Components of a precipitator hopper

Wet, Negative Corona Precipitators

A wet, negative corona precipitator is useful for industrial applications where mists or fogs must be controlled or when solid particulate matter in the gas stream has undesirable electrical or physical properties. Undesirable physical properties include moderate stickiness or a high carbonaceous composition. A washing system, rather than rappers, is used for dust removal. These units, termed either *wet* or *wetted wall*, use power supplies that generate high negative voltages on the small discharge electrodes. The power supplies are essentially identical to those used on dry, negative corona precipitators.

Wet, negative corona ESPs are usually preceded by a quench chamber to ensure that the gas stream is saturated prior to entering the unit. This quench chamber can either be a separate stand-alone vessel as shown in Figure 9-21 or an initial compartment within the wet ESP itself. Due to the presaturation sprays, the operating gas temperatures are usually 130°F - 170°F. This substantially reduces the vulnerability of the system to drying of the collection surfaces. Some systems use a liquid recirculation system and liquid additives to maintain the proper pH in the collection plate sprays. Liquid additives can also help minimize the viscosity of the materials draining from the collection plates and can help minimize foaming in some industrial applications.

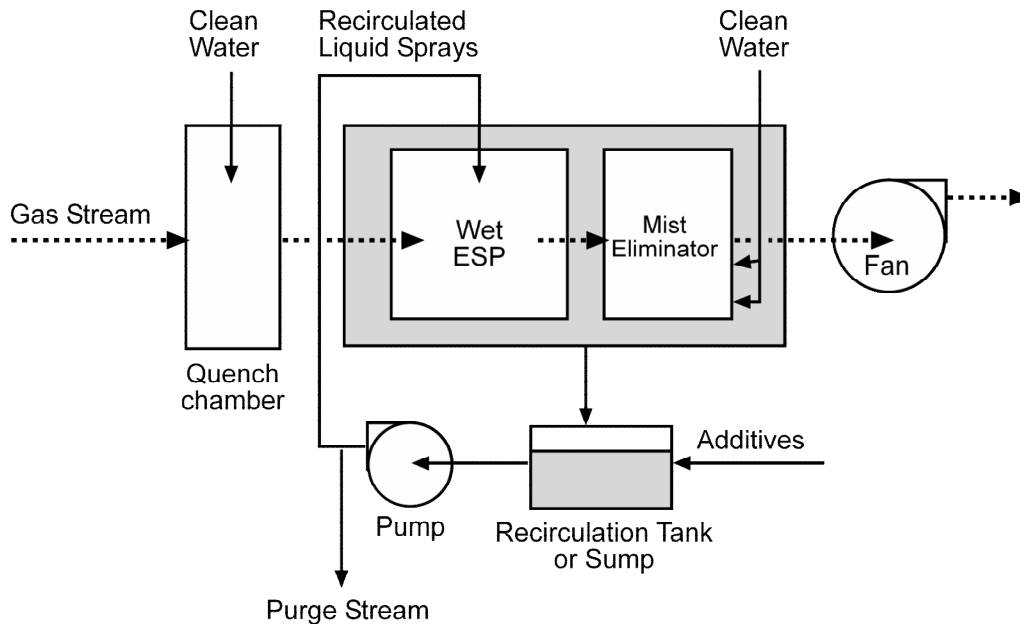


Figure 9-21. Flowchart of a wet, negative corona precipitator

Recirculation liquid must be purged to maintain the solids levels. The rate of liquid purge depends primarily on the rate of collection of solids. Usually, the rate of purge is quite small because the overall recirculation rate of liquid is quite small. A normal liquid-to-gas ratio for a wet, negative corona precipitator is less than 2 gallons per thousand acf.

The gas passages in wet precipitators can be concentric circles, tubes, or parallel rows. Alignment of the negatively charged discharge electrodes and the electrically grounded collection plates is very important to ensure that the field can operate at the necessary voltage. The alignment tolerances are similar to those for dry precipitators.

There are two main design styles for wet, negative corona electrostatic precipitators: (1) vertical flow and (2) horizontal flow. A conventional vertical flow design is illustrated in Figure 9-22. The gas stream enters the presaturator chamber at the top of the unit. The saturated particulate-laden gas stream is distributed to a set of vertical tubes extending to the bottom of the unit. High voltage discharge electrodes are mounted in the center of each tube to generate the negative corona that electrically charges the particles moving down each tube. The charged particles migrate to the wet inner surface of the tube and are collected. Liquid moving down the tube surfaces carries the collected material to the wet ESP sump. Sprays above the tubes are activated on a routine frequency to further clean the tube surface and thereby maintain the required electrical clearances between the high voltage electrode and the electrically grounded tube surface.

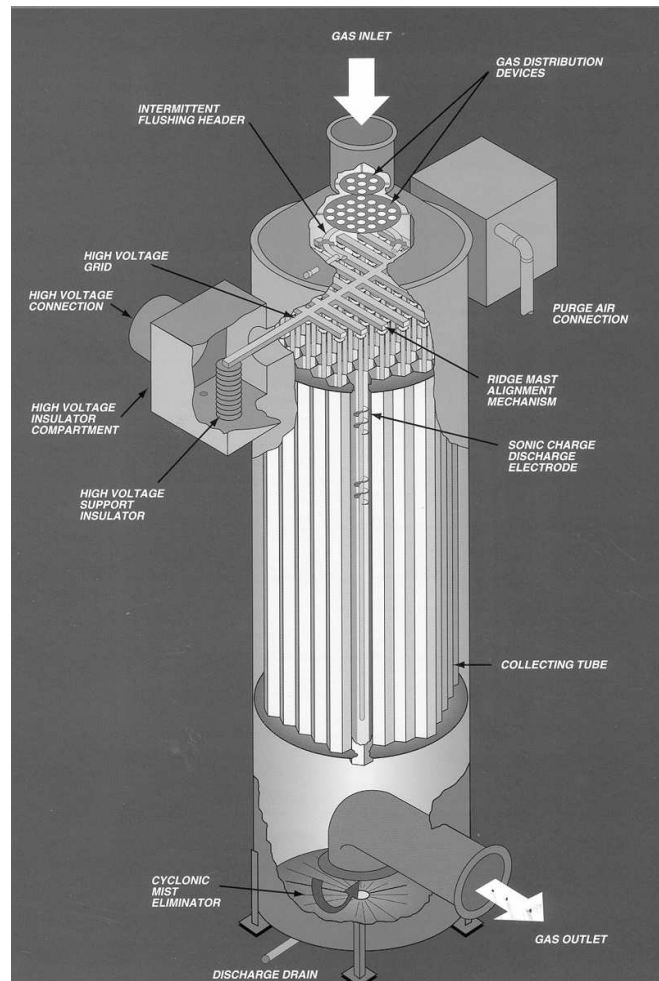


Figure 9-22. Vertical flow wet, negative corona precipitator

Vertical flow wet ESPs have three or more support insulators to suspend the high voltage frame energizing each of the tube discharge wires. These insulators are similar to those used in dry, negative corona units. It is especially important to provide heat and purge air to these insulators due to the relatively cold gas temperatures and the presence of liquid sprays near the tops of the gas passage tubes.

Vertical flow wet, negative corona precipitators use electrical sectionalization differently than dry, negative corona systems. The wet ESPs often have two fields arranged in parallel and only one field in the direction of gas flow. This approach is due, in part, to the difficulty of protecting the high voltage frame support insulators in vertically stacked fields from descending liquid from an upper field.

A horizontal flow wet, negative corona precipitator is shown in Figure 9-23. This unit uses alternating high voltage plates and electrically grounded collection plates to form gas passages. The high voltage plates have discharge electrode points extending from the leading edge of each plate which are energized by a conventional T-R set. The negative corona generated around these discharge points electrically charges particles passing through the unit. The particulate matter is collected on electrically grounded collection plates and drains into the ESP sump. Cleaning of the collection plates is performed by a set of overhead sprays and by a set of sprays on a traversing header on the inlet side of each field (Figure 9-24).

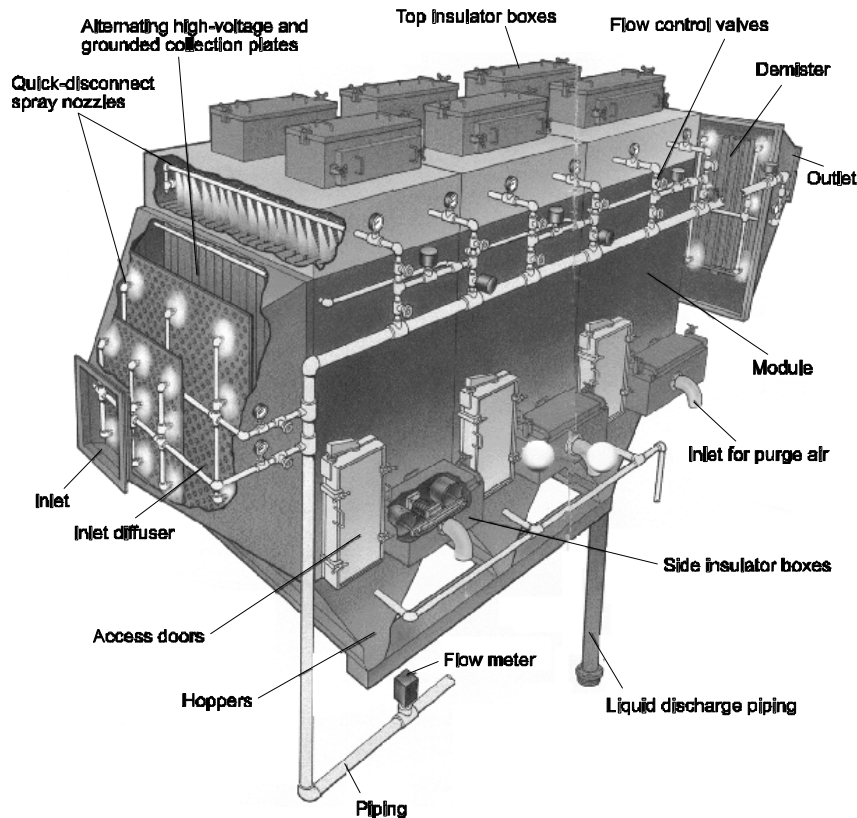


Figure 9-23. Horizontal flow wet, negative corona precipitator

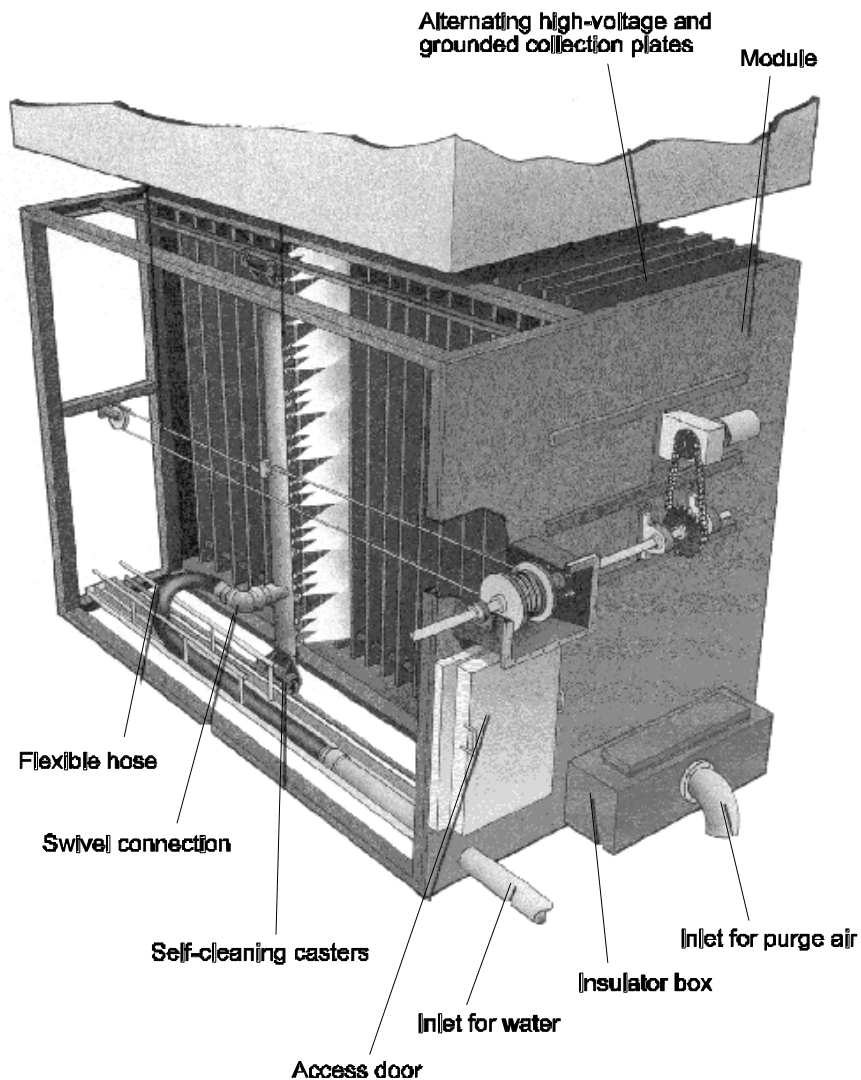


Figure 9-24. View of traversing header sprays

Horizontal flow wet ESPs usually have two or more fields in series. The sectionalization of the fields is similar to the design approach used in dry, negative corona units. The high voltage collection plate support insulators are mounted in insulator boxes on the roof of the unit. As with all wet ESPs, the insulators are heated to minimize the vulnerability to electrical tracking across wet insulator surfaces. Both vertical and horizontal gas flow wet ESPs often use perforated plates to distribute the gas flow entering the units. Sprays are used to occasionally clean these plates.

A set of mist eliminators is often used immediately after a wet, negative corona ESPs. The mist eliminators remove the entrained spray droplets and other solids-containing droplets that would otherwise be emitted to the atmosphere. Mist eliminators have clean water sprays to occasionally clean the droplet-contacting surfaces. Common types of mist eliminators used in wet ESPs include chevrons, tube banks, and baffle plates.

Wet, Positive Corona Precipitators

Wet, positive corona precipitators are used for the collection of organic droplets and mists from relatively small industrial applications such as textile mill tenter frames. As shown in Figure 9-25, the discharge electrodes are separated from the electrically grounded collection plates. The positive voltages applied to the discharge electrodes are in the range of 12 to 15 kilovolts, considerably lower than the negative voltages used in the dry, negative corona or wet, negative corona designs. Electrical charges are applied to particles as they pass through the preionizer section. These particles are then collected on the downstream collection plates. Since wet, positive corona precipitators only collect liquid particles that drain from the plates, they do not require rappers or liquid distributors. The collection plates are designed to allow for easy removal and manual cleaning. The plates are often cleaned on a weekly or monthly basis, depending on the stickiness and viscosity of the collected material.

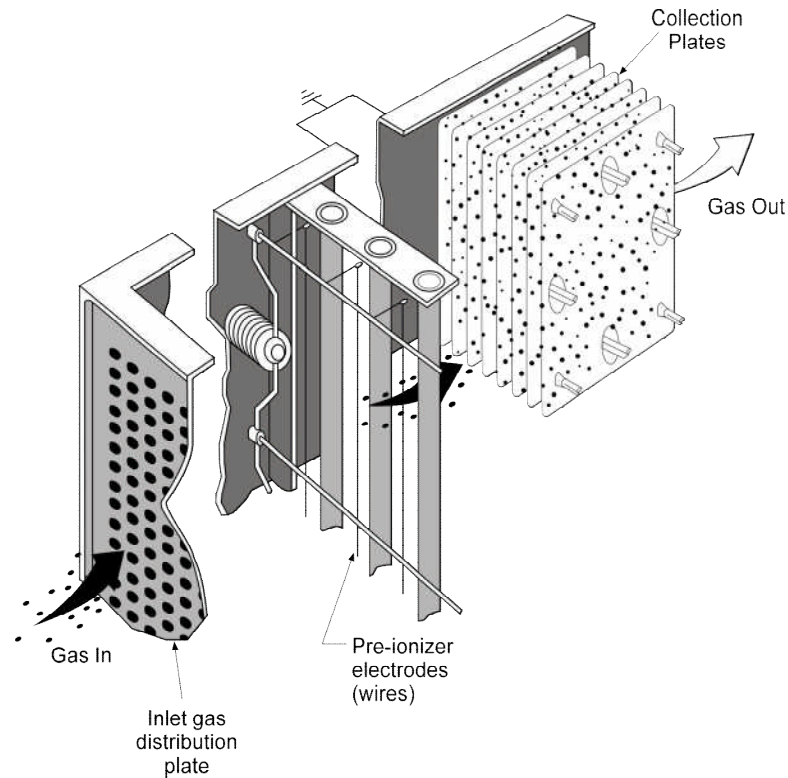


Figure 9-25. Wet, positive corona precipitator

Performance Evaluation

The size of an electrostatic precipitator is important since there is a general relationship between the size of the unit and the attainable particulate matter removal efficiency. The time for particle charging and migration (Step 1 in electrostatic precipitation) is greater in large units. This is important because the migration velocities of particles with diameters less

than 10 μm are relatively low. Large electrostatic precipitators also provide longer gravity settling times for solids rapped from the collection plates and discharge wires (Step 2 in electrostatic precipitation). However, there are practical limits to precipitator size. Units that are too large are extremely expensive. Other problems associated with oversized units include corrosion caused by excessive convective and conductive gas cooling, corrosion caused by multiple air infiltration sites, and gas maldistribution caused by very low gas velocities at the precipitator inlet. Purchasers and designers of electrostatic precipitators must determine the optimum size that balances the requirements for high efficiency with the need for reasonable cost and reliability.

Relationships and techniques for estimating the collection efficiency of electrostatic precipitators will be presented in this section. In addition, several factors affecting precipitator performance will be discussed. These include:

- Specific collection area
- Sectionalization
- Aspect ratio
- Gas superficial velocity
- Collector plate spacing
- Discharge electrodes
- Rapping systems
- Hopper design
- Flue gas conditioning systems
- Instrumentation

A well designed, properly operated, and well maintained electrostatic precipitator system should achieve overall collection efficiencies in excess of 99 percent.

Collection Efficiency

Perhaps the earliest relationship for predicting the collection efficiency of electrostatic precipitators is the Deutsch-Anderson equation (Equation 9-3). It was first developed empirically by Deutsch and then later derived from basic principles by Anderson. It is a relatively simple and straight-forward relationship and, of course, it doesn't work very well. However, it does serve as the basis for more refined models.

$$\eta = 1 - e^{-\frac{\omega A}{Q}} \quad (9-3)$$

where:

- η = efficiency (decimal form)
- ω = migration velocity (ft/sec)
- A = total collection plate area (ft^2)
- Q = total gas flow rate (ft^3/sec)
- e = base of natural logarithm = 2.718

This equation is based on probability theory and generally applies to particles less than approximately 10 μm in diameter. Particles less than this size have migration velocities of 0.3 to 0.8 ft/sec, which is well below the gas velocities through the passages of 3 to 6 ft/sec. Due to the turbulent nature of the gas flow through the passages, the motion of these particles is dependent primarily on the turbulent mixing of the eddy currents. However, particles close to the collection plate will be captured due to electrostatic forces.

The Matts-Ohnfield equation is a refinement of the Deutsch-Anderson equation. As shown in Equation 9-4, an additional exponent is used to provide a more conservative estimate of removal efficiency. Typical values of k range from 0.4 to 0.6.

$$\eta = 1 - e^{-\left[\omega\left(\frac{A}{Q}\right)^k\right]} \quad (9-4)$$

where:

k = dimensionless constant

The migration velocity depends on the electrical field strength, the electrical charge on the particle, and other factors described earlier in Equation 9-2. Accordingly, Equation 9-3 and Equation 9-4 are applicable only for particles of a single size. The migration velocity calculated for a submicrometer particle is well below the migration velocity of larger particles, because to the limited number of electrical charges on the small particles.

Migration velocity is also influenced by the dust resistivity. The migration velocities for particles that create low dust layer resistivities are high since these conditions increase the electrical field strength near the collection plate.

Due to variations in particle size distributions and in dust layer resistivities, it is difficult to use the Deutsch-Anderson type equations directly to determine the necessary precipitator size. Furthermore, this approach does not take into account particulate emissions due to rapping reentrainment, gas sneackage around the fields, and other non-ideal operating conditions.

To take these conditions into account, the migration velocity is often used as an empirical factor. Particulate removal data from a variety of similar units installed previously are reviewed to determine the effective migration velocity. This empirically derived migration velocity is then used to calculate the necessary collection plate area of a new installation. The variability of these values is illustrated in Table 9-1.

Table 9-1. Effective Migration Velocities for Various Industries		
Application	Effective Migration Velocity	
	ft/sec	cm/sec
Utility Coal-Fired Boiler	0.13 - 0.67	4.0 - 20.4
Pulp and Paper Mill	0.21 - 0.31	6.4 - 9.5
Sulfuric Acid Mist	0.19 - 0.25	5.8 - 7.6
Cement (Wet Process)	0.33 - 0.37	10.1 - 11.3
Cement (Dry Process)	0.19 - 0.23	5.8 - 7.0
Gypsum	0.52 - 0.64	15.8 - 19.5
Open-Hearth Furnace	0.16 - 0.19	4.9 - 5.8
Blast Furnace	0.20 - 0.46	6.1 - 14.0

In order to use the Deutsch-Anderson type equations, the collection plate area and average gas velocities must be calculated from the precipitator specifications. The average gas velocity is simply the total gas flow rate in actual cubic feet per minute divided by the area of the precipitator inlet. This calculation is shown in Equation 9-5.

$$V = \frac{\text{actual gas flow rate}}{\text{cross-sectional area}} = \frac{Q \text{ ft}^3 / \text{min} \left(\frac{\text{min}}{60 \text{ sec}} \right)}{HW} = \frac{Q \text{ ft}^3 / \text{min} \left(\frac{\text{min}}{60 \text{ sec}} \right)}{H \left(\frac{S}{12} \times n \right)} \quad (9-5)$$

where:

- V = gas velocity (ft/sec)
- Q = gas flow rate (ft³/min) (actual)
- H = collection plate height (ft)
- S = passage width, inches (normally 9, 10, 12 or 16 in.)
- n = number of passages
- W = precipitator width (ft)

In calculating the plate area, start by counting the number of gas passages in each field as shown in Figure 9-26. If there are n collection plates across the unit, there will be n-1 passages, since gas does not flow next to the exterior walls of the precipitator.

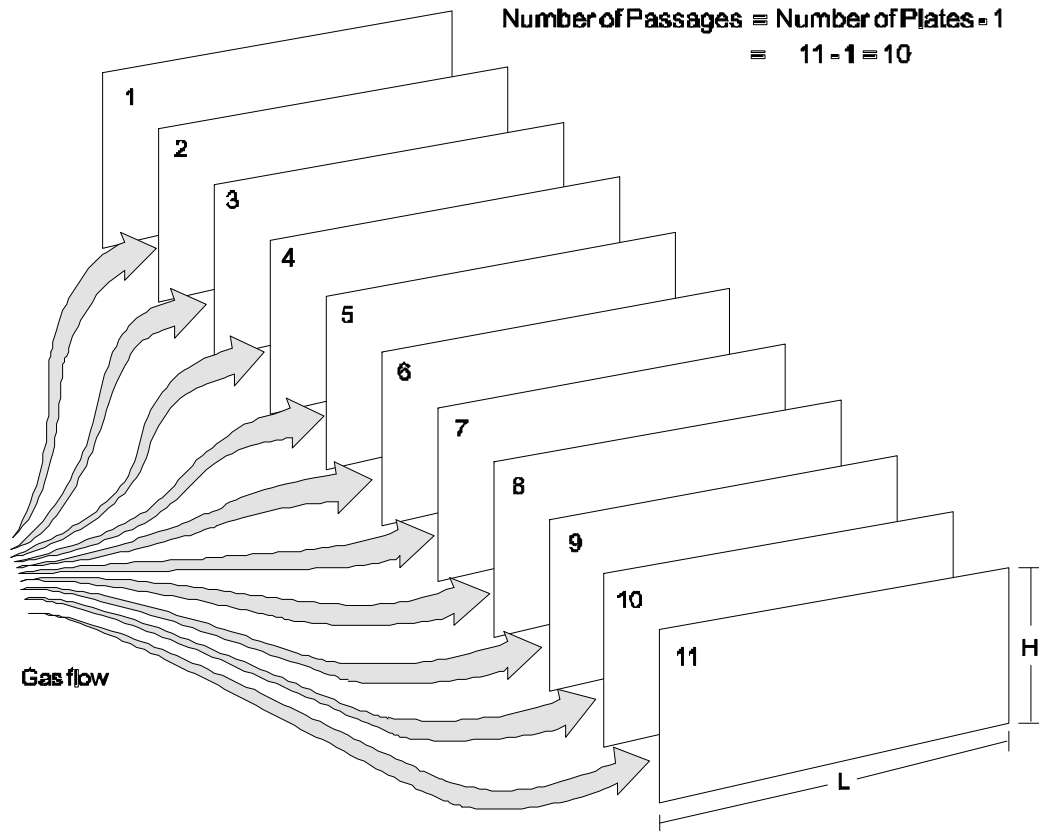


Figure 9-26. Collection plate area calculation

The collection plate area is calculated based on the dimensions of the plate. Since dust collects on both sides of the collection plates in the passages, the collection plate area is calculated using Equation 9-6.

$$A_i = 2 (n-1) (H) (L) \quad (9-6)$$

Where:

- A_i = collection plate area in field i (ft^2)
- n = number of collection plates across unit
- H = height of collection plates (ft)
- L = length of collection plate in direction of gas flow (ft)

The collection plate area for the unit chamber of the precipitator is calculated simply by summing the areas of each of the fields.

Example 9-1

Calculate the expected particulate efficiency for an electrostatic precipitator serving a utility coal-fired boiler. The gas flow rate is 250,000 ACFM. The total collection plate area is 100,000 ft^2 . Use an effective migration velocity of 0.20 ft/sec.

Substituting into the Deutsch-Anderson equation:

$$\eta = 1 - e^{-\omega \frac{A}{Q}} = 1 - e^{-\left[\left(0.20 \frac{\text{ft}}{\text{sec}} \right) \left(\frac{100,000 \text{ft}^2}{250,000 \frac{\text{ft}^3}{\text{min}} \times \frac{\text{min}}{60 \text{sec}}} \right) \right]} = 0.99177$$

This indicates that the overall efficiency of the precipitator would be 99.18%, if the effective migration velocity were 0.20 feet per second. The estimated efficiencies for assumed effective migration velocities of 0.25 and 0.30 ft/sec would be 99.75% and 99.93% respectively. This illustrates the importance of the assumed effective migration velocity.

In the past, this precipitator sizing approach was sufficient to obtain an initial estimate of the required collection plate area, as long as the equipment manufacturer had an extensive data base to select an appropriate effective migration velocity. These plate area data were then refined and adjusted in designing the unit. A variety of other design factors such as average gas flow rate, number of fields in series, number of chambers, and aspect ratio were considered in determining the specifications of the precipitator.

Sizing calculations based only on Deutsch-Anderson type equations have significant limitations in present-day applications, due primarily to the very stringent particulate control requirements. There can be substantial variations in all of the non-ideal modes of particulate emissions that are lumped together in the effective migration velocity term. Also, there can be significant differences in the energization of the precipitator fields. These site-specific energization and non-ideal emission mode variations can be large enough to cause a new unit to fail to meet the required performance specifications.

A computerized performance model, the EPA/RTI or Lawless model, has been developed. It provides a more fundamentally correct representation of the precipitation process than the Deutsch-Anderson type equations. The EPA/RTI model is based on the localized electrical field strengths and current densities prevailing throughout the precipitator. These data can be input based on actual readings from operating units, or it can be calculated based on electrode spacing and resistivity. These data are used to estimate the combined electrical charging on each particle size range due to field dependent charging and diffusional charging. Particle size dependent migration velocities are then used in a Deutsch-Anderson type equation to estimate particle collection in each field of the precipitator. This model takes into account a number of site-specific factors, including gas flow maldistribution, particle size distribution, and rapping reentrainment.

The use of these performance models requires detailed information concerning the anticipated configuration of the precipitator and the characteristics of the gas stream. Information needed to operate the model is provided in Table 9-2. It is readily apparent that not all these parameters are needed in each case since some can be calculated from several of the others.

Table 9-2. Data Used in EPA/RTI Computerized Performance Model for Electrostatic Precipitators

<p>ESP Design</p> <ul style="list-style-type: none"> • Specific collection area • Collection plate area • Collection height and length • Gas velocity • Number of fields in series • Number of discharge electrodes • Type of discharge electrodes • Discharge electrode-to-collection plate spacing
<p>Particulate Matter and Gas Stream Data</p> <ul style="list-style-type: none"> • Resistivity • Particle size mass median diameter • Particle size distribution standard deviation • Gas flow rate distribution standard deviation • Actual gas flow rate • Gas stream temperature • Gas stream pressure • Gas stream composition

The EPA/RTI model is available through the U.S. EPA Technical Transfer Network (TTN) at <http://www.epa.gov/ttnecat1/products.html>. Copies of the instruction manual can also be downloaded. This model should be useful for both permit review and precipitator problem evaluation.

Specific Collection Area

The specific collection area (SCA) is defined as the ratio of the collection surface area to the actual gas flow rate passing through the unit. As shown in Equation 9-7, it is usually expressed in terms of square feet per 1,000 acfm of gas flow.

$$SCA = \frac{A}{Q} \quad (9-7)$$

where:

- SCA = specific collection area (ft²/10³ acfm)
 A = total collection plate area (ft²)
 Q = total gas flow rate (10³ acfm)

There has been a substantial increase in SCAs from levels of 100 to 200 ft² per 1,000 acfm in the 1960s to present-day levels of 300 to 1400 ft² per 1,000 acfm. There is no single value of SCA that guarantees adequate performance for all precipitators. Instead, the SCA must be based on unit-specific factors such as the dust layer resistivities and the particle size distribution. Sources that generate particulate matter with high resistivities or small particle sizes generally use a high SCA.

Sectionalization

The performance of an electrostatic precipitator is not solely a function of the quantity of collection plate surface area. It is also dependent on how that surface area is used. There are a variety of design factors that must be taken into account to ensure proper particulate matter removal capability. Proper sectionalization is one of the most important of these design factors.

The electrostatic precipitator is divided into separately energized areas, termed *fields*, arranged in series along the direction of gas flow. Almost all commercial precipitators have at least three fields in series. Some large units used for high resistivity conditions can have as many as fourteen fields in series. The inlet field removes 60% to 75% of the incoming particulate matter, and each subsequent field removes 50% to 80% of the particulate matter penetrating through the preceding field.

Due to these differences in mass collection rates, there can be significantly more dust on the collection plates in the fields on the inlet side of the precipitator than on the outlet side. These thick dust layers suppress current flow. In addition, the electrical charges residing on the particles moving through the space between the discharge electrode and the collection plate produce what is termed a *space charge* that also suppresses current flow in the inlet fields. By dividing the precipitator into separate electrical fields, the effect of the heavy dust layers and the particle space charge can be minimized.

Electrical sparking occurs preferentially on the inlet side of the precipitator. This sparking is due primarily to the accumulation of electrical charge on the outer surface of the dust layer on the collection plate. Sparking near the inlet is also due to the disturbances caused when large quantities of dust are dislodged during each rapping cycle. Rapping in the inlet fields is more frequent than in the outlet fields. As noted earlier, the automatic voltage controller detects the electrical spark as a current surge and shuts off the applied secondary voltage for a few milliseconds. There is also a short period when the secondary voltage is ramping back to its maximum pre-spark levels. During these short time periods, the field strength is not at optimum levels for collection of particulate matter. By sectionalizing the precipitator into separate fields, the field energization problems associated with frequent sparking can be isolated to the first few fields with high spark rates.

On an infrequent basis, an internal mechanical problem in a field can cause an electrical short circuit. Several conditions can cause shorts:

- Mechanical flex failure of a discharge wire
- Chemical corrosion failure of a discharge wire
- Electrical sparking related erosion failure of a discharge wire
- Electrical tracking and failure across a support insulator surface or an anti-sway insulator surface
- Presence of solids bridging between the high voltage frame and the grounded collection plates due to hopper overflow

The field is automatically taken offline by the primary control cabinet to prevent component damage caused by the high current condition. The field can not be reenergized until maintenance personnel enter the unit to retrieve the failed wire, fix the insulators, or clear the hopper solids bridged material. Often the precipitator must operate for a long period of time before this maintenance work can be completed. If the precipitator has a high degree of sectionalization, the amount of the unit out-of-service is relatively small, and the emission rates do not increase substantially. If there are only a few fields in service, the impact of the loss of a field on performance can be quite high.

In addition to standard sectionalization, most electrostatic precipitators also divide individual fields into *bus sections*. A precipitator field has either one or two bus sections. This is the smallest section of the field that can be energized by the T-R set serving the field. The term bus section is derived from the fact that each of these sections has a separate electrical bus (electrical conduit line) from the T-R set. Precipitators often have two bus sections per field so that these two different areas can be separately energized using half-wave rectified power. The advantages and disadvantages of half wave versus full wave rectification are outside the scope of this course.

Example 9-2

One electrostatic precipitator serving a coal-fired boiler has a gas stream of 500,000 ACFM, an inlet particulate mass concentration of 2 grains per ACF, and an SCA of 300 ft²/1000 ACFM. What is the increase in the emission rate if one of the four fields trips offline due to an internal mechanical-electrical problem? Assume the inlet field has an efficiency of 80%, the two middle fields have an efficiency of 70%, and the outlet field has an efficiency of 60%.

A second electrostatic precipitator serving a similar coal-fired boiler also has a gas flow rate of 500,000 ACFM, an inlet particulate mass concentration of 2 grains per ACF, and an SCA of 300 ft²/1000 ACFM. However, this unit only has three fields in series. What is the increase in the emission rate when a field trips offline if the inlet field has an efficiency of 85%, the middle field has an efficiency of 81%, and the outlet field has an efficiency of 75%?

Solution:

For the first precipitator, the efficiency of four fields in series during routine operation can be estimated as follows.

$$\text{Emissions}_{\text{Routine}} = \frac{2 \text{ grains}}{\text{ACF}} \left(1 - \frac{\text{eff}_1}{100}\right) \left(1 - \frac{\text{eff}_2}{100}\right) \left(1 - \frac{\text{eff}_3}{100}\right) \left(1 - \frac{\text{eff}_4}{100}\right)$$

$$\text{Emissions}_{\text{Routine}} = \frac{2 \text{ grains}}{\text{ACF}} \left(1 - \frac{80}{100}\right) \left(1 - \frac{70}{100}\right) \left(1 - \frac{70}{100}\right) \left(1 - \frac{60}{100}\right)$$

$$\text{Emissions}_{\text{Routine}} = \frac{2 \text{ grains}}{\text{ACF}} (0.20)(0.30)(0.30)(0.40) = 0.014 \text{ grains / ACF}$$

When one of the four fields is out of service, the performance of the precipitator can be calculated as follows:

$$\text{Emissions}_{\text{Upset}} = \frac{2 \text{ grains}}{\text{ACF}} \left(1 - \frac{\text{eff}_1}{100}\right) \left(1 - \frac{\text{eff}_2}{100}\right) \left(1 - \frac{\text{eff}_3}{100}\right) \left(1 - \frac{\text{eff}_4}{100}\right)$$

$$\text{Emissions}_{\text{Upset}} = \frac{2 \text{ grains}}{\text{ACF}} \left(1 - \frac{80}{100}\right) \left(1 - \frac{70}{100}\right) \left(1 - \frac{70}{100}\right) \left(1 - \frac{0}{100}\right)$$

$$\text{Emissions}_{\text{Upset}} = \frac{2 \text{ grains}}{\text{ACF}} (0.20)(0.30)(0.30)(1.0) = 0.036 \text{ grains / ACF}$$

In this case, the emissions increased from 0.014 to 0.036 grains/ACF.

In this general calculation approach, it is assumed that the outlet field, the one with the lowest efficiency, is not available. This is an appropriate calculation approach regardless of which of the four is tripped offline. The roles of the four fields in series will shift as soon as one is lost. For example, the second field becomes the first field if the inlet field trips offline. If one of the middle fields is lost, the gas stream entering the outlet field has high mass loadings and larger sized particulate than during routine operation. Accordingly, the outlet field operates at the efficiency of a middle field.

For the second precipitator, the efficiency during routine operation and during upset conditions after the loss of one of the fields is estimated as follows:

$$\text{Emissions}_{\text{Routine}} = \frac{2 \text{ grains}}{\text{ACF}} \left(1 - \frac{85}{100}\right) \left(1 - \frac{81}{100}\right) \left(1 - \frac{75}{100}\right)$$

$$\text{Emissions}_{\text{Routine}} = \frac{2 \text{ grains}}{\text{ACF}} (0.15)(0.19)(0.25) = 0.014 \text{ grains / ACF}$$

$$\text{Emissions}_{\text{Upset}} = \frac{2 \text{ grains}}{\text{ACF}} \left(1 - \frac{85}{100}\right) \left(1 - \frac{81}{100}\right) \left(1 - \frac{0}{100}\right)$$

$$\text{Emissions}_{\text{Upset}} = \frac{2 \text{ grains}}{\text{ACF}} (0.15)(0.19)(1.0) = 0.057 \text{ grains / ACF}$$

The second precipitator has an emission increase from 0.014 to 0.057 grains/ACF. This is a substantially higher increase than the first precipitator.

It is apparent from the relatively simple calculation that the emission increases resulting from the loss of a field are more severe for units with limited sectionalization, such as the second unit in Example 9-2.

Aspect Ratio

Precipitators with the proper aspect ratios are less sensitive to gravity settling problems. The aspect ratio is defined as the total length of the collection plates (all fields added together) divided by the collection plate height:

$$\text{AR} = \frac{\sum_{i=1}^n L_i}{H} \quad (9-8)$$

where:

- AR = aspect ratio (dimensionless)
- L_i = length of plates in field i (ft)
- H = collection plate height (ft)
- n = number of fields in series

The aspect ratio is important because it directly affects the ability of the precipitator to capture solids rapped from the collection plates and falling toward the hoppers. If the aspect ratio is too low, the small particles or small agglomerates of particles are swept out of the precipitator before they can reach the hopper. This increases rapping reentrainment emissions.

Modern precipitators are designed with aspect ratios of at least 1.0, and the normal range extends to more than 1.5. This means that they are longer than they are high. This provides more time for gravity settling to carry the particulate agglomerates to the hoppers. The average gas velocities in new designs are also slightly lower than pre-1970 units in order to provide more time for settling and reduce rapping reentrainment losses.

Example 9-3

An electrostatic precipitator serving a cement kiln has four fields in series. All of the fields have collection plates that are 24 feet high. The first two fields have collection plate lengths of 9 feet each. The last two fields have collection plate lengths of 6 feet. What is the aspect ratio?

Solution:

$$AR = \frac{\sum_{i=1}^n L_i}{H} = \frac{9+9+6+6}{24} = 1.25$$

Gas Superficial Velocity

High gas velocities adversely affect the performance of precipitators, reducing the time available for particle charging and migration. High velocities through the gas passages can also scour particles from the outer surfaces of the dust layers and, thereby, add to reentrainment emissions. Furthermore, high gas velocities reduce the time available for rapped solids to settle by gravity into the hoppers. The average gas velocities in modern precipitators are generally between 3 and 6 ft/sec.

Variations in the gas velocity should be minimized. Localized high velocity zones in the precipitator could significantly increase particulate emissions. The variations should be limited to $\pm 20\%$ of the average gas velocity. In the past, equipment manufacturers have used 1/32 and 1/16 scale models in order to optimize gas velocities. During the last 10 years, air flow computational fluid dynamic models (often termed CFD models) have also been successfully applied to correct gas flow maldistribution problems.

Collector Plate Spacing

A trend toward increased plate-to-plate spacings started in the 1980s because of the interest in rigid frame type discharge electrode supports. Due to the width of the support tube, the plate spacings were increased from a typical value of 9 in. to the 11 to 12 in. range. This practical consideration was not the only motivation for increased plate spacings. It has been recognized for more than 35 years that improved electrical field strengths could be obtained by increased discharge electrode-to-collection plate spacing. Due, in part, to stringent particulate matter control requirements, many new units will have plate-to-plate spacings in the range of 10 to 20 inches.

Summary of Sizing Parameters

A summary of the typical sizing parameters for electrostatic precipitators is provided in Table 9-3. Some caution is warranted in comparing an existing unit with the ranges shown in this

table. The necessary precipitator size and design characteristics vary substantially from site-to-site due to factors such as differences in particulate resistivity distributions, particle size distributions, and process operating rate variations.

Table 9-3. Typical Sizing Parameters Dry Negative Corona ESPs	
Sizing Parameter	Common Range
Specific Collection Area, (ft ² /1000 ACFM)	400 - 1000
Number of Fields in Series	3 - 14
Aspect Ratio	1 - 1.5
Gas Velocity, ft/sec	3 - 6
Plate-to-plate spacing, inches ¹	9 - 16

¹One manufacturer uses 6 in. spacing

Discharge Electrodes

Discharge electrode designs have evolved substantially since the early 1970s, when discharge wire failure was a common problem. The introduction of rigid discharge electrodes and electrode frames has substantially reduced this problem. The use of protective shrouds (shown in Figure 9-16) over the top and bottom 18 inches of the wire-type discharge electrodes has also reduced the frequency of failure. Because of these improvements, present-day failures are usually due to either corrosion or misalignment problems. The failure of discharge wires has become a symptom of other problems rather than a fundamental problem.

Rapping Systems

As noted previously, the rapping frequency is not constant throughout the precipitator. The calculated data shown in Example 9-4 present some assumed field-by-field performance values for a four-field unit. It is apparent that large quantities of particulate are captured in the inlet field, and frequent rapping is needed.

Example 9-4

Estimate the quantities of dust in each field of a four-field electrostatic precipitator having efficiencies of 80%, 75%, 70%, and 65% respectively. Assume a gas flow rate of 250,000 ACFM and a particulate matter loading of 2 grains per actual cubic foot.

Field	Assumed Efficiency	Particulate Entering (lb _m /hr)	Particulate Leaving, (lb _m /hr)	Particulate Collected (lb _m /hr)
1 (inlet)	80	4,286	857	3,429
2 (middle)	75	857	214	643
3 (middle)	70	214	64	150
4 (outlet)	65	64	22	42

Due to the general pattern of particulate removal in a precipitator, the rapping frequency for the inlet field collection plates is usually once every 5 to 15 minutes. This means that the entire set of rappers on this field is activated once during each cycle of 5 to 15 minute duration. The outlet fields collection plates have cycle times that occur as often as one cycle per hour to as infrequently as one cycle every 24 hours. The discharge electrode frame rappers and the gas distribution screen rappers are generally operated on a relatively high frequency, ranging from cycle times of 5 minutes to more than 2 hours.

Many industrial processes served by electrostatic precipitators have process operating rate-related gas flow changes, changes in particulate matter loadings, and changes in particle characteristics. New microprocessor rapping system controllers have several rapping frequency programs. These can be selected manually or automatically based on the process operating conditions. These systems are very effective at tailoring the rapping practices to the prevailing operating conditions. Many of the systems also provide useful diagnostic data concerning the operating status of each of the rappers.

Rapping collection plates generally results in some rapping reentrainment regardless of the resistivity conditions and gas flow rates. Accordingly, collection plate rappers in different portions of the precipitator should not be activated simultaneously. The transient wave of particulate matter can impair the electrical performance of downstream precipitator fields. Most new microprocessor-based rapper controllers include features to preclude simultaneous rapping.

Hopper Design

The removal of solids from the hopper is the important third step in the overall electrostatic precipitation process. Failure to remove solids from the hoppers in a timely manner can cause collection plate misalignment and discharge electrode frame misalignment. Short circuit paths between the high voltage electrodes and the electrically grounded collection plates can result in the formation of large fused clinkers, which usually have to be removed manually. Hopper overflow can also cause deposition on anti-sway insulators.

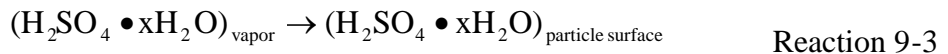
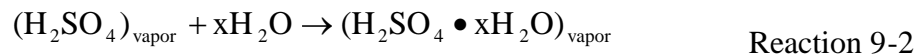
There are a variety of design features that can reduce vulnerability to hopper overflow. Hoppers should have steep sides to facilitate solids movement. They should have thermal insulation and an outer protective lagging to prevent heat loss. Hopper heaters are often

mounted in the bottom portions of the hopper to provide supplemental heat in the area where convective and conductive cooling is most rapid. Maintaining proper solids temperatures in the hoppers is important because the hot area partially surrounding the deposited solids facilitates solids flow into the small throat at the bottom. If the solids and trapped air cool, the solids flow less readily and may bridge over the throat. One of the most useful techniques for minimizing hopper overflow is to empty the hoppers continuously or as frequently as possible.

Flue Gas Conditioning Systems

Flue gas conditioning (FGC) systems are used exclusively to adjust the resistivity conditions in cold side electrostatic precipitators serving coal-fired boilers. These units operate at gas temperatures between 200°F and 400°F and are vulnerable to both low and high resistivity conditions under some boiler operating conditions. These resistivities can be adjusted back into the moderate range where precipitators work well by injecting either sulfur trioxide or sulfur trioxide and ammonia. Sulfur trioxide reacts to form sulfuric acid vapor and heterogeneously nucleates on the surfaces of particles to adjust the surface conductivity. Ammonia reacts with sulfur trioxide in the flue gas stream to form ammonium sulfate and ammonium bisulfate, which also nucleates on particle surfaces and adjusts the surface conductivity. Sulfur trioxide injection and ammonia injection have been used successfully since the 1970s.

A conventional sulfur trioxide system is shown in Figure 9-27. Elemental sulfur is melted and pumped to the oxidation chamber where sulfur dioxide is formed. The gas stream then enters a vanadium pentoxide catalyst bed where the sulfur dioxide is oxidized further to yield sulfur trioxide. This is transported at a temperature range of 600°F to 700°F to a set of injection nozzles placed upstream of the precipitator inlet. As the sulfur trioxide disperses into the gas stream, it cools and forms vapor phase sulfuric acid as indicated by Reaction 9-1. The sulfuric acid molecules are highly hygroscopic and attract water molecules as indicated in Reaction 9-2.



The sulfuric acid then adsorbs on the surfaces of the particles. The sulfur trioxide injection rates provide concentrations of 5 to 25 ppm of sulfuric acid in the gas stream passing through the precipitator. The large majority of the sulfuric acid formed due to a flue gas conditioning system is removed in the precipitator.

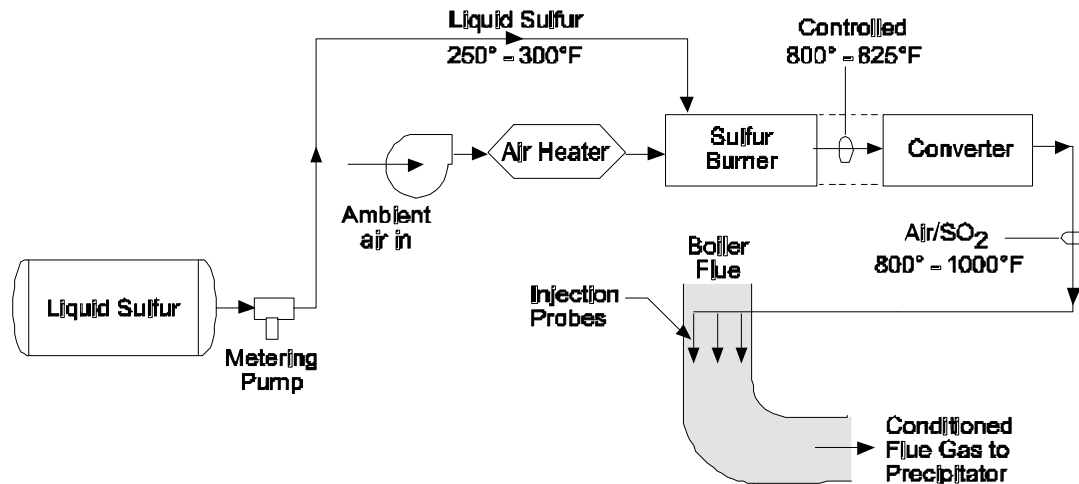


Figure 9-27. Sulfur trioxide conditioning system

Example 9-5

A coal-fired utility boiler generates 5 ppm of sulfuric acid. Diagnostic tests have indicated that 17 ppm of sulfuric acid are needed in the gas stream to maintain the flyash resistivity in the moderate range. Calculate the sulfur required to operate a sulfur trioxide conditioning system for a period of one year. Assume that the boiler has a gas flow rate of 1.0×10^6 ACFM, the gas temperature is 310°F , the boiler operates 82% of the year, and the sulfur trioxide system is needed 85% of the operating time.

Solution:

Sulfur Trioxide System Operating Hours:

$$\begin{aligned} \text{Operating hours} &= 8,760 \text{ total hours} \left(\frac{0.82 \text{ boiler hours}}{\text{total hours}} \right) \left(\frac{0.85 \text{ FGC hours}}{\text{boiler hours}} \right) \\ &= 6,106 \text{ FGC hours} \end{aligned}$$

Sulfur Trioxide Demand:

$$\text{SO}_3 \text{ needed} = 17 \text{ ppm} - 5 \text{ ppm} = 12 \text{ ppm} = 1.2 \times 10^{-5} \text{ lb moles SO}_3/\text{lb mole flue gas}$$

Sulfur Trioxide Injection Requirements:

$$\begin{aligned} \text{SO}_3 \text{ needed} &= \left(1 \times 10^6 \frac{\text{ft}^3}{\text{min}} \right) \left(\frac{528^\circ\text{R}}{770^\circ\text{R}} \right) \left(\frac{\text{lb-mole}}{385.4 \text{ std ft}^3} \right) \left(60 \frac{\text{min}}{\text{hr}} \right) \left(1.2 \times 10^{-5} \frac{\text{lb-mole SO}_3}{\text{lb-mole}} \right) \\ &= 1.28 \text{ lb-moles/hr} \end{aligned}$$

Sulfur Required:

Sulfur lb moles = SO₃ lb moles = 1.28 lb moles/hour

$$\begin{aligned} \text{Sulfur required} &= \left(1.28 \frac{\text{lb-moles}}{\text{hr}}\right) \left(6,106 \frac{\text{hrs}}{\text{year}}\right) \left(32 \frac{\text{lbs}}{\text{lb-mole}}\right) \left(\frac{\text{ton}}{2,000 \text{ lbs}}\right) \\ &= 125 \text{ tons/year} \end{aligned}$$

There are a number of sulfur trioxide conditioning systems in commercial service. The unit shown in Figure 9-28 stores the necessary sulfur in a pelletized form. The sulfur is fed to a melter and then oxidized to form sulfur trioxide. This approach avoids the possible problems and energy costs associated with storing sulfur in a molten form on a continuous basis.

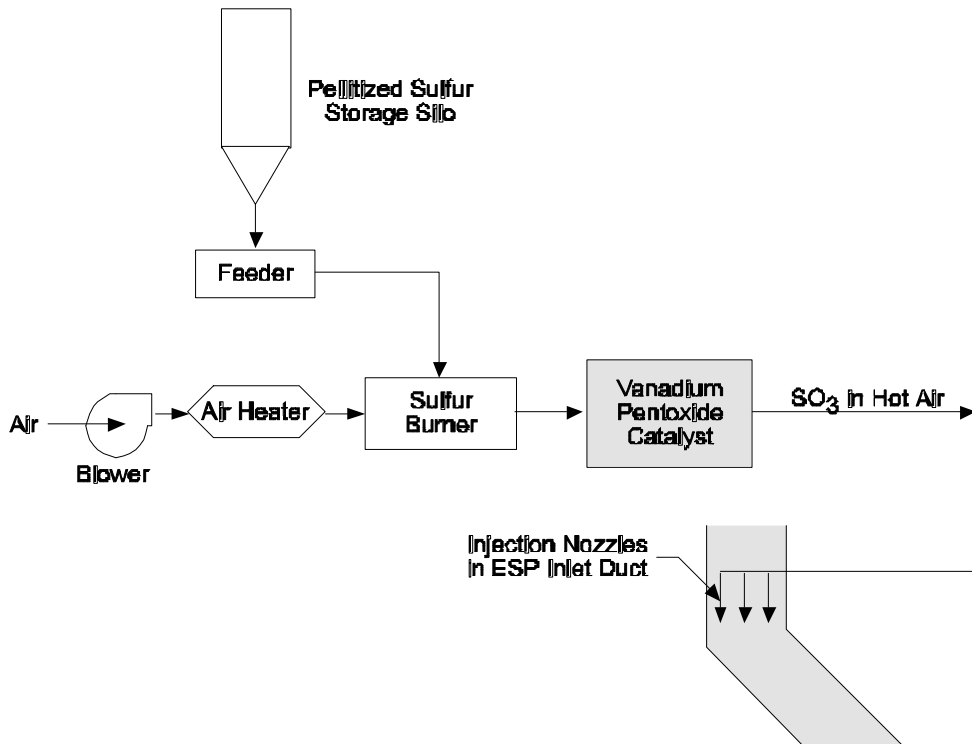


Figure 9-28. Pelletized-type sulfur trioxide conditioning system

Another commercial version of a sulfur trioxide conditioning system uses a set of small catalyst chambers rather than a single large unit for oxidizing sulfur dioxide to sulfur trioxide. The sulfur dioxide gas formed in the sulfur burner is then distributed to a set of pipes leading to the precipitator inlet. Catalyst modules are present on each of the injection lines.

Ammonia FGC systems are very similar to the ammonia feed systems used with Selective Catalytic Reduction (SCR) and Selective Non-Catalytic Reduction (SNCR) for nitrogen oxides control. The ammonia FGC systems can use either anhydrous ammonia or aqueous ammonia as a feedstock. The ammonia is fed from the storage tank at a rate necessary to achieve a preset concentration level, normally 10 to 20 ppm. The ammonia is diluted by a carrier gas, usually air, to a concentration well below its Lower Explosive Limit (LEL) of 15%. Ammonia feed concentrations are usually less than 3% by volume. The ammonia is then injected into the flue gas streams through a set of pipes mounted at the precipitator inlet. Due to the low ammonia concentrations, the large majority quickly reacts and nucleates on the surfaces of the flyash. Ammonia emissions from the precipitator are usually near negligible levels.

Ammonia conditioning systems can be used as stand-alone units for cold side electrostatic precipitators subject to low resistivity related particulate matter emission problems. In this type of application, the main impact of the ammonia and its gas phase reaction process appears to be improved particle agglomeration of the dust on the collection plate surfaces.

Instrumentation

New state-of-the art automatic voltage controllers include digital gauges for all of the following electrical parameters of interest in the precipitator field:

- Primary voltage, volts A.C.
- Primary current, amperes A.C.
- Secondary voltage, kilovolts D.C.
- Secondary current, milliamps D.C.
- Spark rate
- SCR Conduction angle, degrees
- Field limiting condition
- Power input, kilowatts

In a few new systems, these parameters are logged and processed in data acquisition systems to provide routine operating records for the unit. In most existing units, the electrical data is logged manually by plant operators.

Information concerning the rappers is usually provided by instrumentation mounted in the rapper control panel. New microprocessor-based control cabinets provide visual information concerning the rapper program in use at the present time, the specific rappers being activated, the presence of any probable rapper activation faults, and the rapping intensities.

Gas stream temperature and oxygen monitors are often used upstream and downstream of electrostatic precipitators to detect the onset of air infiltration problems. Air infiltration can increase gradually due to wear of mechanical parts in the solids discharge system, deterioration of fabric type expansion joints on ductwork, and corrosion of exterior metal parts. The rate of infiltration can increase rapidly because the corrosion caused by acid

deposition in cold areas increases gaps and holes where air is entering. One way to identify the presence of significant air infiltration is to install gas stream temperature monitors immediately upstream and downstream of the precipitator. A change in the temperature drop across the unit at a given load condition provides one relatively inexpensive and useful indicator. Increases from the baseline range of temperature drops would indicate the need to identify and repair the infiltration sites.

Oxygen concentration measurements at the inlet and outlet of the units can also be used to identify increased air infiltration. An increase of more than 0.5% in the oxygen composition of the gas stream is generally associated with significant air infiltration-related problems. For example, a unit with an inlet concentration of 4% oxygen and an outlet concentration of 5% oxygen requires further attention.

Hopper level detectors are often used to provide an early warning of high solids levels in precipitator hoppers. It is important that the detectors be mounted in the proper location. If they are mounted too low in the hoppers, they alarm unnecessarily and may be ignored by the operators. If they are mounted too high in the hoppers, there may be insufficient time for the operator to respond to the alarm and begin removing solids from the hoppers.

This page intentionally left blank.

Review Questions

1. What type of electrostatic precipitator generally uses a presaturator chamber or presaturator water sprays before the unit? Select all that apply.
 - a. Dry, negative corona
 - b. Wet, negative corona
 - c. Wet, positive corona
2. What are the typical superficial gas velocities through a dry, negative corona precipitator?
 - a. 1 to 5 feet per second
 - b. 2 to 10 feet per second
 - c. 3 to 6 feet per second
 - d. 1 to 5 feet per minute
3. What charge is imposed on a collection plate in a dry, negative corona precipitator or a wet, negative corona precipitator?
 - a. Negative
 - b. Positive
 - c. None, the plates are electrically grounded
 - d. None of the above
4. What type of electrostatic precipitator is used to collect organic mists? Select all that apply.
 - a. Dry, negative corona
 - b. Wet, negative corona
 - c. Wet, positive corona
5. What type of electrostatic precipitator is least vulnerable to resistivity problems? Select all that apply.
 - a. Dry, negative corona
 - b. Wet, negative corona
 - c. Wet, positive corona
6. What is the purpose of the T-R set in dry, negative corona precipitators?
 - a. Decrease the voltage and rectify the electricity to alternating current
 - b. Increase the voltage and rectify the electricity to alternating current
 - c. Increase the voltage and rectify the electricity to alternating current
 - d. Increase the voltage and rectify the electricity to direct current

7. What is the normal current in an electrostatic field in good physical condition when the applied secondary voltage is less than the corona onset level?
 - a. Less than 1 ampere
 - b. Less than 0.1 ampere
 - c. Zero
 - d. None of the above

8. What problems can occur if moisture and/or conductive solids accumulate on the surfaces of the high voltage frame support insulators? Select all that apply.
 - a. The insulator can overheat and shatter
 - b. The field served by the insulator could trip offline due to the short circuit
 - c. The discharge wires in the field could be vulnerable to electrical sparking

9. What fraction of the particulate matter entering the precipitator is usually collected in the inlet field?
 - a. 10% to 25%
 - b. 25% to 50%
 - c. 50% to 80%
 - d. 80% to 99%

10. What is the purpose of rapping in dry, negative corona precipitators?
 - a. Remove large clumps of agglomerated solids precipitated in the field
 - b. Keep the collection plate metal clean by intensely redispersing collected solids that have not fallen into the hopper
 - c. Keep the high voltage frame support insulators clean
 - d. Keep the anti-sway insulators clean

11. Under what conditions do dry, negative corona precipitators operate best?
 - a. Low resistivity
 - b. Moderate resistivity
 - c. High resistivity

12. Under what conditions is the dust layer weakly held to the vertical collection plates in a dry, negative corona precipitator?
 - a. Low resistivity
 - b. Moderate resistivity
 - c. High resistivity

13. What factors influence the dust layer resistivity for a precipitator operating at less than 350°F? Select all that apply.
- a. Gas temperature
 - b. Sulfuric acid vapor concentration
 - c. Water vapor concentration
14. The saturation charge is related to _____.
- a. The cube of the particle diameter
 - b. The square of the particle diameter
 - c. The first power of the particle diameter
 - d. The square root of the particle diameter
15. Electrical charge is dissipated through dust layers on the collection plates of dry, negative corona precipitators based on _____. Select all that apply.
- a. Surface conduction
 - b. Bulk conduction
 - c. Electrical sparking
16. Resistivity usually _____ over the gas temperature range of 500°F to 800°F.
- a. Increases
 - b. Decreases
 - c. Remains unchanged
17. The secondary voltage is _____.
- a. The voltage applied on the discharge electrodes
 - b. The voltage applied to the primary side of the T-R set
 - c. The voltage applied by the back-up power supply used in the event that the primary circuit trips offline
 - d. None of the above
18. What conditions are inappropriate for dry, negative corona electrostatic precipitators? Select all that apply.
- a. Explosive gases or vapors
 - b. Sticky particulate matter
 - c. Gas streams vented back into occupied areas

19. Typical secondary voltages in a dry, negative corona precipitator and a wet, negative corona precipitators are in the range of _____.

- a. 5,000 to 10,000 volts
- b. 10,000 to 20,000 volts
- c. 20,000 to 50,000 volts
- d. 50,000 to 100,000 volts
- e. 100,000 to 300,000 volts

20. What is the difficult-to-control particle size range?

- a. 0.1 to 0.5 micrometers
- b. 0.5 to 2 micrometers
- c. 2 to 5 micrometers
- d. 5 to 10 micrometers

Review Question Answers

1. What type of electrostatic precipitator generally uses a presaturator chamber or presaturator water sprays before the unit? Select all that apply.
 - b. Wet, negative corona
2. What are the typical superficial gas velocities through a dry, negative corona precipitator?
 - c. 3 to 6 feet per second
3. What charge is imposed on a collection plate in a dry, negative corona precipitator or a wet, negative corona precipitator?
 - c. None, the plates are electrically grounded
4. What type of electrostatic precipitator is used to collect organic mists? Select all that apply.
 - c. Wet, positive corona
5. What type of electrostatic precipitator is least vulnerable to resistivity problems? Select all that apply.
 - b. Wet, negative corona
 - c. Wet, positive corona
6. What is the purpose of the T-R set in dry, negative corona precipitators?
 - d. Increase the voltage and rectify the electricity to direct current
7. What is the normal current in an electrostatic field in good physical condition when the applied secondary voltage is less than the corona onset level?
 - c. Zero
8. What problems can occur if moisture and/or conductive solids accumulate on the surfaces of the high voltage frame support insulators? Select all that apply.
 - a. The insulator can overheat and shatter
 - b. The field served by the insulator could trip offline due to the short circuit

9. What fraction of the particulate matter entering the precipitator is usually collected in the inlet field?
- c. 50% to 80%
10. What is the purpose of rapping in dry, negative corona precipitators?
- a. Remove large clumps of agglomerated solids precipitated in the field
11. Under what conditions do dry, negative corona precipitators operate best?
- b. Moderate resistivity
12. Under what conditions is the dust layer weakly held to the vertical collection plates in a dry, negative corona precipitator?
- a. Low resistivity
13. What factors influence the dust layer resistivity for a precipitator operating at less than 350°F? Select all that apply.
- a. Gas temperature
 - b. Sulfuric acid vapor concentration
 - c. Water vapor concentration
14. The saturation charge is related to _____.
- b. The square of the particle diameter
15. Electrical charge is dissipated through dust layers on the collection plates of dry, negative corona precipitators based on _____. Select all that apply.
- a. Surface conduction
 - b. Bulk conduction
16. Resistivity usually _____ over the gas temperature range of 500°F to 800°F.
- b. Decreases
17. The secondary voltage is _____.
- a. The voltage applied on the discharge electrodes

18. What conditions are inappropriate for dry, negative corona electrostatic precipitators?
Select all that apply.
- a. Explosive gases or vapors
 - b. Sticky particulate matter
 - c. Gas streams vented back into occupied areas
19. Typical secondary voltages in a dry, negative corona precipitator and a wet, negative corona precipitators are in the range of _____.
- d. 50,000 to 100,000 volts
20. What is the difficult-to-control particle size range?
- a. 0.1 to 0.5 micrometers

This page intentionally left blank.

Review Problems

1. What is the collection efficiency predicted by the Deutsch-Anderson equation for a precipitator having a collection area of 70,000 ft² and a gas flow rate of 440,000 acfm? Assume an effective migration velocity of 0.5 ft/sec.
2. What is the aspect ratio for a five-field electrostatic precipitator having collection plate heights of 30 ft, collection plate lengths of 9 ft, and a precipitator width (normal to gas flow) of 50 ft?
3. What is the average gas velocity passing through the precipitator described in Problem 2 assuming that the gas flow rate is 400,000 acfm?
4. What is the collection plate area of a field having the following characteristics?
 - Plate height: 40 ft
 - Plate length: 6 ft
 - Number of plates: 39
 - Plate-to-plate spacing: 9 in
5. What is the SCA of a five-field precipitator having the following characteristics?
 - Plate height: 40 ft
 - Plate length: 6 ft
 - Number of plates: 39
 - Plate-to-plate spacing: 9 in
 - Number of fields in series: 5
 - Average gas velocity: 4.2 ft/sec

This page intentionally left blank.

Review Problem Solutions

1. What is the collection efficiency predicted by the Deutsch-Anderson equation for a precipitator having a collection area of 70,000 ft² and a gas flow rate of 440,000 acfm? Assume an effective migration velocity of 0.5 ft/sec.

Solution:

$$\eta = 1 - e^{-\frac{A\omega}{Q}} = 1 - e^{-\frac{(70,000 \text{ ft}^2) \left(0.5 \frac{\text{ft}}{\text{sec}}\right)}{\left(440,000 \frac{\text{ft}^3}{\text{min}}\right) \left(\frac{\text{min}}{60 \text{ sec}}\right)}} = 0.9915 = 99.15\%$$

2. What is the aspect ratio for a five-field electrostatic precipitator having collection plate heights of 30 ft, collection plate lengths of 9 ft, and a precipitator width (normal to gas flow) of 50 ft?

Solution:

$$\text{A.R.} = \frac{L}{H} = \frac{(5 \text{ fields}) \left(9 \frac{\text{ft}}{\text{field}}\right)}{30 \text{ ft}} = 1.5$$

3. What is the average gas velocity passing through the precipitator described in Problem 2 assuming that the gas flow rate is 400,000 acfm?

Solution:

$$v = \frac{Q}{A} = \frac{400,000 \frac{\text{ft}^3}{\text{min}}}{(30 \text{ ft})(50 \text{ ft})} = 266.67 \frac{\text{ft}}{\text{min}} = 4.44 \frac{\text{ft}}{\text{sec}}$$

4. What is the collection plate area of a field having the following characteristics?

- Plate height: 40 ft
- Plate length: 6 ft
- Number of plates: 39
- Plate-to-plate spacing: 9 in

Solution:

$$\text{Number of passages} = \text{Number of plates} - 1 = 39 - 1 = 38$$

$$\text{Field plate area} = 2(\text{Number of passages})LH = 2(38)(6 \text{ ft})(40 \text{ ft}) = 18,240 \text{ ft}^2$$

5. What is the SCA of a five-field precipitator having the following characteristics?

- Plate height: 40 ft
- Plate length: 6 ft
- Number of plates: 39
- Plate-to-plate spacing: 9 in
- Number of fields in series: 5
- Average gas velocity: 4.2 ft/sec

Solution:

$$A = 5 \text{ fields}(2)(38)(6 \text{ ft})(40 \text{ ft}) = 91,200 \text{ ft}^2$$

$$Q = \left(4.2 \frac{\text{ft}}{\text{sec}}\right) [(38 \text{ passages})(0.75 \text{ ft})(40 \text{ ft})] = 4,788 \frac{\text{ft}^3}{\text{sec}} = 287,280 \frac{\text{ft}^3}{\text{min}}$$

$$\text{SCA} = \frac{A}{Q} = \frac{91,200 \text{ ft}^2}{287,280 \frac{1,000 \text{ ft}^3}{\text{min}}} = 317.46 \frac{\text{ft}^2}{1,000 \text{ acfm}}$$

References

Beak, W., W. Krawczyk and J. Richards, "Identifying and minimizing the effects of spatial/temporal fly ash resistivity variations to reduce emissions and maintenance requirements", presented at the Independent Power Generation Conference, New Orleans, LA, 1988.

Bickelhaupt, R.E., *A Technique for Predicting Fly Ash Resistivity*, EPA 600/7-79-204, 1979.

Colbert, T.S., "The electrostatic precipitator and its power supply: a circuit analysis", Paper 79-9.2, presented at the 72nd Annual Meeting of the Air Pollution Control Association, Cincinnati, OH, June 1979.

Engelbrecht, H.L., "Increased plate-to-wire spacing to enhance electrostatic precipitator performance", Paper 83-55.6, presented at the 76th Annual Meeting of the Air Pollution Control Association, June 1983.

Eskra, B.J., and B.G. McKinney, "One year's operating experience with SO₃ conditioning on a large coal-fired unit's electrostatic precipitator", Paper 82-49.3, presented at the 75th Annual Meeting of the Air Pollution Control Association, June 1982.

Feldman, P.L., and K.S. Kumar, "Effects of wide plate spacings in electrostatic precipitators", Paper 90-101.7, presented at the Air and Waste Management Association Meeting, Pittsburgh, PA, June 1990.

Fletcher, H.R., "Operating experience at Detroit Edison with various flue gas conditioning systems", Paper 82-49.1, presented at the 75th Annual Meeting of the Air Pollution Control Association, June 1982.

Gooch, J.R., and H.M. Guillaume, Jr., *Electrostatic Precipitator Rapping Reentrainment and Computer Model Studies*, Electric Power Research Institute Publication FP-792, Vol. 3, 1978.

Hall, H.J., "Summary of overall concepts for design, energization, and control of electrostatic precipitators", Paper 83-57.6, presented at the 76th Annual Meeting of the Air Pollution Control Association, June 1983.

Humbert, C.O., "Electrostatic precipitator rappers: their function, operation, and maintenance", Paper 83-57.3, presented at the 76th Annual Meeting of the Air Pollution Control Association, June 1983.

Jonelis, R.E., and J.A. Jonelis, "Economical, innovative methods of straightening ESP collector plates so as to achieve alignment for the purposes of improving particulate control and performance", Paper 85-JPGC-APC-5, presented at the American Society of Mechanical Engineers/IEEE Power Generation Conference, Milwaukee, WI, October 1985.

Katz, J., *The Art of Electrostatic Precipitators*, Scholium International, Port Washington, NY, 1979.

Lawless, P., *Electrostatic Precipitator V-I and Performance Model: Users Manual*, EPA 600/R-92-104a, 1992.

Lurgi, G., *Corrosion-Proof Wet Precipitator*, 1988.

Makansi, J., "Particulate control: optimizing precipitators and fabric filters for today's power plants", *Power*, 1986.

McDonald, J.R., and A.H. Dean, *A Manual for the Use of Electrostatic Precipitators to Collect Fly Ash Particles*, EPA 600/8-80-025, 1980.

Neundorfer, M., *Second Symposium on the Transfer and Utilization of Particulate Control Technology, Vol. 2, Electrode Cleaning Systems: Optimizing Rapping Energy and Rapping Control*, EPA 600/9-9-80-039a, 1980.

Raymond, R.K., *Second Symposium on the Transfer and Utilization of Particulate Control Technology, Vol. 2, Electrostatic Precipitators: Electrical Problems and Solutions*, EPA 600/9-9-80-039a, 1980.

Schwab, M.J., and R. Johnson, "Numerical design method for implementing gas distribution within electrostatic precipitators" presented at the 56th Annual Meeting, American Power Conference, Chicago, IL, April 1994.

Steinsvaag, D., "Smoke abatement for textile finishers", *American Dyestuff Reporter*, September 1992.

Szabo, M.F., and R.W. Gerstle, *Operation and Maintenance of Particulate Control Devices on Coal-fired Utility Boilers*, EPA 600/2-77-129, 1977.

Theodore, L., and A.J. Buonicore, *Industrial Air Pollution Equipment for Particulates*, CRC Press, Cleveland, OH, 1976.

Verhoff, F.H., and J.T. Banchemo, *Chemical Engineering Progress*, pp. 70-71, 1974.

Weyers, L.L., and R.E. Cook, *Operating Experience with Flue Gas Conditioning Systems at Commonwealth Edison Company*, Wahlco, Santa Anna, CA, April 1981.

White, H.J., "Fly ash resistivity", *Journal of the Air Pollution Control Association*, 1977.

CHAPTER 10

HOODS AND FANS

Industrial process systems consist of the process equipment, which generates the pollutants, the air pollution control equipment that removes them, and the fan that moves the gas stream through the necessary equipment. The process equipment and the air pollutant control devices do not work independently. The operating conditions of all the system components are closely linked together by the individual performance of hoods, fans and ductwork.

Hoods

The pollutants generated or released by process equipment must be captured so that they can be transported to the air pollution control device. Pollutant capture occurs in hoods (Figure 10-1). Hoods are often an integral part of the process equipment. The hood can consist of a simple, stationary plenum mounted above or to the side of the source, a large moveable plenum, or the process equipment itself.



Figure 10-1. Stationary hood in an industrial process

If hoods do not capture pollutants generated by process equipment, the pollutants disperse directly into the plant air and eventually pass through roof vents and doors into the atmosphere. Evaluation of the ability of the hoods to capture pollutants at the point of generation is important in many inspections and engineering studies. The USEPA defines fugitive emissions as “emissions that (1) escape capture by process equipment exhaust hoods;

(2) are emitted during material transfer; (3) are emitted to the atmosphere from the source area; and (4) are emitted directly from process equipment.”

$$\text{Fugitive emissions} = \text{Total emissions} - \text{Emissions captured by hood} \quad (10-1)$$

$$\text{Stack emissions} = \text{Emissions captured by hood} \times \left(\frac{100 - \eta}{100} \right) \quad (10-2)$$

where

$$\eta = \text{Collection efficiency (\%)}$$

The importance of hood performance is illustrated by Examples 10-1 and 10-2, which are based on the simplified industrial process shown in Figure 10-2. This system consists of a process unit that generates pollutants, several hoods surrounding the process equipment, the ductwork, an air pollution control device, a fan, and a stack.

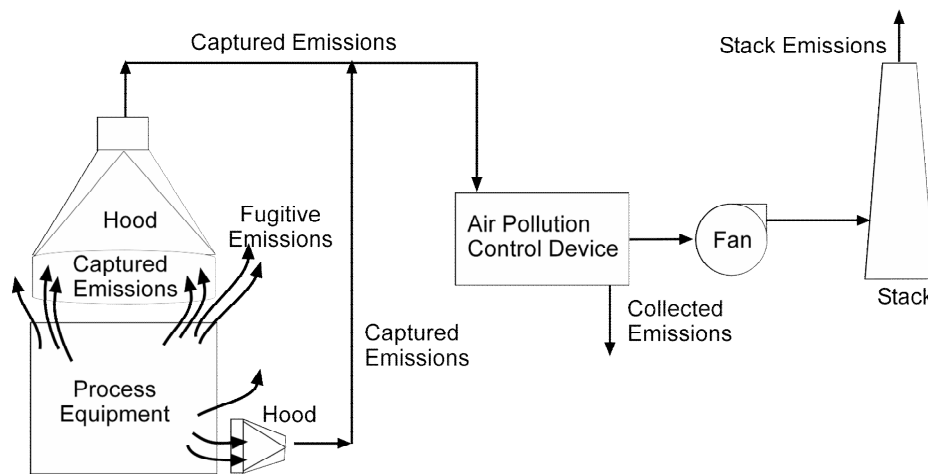


Figure 10-2. Role of hoods in an industrial process

Example 10-1

Calculate the fugitive emissions and the stack emissions if the process equipment generates $100 \text{ lb}_m/\text{hr}$ of particulate matter, the hood capture efficiency is 95%, and the collection efficiency of the air pollution control device is 95%.

Solution:

Calculate fugitive emissions:

$$\begin{aligned} \text{Fugitive emissions} &= \text{Total emissions} - \text{Emissions captured by hood} \\ &= 100 \frac{\text{lb}_m}{\text{hr}} - 95 \frac{\text{lb}_m}{\text{hr}} = 5 \frac{\text{lb}_m}{\text{hr}} \end{aligned}$$

Calculate stack emissions:

$$\text{Stack emissions} = \text{Emissions captured by hood} \times \left(\frac{100 - \eta}{100} \right) = \left(95 \frac{\text{lb}_m}{\text{hr}} \right) \left(\frac{100 - 95}{100} \right) = 4.75 \frac{\text{lb}_m}{\text{hr}}$$

The capture of emissions by the hood is the key step in an air pollution control system. Example 10-1 shows that, even with high hood capture efficiency, fugitive emissions can be higher than emissions leaving the stack.

Example 10-2

Calculate the stack emissions and fugitive emissions if the process equipment generates 100 lb_m/hr of particulate matter, the hood capture efficiency is 90%, and the collection efficiency of the air pollution control device is 95%.

Solution:

Calculate fugitive emissions:

$$\begin{aligned} \text{Fugitive emissions} &= \text{Total emissions} - \text{Emissions captured by hood} \\ &= 100 \frac{\text{lb}_m}{\text{hr}} - 90 \frac{\text{lb}_m}{\text{hr}} = 10 \frac{\text{lb}_m}{\text{hr}} \end{aligned}$$

Calculate stack emissions:

$$\text{Stack emissions} = \text{Emissions captured by hood} \times \left(\frac{100 - \eta}{100} \right) = \left(90 \frac{\text{lb}_m}{\text{hr}} \right) \left(\frac{100 - 95}{100} \right) = 4.5 \frac{\text{lb}_m}{\text{hr}}$$

These two problems illustrate the importance of hoods. Slight changes in the ability of the hood to capture the pollutants can have a large impact on the total fugitive and stack emissions released into the atmosphere.

Unfortunately, it is not always possible to see the fugitive emissions. Gaseous and vapor emissions such as carbon monoxide, sulfur dioxide, hydrogen chloride, and nitric oxide are not visible. Even particulate emissions may be hard to see under the following circumstances:

- If there are numerous small fugitive sites
- If there is one major site that cannot be seen from normal areas accessible to personnel
- If the particulate matter is not in the size range that causes light scattering

Techniques for monitoring hood capture effectiveness are important because the quantities of fugitive emissions can be high, and these emissions are often hard to see.

Hood Operating Principles

Hoods are generally designed to operate under negative pressure. The air is drawn into the hood due to static pressures that are lower inside the hood than those in the process equipment and the surrounding air. Since air from all directions moves toward the low-pressure hood, the hood must be as close as possible to the process equipment in order to capture the pollutant-laden air and not just the surrounding air. At approximately one-hood-diameter away from the hood entrance, the gas velocities are often less than 10% of the velocity at the hood entrance. Figure 10-3 illustrates how quickly the gas velocity decreases as distance from the hood increases.

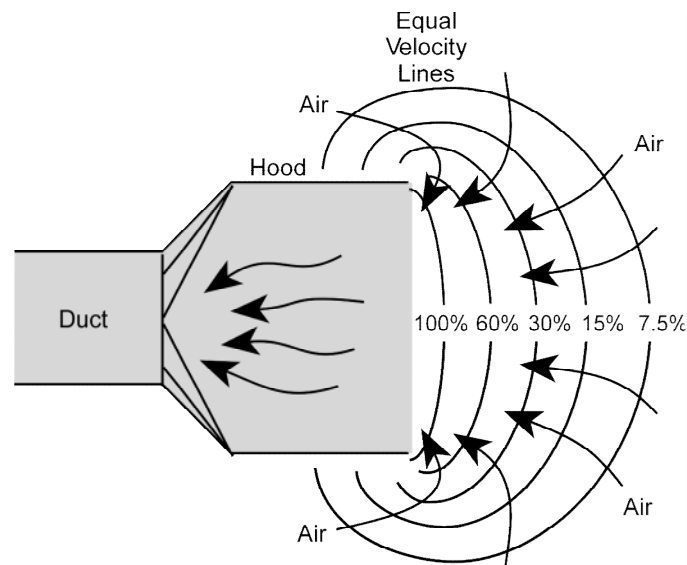


Figure 10-3. Hood capture velocities

Figure 10-3 indicates that the hood has very little influence on gas flow except in the area very close to the hood entrance. In order to ensure good capture of the pollutant-laden gas streams, the hood must be close to the emission source. The *capture velocity* of a hood is defined as the air velocity at any point in front of the hood or at the hood opening necessary to overcome opposing air currents and to capture the contaminated air at that point by pulling it into the hood. A general guide for appropriate capture velocities in several situations is provided in Table 10-1.

Table 10-1. Capture Velocities	
Type of Material Release	Capture Velocity (ft/min)
With no velocity into quiet air	50-100
At low velocity into moderately still air	100-200
Active generation into zone of rapid air motion	200-500
With high velocity into zone of very rapid air motion	500-2,000

The following show conditions that would help determine what part of the capture velocity range should be used for a particular operation. In general, high toxicity contaminants released from small sources into rapidly moving air currents would require higher capture velocities.

- The surrounding air currents
Minimal room air currents vs. disturbing room air currents
- The level of toxicity of the pollutant to be captured
Nuisance value only vs. high toxicity
- The amount of pollutant
Intermittent (low production) vs. high production (heavy use)
- Area of the hood opening
Large hood (large air mass in motion) vs. small hood (local control only)

The following flow/capture velocity equation for a freely suspended hood without a flange demonstrates the importance of the proximity of the hood to the source:

$$Q = v_h(10X^2 + A_h) \quad (10-3)$$

where

- Q = actual volumetric flow rate (ft³/min)
- X = distance from hood face to farthest point of contaminant release (ft)
- v_h = hood capture velocity at distance X (ft/min)
- A_h = area of hood opening (ft²)

It should be noted that this correlation between distance, gas flow rate, and capture velocity should be used for *estimation purposes only* because the vacuum from a hood does not create equal velocity lines or points. Equation 10-1 is also limited to the distance (X) being less than or equal to 1.5 hood diameters. Capture velocity equations for a variety of hoods with different locations and arrangements can be obtained from the ACGIH, *Industrial Ventilation Manual*.

Example 10-3

The recommended capture velocity for a certain pollutant entering a 16-inch diameter hood is 300 ft/min. What is the required volumetric flow rate for the following distances from the hood face (X)?

- A. X = 12 in. (75% of hood diameter)
- B. X = 24 in. (150% of hood diameter)

Solution for Part A:

$$Q = v_h(10X^2 + A_h)$$

Calculate the area of the hood opening:

$$A_h = \frac{\pi D^2}{4} = \frac{\pi \left[16 \text{ in} \left(\frac{1 \text{ ft}}{12 \text{ in}} \right) \right]^2}{4} = 1.40 \text{ ft}^2$$

Calculate the volumetric flow rate, Q , required to obtain the recommended capture velocity of 300 fpm at a distance of 12 inches from the hood:

$$Q = v_h (10X^2 + A_h) = 300 \frac{\text{ft}}{\text{min}} [10(1 \text{ ft})^2 + 1.40 \text{ ft}^2] = 3,420 \frac{\text{ft}^3}{\text{min}}$$

Solution for Part B:

Calculate the volumetric flow rate, Q , required to obtain the recommended capture velocity of 300 fpm at a distance of 24 inches from the hood:

$$Q = v_h (10X^2 + A_h) = 300 \frac{\text{ft}}{\text{min}} [10(2 \text{ ft})^2 + 1.40 \text{ ft}^2] = 12,420 \frac{\text{ft}^3}{\text{min}}$$

The volumetric flow rate requirements increased approximately four times when the distance between the hood and the contaminant source doubled.

Hood Designs for Improved Performance

There are many ways to design hoods to improve capture effectiveness. When the pollutant-laden gas stream is hot, the hood is often positioned above the point of pollutant release to take advantage of the buoyancy of the low-density hot gas stream.

Flanges can be used to block the movement of unwanted air into the hood. The recommended width of a flange for most situations should be equal to the square root of the hood area. The beneficial effect of a flange on the gas velocities near a hood entrance is shown in Figure 10-4.

Hood capture is greatly improved when the enclosure comprised of the hood and the side baffles can encompass the point of pollutant generation. These side baffles can be in the form of metal sheets, strips of fabric or plastic, or any other materials that block the movement of clean air into the low-pressure area of the hood. In addition to reducing the unintentional capture of clean air, these side baffles also prevent cross drafts, which can prevent the intended movement of the pollutant-laden gas into the hood.

Some process equipment inherently creates an entirely enclosed area for pollutant-laden gas capture. For example, coal-fired boilers generate pollutants in an enclosed furnace area that is maintained at a slightly negative static pressure of -0.05 to -0.25 in. WC. In this case, the boiler walls serve as the hood.

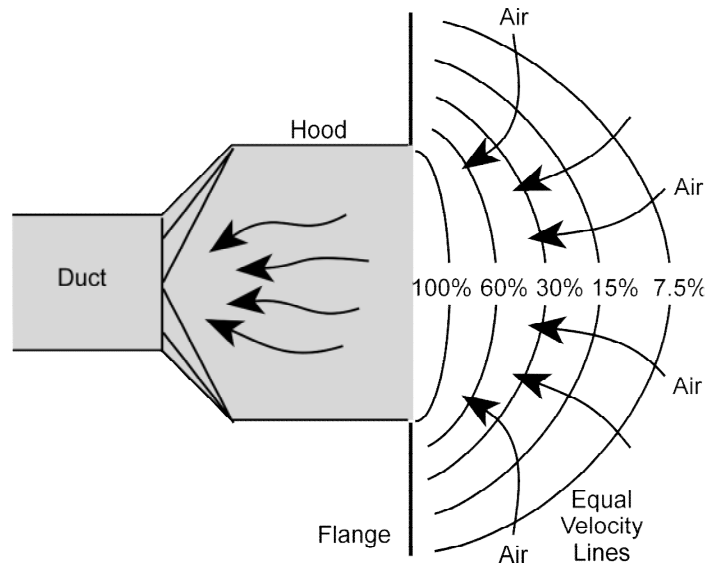


Figure 10-4. Effect of side baffles on hood capture velocities

Another hood design that is used to improve capture effectiveness is called the push-pull hood. As shown in Figure 10-5, a high-velocity clean air stream is blown across the area of pollutant generation into the hood on the opposite side.

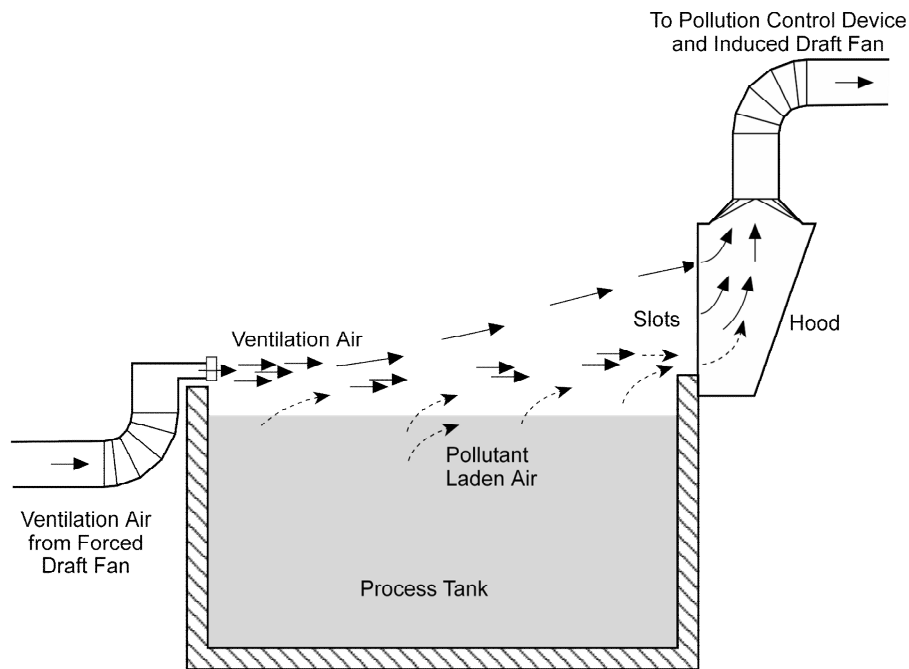


Figure 10-5. Push-pull hood

The high-velocity gas stream does not inherently disperse rapidly. Therefore, it flows toward the hood and is captured. The hood also effectively captures the pollutant-laden gas that is trapped in this strong cross draft. These types of hoods are sometimes used on open tanks

and other sources where access from the top is necessary in order to operate the equipment. However, they may not be appropriate for tanks and other processes handling materials where the cross draft could significantly increase the quantities vaporized. Push-pull hoods can provide very high capture efficiencies where they are applicable.

Monitoring Hood Capture Effectiveness

There are several effective ways to confirm that the hood capture effectiveness has not decreased since it was installed or tested. Visible emission observations for fugitive emissions should be conducted in the case of particulate sources. In general, you should confirm that the hood has not been moved away from the point of pollutant generation and that side baffles and other equipment necessary to maintain good operation have not been damaged or removed.

The hood static pressure should be monitored to ensure that the appropriate gas flow rate is being maintained. The *hood static pressure* is simply the static pressure in the duct immediately downstream from the hood. This static pressure is usually negative and is entirely dependent on the hood geometry and the gas flow rate. As long as the hood has not been damaged or altered, the hood static pressure provides an indirect, but relatively accurate measurement of the gas flow rate. As indicated in Equation 10-4, the hood static pressure is determined from the velocity pressure in the duct from the hood and the hood entry loss. The loss of static pressure caused by air flowing into a system is referred to as entry loss.

$$SP_h = VP_d + h_e \quad (10-4)$$

where

- SP_h = hood static pressure (in WC)
- VP_d = duct velocity pressure (in WC)
- h_e = hood entry loss (in WC)

The velocity pressure term is due to the energy necessary to accelerate the air from zero velocity to the velocity in the duct. The hood entry loss is usually expressed as some fraction of this velocity pressure:

$$h_e = F_h VP_d \quad (10-5)$$

where

- F_h = hood entry loss coefficient (dimensionless)
- VP_d = duct velocity pressure (in WC)

Hood entry loss coefficients are tabulated in standard texts on hoods and ventilation systems.

When air enters a negative pressure duct, the airflow converges as shown in Figures 10-6 through 10-8. The area where air converges upon entering a duct is referred to as *vena contracta*. After the vena contracta, the airflow expands to fill the duct and some of the velocity pressure converts to static pressure. The vena contracta is dependent on the hood

geometry, which determines the resistance to airflow entering the hood. In general, the smoother the entry, the lower the entry loss coefficient.

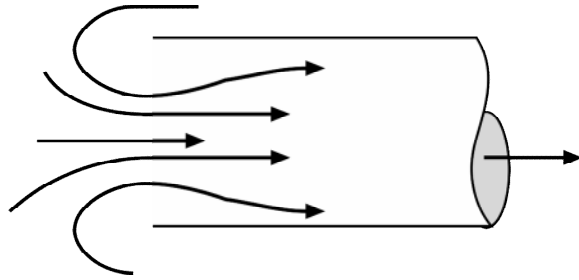


Figure 10-6. Plain duct end ($h_e = 0.93$)

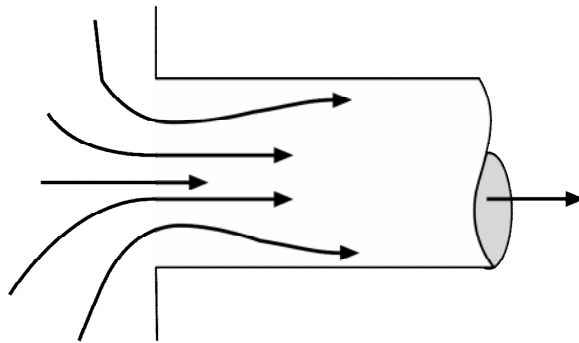


Figure 10-7. Flanged duct end ($h_e = 0.49$)

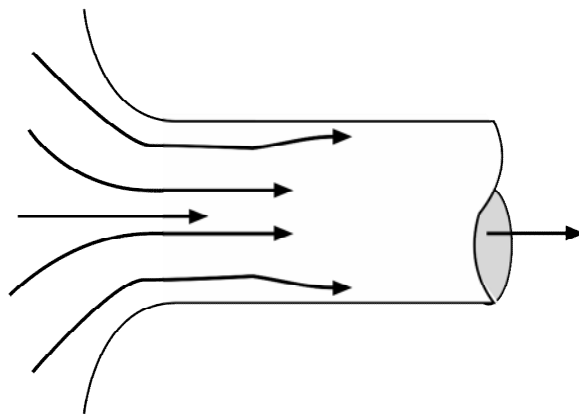


Figure 10-8. Bell-mouth duct inlet ($h_e = 0.04$)

The velocity pressure is related to the square of the gas velocity in the duct and the gas density:

$$VP_d = \rho_g \left(\frac{v_d}{1,096.7} \right)^2 \quad (10-6)$$

where

VP_d = duct velocity pressure (in WC)

v_d = duct gas velocity (ft/min)

ρ_g = gas density (lb_m/ft^3)

As the gas flow rate into the hood increases, the hood static pressure increases. A decrease in hood static pressure (i.e., a less negative value) usually indicates that the gas flow rate entering the hood has decreased from previous levels. This may reduce the effectiveness of the hood by reducing the capture velocities at the hood entrance.

Example 10-4

A hood serving a paint dipping operation has a hood static pressure of 1.10 in WC. The baseline hood static pressure was 1.70 in WC. Estimate the gas flow rate under the following two conditions:

- A. At present operating conditions
- B. At baseline levels

Use the data provided below:

$$F_h = 0.93$$

$$\text{Temperature} = 68^\circ\text{F}$$

$$\text{Duct diameter} = 2 \text{ ft (inside diameter)}$$

Solution for Part A:

Calculate the velocity pressure in the duct:

$$SP_h = (1 + F_h)VP_d$$

$$VP_d = \frac{SP_h}{1 + F_h} = \frac{1.10 \text{ in WC}}{1 + 0.93} = 0.57 \text{ in WC}$$

Calculate the gas velocity in the duct:

$$VP_d = \rho_g \left(\frac{v_d}{1,096.7} \right)^2$$

$$v_d = 1,096.7 \sqrt{\frac{VP_d}{\rho_g}} = 1,096.7 \sqrt{\frac{0.57 \text{ in WC}}{0.0747 \frac{\text{lb}_m}{\text{ft}^3}}} = 3,029.5 \frac{\text{ft}}{\text{min}}$$

Calculate the gas flow rate:

$$Q = v_d A_d = v_d \left(\frac{\pi D^2}{4} \right) = 3,029.5 \frac{\text{ft}}{\text{min}} \left[\frac{\pi (2 \text{ ft})^2}{4} \right] = 9,517.5 \frac{\text{ft}^3}{\text{min}}$$

Solution for Part B:

Calculate the velocity pressure in the duct:

$$SP_h = (1 + F_h) VP_d$$

$$VP_d = \frac{SP_h}{1 + F_h} = \frac{1.70 \text{ in WC}}{1 + 0.93} = 0.88 \text{ in WC}$$

Calculate the gas velocity in the duct:

$$VP_d = \rho_g \left(\frac{v_d}{1,096.7} \right)^2$$

$$v_d = 1,096.7 \sqrt{\frac{VP_d}{\rho_g}} = 1,096.7 \sqrt{\frac{0.88 \text{ in WC}}{0.0747 \frac{\text{lb}_m}{\text{ft}^3}}} = 3,764.2 \frac{\text{ft}}{\text{min}}$$

Calculate the gas flow rate:

$$Q = v_d A_d = v_d \left(\frac{\pi D^2}{4} \right) = 3,764.2 \frac{\text{ft}}{\text{min}} \left[\frac{\pi (2 \text{ ft})^2}{4} \right] = 11,819.9 \frac{\text{ft}^3}{\text{min}}$$

The change in hood static pressure from 1.7 in WC to 1.1 in WC indicates a drop in the gas flow rate from 11,820 acfm to 9,518 acfm. This is nearly a 20% decrease in the gas flow rate.

Transport Velocity

When a particulate contaminant is captured by a hood system and enters the ductwork, a minimum *transport velocity* must be maintained to keep the contaminant from settling out of the gas stream and building up deposits in the ductwork. This would lead to decreased hood

capture efficiencies and increased fugitive emissions. Systems with heavy particulate-laden gas streams should have clean-out ports installed to remove particles that have settled out. Typical transport velocities for different types of contaminants are shown in Table 10-2.

Table 10-2. Transport Velocities	
Contaminant	Transport Velocity (ft/min)
Vapors, gases, smoke	Any (usually 1,000-2,000)
Fume	1,400-2,000
Very fine, light dusts	2,000-2,500
Dry dusts and powders	2,500-3,500
Average industrial dusts	3,500-4,000
Heavy dusts	4,000-4,500
Very heavy or moist dusts	>4,500

Proper duct diameter is a key element when addressing minimum transport velocity. If a section of ductwork has a larger than necessary diameter, then settling out will most likely occur. If a section of ductwork is too small, the pressure drop will increase across this section, thus requiring the fan to handle more static pressure. Another concern when dealing with transport velocities is the abrasion of the ductwork, especially at elbows and the areas opposite entries. The amount of abrasion that occurs is dependent upon several factors, including the duct velocity, the amount and type of particulate matter in the gas stream, and the construction of the ductwork.

Example 10-5

A duct system transporting a dry dust requires a minimum transport velocity of 2,800 ft/min. The volumetric flow rate for the system is 978 acfm. What is the necessary duct diameter in inches for this section of ductwork to maintain the minimum transport velocity?

Solution:

Calculate the duct area:

$$A_d = \frac{Q}{v_d} = \frac{978 \frac{\text{ft}^3}{\text{min}}}{2,800 \frac{\text{ft}}{\text{min}}} = 0.349 \text{ft}^2$$

Calculate the duct diameter:

$$A_d = \frac{\pi D^2}{4}$$

$$D = \sqrt{\frac{4A_d}{\pi}} = \sqrt{\frac{4(0.349 \text{ ft}^2)}{\pi}} = 0.667 \text{ ft} = 8 \text{ in}$$

Summary

Hoods are the first component of the air pollution control system and are of critical importance. If they fail to capture the pollutant, the overall collection efficiency of the system is reduced. Pollutants not captured by hoods become fugitive emissions. Many factors affect a hood's capture efficiency; however, one of the key factors is the distance between the pollutant source and the hood.

The geometry of a hood opening influences the hood entry loss coefficient and the hood static pressure due to the formation of the vena contracta. Comparing the hood static pressure against baseline condition provides a good indicator if the system has developed any problems.

Maintaining a system's minimum transport velocity is necessary to ensure that all of the captured pollutant reaches the air pollution control device and to prevent build-up of the pollutants in the ductwork.

Fans

Fans are the heart of the system. They control the gas flow rate at the point of pollutant generation in the process equipment and through the air pollution control devices. Fans provide the necessary energy for the gas stream to overcome the resistance to gas flow caused by the ductwork and air pollution control devices. Data concerning fan performance is important during inspections and all other technical evaluations of system performance.

Types of Fans and Fan Components

There are two main types of fans: *axial* and *centrifugal*. Most fans used in air pollution control systems are centrifugal fans. An axial fan is shown in Figure 10-9. The term, axial, refers to the use of a set of fan blades mounted on a rotating shaft aligned in the direction of air movement. A standard house ventilation fan is an axial fan.

A centrifugal fan has a wheel composed of a number of fan blades mounted around a hub. As shown in Figure 10-10, the hub turns on a shaft that passes through the fan housing. The gas enters from the side of the fan wheel, turns 90° and is accelerated as it passes over the fan blades. The term, centrifugal, refers to the trajectory of the gas stream as it passes out of the fan housing.

Centrifugal fans can generate high-pressure rises in the gas stream. Accordingly, they are well-suited for industrial processes and air pollution control systems. The remainder of this section concerns centrifugal fans.

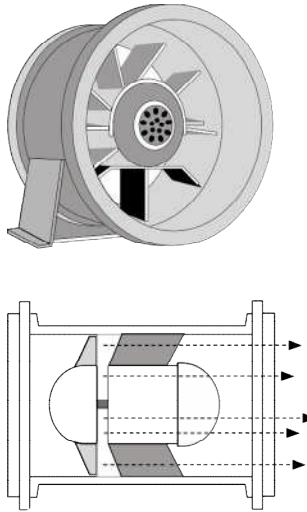


Figure 10-9. Axial fan

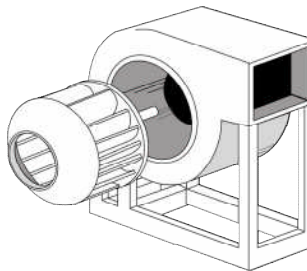


Figure 10-10. Centrifugal fan

The major components of a typical centrifugal fan include the fan wheel, fan housing, drive mechanism, and inlet dampers and/or outlet dampers. A wide variety of fan designs serve different applications.

The fan drive determines the speed of the fan wheel and the extent to which this speed can be varied. The types of fan drives can be grouped into three basic categories:

- Direct drive
- Belt drive
- Variable drive

In a *direct drive* arrangement, the fan wheel is linked directly to the shaft of the motor. This means that the fan wheel speed is identical to the motor rotational speed. With this type of fan drive, the fan speed cannot be varied.

Belt driven fans use multiple belts which rotate over a set of sheaves or pulleys mounted on the motor shaft and the fan wheel shaft. This type of drive mechanism is illustrated in Figure 10-11.

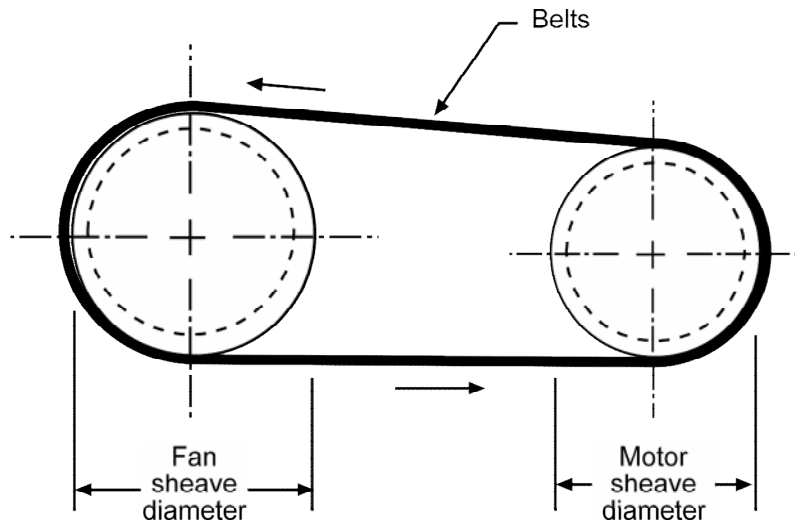


Figure 10-11. Centrifugal fan and motor sheaves

The belts transmit the mechanical energy from the motor to the fan. The fan wheel speed is simply the ratio of the fan wheel sheave diameter to the motor sheave diameter:

$$\text{RPM}_{\text{fan}} = \text{RPM}_{\text{motor}} \frac{D_{\text{motor}}}{D_{\text{fan}}} \quad (10-7)$$

where

- RPM_{fan} = fan speed (revolutions per minute)
- $\text{RPM}_{\text{motor}}$ = motor speed (revolutions per minute)
- D_{fan} = diameter of fan sheave (inches)
- D_{motor} = diameter of motor sheave (inches)

Fan wheel speeds in belt-driven arrangements are fixed unless the belts slip. Belt slippage normally reduces fan wheel speed several hundred rpm and creates a noticeable squeal. If it is necessary to change the fan wheel speed in a belt-driven arrangement, the motor and/or fan wheel sheaves must be replaced with units having different diameters. However, there are very definite safety limits to the extent to which the fan speed can be increased. If the fan rotational speed is excessive, the fan can disintegrate.

Variable speed fans use hydraulic or magnetic couplings that allow operator control of the fan wheel speed independent of the motor speed. The fan speed controls are often integrated into automated systems to maintain the desired fan performance over a variety of process operating conditions.

Fan dampers are used to control gas flow into and out of the centrifugal fan. These dampers can be on the inlet side and/or on the outlet side of the fan. Dampers on the outlet side simply impose a flow resistance that is used to control gas flow. Dampers on the inlet side are designed to control gas flow and to change how the gas enters the fan wheel at different operating conditions. Inlet dampers conserve fan energy due to their ability to affect the airflow pattern into the fan.

The fan wheel consists of a hub and a number of fan blades. The fan blades on the hub can be arranged in three different ways:

- Forward curved
- Backward curved
- Radial

Forward curved fans (Figure 10-12a) use blades that curve or slant toward the direction of rotation of the fan wheel. These are especially sensitive to particle accumulation and are not used extensively in air pollution control systems.

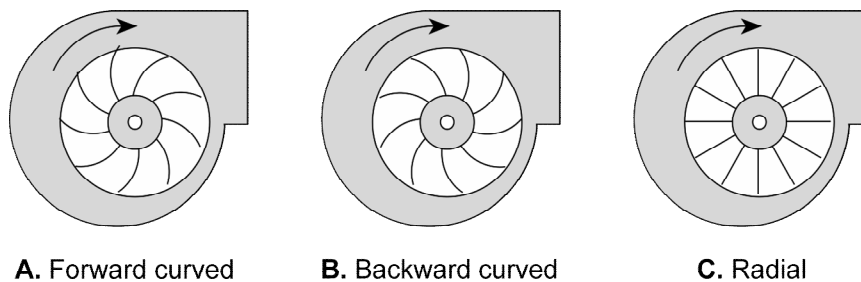


Figure 10-12. Types of fan wheels

Backward curved fans (Figure 10-12b) use straight plates, curved plates, or curved airfoils that angle away from the direction of rotation. These types of fan wheels are used in fans designed to handle gas streams with relatively low particulate loadings because they are prone to solids build-up. Backward curved fans are more energy efficient than radial fans.

Radial fans use fan wheel blades that extend straight out from the hub. A radial blade fan wheel, as shown in (Figure 10-12c), is often used on particulate-laden gas streams because it is the least sensitive to solids build-up.

Centrifugal Fan Operating Principles

A basic understanding of fan operating principles is necessary to evaluate the performance of an industrial ventilation system. The fan operating speed is one of the most important operating variables. Most fans can operate over a modest range of speeds. The flow rate of gas moving through the fan depends on the fan wheel rotational speed. As the speed increases, the gas flow rate increases proportionally. This relationship is expressed as one of the fan laws:

$$Q_2 = Q_1 \left(\frac{RPM_2}{RPM_1} \right) \quad (10-8)$$

where

Q_1 = baseline gas flow rate (acfm)

Q_2 = present gas flow rate (acfm)

RPM_1 = baseline fan wheel rotational speed (revolutions per minute)

RPM_2 = present fan wheel rotational speed (revolutions per minute)

The rate of gas flow through a fan is always expressed in actual conditions. This is helpful because this value does not change, regardless of the gas density. In this respect, a fan is much like a shovel. It moves a specific amount of gas per minute, regardless of whether the gas is dense cold gas or light hot gas.

The gas stream moving through the fan has a static pressure rise due to the mechanical energy expended by the rotating fan wheel. As indicated in Figure 10-13, the static pressure at the outlet is always higher than the static pressure at the inlet. The static pressure rise across the fan is denoted as Fan SP:

$$\text{Fan SP} = SP_{\text{out}} - SP_{\text{in}} - VP_{\text{in}} \quad (10-9)$$

For the conditions shown in the figure, Fan SP = 0.05 – (-10) – 0.50 = 9.55 in WC.

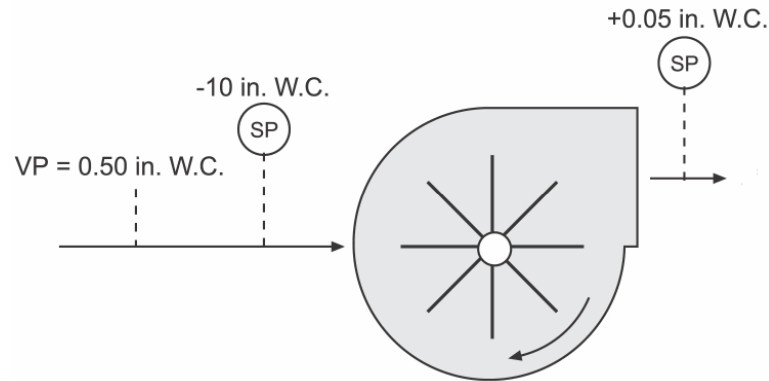


Figure 10-13. Fan static pressure rise

Fan SP is related to the square of the fan speed, as indicated in the second fan law:

$$\text{Fan SP}_2 = \text{Fan SP}_1 \left(\frac{RPM_2}{RPM_1} \right)^2 \quad (10-13)$$

where

Fan SP₁ = baseline fan static pressure (in WC)

Fan SP₂ = present fan static pressure (in WC)

RPM_1 = baseline fan wheel rotational speed (revolutions per minute)

RPM_2 = present fan wheel rotational speed (revolutions per minute)

The specific fan for an industrial ventilation system must be selected based on the specific air flow rate and fan static pressure rise needed to properly capture, transport, and control the emissions. Each industrial ventilation system includes one or more capture hoods, ductwork, air pollution control systems, the fan, and a stack. The gas flow rate through the ventilation system must be sufficient to provide adequate pollutant capture at the hoods and to ensure proper transport of the pollutant-laden air to the air pollution control systems. The fan static pressure rise must be sufficient to accelerate the air entering the hoods and to overcome the flow resistances of the hoods, ductwork, air pollution control systems, and stack.

The designer of an air pollution control system starts by specifying the air volumes and velocities in the hoods, ductwork, air pollution control systems, and stack. These values are selected based on established engineering design principles to ensure high efficiency hood capture, proper operation of the air pollution control systems, and proper dispersion of the effluent gas stream from the stack. Using this information, the designer next calculates the flow resistance of the system and determines the fan static pressure needed to move the design volume.

The static pressure drop across each component of the system is related to the square of the air flow rate. This general relationship is shown in Figure 10-14 and is termed the *system characteristic curve*. The designer will select a fan that will deliver performance corresponding to one point on this curve--the required volume at the necessary fan static pressure. The data necessary for doing this are provided in *multi-rating tables* published by manufacturers for each specific fan model and size they produce. Based on these data, it is possible to select a fan model, the specific model size, the fan speed and the motor horsepower necessary to achieve the necessary air flow rate and fan static pressure condition. An excerpt from a multi-rating table for a centrifugal fan is shown below in Figure 10-15.

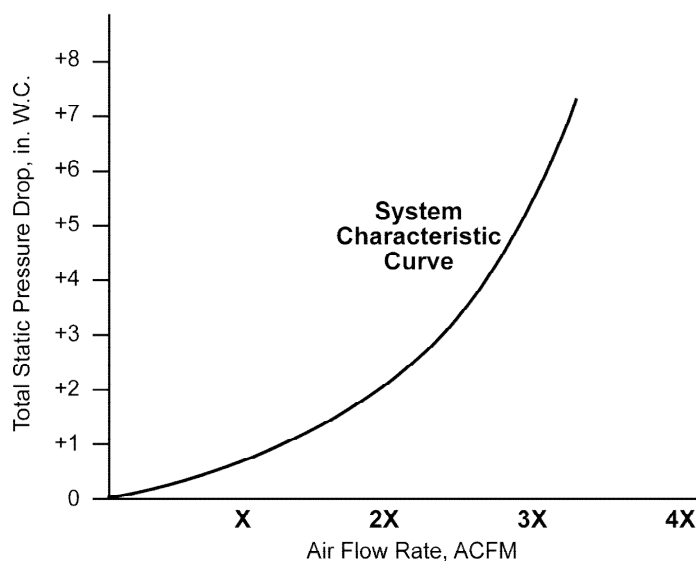


Figure 10-14. System characteristic curve


194 LS				Inlet diameter: 11" O.D.				Wheel diameter: 19 1/2"											
				Outlet area: .660 sq. ft. inside				Wheel circumference: 5.01 ft											
CFM	OV	2"SP		4"SP		6"SP		8"SP		10"SP		12"SP		14"SP		16"SP		18"SP	
		RPM	BHP	RPM	BHP	RPM	BHP	RPM	BHP	RPM	BHP	RPM	BHP	RPM	BHP	RPM	BHP	RPM	BHP
660	1000	995	0.48	1392	1.01	1698	1.60	1960	2.27	2191	2.98	2399	3.74	2592	4.55	2769	5.38	2938	6.27
792	1200	1008	0.55	1398	1.11	1703	1.75	1962	2.45	2192	3.20	2398	3.99	2588	4.83	2767	5.71	2936	6.65
924	1400	1023	0.62	1405	1.23	1708	1.90	1965	2.64	2194	3.43	2401	4.27	2589	5.14	2766	6.05	2932	7.01
1056	1600	1042	0.71	1418	1.35	1716	2.07	1971	2.84	2197	3.67	2401	4.53	2593	5.46	2769	6.42	2935	7.41
1188	1800	1061	0.80	1431	1.49	1726	2.24	1980	3.06	2203	3.92	2407	4.83	2593	5.78	2771	6.79	2936	7.81
1320	2000	1084	0.90	1447	1.64	1739	2.44	1987	3.29	2209	4.19	2414	5.15	2600	6.13	2773	7.16	2940	8.21
1452	2200	1109	1.01	1465	1.80	1753	2.65	1999	3.54	2221	4.49	2422	5.47	2607	6.50	2778	7.55	2943	8.61
1584	2400	1136	1.13	1485	1.98	1769	2.87	2012	3.80	2229	4.78	2431	5.82	2612	6.87	2786	7.98	2949	9.01
1716	2600	1162	1.26	1505	2.16	1784	3.10	2025	4.08	2242	5.11	2441	6.18	2623	7.28	2791	8.40	2956	9.41
1980	3000	1223	1.56	1554	2.58	1824	3.62	2059	4.70	2272	5.82	2464	6.95	2644	8.14	2815	9.38	2973	10.21
2244	3400	1290	1.91	1606	3.04	1867	4.19	2098	5.38	2305	6.59	2495	7.83	2671	9.09	2838	10.4	2995	11.01
2508	3800	1361	2.33	1661	3.56	1917	4.84	2141	6.12	2345	7.44	2531	8.78	2703	10.1	2866	11.5	3011	11.81
2772	4200	1439	2.83	1723	4.16	1968	5.54	2189	6.95	2387	8.37	2569	9.80	2740	11.3	2900	12.8	3021	12.61
3036	4600	1519	3.40	1788	4.84	2025	6.32	2239	7.85	2432	9.36	2611	10.9	2780	12.5	2937	14.1	3027	13.41
3300	5000	1603	4.07	1855	5.58	2086	7.20	2294	8.83	2483	10.5	2660	12.1	2825	13.8	2978	15.5	3027	14.21
3564	5400	1691	4.84	1929	6.45	2148	8.14	2350	9.88	2536	11.6	2708	13.4	2869	15.2	3024	17.0	3024	15.01
3828	5800	1781	5.73	2005	7.41	2214	9.18	2409	11.0	2591	12.9	2759	14.8	2917	16.7	3069	18.1	3069	15.81

Figure 10-15. Portion of a typical multi-rating table (reprinted courtesy of The New York Blower Company)

The match between the fan performance data and the system characteristic curve is illustrated in Figure 10-16 for the specific fan rotational speed chosen. As long as the overall system remains in good condition and the fan remains in good condition, the system will operate at the point shown in Figure 10-16. This is termed the *operating point*. When the total system static pressure drop and the fan static pressure rise are shown on the same graph, as in the case with Figure 10-16, it is convenient to simply delete the total system static pressure drop axis.

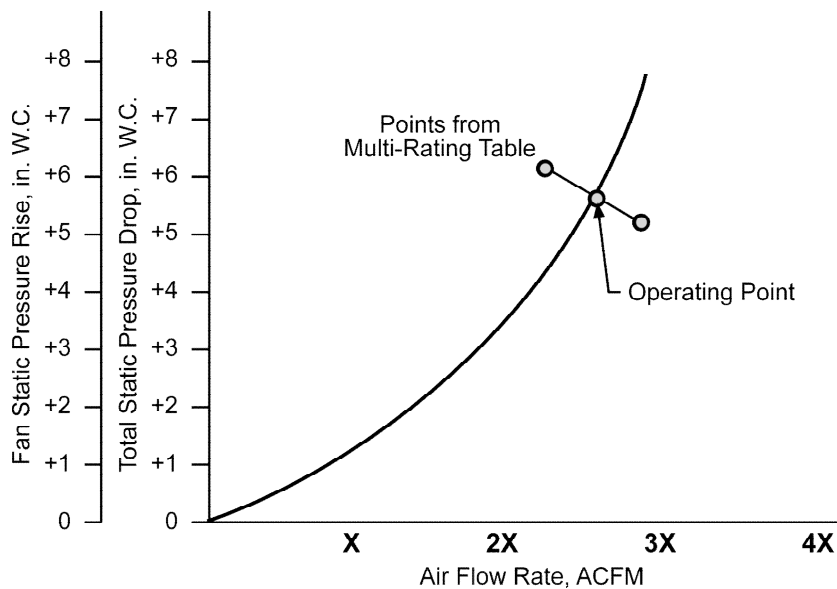


Figure 10-16. Operating point

Figure 10-17 illustrates an example fan curve for a given fan speed. The multi-rating data used to select the fan represented a subset of the total data set that defines this fan curve. There is a specific fan curve for each fan model, model size, and speed. The intersection of the fan curve and the system characteristic curve is illustrated as Point A. This is the point that was determined by the system designer selecting the fan.

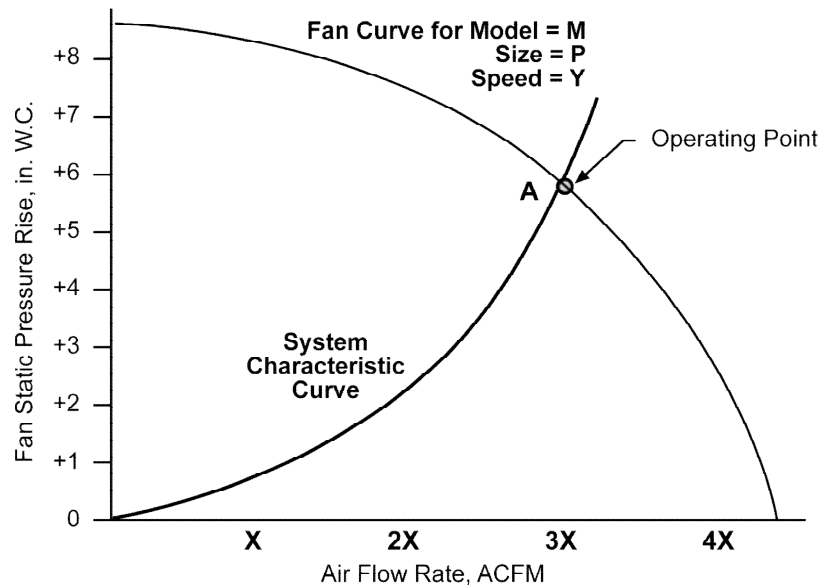


Figure 10-17. Fan characteristic curve

Air pollution control systems and other types of industrial ventilation systems, however, do not necessarily remain exactly at the conditions anticipated by the system designer and the fan manufacturer. A number of normal operating changes and operating problems can cause changes in the overall system air flow rates and the static pressure rises across the fan. The extent of the air flow and static pressure rise changes depend on the fan's performance conditions and the system characteristic curve.

If the gas flow resistance increases due to the build-up of dust in an air pollution control device or because a damper is closed, the system characteristic curve will shift upwards as indicated in Figure 10-18. With this increased gas flow resistance there will be a new operating point, labeled "B". At this new operating point, the fan static pressure rise will be slightly higher while the air flow rate will be slightly lower.

If the air flow resistance decreases due to changes in an air pollution control device or opening of a damper, the system characteristic curve will shift downwards. This results in a new operating point (labeled "C") that has a slightly reduced fan static pressure and increased air flow rate.

Some changes in the system characteristic curve are normal due to factor such as (1) air pollution control system cleaning cycles, (2) gradually increasing air infiltration between maintenance cycles, (3) the opening and closing of individual dampers on individual process sources, and (4) opening and closing of fan inlet or outlet dampers. The system must be

designed to provide adequate pollutant capture even at the lowest normally occurring air flow rates.

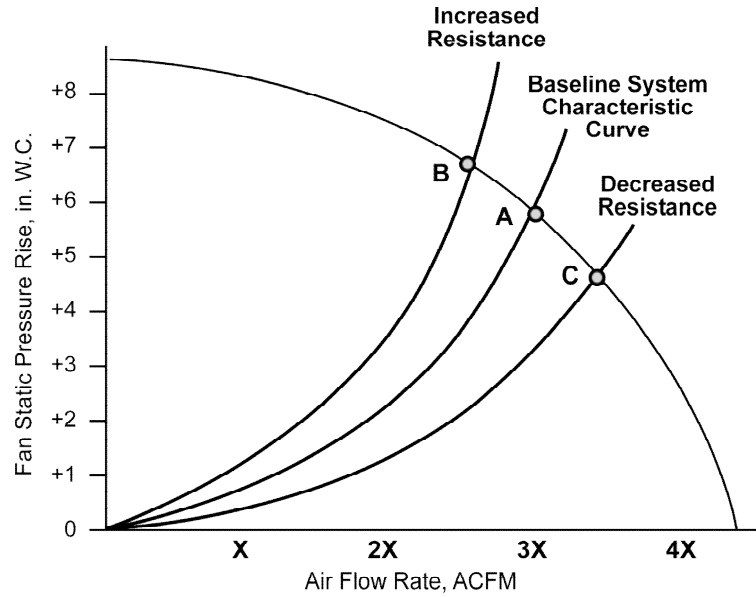


Figure 10-18. Changes in system resistance curve

When changes in the system characteristic curve are outside of the anticipated range, operators often have the option of modifying the fan to increase its capability. Most fans on industrial systems are selected to operate at a speed near the middle of its safe operating range. Slight increases in the fan speed can increase air flow rates and static pressure rises without exceeding the safe operating speed limits. The impact of a slight increase in the fan speed is illustrated in Figure 10-19.

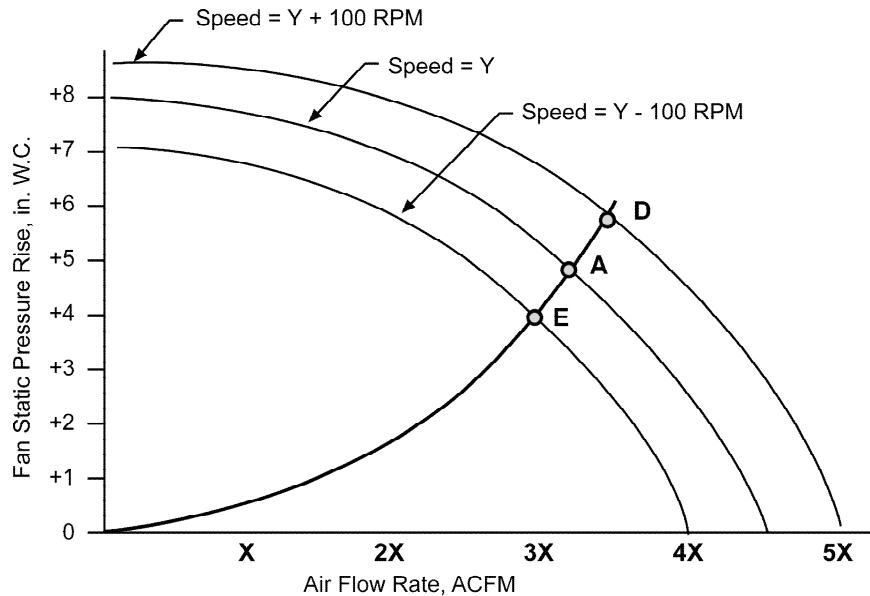


Figure 10-19. Changes in fan speed

It is apparent that the increased fan speed results in a new operating point (labeled "D") having an air flow rate and fan static pressure rise that are both larger than the conditions represented by operating point "A." Not all fans can be easily adjusted to change the fan speed. For example, direct drive fans where the fan wheel shaft is directly driven by the fan motor operate only at the motor rotation speed and can not be adjusted. Belt driven fans can be adjusted but only by changing one or both of the sheaves on the fan and motor. Some large fans with hydraulic or magnetic drives have easily adjusted fan speeds.

Some inadvertent reductions in fan speed are possible for belt driven fans. If the drive belts become slightly loose, they can slip as they move across the sheaves. This often results in a decreased air flow rate of 100 to 200 rpm. The decrease in the air flow rate is directly proportional to the decrease in the fan speed.

As noted earlier, the operating point of a system can be changed by the opening and closing of a fan inlet damper. This is a special damper mounted immediately ahead of the fan, and this damper changes how air enters the fan wheel. As the inlet damper is closed, the operating point shifts to the left, giving lower air flow rate at the higher fan static pressure. Opening the damper shifts the operating point to the right, giving higher air flow rate at the lower fan static pressure.

The fan inlet damper is often used to ensure safe opening of a fan that operates with air streams at elevated gas temperatures. During start-up when the air is cold, the fan inlet damper is kept partially closed to minimize the quantity of heavy cold air moved through the system. As the air heats and becomes less dense, the fan inlet damper opens to increase the air flow rate and fan static pressure rise. This approach minimizes the electrical power demand on the fan motor. Starting with the fan inlet dampers wide open would often exceed the safe current levels for the motor and thereby result in burnout of the motor windings. It is very important to avoid overloading fan motor currents.

Example 10-6

The static pressure drop across a ventilation system, measured at the fan inlet, is -16.5 in WC at a gas flow rate of 8,000 acfm. Estimate the static pressure drop if the flow rate is increased to 12,000 acfm.

Solution:

$$\frac{\Delta SP_{\text{high flow}}}{\Delta SP_{\text{low flow}}} = \left(\frac{Q_{\text{high flow}}}{Q_{\text{low flow}}} \right)^2$$

$$\Delta SP_{\text{high flow}} = \Delta SP_{\text{low flow}} \left(\frac{Q_{\text{high flow}}}{Q_{\text{low flow}}} \right)^2 = -16.5 \text{ in WC} \left(\frac{12,000 \text{ acfm}}{8,000 \text{ acfm}} \right)^2 = -37.1 \text{ in WC}$$

Note: This solution is based on the assumption that there are no significant changes in gas density due to the increase in gas flow rate.

Decreased system resistance can sometimes be a problem. In this situation, the system operating point shifts to the right to a position of higher gas flow rate and lower static pressure rise. While this change would favor improved hood capture, it could reduce the collection efficiency of the air pollution control device. High gas velocities through certain types of air pollution control systems, such as fabric filters, electrostatic precipitators, carbon adsorbers and catalytic oxidizers, can reduce efficiency.

It is helpful to be able to determine when the system characteristic curve has shifted. The most direct way to check the fan performance is to measure the gas flow rate. However, this is time consuming. The fan motor current data provides an indirect, but sometimes very useful, indication of gas flow changes from the baseline conditions. If the system resistance has not changed, an increase in fan motor current is associated with an increase in the gas flow rate. Likewise, decreases in fan current occur when the gas flow rate drops in systems whose resistance has not changed. Unfortunately, the relationship between gas flow rate and motor current is not linear and system resistances can change. The nonlinear characteristic of the relationship is indicated by the brake horsepower curve shown in Figure 10-20. The fan motor current is directly proportional to the brake horsepower, as indicated by the following equation for a three-phase motor:

$$\text{BHP} = \frac{1.73 I \cdot E \cdot \text{Eff} \cdot \text{PF}}{745} \quad (10-14)$$

where

BHP = brake horsepower
 I = fan motor current (amperes)
 E = voltage (volts)
 Eff = efficiency expressed as a decimal
 PF = power factor

While the shape of the horsepower curve varies for different types of fan wheels, this general relationship applies to all centrifugal fans in their normal operating range.

The brake horsepower is also related to the cube of the fan speed, as indicated by the third fan law:

$$\text{BHP}_2 = \text{BHP}_1 \left(\frac{\text{RPM}_2}{\text{RPM}_1} \right)^3 \quad (10-15)$$

where:

BHP₁ = baseline brake horsepower
 BHP₂ = present brake horsepower
 RPM₁ = baseline fan wheel rotational speed (revolutions per minute)
 RPM₂ = present fan wheel rotational speed (revolutions per minute)

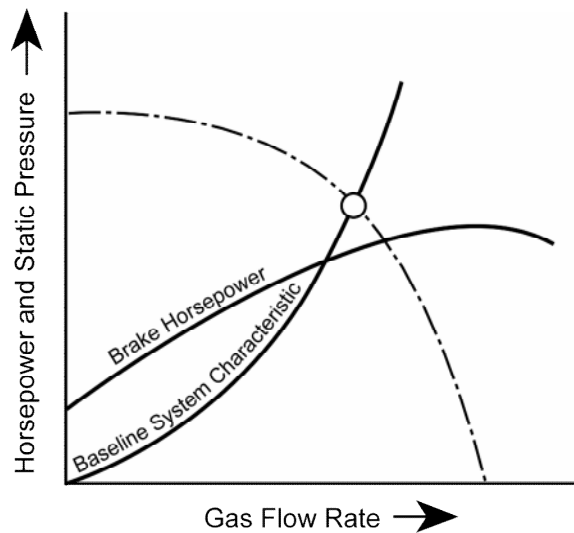


Figure 10-20. Brake horsepower curve

Effect of Gas Temperature and Density

A fan operates like a high-speed shovel. Every rotation of the fan wheel at a given operating point moves a constant volume of air. While the volume is constant, the weight of the air being moved may not be constant. The density of the gas being handled by the fan is a function of the gas temperature. At high gas temperatures, the gas has a low density, and the gas is relatively light. When the gas temperature is cold, for example at ambient temperature, the gas is dense, and its weight is substantial. In addition to gas temperature, gas density is also a function of the absolute gas pressure.

The gas density has a direct effect on the fan motor current. The current will be high when the gas stream is cold, such as the times when the process is starting up. If steps are not taken to minimize gas flow during cold operating periods, the fan motor could burn out due to excessive current flow. To prevent this, the fan inlet or outlet dampers are usually partially closed during start-up to restrict the amount of dense air being handled. As the process heats up and the gas stream becomes less dense, the dampers can be opened to permit normal gas flow rates.

When using the fan motor current as an indicator of gas flow rate, it is important to correct the motor currents at the actual conditions back to standard conditions:

$$I_{\text{STP}} = I_{\text{actual}} \left(\frac{\rho_{\text{STP}}}{\rho_{\text{actual}}} \right) \quad (10-16)$$

where

- I_{STP} = fan motor current at standard conditions (amperes)
- I_{actual} = fan motor current at actual conditions (amperes)

$$\begin{aligned}\rho_{STP} &= \text{gas density at standard conditions (lb}_m\text{/ft}^3\text{)} \\ \rho_{\text{actual}} &= \text{gas density at actual conditions (lb}_m\text{/ft}^3\text{)}\end{aligned}$$

Example 10-7

A fan motor is operating at 80 amps and the gas flow rate through the system is 10,000 acfm at 300°F and -10 in WC (fan inlet). What is the motor current at standard conditions?

Solution:

$$I_{STP} = I_{\text{actual}} \left(\frac{\rho_{STP}}{\rho_{\text{actual}}} \right)$$

Calculate the gas density at actual conditions:

$$\rho = \frac{P \cdot MW}{RT}$$

$$P = (407 \text{ in WC} - 10 \text{ in WC}) \left(\frac{1 \text{ atm}}{407 \text{ in WC}} \right) = 0.975 \text{ atm}$$

$$T = 300^\circ\text{F} + 460 = 760^\circ\text{R}$$

$$\rho = \frac{P \cdot MW}{RT} = \frac{(0.975 \text{ atm}) \left(29 \frac{\text{lb}_m}{\text{lb-mole}} \right)}{\left(0.73 \frac{\text{atm} \cdot \text{ft}^3}{\text{lb-mole} \cdot ^\circ\text{R}} \right) (760^\circ\text{R})} = 0.0510 \frac{\text{lb}_m}{\text{ft}^3}$$

Calculate the motor current at standard conditions:

$$I_{STP} = I_{\text{actual}} \left(\frac{\rho_{STP}}{\rho_{\text{actual}}} \right) = 80 \text{ amps} \left(\frac{0.0747 \frac{\text{lb}_m}{\text{ft}^3}}{0.0510 \frac{\text{lb}_m}{\text{ft}^3}} \right) = 117 \text{ amps}$$

Note 1: The problem could have been solved quickly by using tabulated values of the gas density. However, this approach also reduces the risk of a gas density error caused by not taking into account the effect of pressure changes.

Note 2: The gas composition could be taken into account by calculating the weighted average molecular weights of the constituents rather than assuming 29 pounds per pound mole, which is close to the value for air. This correction is important when

the gas stream has a high concentration of compounds such as carbon dioxide or water, which have molecular weights that are much different than air.

The gas temperature and pressure corrections for gas density must also be used when selecting a fan. The fan multi-rating tables are expressed in standard temperature (70°F) and pressure (1 atm). These corrections are needed to ensure that the fan will deliver the necessary gas flow rates and fan static pressure increases under the actual operating conditions anticipated in the process. As the gas flows through the fan, the pressure usually changes from negative to positive. This increase in pressure can cause the gas temperature to increase slightly.

Summary

Centrifugal fans are the most commonly used type of fan in air pollution control systems because of their ability to generate high pressure rises in the gas stream. The major components of a typical centrifugal fan include the fan wheel, fan housing, drive mechanism, and inlet dampers and/or outlet dampers.

The intersection of the fan characteristic curve and the system characteristic curve is called the operating point for the fan. The factors that affect the fan characteristic curve are the type of fan wheel and blade, the fan wheel rotational speed, and the shape of the fan housing. The system characteristic curve takes into account the energy losses throughout the ventilation system. These curves are helpful indicators in determining if a change in the system has occurred. A change in the system can also be detected through the fan motor current data that corresponds with the gas flow rate, provided the system resistance has not changed.

The fan laws can predict how a fan will be affected by a change in an operating condition. The fan laws apply to fans having the same geometric shape and operating at the same point on the fan characteristic curve.

A fan will move a constant volume of air; however the amount of work required to move the gas flow is dependent on the density of the gas. Two factors that affect density are temperature and pressure. The gas flow density has a direct effect on the fan motor current.

Review Problems

1. Calculate the hood static pressure if the hood coefficient of entry is 0.49 and the gas flow rate through a 1.5-foot diameter duct from the hood is 6,200 ft³/min. Use standard temperatures and pressures.
 - a. 2.1 in WC
 - b. 1.15 in WC
 - c. 0.38 in WC
 - d. 0.85 in WC

2. Find the farthest distance away that a flanged hood, 6 in by 12 in, can be placed away from the contaminant source and maintain the capture velocity of 300 fpm and a volumetric flow rate of 2,000 acfm. The equation for a flanged hood is:

$$Q = 0.75v_h(10X^2 + A_h)$$

- a. 15 inches
 - b. 24 inches
 - c. 3 inches
 - d. 11 inches
3. Estimate the rotational speed of a belt-driven centrifugal fan based on the following data:

Motor rotational speed, $RPM_{Motor} = 1778$ rpm

Motor sheave diameter, $D_{Motor} = 8$ in.

Fan sheave diameter, $D_{Fan} = 14$ in.

- a. 1,239 rpm
 - b. 2,000 rpm
 - c. 400 rpm
 - d. 1,016 rpm
4. A system consists of the following components (in order): hood, fabric filter, centrifugal fan, and stack. The fabric filter static pressure drop has increased from 4.5 inches of water to 6.5 inches of water. If the fan dampers do not move to compensate for this change, what will happen to the hood static pressure?
 - a. It will be less negative (closer to zero)
 - b. It will be more negative
 - c. It will become positive
 - d. It will remain unchanged

5. A centrifugal fan is moving 1,000 cubic feet of air per minute at a temperature of 450°F and a fan inlet pressure of -15 inches of water. What will the actual air flow rate be if the gas temperature decreases to 68°F, the inlet pressure remains unchanged, and the fan rotational speed remains the same?
 - a. The air flow rate will increase to 1,723 acfm
 - b. The air flow rate will decrease to 580 acfm
 - c. The air flow rate will remain at 1,000 acfm

6. A centrifugal fan is operating with a motor current of 120 amps. The gas density entering the fan during normal operation is 0.045 pounds per cubic foot. Estimate the motor current at standard conditions when the gas density is approximately 0.075 pounds per cubic foot.
 - a. 500 amps
 - b. 200 amps
 - c. 159 amps
 - d. 90 amps

7. The static pressure drop through a section of ductwork is -1.2 inches of water when the gas flow rate is 5,000 acfm. Estimate the static pressure drop across this section if the gas flow rate increases to 8,000 acfm. Assume that there are no gas density changes associated with the increased gas flow rate.
 - a. -3.07 in WC
 - b. -1.1 in WC
 - c. -2 in WC
 - d. -4 in WC

8. The hood capture efficiency is 92% and the wet scrubber control system has a collection efficiency of 95%. If the process served by this system is generating 140 pounds of pollutant per hour, calculate the fugitive emissions and the stack emissions.
 - a. 20.50 lb_m/hr fugitive emissions and 9.80 lb_m/hr stack emissions
 - b. 1.50 lb_m/hr fugitive emissions and 0.80 lb_m/hr stack emissions
 - c. 11.2 lb_m/hr fugitive emissions and 6.4 lb_m/hr stack emissions
 - d. 14.0 lb_m/hr fugitive emissions and 3.54 lb_m/hr stack emissions

9. Assume a fan is presently operating with the following conditions: 20,000 acfm, 2.5 in WC fan static pressure, 400 rpm, and 12 brake horsepower. Using the fan laws determine the new rpm, brake horsepower, and static pressure when the volumetric increases to 22,500 acfm.
- a. 490 rpm, 19.1 bhp, 5.7 in WC
 - b. 350 rpm, 9.5 bhp, 3.9 in WC
 - c. 400 rpm, 10.2 bhp, 2.8 in WC
 - d. 450 rpm, 17.1 bhp, 3.2 in WC
10. What would happen to the desired operating point of a fan if a hole developed in the inlet ductwork. Which characteristic curve will shift, what will happen to the operating point, volumetric flow rate, and hood static pressure?
- a. The system characteristic curve will shift down, the volumetric flow rate will increase, and the hood static pressure will increase.
 - b. The system characteristic curve will shift down, the volumetric flow rate will decrease, and the hood static pressure will decrease.
 - c. The system characteristic curve will shift down, the volumetric flow rate will increase, and the hood static pressure will decrease.
 - d. The system characteristic curve will shift up, the volumetric flow rate will increase, and the hood static pressure will decrease.

This page intentionally left blank.

Review Problem Solutions

1. Calculate the hood static pressure if the hood coefficient of entry is 0.49 and the gas flow rate through a 1.5-foot diameter duct from the hood is 6,200 ft³/min. Use standard temperatures and pressures.

b. 1.15 in WC

Solution:

$$SP_h = VP_d + h_e = (1 + F_h)VP_d$$

Calculate the velocity pressure:

$$v = \frac{Q}{A} = \frac{6,200 \frac{\text{ft}^3}{\text{min}}}{\frac{\pi(1.5\text{ft})^2}{4}} = 3,508 \frac{\text{ft}}{\text{min}}$$

$$VP_d = \rho_g \left(\frac{v_d}{1,096.7} \right)^2 = 0.075 \frac{\text{lb}_m}{\text{ft}^3} \left(\frac{3,508 \frac{\text{ft}}{\text{min}}}{1,096.7} \right)^2 = 0.77 \text{ in WC}$$

Calculate the hood static pressure:

$$SP_h = (1 + 0.49) 0.77 \text{ in WC} = 1.15 \text{ in WC}$$

2. Find the farthest distance away that a flanged hood, 6 in by 12 in, can be placed away from the contaminant source and maintain the capture velocity of 300 fpm and a volumetric flow rate of 2,000 acfm. The equation for a flanged hood is:

$$Q = 0.75v_h(10X^2 + A_h)$$

d. 11 inches

Solution:

$$X = \sqrt{\frac{Q}{0.75v_h} - A_h} = \sqrt{\frac{2,000 \frac{\text{ft}^3}{\text{min}}}{0.75 \left(300 \frac{\text{ft}}{\text{min}} \right)} - \frac{(6\text{in})(12\text{in})}{144 \frac{\text{in}^2}{\text{ft}^2}}} = 0.92 \text{ ft} = 11 \text{ in}$$

3. Estimate the rotational speed of a belt-driven centrifugal fan based on the following data:

Motor rotational speed, $\text{RPM}_{\text{motor}} = 1,778 \text{ rpm}$

Motor sheave diameter, $D_{\text{motor}} = 8 \text{ in}$

Fan sheave diameter, $D_{\text{fan}} = 14 \text{ in}$

- d. 1,016 rpm

Solution:

$$\text{RPM}_{\text{fan}} = \text{RPM}_{\text{motor}} \frac{D_{\text{motor}}}{D_{\text{fan}}} = 1,778 \text{ rpm} \left(\frac{8 \text{ in}}{14 \text{ in}} \right) = 1,016 \text{ rpm}$$

4. A system consists of the following components (in order): hood, fabric filter, centrifugal fan, and stack. The fabric filter static pressure drop has increased from 4.5 inches of water to 6.5 inches of water. If the fan dampers do not move to compensate for this change, what will happen to the hood static pressure?

- a. It will be less negative (closer to zero)

5. A centrifugal fan is moving 1,000 cubic feet of air per minute at a temperature of 450°F and a fan inlet pressure of -15 inches of water. What will the actual air flow rate be if the gas temperature decreases to 68°F, the inlet pressure remains unchanged, and the fan rotational speed remains the same?

- c. The air flow rate will remain at 1,000 acfm

6. A centrifugal fan is operating with a motor current of 120 amps. The gas density entering the fan during normal operation is 0.045 pounds per cubic foot. Estimate the motor current at standard conditions when the gas density is approximately 0.075 pounds per cubic foot.

- b. 200 amps

Solution:

$$I_{\text{STP}} = I_{\text{actual}} \left(\frac{\rho_{\text{STP}}}{\rho_{\text{actual}}} \right) = 120 \text{ amps} \left(\frac{0.075 \frac{\text{lb}_m}{\text{ft}^3}}{0.045 \frac{\text{lb}_m}{\text{ft}^3}} \right) = 200 \text{ amps}$$

7. The static pressure drop through a section of ductwork is -1.2 inches of water when the gas flow rate is 5,000 acfm. Estimate the static pressure drop across this section if the gas

flow rate increases to 8,000 acfm. Assume that there are no gas density changes associated with the increased gas flow rate.

- a. -3.07 in WC

Solution:

$$\Delta SP_{\text{high flow}} = \Delta SP_{\text{low flow}} \left(\frac{Q_{\text{high flow}}}{Q_{\text{low flow}}} \right)^2 = -1.2 \text{ in WC} \left(\frac{8,000 \text{ acfm}}{5,000 \text{ acfm}} \right)^2 = -3.07 \text{ in WC}$$

8. The hood capture efficiency is 92% and the wet scrubber control system has a collection efficiency of 95%. If the process served by this system is generating 140 pounds of pollutant per hour, calculate the fugitive emissions and the stack emissions.

- c. 11.2 lb_m/hr fugitive emissions and 6.4 lb_m/hr stack emissions

Solution:

$$\text{Fugitive emissions} = (1 - 0.92)140 \text{ lb}_m/\text{hr} = 11.2 \text{ lb}_m/\text{min}$$

$$\text{Stack emissions} = (1 - 0.95)(0.92)140 \text{ lb}_m/\text{min} = 6.4 \text{ lb}_m/\text{min}$$

9. Assume a fan is presently operating with the following conditions: 20,000 acfm, 2.5 in WC fan static pressure, 400 rpm, and 12 brake horsepower. Using the fan laws determine the new rpm, brake horsepower, and static pressure when the volumetric increases to 22,500 acfm.

- d. 450 rpm, 17.1 bhp, 3.2 in WC

Solution:

$$\frac{Q_1}{Q_2} = \frac{\text{RPM}_1}{\text{RPM}_2}$$

$$\text{RPM}_2 = \text{RPM}_1 \frac{Q_2}{Q_1} = 400 \text{ rpm} \left(\frac{22,500 \text{ acfm}}{20,000 \text{ acfm}} \right) = 450 \text{ rpm}$$

$$\frac{\text{BHP}_1}{\text{BHP}_2} = \left(\frac{\text{RPM}_1}{\text{RPM}_2} \right)^3$$

$$\text{BHP}_2 = \text{BHP}_1 \left(\frac{\text{RPM}_2}{\text{RPM}_1} \right)^3 = 12 \text{ bhp} \left(\frac{450 \text{ rpm}}{400 \text{ rpm}} \right)^3 = 17.1 \text{ bhp}$$

$$\frac{SP_1}{SP_2} = \left(\frac{RPM_1}{RPM_2} \right)^2$$

$$SP_2 = SP_1 \left(\frac{RPM_2}{RPM_1} \right)^2 = 2.5 \text{ in WC} \left(\frac{450 \text{ rpm}}{400 \text{ rpm}} \right)^2 = 3.2 \text{ in WC}$$

10. What would happen to the desired operating point of a fan if a hole developed in the inlet ductwork. Which characteristic curve will shift, what will happen to the operating point, volumetric flow rate, and hood static pressure?
- c. The system characteristic curve will shift down, the volumetric flow rate will increase, and the hood static pressure will decrease.

References

American Conference of Governmental Industrial Hygienists, *Industrial Ventilation - A Manual of Recommended Practice*, 23rd Edition, 1998.

Cengel, Y.A., and M.A. Boles, *Thermodynamics: An Engineering Approach*, McGraw-Hill, New York, 1989.

Code of Federal Regulations, Title 40, Part 60, Method 22, July 1, 1997.

This page intentionally left blank.

APPENDIX A

CONVERSION FACTORS

Length

$$1 \text{ in} = 2.54 \text{ cm}$$

$$1 \text{ m} = 3.281 \text{ ft}$$

$$1 \text{ ft} = 0.3048 \text{ m}$$

Mass

$$1 \text{ lb}_m = 453.6 \text{ g}$$

$$1 \text{ lb}_m = 7,000 \text{ grains}$$

$$1 \text{ kg} = 2.205 \text{ lb}_m$$

Pressure

$$1 \text{ atm} = 101,325 \text{ Pa}$$

$$1 \text{ atm} = 760 \text{ mm Hg}$$

$$1 \text{ atm} = 14.7 \text{ psia}$$

Force

$$1 \text{ N} = 1 \text{ kg}\cdot\text{m}/\text{sec}^2$$

$$1 \text{ N} = 0.225 \text{ lb}_f$$

$$1 \text{ dyne} = 1 \text{ g}\cdot\text{cm}/\text{sec}^2$$

$$1 \text{ N} = 1 \times 10^5 \text{ dynes}$$

Energy

$$1 \text{ cal} = 4.18 \text{ J}$$

$$1 \text{ J} = 9.486 \times 10^{-4} \text{ Btu}$$

$$1 \text{ Btu} = 252.2 \text{ cal}$$

Power

$$1 \text{ watt} = 1 \text{ J}/\text{sec}$$

$$1 \text{ watt} = 3.414 \text{ Btu}/\text{hr}$$

$$1 \text{ watt} = 1.341 \times 10^{-3} \text{ hp}$$

$$1 \text{ hp} = 33,479 \text{ Btu}/\text{hr}$$

Density

$$1 \text{ kg}/\text{m}^3 = 0.0624 \text{ lb}_m/\text{ft}^3$$

$$1 \text{ kg}/\text{m}^3 = 1 \times 10^{-3} \text{ g}/\text{cm}^3$$

Absolute viscosity

$$1 \text{ Pa}\cdot\text{sec} = 1 \text{ kg}/\text{m}\cdot\text{sec} = 1,000 \text{ cp}$$

$$1 \text{ cp} = 6.72 \times 10^{-4} \text{ lb}_m/\text{ft}\cdot\text{sec}$$

Kinematic viscosity

$$1 \text{ m}^2/\text{sec} = 3.875 \times 10^4 \text{ ft}^2/\text{hr}$$

Area

$$1 \text{ m}^2 = 10.764 \text{ ft}^2$$

$$1 \text{ cm}^2 = 0.155 \text{ in}^2$$

$$1 \text{ m}^2 = 1.196 \text{ yd}^2$$

Volume

$$1 \text{ m}^3 = 35.31 \text{ ft}^3$$

$$1 \text{ cm}^3 = 0.061 \text{ in}^3$$

$$1 \text{ m}^3 = 264.2 \text{ gal}$$

$$1 \text{ ft}^3 = 28.317 \text{ liters}$$

$$1 \text{ m}^3 = 1 \times 10^3 \text{ liters}$$

$$1 \text{ ft}^3 = 7.48 \text{ gal}$$

Volumetric flow

$$1 \text{ m}^3/\text{sec} = 35.31 \text{ ft}^3/\text{sec}$$

$$1 \text{ ft}^3/\text{min} = 1.7 \text{ m}^3/\text{hr}$$

$$1 \text{ gpm} = 0.227 \text{ m}^3/\text{hr}$$

Velocity

$$1 \text{ m}/\text{sec} = 3.28 \text{ ft}/\text{sec}$$

$$1 \text{ m}/\text{sec} = 196.85 \text{ ft}/\text{min}$$

$$1 \text{ mph} = 0.447 \text{ m}/\text{sec}$$

Geometry

$$\text{Area of circle} = \pi r^2 = \pi d^2/4$$

$$\text{Circumference of circle} = 2\pi r = \pi d$$

$$\text{Surface area of sphere} = 4\pi r^2 = \pi d^2$$

$$\text{Surface area of cylinder} = 2\pi rh = \pi dh$$

$$\text{Volume of sphere} = 4\pi r^3/3 = \pi d^3/6$$

This page intentionally left blank.

APPENDIX B

CONSTANTS AND USEFUL INFORMATION

Gas constants

$$R = 82.06 \text{ atm}\cdot\text{cm}^3/\text{g}\cdot\text{mole}\cdot\text{K}$$

$$R = 8.31 \times 10^3 \text{ kPa}\cdot\text{m}^3/\text{kg}\cdot\text{mole}\cdot\text{K}$$

$$R = 10.73 \text{ psia}\cdot\text{ft}^3/\text{lb}\cdot\text{mole}\cdot^\circ\text{R}$$

$$R = 0.73 \text{ atm}\cdot\text{ft}^3/\text{lb}\cdot\text{mole}\cdot^\circ\text{R}$$

Acceleration of gravity

$$g = 32.17 \text{ ft}/\text{sec}^2 = 980.7 \text{ cm}/\text{sec}^2 = 9.8 \text{ m}/\text{sec}^2$$

Newton's conversion constant

$$g_c = 32.17 \text{ lb}_m\cdot\text{ft}/\text{lb}_f\cdot\text{sec}^2$$

Molar volume

$$1 \text{ lb}\cdot\text{mole} = 385.4 \text{ ft}^3 \text{ at } 20^\circ\text{C} \text{ and } 1 \text{ atm}$$

$$1 \text{ g}\cdot\text{mole} = 24.1 \text{ liters at } 20^\circ\text{C} \text{ and } 1 \text{ atm}$$

Specific heat

$$C_p \text{ for water} = 1 \text{ Btu}/\text{lb}_m\cdot^\circ\text{F} = 1 \text{ cal}/\text{g}\cdot^\circ\text{C} \text{ (at } 20^\circ\text{C} \text{ and } 1 \text{ atm)}$$

$$C_p \text{ for air} = 0.244 \text{ Btu}/\text{lb}_m\cdot^\circ\text{F} = 0.244 \text{ cal}/\text{g}\cdot^\circ\text{C} \text{ (average over } 0\text{-}2,000^\circ\text{F)}$$

Absolute viscosity

$$\text{Viscosity of water} = 1 \text{ cp} = 0.01 \text{ g}/\text{cm}\cdot\text{sec} = 6.72 \times 10^{-4} \text{ lb}_m/\text{ft}\cdot\text{sec} \text{ (at } 20^\circ\text{C} \text{ and } 1 \text{ atm)}$$

$$\text{Viscosity of air} = 1.8 \times 10^{-4} \text{ g}/\text{cm}\cdot\text{sec} = 1.21 \times 10^{-5} \text{ lb}_m/\text{ft}\cdot\text{sec} \text{ (at } 20^\circ\text{C} \text{ and } 1 \text{ atm)}$$

Density

$$\text{Density of water} = 1 \text{ g}/\text{cm}^3 = 62.4 \text{ lb}_m/\text{ft}^3 \text{ (at } 20^\circ\text{C} \text{ and } 1 \text{ atm)}$$

$$\text{Density of air} = 1.2 \times 10^{-3} \text{ g}/\text{cm}^3 = 7.47 \times 10^{-2} \text{ lb}_m/\text{ft}^3 \text{ (at } 20^\circ\text{C} \text{ and } 1 \text{ atm)}$$

This page intentionally left blank.